GEM TN-93-473

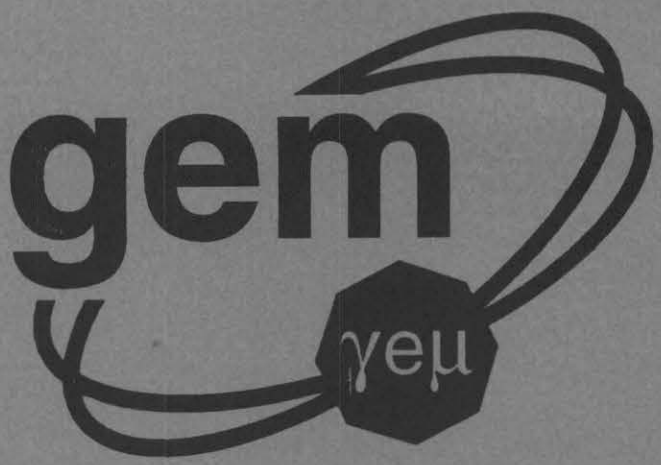

Technical Note
GEM R&D and Test Beam Plan
Fermilab 1995 - 1996 Run

by the
Gammas, Electrons, and Muons
Collaboration

Edited by:
Harvey Newman
Henk Uijterwaal
Gary Word

October 28, 1993

Technical Note
GEM R&D and Test Beam Plan
Fermilab 1995–1996 Run

The GEM Collaboration

Editors:

Harvey Newman
Henk Uijterwaal
Gary Word

October 28, 1993

GEM-TN-93-473

Technical Note
GEM R&D and Test Beam Plan
Fermilab 1995–1996 Run

by the

Gammas, Electrons, and Muons Collaboration

October 28, 1993

Edited by:
Harvey Newman
Henk Uijterwaal
Gary Word

Collaboration contact persons:

Barry Barish
Division of Physics, Mathematics and Astronomy
256-48 HEP
California Institute of Technology
Pasedena, California 91125

William Willis
Nevis Laboratory
Columbia University
P.O. Box 137
Irvington-on-Hudson
New York 10533

GEM Collaborators List

ALBANIA

Institute of Nuclear Physics of the Albanian Academy of Sciences : B. Cico, A. Dodbibaj, N. Domi, P. Fuga, L. Karcanaj, A. Kasneci, M. Kedhi, S. Koji, Agim Minxhozi, B. Nevruzaj, D. Rexha, P. Skendo, J. Thereska, F. Ylli, S. Zaganjori, D. Zeneli, J. Zoto

Polytechnical Institute of Tirana : B. Taullahu

University of Tirana : L. Aliko, P. Berzhani, A. Borici, E. Cabej, O. Ciftja, Edlira Ciu, A. Dede, M. Dede, B. Duka, A. Fuga, A. Gashi, Z. Gionai, D. Gjiknodi, B. Guda, E. Hysengegasi, M. Ifiti, K. Islami, F. Klosi, M. Kuqo, V. Laska, G. Leka, R. Maksim, R. Mejdani, I. Mele, Z. Mulaj, N. Nosi, M. Panariti, K. Pance, I. Prifti, R. Sharko, M. Spiro, H. Sykja, N. Thomo, M. Treska, F. Vila, D. Xhuglini, I. Xhunga, E. Xhuvani

BELARUS

Byelorussian Research and Production Association of Powder Metallurgy : S. G. Barai, N. Naumovich, Oleg Roman, V. Shelekhina, A. Shevchionok

Institute of Heat and Mass Exchange of Academy of Science of Belarus : V. Kolpaschikov

National Scientific and Educational Center of Particle and High Energy Physics : Mikhail Baturitsky, Sergei Degtjarev, Oleg Dvornikov, Igor Emeljanchik, A. Kurilin, A. Litomin, Vitaly Mikhailov, Victor Shuljak, Nikolai Shumeiko, A. Solin, A. Soroko, Vladimir Stepanets

Scientific Research Institute of Nuclear Problems, Belarussia State University : V. G. Baryshevsky, A. Fjodorov, M. Korzhik, A. Lobko

BRAZIL

University of Sao Paulo : Oscar P. Eboli, Carlos O. Escobar, Philippe Gouffon, Miguel Luksys, S. F. Novaes

CHINA

Beijing Glass Research Institute (BGRI) : G. Chen, Z. Z. Dai, X. Y. Dong, Y. C. Gao, T. Z. Li, G. T. Liu, Z. Q. Liu, S. Q. Man, S. X. Ren, Z. L. Su, Y. T. Wang, Ou Wen, H. Xiao, H. Z. Yang, F. C. Zhang, F. Y. Zhang, J. Zhang, J. Q. Zhang, Y. N. Zheng

Institute of High Energy Physics (IHEP) : Yuan-bo Chen, Xiang-zong Cui, Wei-Xin Gu, Yifan Gu, Ya-Nan Guo, Yu-yi Guo, Tao Hu, Yinzhi Huang, Chun-hua Jiang,

Ying-yuan Jiang, Yuan-fen Lai, Jin Li, Zhi-gang Li, Jian-feng Lin, Zhen-an Liu, Chen-Sheng Mao, Ze-pu Mao, Qun Ouyang, Huai-Yi Sheng, Man Wang, Yun-yong Wang, De-ming Xi, Ji-wei Xi, Yi-gang Xie, Rongsheng Xu, Yu-ling Xu, Chuan-song Yu, Bing-yun Zhang, Cai-di Zhang, Chang-chun Zhang, Da-Hua Zhang, Qin-jian Zhang, Yu Zhang, Di-xin Zhao, Jing-wei Zhao, Zi-ming Zhu, Bao-An Zhuang

Nanjing University : Ting-Yang Chen, Dungtang Gao, G. X. Gao, Ming Qi, De-Xung Xi, Nai-Guo Yao, Zheu-Wu Zhang

Peking University : C. X. Lai, H. T. Liu, Song-Juang Xia, Y. L. Ye

Shanghai Institute of Ceramics (SIC) : X. L. Fang, P. X. Gu, J. K. Guo, G. Q. Hu, S. K. Hua, Pe-Jung Li, D. Z. Shen, E. W. Shi, W. T. Su, Z. Y. Wei, Y. Y. Xie, L. Xu, Z. L. Xue, D. S. Yan, Zhi-wen Yin, X. L. Yuan, G. M. Zhao, Y. L. Zhao, W. Z. Zhong, R. M. Zhou

Shanghai Institute of Nuclear Research (SINR) : X. P. Li, F. H. Yu, W. H. Zheng

Tongji University : Lingyan Chen, J. Du, M. Gu, J. Wang, L. M. Wang, X. Wu, K. H. Xiang

Tsinghua University : M. Cao, Hong Yi Chen, Ze Ming Chen, Jing Kang Deng, Wen Huan Gao, Ke Jun Kang, Y. P. Kuang, Da Cheng Li, Yan Xiang Li, L. S. Liu, Y. Q. Liu, W. Z. Luo, D. H. Nan, Wei Dou Ni, Yong Gen Qian, Jia Lie Ren, Ren Cheng Shang, K. Shen, Bing Xue Shi, Ke Ren Shi, J. Wang, Jing Jin Wang, Jun Ming Wang, Q. Wang, Yue Min Wang, Ke Ling Wen, Si Da Xu, Y. P. Yi, Guan Zheng Yu, Y. Zhao, H. Y. Zhou, Sheng Jiang Zhu

University of Science & Technology of China (USTC) : Z. H. Bian, M. F. Cai, Y. M. Fang, R. D. Han, L. Y. Hao, X. S. Lin, B. A. Liu, W. Mei, Q. C. Shi, H. M. Wang, Z. M. Wang, S. L. Wu, S. L. Xing, J. H. Xu, K. Z. Xu, X. L. Xu, B. X. Yang, B. J. Ye, X. Q. Yu, J. Zhang, Y. Z. Zhou

CZECH REPUBLIC

Charles University : I. Wilhelm

Czech Technical University : V. Bouda, V. Haulena, J. John, P. Kocourek, L. Musilek, J. Navratil, L. Pina, S. Pospisil, V. Sochor, B. Sopko, J. Stecha, J. Tolar, J. J. Venkrbec

Institute of Electrical Engineering : M. Polak

Institute of Nuclear Physics, Academy of Sciences : A. Kugler, R. Mach, P. Chraska, J. Hladky

University Karlovy : V. Malat

EQUADOR

Universidad San Francisco de Quito : S. Gangotena, Bruce Hoeneisen, C. Marin

GEORGIA

Tbilisi State University : J. S. Bagaturia, W. P. Djordjadze, M. Khaindrava, G. V. Melitauri, D. A. Mzavia, T. M. Sakhelashvili, R. G. Shanidze, A. Tavkhelidze, Z. Tsamalaidze

INDIA

Bhabha Atomic Research Center : G. Govindarrdan, S. S. Kapoor, G. P. Srivastava

Panjab University : S. B. Beri, V. Bhatnagar, S. Chopra, Jatinder M. Kohli, J. B. Singh, P. M. Sood

University of Delhi, South Campus : V. S. Bhasin, R. Gang, S. K. Jha, Vijay Kapoor, N. Parashar, Ram K. Shivpuri, S. Soni, K. N. Tripathi

Variable Energy Cyclotron Center : R. Bhandari, B. Simha

ISRAEL

Tel Aviv University : G. Bella, Odette Benary, Rachel Heifetz, Yona Oren

ITALY

INFN, Trieste : A. Bravar, R. Giacomich, A. Penzo, P. Schiavon, A. Vacchi

KAZAKHSTAN

High-Energy Physics Institute of National Academy of Sciences of Kazakhstan Republic (HEPI of NAS KR) : E. Khusainov, N. Nurgozhin, N. Pokrovsky, A. Temiraliev, B. Zhautykov, Ernst G. Boos, I. Kouchin

KOREA

Changwon National University : C. H. Hahn

Chonnam National University : H. I. Jang, Jae Yool Kim, I. T. Lim

Choongnam National University : H. Y. Lee

Chosun University : B. N. Park

Dongshin University : M. Y. Pac

Gunsan National University : J. Y. Ryu

Gyeongsang National University : S. K. Choi, K. S. Chung, I. G. Park, J. S. Song

KAIST : J. K. Kim

Kangnung National University : Kyu-Seok Kang, D. W. Kim

Kangwon National University : S. K. Nam

Korea University : JooSang Kang, Chong Oh Kim, S. K. Park, K. S. Sim

Kyungpook National University : Donghee Kim, S. Y. Noh, D. Son, Y. M. Park

National Teacher's University : S. N. Kim

Seongkyunkwan University : Y. I. Choi

Seoul National Teacher's College : D. G. Ku, E. H. Lee

Seoul National University : Jewan Kim, Sunkee Kim, Seong Sook Myung

Sookmyeong Women's University : J. N. Park

Wonkwang University : S. Y. Bahk

MEXICO

CINVESTAV : Gerardo Herrera Corral, Heriberto Castilla Valdez

Universidad de Guanajuato : Arturo Gonzalez, Antonio Morelos, Gerardo Moreno, Luis Villasenor

POLAND

Institute of Nuclear Physics : Andrzej Eskreys, Jan Figiel, Bogdan Pawlik, Piotr Stopa, Maciej Zachara

ROMANIA

Bucharest University : C. Besliu

Institute of Atomic Physics : A. Aculai, Christian Blaj, Horia Bozdoc, Liviu Butacu, Mircea Ciobanu, A. Dorobantu, Daniel Ighicianu, Gheorghe Pascovici, V. Popa, Gheorghe Radulescu, Dan Spanu, C. Stan-Sion, Vlad Valeanu, K. Zimmer

RUSSIA

Bochvar Institute for Inorganic Materials : V. Ya. Filkin, A. D. Nikulin, E. I. Plashkin, G. K. Zelensky

Central Institute for Structural Materials, "Prometei" : V. V. Chizhikov, V. I. Kondakov

Institute for Assembling Technology, NIKIMT : I. A. Bachelis, O. K. Drujilovsky, A. A. Kurkumeli

Institute for Nuclear Research, Moscow : V. N. Bolotov, O. Goncharenko, A. Proskuryakov, B. Semenov, V. Suchov, V. Urazmetov

Institute of High Energy Physics, Serpukhov : N. N. Fedyakin, R. N. Krasnokutsky, R. S. Shuvalov, V. V. Sushkov

Institute of Nuclear Physics, Novosibirsk : V. Aulchenko, Stanislav V. Klimenko, G. Kolachev, Mikhail Leltchouk, L. Leontiev, V. Malishev, A. Maslennikov, A. Onuchin, V. Panin, S. Peleganchuk, S. Pivovarov, Veniamiin A. Sidorov, V. Tayursky, Yu. Tikhonov

Institute of Theoretical and Experimental Physics, (ITEP) : Vladislav Balagura, S. Bojarinov, S. Burov, V. Chudakov, Michael Danilov, A. Droutskoi, Yuri Efremenko, V. B. Gavrilov, Yu. Gershtein, Andrei Golutvin, Anatoly Gordeev, Yuri Kamyshkov, I. Korolko, S. V. Kuleshov, L. Laptin, Vasiliy L. Morgunov, Paul Murat, A. A. Nikitin, Dmitri Onoprienko, Audrey Ostapchuk, V. S. Popov, F. Ratnikov, V. Rusinov, Alexander Savin, Sergei Shevchenko, V. Shibaev, Konstantine Shmakov, Alexander Smirnov, V. Stolin, Evgueni I. Tarkovsky, V. Tchistilin, I. Tikhomirov, A. Zhokin

Joint Institute for Nuclear Research : A. V. Bannikov, Leonid S. Barabash, S. A. Baranov, D. A. Belosludtsev, Yuri E. Bonushkin, V. N. Bychkov, A. P. Dergunov, Yu. V. Ershov, V. Frolov, Igor A. Golutvin, N. V. Gorbunov, Yuri A. Gornushkin, A. B. Ivanov, V. D. Kalagin, A. G. Karev, V. Yu. Karzhavin, M. Yu. Kazarinov, S. V. Khabarov, V. S. Khabarov, B. A. Khomenko, N. N. Khovansky, Y. T. Kiryushin, O. N. Klimov, V. D. Kondrashov, A. V. Korytov, V. M. Kotov, Zinovi V. Krumstein, P. A. Kulinich, Vadim N. Lysiakov, A. L. Lyubin, A. V. Makhankov, V. L. Malyshev, I. M. Melnichenko, Yu. P. Merekov, S. A. Movchan, A. A. Nozdrin, A. G. Olshevski, V. V. Perelygin, V. D. Peshekhonov, Yu. P. Petukhov, D. Pose, T. Predo, V. P. Rashevsky, Yu. V. Sedykh, S. Y. Selyunin, S. V. Sergeev, L. M. Smirnov, D. A. Smolin, L. G. Tkachev, V. V. Tokmenin, L. S. Vertogradov, Y. B. Viktorov, A. V. Vishnevsky, V. S. Yamburenko, V. E. Zhiltsov

Kurchatov Institute of Atomic Energy : Spartak T. Belyaev, Yu. Dubovik, S. L. Fokin, M. S. Ippolitov, A. L. Lebedev, V. I. Manko, N. Martovetsky, George Mgebrischvili, E. Monitch, A. S. Nianine, R. I. Scherbachev, A. A. Vasiliev, Maxim A. Vasiliev

Lebedev Physical Institute : A. Chikanian, A. Shmeleva, V. Tikhomirov

Moscow Engineering Physics Institute : A. Medvedev, M. Potekhin, V. Staroseltsev, Alexei Sumarokov, V. Tcherniatin, Alexandre Vanyashin, S. Voloshin

Moscow State University : Anatoli A. Arodzero, George L. Bashindzhagyan, Pavel Ermolov, Yuri V. Fisyak, Dmitri Karmanov, Viktor Kramarenko, Eugene Kuznetsov, Alexandre N. Larichev, A. Leflat, Michael M. Merkin, E. K. Shabalina, N. B. Sinev, Natalia A. Sotnikova, Alexandre G. Voronin, Valery Yu. Zhukov, Sergei A. Zotkin

St. Petersburg Nuclear Physics Institute : V. M. Andreev, V. Astashin, N. Bondar, A. Denisov, A. Golyash, V. T. Gratchev, M. Guriev, N. Isaev, M. Ishmukhametov, V. Ivochkin, S. Kalentarova, O. Kiselev, A. G. Krivshich, L. Lapina, P. Levtchenko, V. Maleev, M. Nesvizhevskaya, S. Patrichev, Yu. Platonov, O. E. Prokofiev, V. Razmislovich, N. Sagidova, Vladimir M. Samsonov, V. V. Sarantsev, A. Schetkovski,

V. Scorobogatov, D. M. Seliverstov, A. Sergeev, V. Sknar, A. Smirnov, Edouard M. Spiridenkov, V. M. Suvorov, I. Tkatch, G. Velichko, S. Volkov, Yu. Volkov, Alexei A. Vorobyov, Yu. Zhelamkov, O. L. Fedin

TAIWAN

Institute of Physics, Academia Sinica : Jaroslav Antos, Hsiao-Ying Chao, Yen-Chu Chen, Mao-Tung Cheng, C. N. Chiou, T. L. Chu, C. L. Ho, Melin Huang, Shih-Chang Lee, Ping-Kun Teng, Ming-Jer Wang, P. Yeh

UNITED STATES of AMERICA

Adelphi University : W. C. Lefmann, Robert V. Steiner

Boston University : Steven P. Ahlen, Ed Booth, Robert Carey, Steve Dye, Mitchell Golden, Eric Hazen, Dan Higby, Anthony S. Johnson, Kenneth D. Lane, Alex Marin, James P. Miller, David Osborne, B. Lee Roberts, James T. Shank, Elizabeth H. Simmons, James L. Stone, Lawrence R. Sulak, Gary Varner, David Warner, Scott Whitaker, William A. Worstell, Bing Zhou

Brookhaven National Laboratory : Maged S. Atiya, Steven Bellavia, I-Hung Chiang, M. Citterio, Bruce Gibbard, Howard Gordon, John S. Haggerty, Stephen Kahn, Hobart W. Kraner, David Lissauer, Laurence S. Littenberg, Hong Ma, Donald Makowiecki, Sean R. McCorkle, Michael J. Murtagh, Paul O'Connor, Venetios A. Polychronakos, Serban Protopopescu, Veljko Radeka, David C. Rahm, Sergio Rescia, Lee Rogers, Nicholas P. Samios, John Sondericker, D. Stephani, Iuliu Stumer, Helio Takai, Michael J. Tannenbaum, S. Peter Yamin, Bo Yu

Brown University : Mildred Widgoff

California Institute of Technology : Barry C. Barish, Daniel Burke, Giorgio Gratta, David Kirkby, Gary Liu, Wenwen Lu, Da An Ma, Richard Mount, Steve Mrenna, Harvey B. Newman, Xiaorong Shi, Hiroaki Yamamoto, Ren-yuan Zhu

Carnegie Mellon University : Richard M. Edelstein, Arnold Engler, Tom Ferguson, Robert W. Kraemer, Douglas Potter, Michael Procario, James R. Russ, R. B. Sutton, Helmut Vogel

Columbia University : Elena Aprile, Yin Au, Aleksey E. Bolotnikov, Tim Bolton, Allen C. Caldwell, D. Chen, Herbert Robert Cunitz, J. Dodd, Alan Gara, Y. Ho, Wonyong Lee, Eric J. Mannel, M. Moulsen, R. Mukherjee, John Parsons, Peter C. Rowson, Michael Seman, Michael Shaevitz, Frederick W. Sippach, E. Stern, William Willis, L. Zhang

Draper Laboratory : Howard Baker, E. C. Berk, M. J. Furey, Dick Gustavson, M. Hansberry, T. P. Hinds, Tom W. Lee, Frank Nimblett, Joe Paradiso, Peter Sebelius, Ed Womble

Drexel University : Charles Lane

Fairfield University : David R. Winn

Indiana University : Ethan D. Alyea, Chuck Bower, Mark Gebhard, Richard M. Heinz, Stuart Mufson, James Musser, James Pitts

Jackson State University : F. Lott, Huazhong Zhang

Lawrence Livermore National Laboratory : Elden Ables, O. Alford, Frederick Curt Belser, Jack Berkey, Richard M. Bionta, Joel M. Bowers, D. Bupp, Anthony K. Chargin, Otis Clamp, J. Clements, Gary A. Deis, Orrin D. Fackler, Don Garner, Max Haro, J. R. Heim, Fred Holdener, John Horvath, W. Hsu, Coleman V. Johnson III, Norm Lau, Daniel M. Makowiecki, R. Martin, G. Joseph Mauger, Kerry Miller, T. Moore, D. Ng, Gene Oberst, Harlan Olson, Lawrence (Buzz) Pedrotti, R. Pico, Steve Pratuch, K. M. Skulina, J. Swan, Karl A. Van Bibber, Richard Warren, Torre J. Wenaus, Carl Williams, Jeff Williams, V. Williamson, Sarah Wineman, Winston Wong, D. Wright, Craig R. Wuest, Robert Yamamoto, Ted Yokota

Los Alamos National Laboratory : Ron Barber, Jan G. Boissevain, Melynda L. Brooks, Maureen Cafferty, Brad Cooke, K. R. Fuller, Sangkoo F. Hahn, J. E. Hinckley, C. S. Johnson, Jon S. Kapustinsky, W. Wayne Kinnison, David M. Lee, Richard A. Martin, Geoffrey B. Mills, D. I. Montoya, R. E. Prael, Gary H. Sanders, Brian G. Smith, R. L. Smith, Walter E. Sondheim, R. Robert Stevens, Tim Thompson, J. R. VanAnne, L. S. Waters, Bernie Weinstein

Louisiana State University : Richard Imlay, Hong Joo Kim, Christopher Lyndon, Roger McNeil, William Metcalf

Martin Marietta Astronautics, Y-12 Oak Ridge Laboratory : J. Bohanon, B. Bowden, V. Galyon, J. Gertsen, J. Heck, N. Howell, J. King, S. Robinson, J. Rollins

Martin Marietta Astronautics Group : T. Adams, Kim Barnstable, J. Coulon, Nicholas Joseph DiGiacomo, Brian Easom, R. Humphreys, Lyle Mason, Greg Velasquez

Massachusetts Institute of Technology : Philip Burrows, Wit Busza, Richard T. Camille Jr., Y. H. Chang, M. Chaniotakis, G. H. East, Jun Feng, Jerome I. Friedman, Elizabeth D. Hafen, Padmanabh Haridas, J. Kelsey, Henry Kendall, Peter Marston, Joseph V. Minervini, D. B. Montgomery, R. L. Myatt, Louis S. Osborne, Z. Piek, I.R.D. (Bob) Pillsbury Jr., Jaroslaw W. Pisera, Irwin A. Pless, Shahin Pourahimi, Lawrence Rosenson, Bradford Smith, Paraskevas Sphicas, James D. Sullivan, K. Sumorok, Frank E. Taylor, Robin Verdier, Rui F. Vieira, Bernard Wadsworth, E. Wyslovch

Memphis State University : D. R. Franceschetti, S. Jahan, D. W. Jones

Michigan State University : Maris A. Abolins, R. Brock, Carl Bromberg, J. Huston, J. Linnemann, Robert J. Miller, B. Pope, H. Weerts

Northwestern University : David Buchholz, Bruno Gobbi

Oak Ridge National Laboratory : Martin L. Bauer, H. R. Brashear, Charles A. Britton Jr., Steve Chae, L. G. Clonts, Hans O. Cohn, E. F. Kennedy, Frank Plasil, Ken Read, Mark J. Rennich, M. L. Simpson, Richard A. Todd, A. L. Wintenberg, C. C. Wynn, Kathy Young

Princeton University : Peter P. Denes, Mark M. Ito, Daniel R. Marlow, Eric Prebys, Robert Wixted

Rutgers University : Pieter Jacques, Mohan S. Kalelkar, Richard R. Plano, Peter Stamer

Southern Methodist University : Fredrick Olness, Tomasz Skwarnicki, Ryszard Stroynowski, Vigdor Teplitz

State University of New York at Albany : Mohammad Saj Alam, Ick-Joh Kim, Z. C. Ling, Bijan Nemati, John O'Neill, Horst Severini, Chih-Ree Sun

State University of New York at Stony Brook : Roderich J. Engelmann, Chang Kee Jung, Michael D. Marx, Robert L. McCarthy, Mohammad M. Mohammadi, Michael Rijsenbeek, Amir H. Sanjari, Chiaki Yanagisawa

Superconducting Super Collider Laboratory : Neil Baggett, Mark Bowden, Gerry Chapman, Zukun Chen, Laird R. Cormell, Dario Crosetto, Nasser Danesh, Peter Dingus, Milind Diwan, Howard Fenker, Kenneth Freeman, Michael Gamble, Vladimir Glebov, Norm Gober, Mike Harris, John Hilgart, Vishal Kapoor, Alfred W. Maschke, Kenneth W. McFarlane, Rainer Meinke, Cas Milner, Gena Mitselmakher, Nikolai Mokhov, Kate Morgan, Paul Padley, Frank E. Paige, Brett Parker, Lynn Parlier, Paul Reardon, Lee Alan Roberts, Emile Sabin, Brian L. Scipioni, Irwin Sheer, Rickey L. Shypit, Rayappu Soundranayagam, Francois Stocker, Kent Swarts, Jennifer Thomas, Henk A. J. R. Uijterwaal, Bill Wisniewski, John Womersley, Ronn Woolley, Gary B. Word, Jin Chu Wu, George P. Yost, Ewald Zimmer-Nixdorf

Syracuse University : Geoffrey C. Fox, W. Furmanski, T. Haupt

Texas A&M University : C. Gagliardi, G. Glass, Younan Lu, R. Tribble, Robert C. Webb

University of Arizona : Geoffrey E. Forden, Kenneth A. Johns, John P. Rutherfoord, Leif Shaver, Michael A. Shupe, Joel Steinberg, Christian Zeitnitz

University of California, San Diego : James G. Branson, W. Brower, Hans E. G. Kobrak, R. Masek, Hans Peter Paar, Michael Sivertz, Robert A. Swanson

University of Colorado : Bruce Broomer, Mark Christopher, Eric Erdos, Uriel Nauenberg, Gerhard Schultz

University of Houston : Kwong Lau, Bill W. Mayes, Lawrence Pinsky, J. Pyrlik, Roy Weinstein

University of Iowa : Nural Akchurin, D. Kadrmas, Jerry Langland, Edward R. McCliment, Y. Meurice, Charles Newsome, F. Olchowski, Yasar Onel, M. Halsie Reno, Vincent Rodgers

University of Michigan : Shawn McKee, Scott Nutter, Gregory Tarle

University of Mississippi : K. Bhatt, L. N. Bolen, M. L. Booke, Lucien M. Cremaldi, K. Hendrix, Brent Moore, James J. Reidy, J. R. Weinstein

University of Oregon : James E. Brau, Raymond E. Frey, Koichiro Furuno, D. Gao, R. Kollipara, David M. Strom, X. Yang

University of Pittsburgh : Wilfred E. Cleland, Mark J. Clemen, Eugene Engels Jr., J. Rabel, P. Shepard, V. J. Sonnadara

University of Rochester : James Dunlea, George Fanourakis, Thomas Ferbel, George Ginther, Frederick Lobkowicz, Paul Slattery, Marek Zielinski

University of South Carolina : Carl Rosenfeld, Jeffrey R. Wilson

University of Tennessee : Steve Berridge, William M. Bugg, Y. C. (Peter) Du, R. Kroeger, A. Weidemann

University of Texas at Austin : Charles C. Allen, Gerald W. Hoffmann, Karol Lang, M. R. Marcin, Jack L. Ritchie

University of Washington : Toby Burnett, Victor Cook, D. Forbush, J. Franklin, Paul M. Mockett, J. Rothberg, F. Toeus, S. Wasserbaech

University of Wisconsin : J. Pfotenhauer

Vanderbilt University : Robert Panvini, T. W. Reeves, S. Rousakov, John Paul Venuti

Vassar College : Cindy Schwarz

Yale University : Robert K. Adair, Charles Baltay, Basem Barakat, Ram Ben-David, W. Emmet, Henry Kasha, Steven Laurens Manly, D. Pilon, Sumit Sen, John Sinnott, E. Wolin

York College CUNY : Samuel R. Borenstein

Editors' Note

This document was almost entirely produced via electronic means. The only exceptions are two figures in chapter 4 and most of chapter 5.

The individual TEX (.tex) and postscript (.ps) files that were used to produce most of this document may be found on sscux1.ssc.gov in the area: /usr/ssc/gem/doc/technotes/GEM-TN-93-473. Except for the two noted exceptions, the postscript file rdt.ps includes the entire document, including the figures.

Most of the figures are available separately, both as postscript files (.ps files) and in whatever format was used to create the postscript files, such as FrameMaker (.fm) or Canvas (.canvas).

The Microsoft Word file containing the text of chapter 5 can be found in the "5_tracker" sub-directory as file "tracker.msw."

Additionally, these files can be obtained via anonymous ftp from "sscux1.ssc.gov" in the directory "gem/doc/technotes/GEM-TN-93-473."

October 28, 1993

H. Newman
H. Uijterwaal
G. Word

Contents

List of Tables

List of Figures

Chapter 1

Overview

The Gamma, Electron Muon (GEM) collaboration was formed in June 1991 to develop a major detector for the Superconducting Super Collider (SSC). When installed at the SSC, the GEM detector will be used to study high transverse-momentum physics, such as searching for the Higgs boson, and to search for new physics beyond the standard model.

This R&D and Test document (the "RDT") sets forth the plans of GEM for Research and Development of its detector systems over the next three years. An important part of this work is focused on a beam test at FNAL. We are following as far as practical a plan to produce final engineering prototypes for this test. According to our present schedule, we can use the results of these tests not only to verify our predictions of the performance of the detector systems under realistic conditions, but also to fine-tune the design to meet performance goals or to reduce costs in the production phase.

Since most of the R&D issues must be solved in order to produce the final modules which we will test in the beam, a major part of the R&D is described here under the heading of preparation for the beam test. There are, of course, some items which are not of this character which must go on in parallel. An example is studies of the effects of radiation damage and their mitigation, which will not be encountered in the beam test, but must be understood on the same time scale, to feed back into the final detector construction.

The scope of the beam tests has been studied extensively. It is important to select a configuration which provides the full scale of detector modules, in the sense that crucial phenomena which might not appear in small units can be confidently understood. It is also vital to provide a setup which allows the evaluation of detector response with a known incoming beam, particularly in cases where our ability to simulate the physics of the detector response is in some doubt. This calibration information will be very valuable in analyzing the physics data from the final detector. On the other hand, considerations of schedule as well as resources motivate us to restrain the size of what is certainly a major fixed target experiment in any case.

For example, we have determined that the added costs of producing a "sector" of GEM which is a faithful replica of a portion of the final detector, with an accurate reproduction of the radial spacing between the elements of different detector systems, is substantially higher than that of a more loosely integrated assembly of detectors. No important issues were identified which required the full sector configuration, and we are following the less

expensive approach.

Many of the comments we received in the report of the PAC review of the GEM Technical Design Report[1] suggested that the beam test at FNAL we will carry out starting in 1995 be used to verify particular features of our detectors. We are in agreement with these suggestions and this RDT sets forth exactly how we propose to follow these recommendations. At the time of the review, the schedule did not allow much time for feedback into the production of final modules, except in the case of serious faults. As noted above, we will now have sufficient time to take full advantage of the results of these tests.

The results we seek are of two sorts. One is to verify that the technical performance of the detector systems is in accordance with our design. An example would be the confirmation of the alignment accuracy in the tracking systems, or the level of noise in the precision electronics chains. The second kind of result is an extension of our ability to simulate the physical conditions of the detectors. An example is the simulation of hadrons jets in the calorimeter. It is important to be able to simulate jet response at a fundamental level, by including all the physical processes in sufficient detail to achieve the desired accuracy. This is particularly necessary because the range of particle energies at the SSC considerably exceeds that available in any test beam, and also because it is not adequate to try to measure directly non-uniform aspects in the detector such as the transition regions between the barrel and the end cap by direct measurement in a beam. A deeper understanding is required, and the way to achieve this has been shown in the case of electromagnetic showers, where after many years of effort, a very accurate simulation of the showers has been achieved and verified in experimental measurements.

We plan to reach the required accuracy in the case of hadrons by a similar approach, that is, an accuracy of about one per cent, substantially worse than that achieved for the electromagnetic showers. A parallel effort is being mounted on the simulation and on the acquisition of data for verification. We required precise data for the calorimeter configurations which exemplify the range of conditions we encounter in the GEM experiment. We will include the different varieties of detector modules present in the experiment, in the final form. We also include the cracks and other non-uniform aspects in configurations typical of the experiment. These are the places where we depend most crucially on the simulations. We do not attempt to measure each different projective view of the cracks, for example, since that would be long and expensive, and we will have quite a sufficient range of data to allow us to establish the accuracy of our simulations. Since this work involves an improvement in the present understanding of this kind of simulation at a scientific level, we feel that our program is indeed a scientific experiment rather than just a technical proof of performance.

Similar comments apply to the investigation of the accuracy in our tracking systems under conditions of high rates and realistic environmental conditions. In the case of the electromagnetic calorimetry, the maintenance of the channel-to-channel accuracy is one of the important elements in obtaining the good energy resolution at high energies. An important feature of our beam test is the investigation of the factors which must be controlled in order to achieve this, over large area and a range of angles. There is not much experience at the sub-percent level which we must maintain, and the results of our experiment will have interest beyond the SSC experiments.

The electronics R&D program cannot be entirely paced by the beam test, because of

the long lead time and large costs of monolithic circuit development. We do need to use in the beam test final versions of the electronics which is intimately involved in the performance characteristics of the detector systems, such as the front-end electronics and the wide dynamic range readout of the calorimeters.

The data acquisition presents special circumstances, since it is largely based on the very rapidly developing field of industrially available wide bandwidth networks. The systems which will finally be used are not yet available. For this reason, and because the data rate requirements of the beam tests are so far below those in GEM, this test is not an appropriate venue for a full scale test of the GEM data acquisition system. Certain aspects of our design, on the other hand, should be demonstrated in the R&D program before the design for the final system is frozen.

We are fortunate to have available an experimental area for our beam test which is uniquely suitable for our purposes, with cryogenics facilities, beam characterization, magnets for chamber tests and the like. We are trying to remake the area to fit our needs in the most economical manner possible, and our studies of the scope and configuration of the tests have made every effort to adapt our needs to the area with fewest new expenses.

Some areas of R&D are unrelated to the beam test because they involve features of the GEM environment which are far removed from the conditions in the test beam. We have mentioned the data acquisition, and another example is the studies of radiation damage, which can best be pursued with exposures to well-characterized sources of radiation, photons and neutrons. Similarly, the measurements of ion loading in the calorimeters requires a dedicated set up where the radiation level can be adjusted over a wide range and precisely calibrated. The optimization of the optics of the scintillator-fiber readout system is another example where is the main thrust of the R&D program is outside the test beam setup. These other functional measurements have been carefully integrated into the whole program.

Chapter 2

GEM Sector Test

2.1 Overview

2.1.1 Introduction

The highest energy beams in the world are those available at Fermilab, making this laboratory the most desirable location at which to test and calibrate the components of the GEM detector. GEM proposes to mount a comprehensive test beam program in the Meson West (MWEST) area at Fermilab. This is an ideal location from GEM's perspective. The MWEST experimental hall is adequately large (200×63 ft^2), and is spanned by a 25 ton crane with a hook height of approximately 30 ft. There is also a spacious external control room and working area adjacent to the experimental hall, as well as several smaller internal counting houses. The area has extensive cryogenic facilities, including external LN_2 and LAr storage tanks, full ODH (oxygen deficiency hazard) protection, including an inter-connected trench and deep pit for containing a massive cryogenic spill, and an existing rail system capable of supporting a calorimeter test cryostat and its associated transporter.

There are also a large number of existing tracking chambers in the MWEST hall (including silicon strip detectors, multiwire proportional chambers, and straw tube drift chambers), plus associated readout electronics, that could be reconfigured for test beam use, as well as a large aperture (50×36 in^2) analysis magnet which could be employed for testing components of the GEM central tracker and muon tracker in a 0.8 T magnetic field. The existing MWEST beam is capable of transporting particles of either polarity, up to and including 800 GeV primary protons. The beam transport includes sufficient bending (incorporating two bends of 4.8 mr and 2.4 mr, respectively) that momentum tagging to a fractional precision of 0.2% is possible using existing strip detectors and electronics. The beamline is also equipped with a Čerenkov counter capable of tagging electrons up to $\sim$ 150 GeV.

A schematic layout of the MWEST hall as configured for GEM is shown in figure 2.1. As indicated in the figure, each of the detector subsystems – the calorimeter, the central tracker, and the muon tracker – is to be provided with its own dedicated area. Each subsystem will require its own mechanism for orienting itself relative to its individual simulated intersection point, independent of the orientation of the other subsystems. The types of tests to be performed on each detector subsystem are summarized below. In addition, other GEM

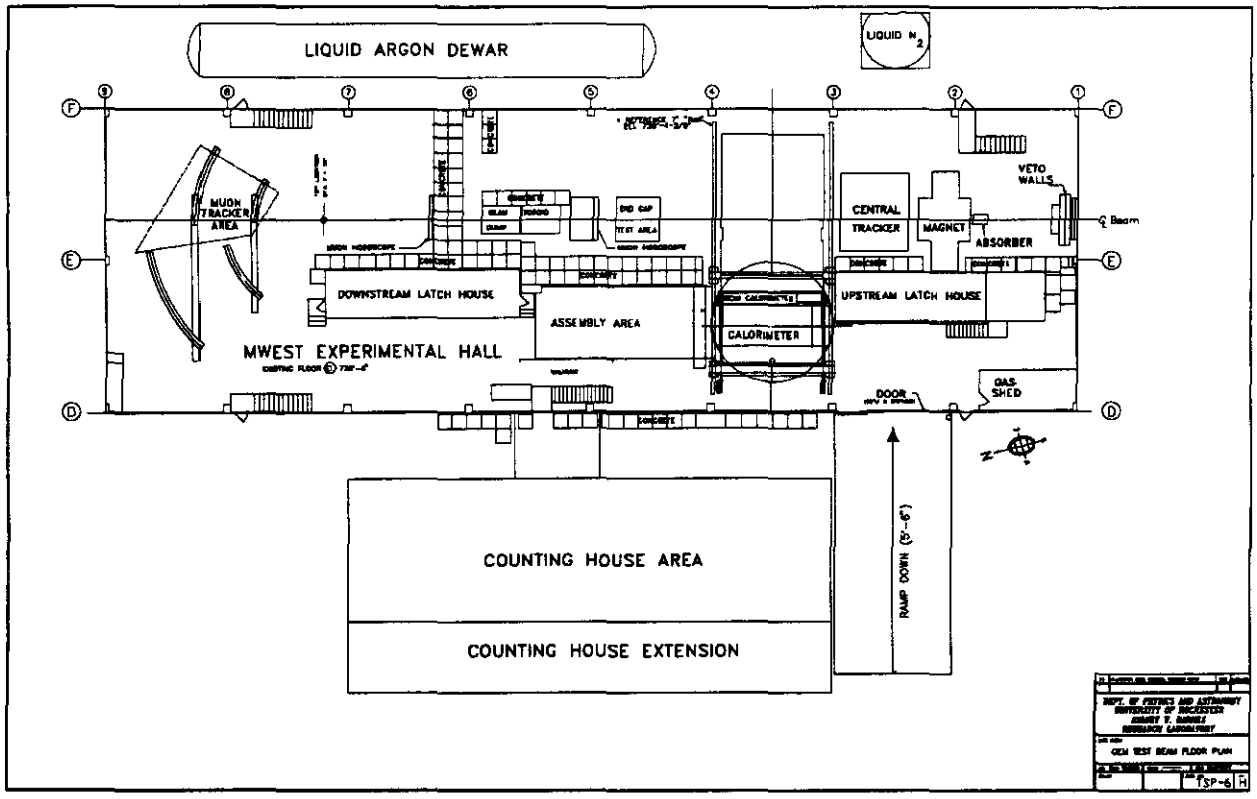

Figure 2.1: Schematic layout of the MWEST hall.

systems – data acquisition, slow controls, on-line and off-line computing – will be developed in an evolutionary manner through the MWEST testing program.

2.1.2 Calorimeter Testing

The primary goals of the calorimeter testing program are the following:

- Perform full-scale engineering studies of all calorimeter subsystems: mechanical, electronic and cryogenic;
- Achieve full system integration of the electromagnetic and hadronic cryogenic calorimetry, and of the external scintillating calorimetry;
- Carry out a full system test of the calorimeter readout and calibration systems;
- Measure the response of the scintillating calorimetry, and determine the reproducibility of its performance from tower to tower and from module to module;
- Study the calorimeter's energy and spatial resolution up to the highest available energies using both electrons and hadrons;

- Investigate the calorimeter's response to single particles in the vicinity of representative cracks;
- Study the calorimeter's response to single particles across the barrel to end cap transition region;
- Investigate the calorimeter's response to high energy muons.

To carry out these tests, a versatile calorimeter transporter will be constructed and mounted on the existing MWEST rail system. This transporter will provide for independent horizontal and vertical motions, as well as rotation and limited tilting capability. The test cryostat will be a double-walled, flanged stainless steel cylinder equipped with a thin upstream beam window. It will be loaded from one end using an insertion bridge.

Plans call for calorimeter testing using first LAr, and then LKr. To minimize the amount of LKr required for the second phase of testing, the cryostat will contain separate bath boxes for the barrel and end cap calorimetry. A comprehensive program of Monte Carlo simulation will provide the critical link between the test beam results and the performance of the operational GEM calorimeter.

Our strategy allows great flexibility in the mix of modules included in a given load of the test cryostat. Options include starting with only one side of the barrel hadron calorimetry, thus postponing the study of the 90° crack, or delaying the installation of some of the end cap prototypes, thus postponing full investigation of the transition region. To accommodate these options, the test cryostat and transporter are being designed to accommodate multiple loads with minimum down time. It is anticipated that MWEST beam time will be available for other GEM test beam purposes during these transition periods.

2.1.3 Central Tracker Testing

The function of the central tracker testing in MWEST is to extend and complement Interpolating Pad Chamber (IPC) testing carried out in 1992 at Indiana University and at BNL in 1993 and 1994. The primary goals to be achieved are:

- Investigate the rate capability of full size barrel and end cap IPC's using final design electronics;
- Complete IPC resolution and efficiency studies begun at BNL, incorporating new ideas and improved electronics;
- Investigate IPC performance in a 0.8 T magnetic field;
- Mount and operate a complete 18° sector of the GEM central tracker (silicon plus IPC's);
- Carry out full scale system tests of the gas circulation, cooling, and mechanical support systems;
- Investigate the position stability of the central tracker silicon system.

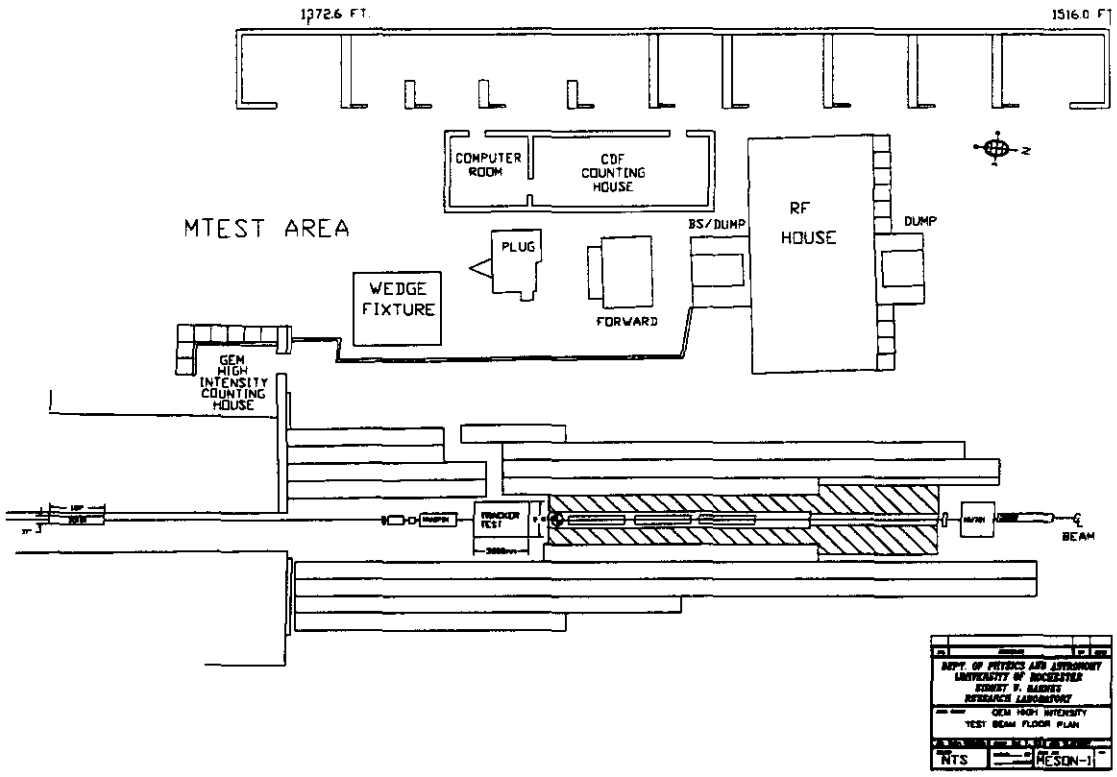

Figure 2.2: Schematic layout of the MWEST beam dump area.

The rate studies are to be carried out in a dedicated area near the MWEST primary beam dump using a setup similar to that employed for the BNL testing. A schematic layout of this area depicting the central tracker setup in place is shown in figure 2.2. The magnetic field tests are to be performed inside the MWEST analysis magnet using a special fixture designed to study Lorentz angle effects for both the central and muon tracking chambers.

2.1.4 Muon Tracker Testing

The purpose of the muon tracker testing in MWEST is to extend and complement Cathode Strip Chamber (CSC) studies carried out using the Texas Test Rig at the SSCL and other facilities. The primary goals to be achieved are:

- Test several small (30×30 cm^2) CSC chambers in a 0.8 T magnetic field;
- Study the effect of the upstream calorimetry on the performance of CSC's operating in a magnetic field;
- Mount and operate a full size sector of the barrel muon tracker.

- Carry out full scale system tests of the gas circulation and mechanical support systems;
- Investigate the large scale spatial and timing resolution of the muon tracker.

Some of the questions to be investigated in the CSC testing—studying Lorentz angle effects and measuring two track resolutions in a 0.8 T magnetic field—are identical to those of interest in the IPC studies. Of special interest to the muon studies is investigating the importance of hadron punch-through at Tevatron energies and the influence of high energy muon radiation in the calorimetry on the performance of the muon system. For these studies, the GEM calorimeter will be simulated by passive absorber mounted directly upstream of the CSC's and penetrating into the analysis magnet. The muon sector test will use high energy particles to study the operational precision achieved using a full-scale, dynamically alignable (via software) sector fixture by measuring the false sagitta induced in high energy tracks passing through a simulated intersection point.

2.2 Beam Requirements

2.2.1 Particle Identification

We plan to employ primarily negative secondary beams, which are preferable to positive secondaries because of radiation safety considerations. We also plan to take data with primary protons using pinhole collimators.

The beam line must be instrumented to reliably tag e^- and μ^-. The former tagging will be accomplished using the existing MWEST Čerenkov counter. A Monte Carlo simulation, tuned to reproduce the measured π/p discrimination of the counter at 530 GeV/c, indicates that it is capable of tagging electrons with an efficiency of 80% up to a momentum of $\sim$ 125 GeV/c, with a background due to misidentified pions of $<$ 10%. The performance of the Čerenkov counter at higher momenta is strongly dependent on the electron fraction of the beam, and schemes for enriching this fraction are being explored. A synchrotron radiation detector will be employed to tag very high energy electrons. Muon tagging will be achieved by a combination of running with the beamline collimators closed, and tagging particles that emerge from the MWEST secondary beam dump. We also intend to record randomly generated pulser triggered events to measure electronic noise during the beam spill.

2.2.2 Particle Intensity

We plan to run typically at secondary particle intensities of $10^3 - 10^4$ particles per second, and accumulate data at a rate of $\sim$ 100 events/s. Limited running at higher beam intensities to study rate dependent effects may be requested.

An exception to the above are the rate studies planned for the central tracker. These investigations require beam intensities of 10^9 s^{-1} over an area of roughly 30 cm^2. Such rates are challenging to achieve in the MWEST hall because of radiation safety considerations. A second difficulty is that a suitable "pinged" beam, which would supply the desired intensity in bursts of $\sim$ 1 ms duration, places special demands on the accelerator and would significantly

impact the rest of the Fermilab program. For these reasons, it is planned to carry out these investigations in the vicinity of the MWEST primary beam dump.

2.2.3 Momentum Tagging

The MWEST beamline will be instrumented with existing 50 μm pitch silicon strip detectors, in a configuration that is capable of tagging the momentum of incident particles to a precision of $\pm 0.2\%$. This accuracy is necessary to provide the capability of measuring the constant term in the calorimeter's energy resolution, which in the case of the electromagnetic accordion is expected to be of the order of 0.4%.

2.2.4 Beam Definition

The beam defining counters must provide both pulse height and timing resolution. The pulse height resolution should permit the rejection of events with more than one beam particle per bunch. The timing resolution must be on the order of 100 ps to enable measurement of the timing capability of the calorimeter, which is expected to be of the order of 200 ps for electron energies above 25 GeV. Fast scintillating materials and photomultipliers, such as the Hammamatsu R2083, will be required.

A beam spot size on the face of the calorimeter of 2×2 cm^2 will be defined by a suitable set of veto counters.

2.2.5 Particle Tracking

To study the position resolution of the electromagnetic calorimetry, tracking chambers capable of a spatial resolution of ~ 100 μm will be mounted directly upstream of the test cryostat at the simulated intersection point. For high energy electrons, the position resolution of the calorimeter is expected to be of the order of 200 μm.

To measure the calorimeter's angular resolution, which will be of the order of 2 mrad at high energies, a second set of tracking chambers will be mounted sufficiently far upstream of the calorimetry to establish incident angles to a precision of ± 1 mrad.

2.3 Test Beam Data Acquisition

The primary consideration influencing the design of the Fermilab data acquisition system is the requirement that the system be fully functional prior to the arrival of beam. A secondary consideration is the desirability of building in sufficient flexibility that ideas relevant to the design and implementation of the final GEM data acquisition system can be explored and developed in the course of MWEST test beam operations.

To maintain maximum compatibility with existing data acquisition systems, it is proposed to employ a two-level architecture employing VME crates at both the subsystem and master crate levels. The subsystem crates will employ consistent hardware (Motorola CPU's, VME modules, ...) and a common software system (VxWorks). The Fermilab-specific front end software is to be developed in an evolutionary manner from existing code used at BNL and

SSCL for various subsystem beam tests (calorimetry and central tracker) and cosmic ray studies (muon tracker). The master crate level will handle data collection, event building, and data distribution. Two options will be explored: A hardware switch, which will allow the investigation of some final GEM data acquisition concepts, and a backup scheme based upon the same sort of hardware and software employed at the subsystem level. The choice between these options will be made sufficiently early to avoid compromising the primary design goal of having a working data acquisition system in advance of MWEST beam operations.

2.4 Run Plan

The overall run plan for GEM's Fermilab test beam program is provided below. It assumes a 1995-96 fixed target run that starts in the middle of calendar 1995 and consists of two five month running periods separated by a one month gap. To the degree practical, the plan involves parallel rather than sequential testing of the various GEM subsystems. In general, it is anticipated that the beam requirements for the tracker tests will not conflict with the needs of the calorimetry studies. When simultaneous operation is precluded by technical constraints, such as the need for beamline access or incompatible beam demands, the response will be a combination of scheduling open access during day shifts and restricting beam-on testing to evenings and nights, and dedicated interleaved runs to provide each subsystem with the opportunity to obtain maximum feedback as the data is being acquired.

2.4.1 Central Tracker Rate Tests

These tests are to be carried out in the MWEST primary beam line upstream of the MWEST production target using essentially the same test setup as employed for the 1993 and 1994 testing at BNL. This testing is to commence at the very beginning of the 1995 half of the fixed target run. This schedule has the following advantages:

1. The test setup can be rigged into place before the start of fixed target operations so as not to interfere with establishing beam in the Meson Area. This is an important consideration since these high rate tests will require a considerable amount of rigging.

2. It will enable these tests to be carried out when induced radioactivity in this area is at a minimum, $\sim$ 3.5 years having elapsed since beam was last dumped in this vicinity. This will not only be advantageous to the installation of the test apparatus, but will also be helpful in assuring unimpeded access during the testing period.

3. This testing can commence as soon as primary beam is brought to the Meson hall, which is the first step in bringing beam to the downstream Meson experimental areas. It can be interleaved with tuning the MWEST secondary beam.

4. Since operations in the primary beam dump area will not interfere with activities in the MWEST hall, these stand-alone high rate tests can occur in parallel with the shake-down phases of these other studies, most of which will involve bringing into reliable

operation a great deal of previously untested apparatus, as well as the commissioning of new triggering and data acquisition systems.

It is estimated that the high rate central tracker studies will require approximately one month to complete, split roughly equally between beam-on checkout (beam-off checkout having been completed prior to the onset of fixed target operations) and the acquisition of data.

2.4.2 Calorimeter Sector Tests

These tests will initially involve filling the cryostat with liquid argon. The switch-over to liquid krypton will occur during the mid-run break. The mode of operation will be dedicated calorimeter runs interleaved with runs devoted to various tracking tests (see below), which in general do not place incompatible demands on the MWEST beam. This strategy will free up periods to be devoted to the analysis of the data acquired, and reflection on and reaction to the results thereby obtained.

The calorimeter tests will be organized as follows:

1. Energy Resolution Studies

   - Take e^-, π^- and μ^- at $\sim$ 10 energies from $20 - 600$ GeV, plus protons at 800 GeV.
   - Accumulate $\sim 10^5$ events at ≥ 3 calorimeter positions for each particle type, implying $\sim 10^7$ total events.
   - Accumulate $\sim 5 \times 10^5$ events in dedicated energy scans of the scintillating barrel calorimeter wedges to complement data collected in conjunction with the overall calorimeter testing program.

2. Phi and Eta Scans

   - Accumulate $\sim 10^5$ events at $\geq$4 energies for each particle type at 20 ϕ and η points for a total of $\sim 2.5 \times 10^7$ events.
   - Accumulate $\sim 10^6$ events in dedicated angular scans of the scintillating barrel calorimetry in addition to the data acquired with these wedges mounted behind the cryogenic calorimetry.

3. Pointing Studies, Shower Shape Analysis, and e/π Separation

   - Employ the same data samples used for the energy studies and the ϕ and η scans.

4. Electronics Testing

   - Employ two readout chains for one of the electron energy scans, implying $\sim 10^6$ additional events.

5. LAr and LKr Comparison

   - Repeat representative aspects (~25%) of the preceding calorimeter testing using LKr instead of LAr, implying $\sim 10^7$ additional events.

6. "Jet" Studies

   - Approximate hadron jets by studying events from a tertiary target positioned at the simulated intersection point.
   - Accumulate $\sim 10^7$ events at several different energies and ϕ and η positions.

7. Studies of Quartz Fiber Calorimetry

   - Accumulate $\sim 3.5 \times 10^6$ events in a variety of tests of this technological option for the GEM forward calorimetry.

At 100 events/s and a $\sim$ 23 s/57 s beam cycle, and assuming 25% efficiency during data taking, 10^8 events can be accumulated in 10^7s, or ~4 months.

2.4.3 Magnetic Field Studies of Prototype CSC's and IPC's

After an initial period devoted to checking out the performance of the prototype CSC's, the initial phase of the magnetic field studies will involve investigating Lorentz angle effects and measuring two track resolutions in a 0.8 T magnetic field using the existing MWEST dipole to simulate the barrel region of GEM, and a smaller magnet (rigged into the space immediately downstream of the calorimeter testing area) to simulate GEM's end cap region. These magnets will be equipped with fixtures capable of handling both CSC's and IPC's.

This phase of the MWEST magnetic field tests will not involve the insertion of any passive absorber into the beam, and will be carried out in coordination with the calorimeter tests. The testing will begin with investigating the performance of muon chamber prototypes, followed by central tracker studies. The mode of operation will involve shared use of the beam between the calorimeter studies and the tracking chamber tests, which will involve investigating two technologies (CSC's and IPC's) and the use of two test setups (for barrel and end cap simulation). Typically, the pattern will be a sequence of relatively short (1—3 days in duration) runs devoted to the tracking chambers, separated by longer periods devoted to data analysis during which calorimetry testing will take place.

2.4.4 Hadron Punch-Through and Muon Radiation Studies

The second phase of the magnetic field studies will involve investigating the importance of hadron punch-through at Tevatron energies and the influence of high energy muon radiation in the calorimetry on the performance of the muon tracker. These tests will be carried out in the MWEST dipole behind passive copper absorber installed inside the magnet aperture. This testing will take place during the final month of the first half of the 1995—96 fixed target run. There are several advantages to this schedule:

1. It is probable that additional radiation shielding will have to be installed to accommodate these tests, and this schedule minimizes the loss of beam time as the result of any necessary shielding reconfiguration(s).

2. This running will not be very useful for calorimeter testing due to the upstream absorber, and this is the period planned for the switch-over from argon to krypton.

3. By scheduling these tests after the earlier CSC testing, they can build on the knowledge gained in this earlier testing, and therefore be carried out more swiftly and efficiently, thus minimizing the interference between these tests and the other uses of the MWEST beam.

2.4.5 Central Tracker Sector Tests

The installation of the full scale sector of the GEM central tracker directly upstream of the calorimeter testing area will be completed by the end of the mid-run break. The subsequent mode of operation will be the same as that described above in section 2.4.4—shared use of the beam with dedicated subsystem running when this is more appropriate. Provision should be made for moving the central tracker unit completely out of the beam to permit some calorimeter runs to take place with a minimum amount of upstream material.

2.4.6 Muon Tracker Sector Tests

The full size sector of the GEM muon tracker will also be installed during the mid-run break into the area downstream of the MWEST beam stop. This location has two advantages:

1. This area allows for the largest motion transverse to the beam to provide maximum flexibility for these tests.

2. Access to this area during upstream testing is a distinct possibility, which would be of considerable benefit to maximizing the overall use of beam time by GEM.

The overall mode of operation will be the same as that described above for the central tracker sector tests—shared use of the beam with dedicated subsystem running when this is more appropriate. A significant flux of muons into this downstream area during upstream beam operations is anticipated. In addition, dedicated runs with an enhanced muon beam will be provided when required. Should neither of these options provide sufficient flux for some purposes, the upstream beam stop can be rigged to one side to allow for dedicated muon tracker runs using incident hadrons, there being a second beam dump buried in the ground just downstream of the MWEST hall.

Chapter 3

Calorimeters

3.1 Calorimeter Research and Development Program

The GEM Calorimeter design, as given in detail in the TDR [1], and shown schematically in Fig. 3.1 has many capabilities to be able to confront the new physics that must emerge in the energy region of the SSC. The design uses the accordion[4] concept for the electromagnetic calorimeter (EM) with krypton in the barrel and argon in the endcaps. The first section of the barrel hadronic (HAD) calorimeter also uses liquid krypton in the barrel while the entire active HAD section in the endcap uses liquid argon. A Scintillating Barrel Calorimeter (SBC) backs up the liquid calorimeter. There will also be a Forward Calorimeter (FC) in the region $\eta > 3.0$ which will use a radiation hard technique of either liquid argon filled tubes or Čerenkov Quartz Fibers (CQF).

In the barrel electromagnetic section (EM) we expect to have excellent energy resolution ($\Delta E/E = 6\%/\sqrt{E} \oplus 0.4\%$) to facilitate the detection of a narrow $H^0 \rightarrow \gamma\gamma$ or $H^0 \rightarrow ZZ^* \rightarrow e^+e^-e^+e^-$; transverse segmentation to allow the rejection of multiphoton backgrounds and to allow pointing of a photon to the vertex ($\Delta\theta/\theta = 40 > \text{mrad}/\sqrt{E} + 0.5$ mrad); longitudinal segmentation to aid in hadron rejection; excellent position resolution (4.4 mm/$\sqrt{E}$); and good timing resolution(5 GeV $\times$ ns/E).

The transverse and longitudinal segmentation of the EM barrel is shown in Fig. 3.2. These 6×6 ($\Delta\eta \times \Delta\phi = 0.16 \times 0.16$) towers also represent an EM trigger tower. The fine strips in the first EM layer match the trigger towers in ϕ while providing jet rejection and pointing in η. Fig. 3.3 shows the layout of the signal electrode to achieve this segmentation. The effect of the pointing resolution is seen in Fig. 3.4 on the width of the invariant mass of two photons coming from a possible Higgs of mass=80 GeV. The pointing ability of the calorimeter will be a benefit at standard SSC luminosity and crucial at higher luminosities as the number of vertices per event increases.

The hadronic calorimeter (HAD) will have good jet energy resolution, will aid in hadron/(e or γ) discrimination, and will be able to identify μ's. Our simulations have shown that the choice of lead for the absorber in the barrel liquid krypton calorimeter will lead to approximately the same e/π response as the copper absorber in the liquid argon endcaps. Therefore we have chosen lead for the barrel to minimize the constant term in the energy resolution. It is crucial to verify our simulation in these beam tests. Also since

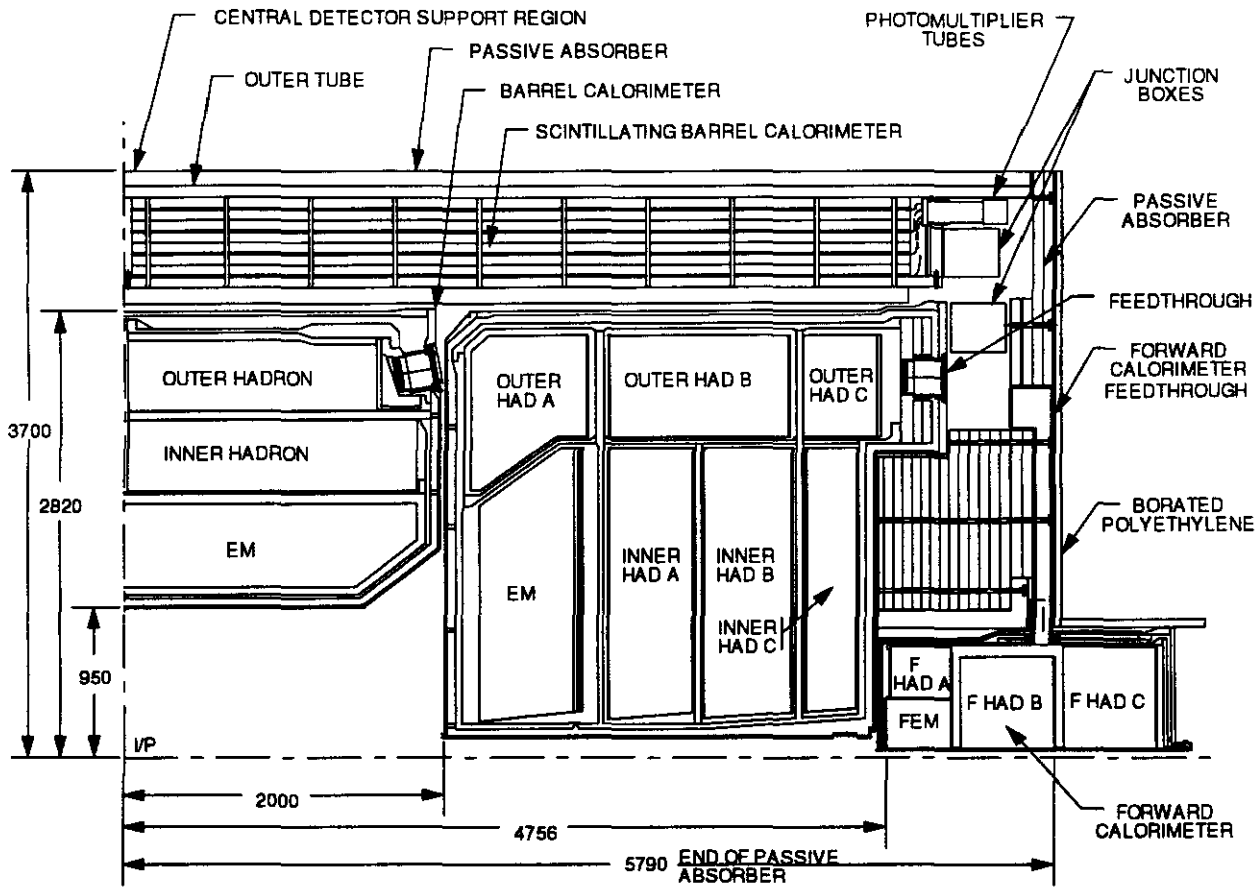

Figure 3.1: Overall layout of the GEM Calorimeter showing the Inner Barrel with LKr, the Outer Scintillating Barrel Calorimeter(SBC), the Endcap with LAr, and the Forward Calorimeter

we will probably start taking data using argon in the barrel to verify everything is working properly before changing to krypton, we can check the difference in the energy resolution between the two liquids for the barrel modules. In fact we may be able to use both liquids for the copper absorber endcap modules if this proves useful.

In the concept of calorimeter system developed in GEM TDR [1], the barrel noble liquid calorimeter is followed by SBC modules. The purpose of SBC is to extend the instrumented absorption thickness of GEM calorimeter and improve hadronic jet and missing E_T resolution by measurement of the tails of late developing showers. The role of SBC becomes significant for the detection of events with high transverse energy jets (5–10 TeV). The detection system of SBC will be also capable of distinguishing minimum ionizing particles above the level of noise and neutron background with resolution time of ~ 3 ns.

Three technologies for the forward calorimeter have been pursued by groups within the GEM collaboration. These are 1) liquid argon sampling calorimetry, 2) liquid scintillator spaghetti calorimetry, and 3) Čerenkov quartz fiber spaghetti calorimetry. In August of 1993 the proponents of the liquid scintillator technology decided to drop this option.

The GEM collaboration has set March of 1994 as the date for a technology decision

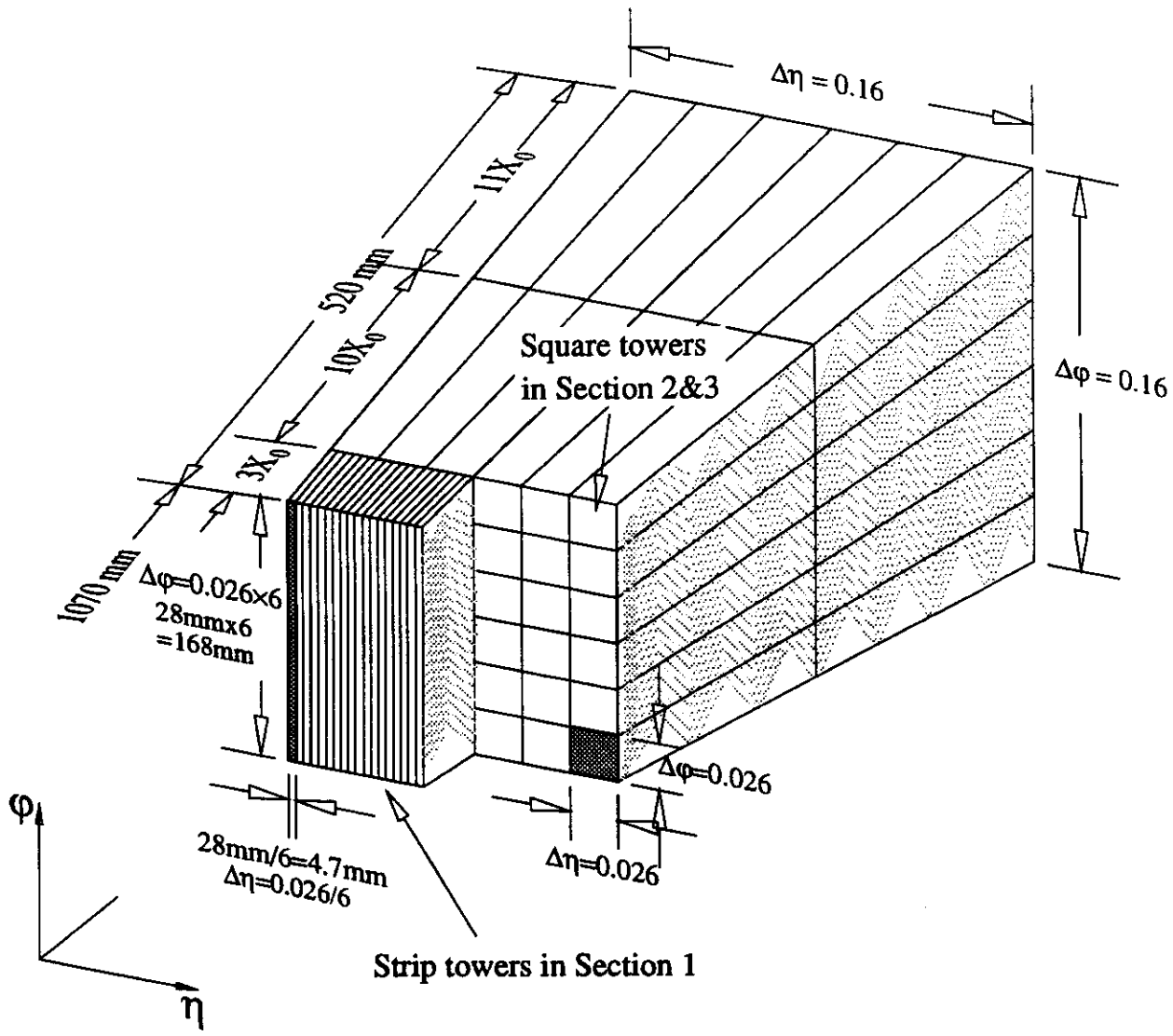

Figure 3.2: Transverse and longitudinal segmentation of the Inner Barrel EM Calorimeter

on forward calorimetry. Representatives for the liquid argon and quartz fiber options will prepare documents summarizing the features of their technology. The executive committee will appoint a panel to review these documents, to hear oral presentations on the merits and problems, and to recommend the preferred technology to the GEM management.

3.1.1 R&D and Engineering Progress as of October, 1993

3.1.1.1 EM

The EM section consists of corrugated absorbers and readout planes stacked in an accordion-like design. The EM barrel calorimeter is segmented longitudinally and transversely (see figure 3.2 and 3.3). In the longitudinal direction the module is segmented into three floors which are subdivided differently in the transverse direction. The third and second floors are

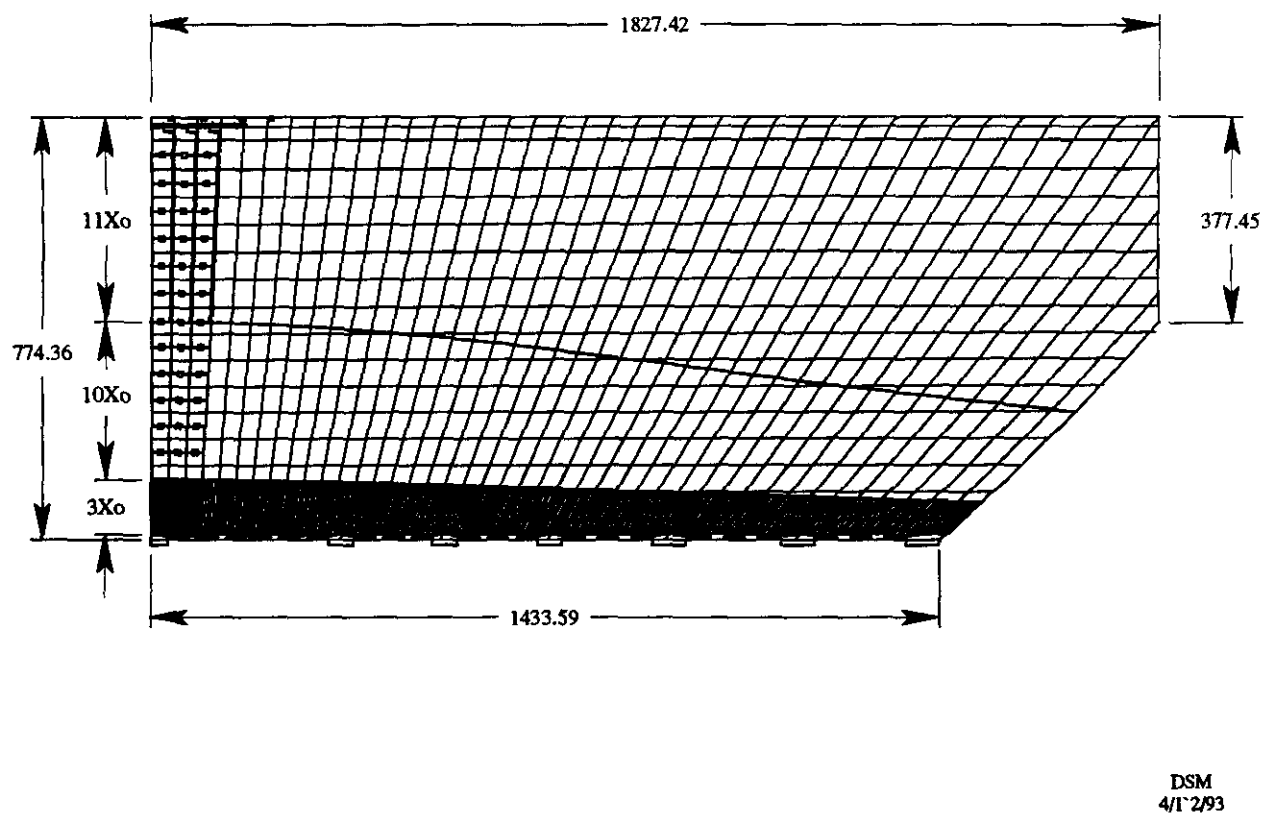

Figure 3.3: Layout of the signal electrode for half of the Inner Barrel EM Calorimeter

segmented as square towers. The first floor, however, is segmented in narrow strips (its main purpose is to aid in the π^0 rejection). The number of strip and square towers is the same in Fig. 3.2 by construction.

Substantial progress has been made on the GEM design. In the summer of 1992 a test was performed at the BNL AGS to study the properties of an accordion calorimeter with 1.3 mm lead plates clad in 0.2 mm of stainless steel (the GEM design will use 1.0 mm lead in the barrel) with krypton. The energy resolution with electrons was measured up to 20 GeV:

$$\frac{\Delta E}{E} = (0.00 \pm 0.2)\% \oplus \frac{(6.72 \pm 0.04)\%}{\sqrt{E}} \oplus \frac{0.08\ GeV}{E}\ [5].$$

Also the timing resolution for a single sample was measured:

$$\sigma_t = (0.19 \pm 0.01) ns \oplus \frac{(4.15 \pm 0.06) GeV \cdot ns}{E}\ [3].$$

Thus for a 20 GeV electron, a timing resolution of 280 ± 30 ps was obtained which was dominated by the scintillator timing resolution of 180 ps. Also very similar results were

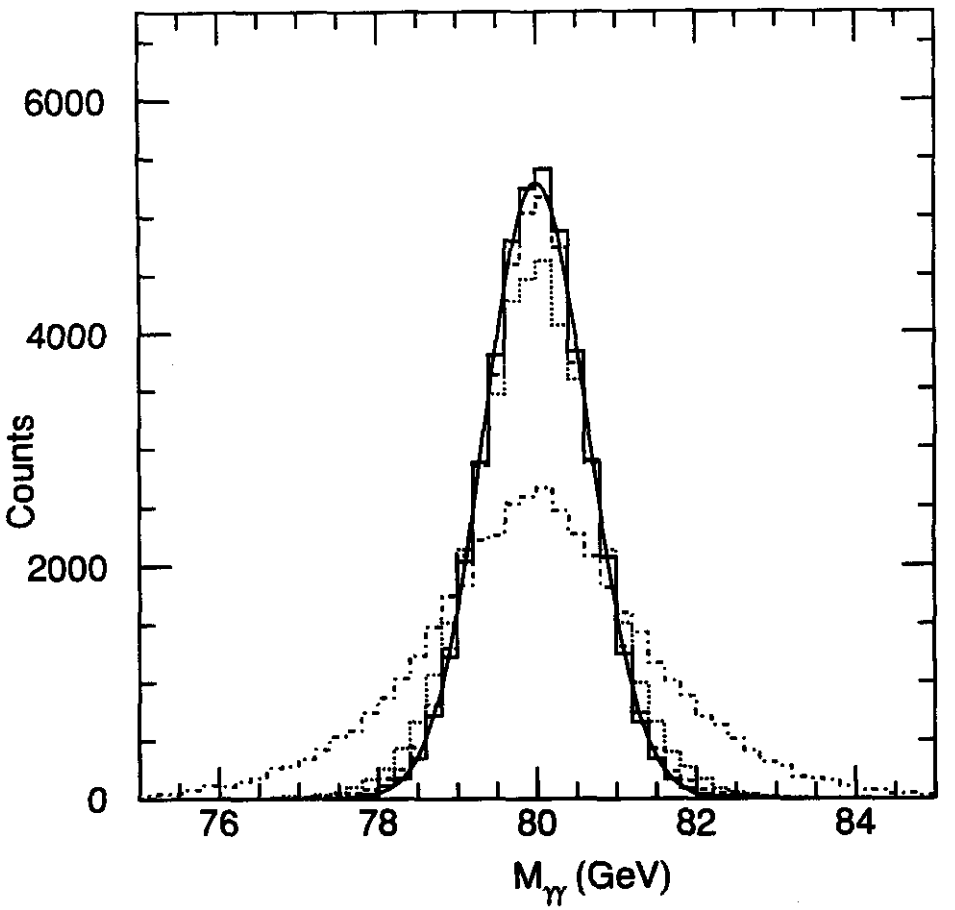

Figure 3.4: Invariant mass of two photons from H^0 with mass of 80 GeV. Solid histogram and fitted line are with all resolution and expected noise at standard luminosity $\sigma = 0.65$ GeV). The dashed histogram puts in the uncertainty of the vertex as determined using the pointing resolution to find the most probable Higgs vertex, out of all the vertices reconstructed by the tracker $\sigma = 0.69$ GeV). The dotted histogram used only the angular resolution of the calorimeter to determine the vertex $\sigma = 0.79$ GeV). The dot-dash histogram is obtained when no vertex information is used $\sigma = 1.48$ GeV).

obtained by digitizing the shaped signals every 18 ns, thus simulating the mode of data acquisition system likely to be employed at the SSC [6]. Clearly we intend to build on this experience in the Fermilab Beam Test Program described in the section 3.2 which will allow the test of real GEM EM modules with electrons with energies up to 600 GeV. The higher energy will allow a direct measurement of the constant term since the sampling term will be negligible there.

There has also been substantial progress in the engineering design of the GEM calorime-

ter. Much of this was documented at the time of the TDR in several GEM Technical notes. Now we have a detailed description of the geometry of the entire calorimeter, including the cryostats. The signal electrodes for the barrel EM have progressed to an almost final design, see Fig. 3.3.

A small but automated bending machine to produce non-projective accordion plates was designed, built and operated successfully at Brookhaven National Laboratory. The absorber plates produced are the same size as used in last summer's test. There were several reasons for the construction of this machine as follows:

1. To demonstrate unique concepts for the full size bending machine:
   (a) Semi-automatic die return and alignment system
   (b) Insulated Die tips to preclude time consuming die heating and cooling
   (c) Integrated End Die/Clamping scheme
   (d) Hydraulic cylinders for load application
2. To determine and measure various engineering parameters:
   (a) Assessment of free-machining, heat treated die material
   (b) Friction and load capacity of pestle-type roller cars
   (c) Deflection of dies and structure
   (d) Load requirements for the 1.56 mm thick absorber plate prior to molding
3. To replace the CERN-RD3 supplied manually operated machine for any future R&D on absorber plate production.

The machine was completed at the end of May and proved to be a complete success. All of the above mentioned unique design concepts met or exceeded expectations. Several absorber plates have been bent using the machine. From the pre-heating oven, plates were placed into the machine, bent and removed in less than 3 minutes. There were no signs of cooling of the pre-preg at the die tips, and the plates cooled quickly once in contact with the die surfaces, allowing timely removal. All bends occurred at once, eliminating the need to reheat and bend the ends, as was required for the RD3 supplied machine.

At a load of 50 tons (equivalent to 400 tons on the full size bending machine), the plates fit well in the mold. Loads of 40 and 30 tons (320 and 240 tons respectively for the full size machine) yielded accordion plates which fit the mold loosely, but which would be acceptable since the mold gives the final shape.

The rollers, structure, and all other mechanisms survived all load conditions without failure. Measurements of structural deflection in several key locations indicated acceptable results which are directly applicable to the full size machine. (Though reduced in length, this small machine was designed to have exactly the same load per die, roller, and traveler beam as the full size machine).

Testing on the small machine will continue and also be used to produce non-projective plates for thermal deflection testing of absorber and signal electrode accordion plates.

The details of the signal cables and feedthroughs have made a great amount of progress in the last few months. These aspects of the calorimeter need a long lead time and are extremely important. We have been working with cable vendors to meet the demanding specifications for both inside and outside the calorimeter. We have developed a concept for the feedthroughs which seems both conservative and compact. We will be placing orders for feedthrough prototypes very soon which will match the signal cables that have been identified.

We have also been working on a new cooling system for the cryostats which pumps the liquid in a closed loop outside the cryostat for direct cooling. This should eliminate the need for numerous additional penetrations in the cryostat for a separate tubes inside the cryostat for cooling.

3.1.1.2 Barrel HAD

The GEM barrel hadronic modules provide a total of 4.7 λ at 90°; of this 4.3 λ is active volume, while the rest is consumed by supports, electronics motherboards, cables etc. A more detailed discussion is available in [13]; here we present only a summary of the design.

A hadronic tower is $\Delta\eta \times \Delta\phi = 0.07854 \times 0.07854$; thus each hadronic tower overlaps nine towers in the EM calorimeter. Mechanically there are two separate layers in depth, each one consisting of individual modules which cover 0.1570 rad = 9°, and extend from the center support washer to one end in z. The modules in the second hadronic layer are rotated by 4.5° in relative to the modules in the first layer; thus any particle going through the crack between modules in the first layer impinges onto the center of a module in the second layer.

We want the modules for the testbeam to be as identical as possible to the planned production units for the real GEM barrel calorimeter. The central washer in the barrel cryostat divides the hadronic calorimetry into two halves, one for positive η and one for negative η. Our testbeam modules will be built the same way, with a simulated central washer between the two halves of the barrel.

However, it is neither possible nor desirable to cover a region in ϕ larger than necessary for complete shower containment. Thus while there are 80 modules in each layer of the final GEM detector, the testbeam program requires only eight inner hadronic modules and six outer hadronic modules. Electrically there are three (four) layers in depth, as discussed below. An end view of one module from each layer is shown in Fig. 3.5 and the side view is in Fig. 3.6.

3.1.1.2.1 The electrostatic transformer arrangement; unit cell: The noise/signal ratio in a ionization calorimeter is proportional to the electrostatic capacitance of such a detector. The noise can be reduced by transforming the impedance of the detector before the amplifier input. Since our calorimeter is inside the magnetic field of the GEM superconducting coil, one cannot use a conventional magnetic transformer. Instead we use the electrostatic transformer principle, where several readout gaps are in in series for readout purposes, rather than setting all ionization gaps in parallel as one would do otherwise. This arrangement increases the effect of the cross capacitance between neighboring channels, and this effect is proportional to the absorber thickness in each gap. An optimum transformer

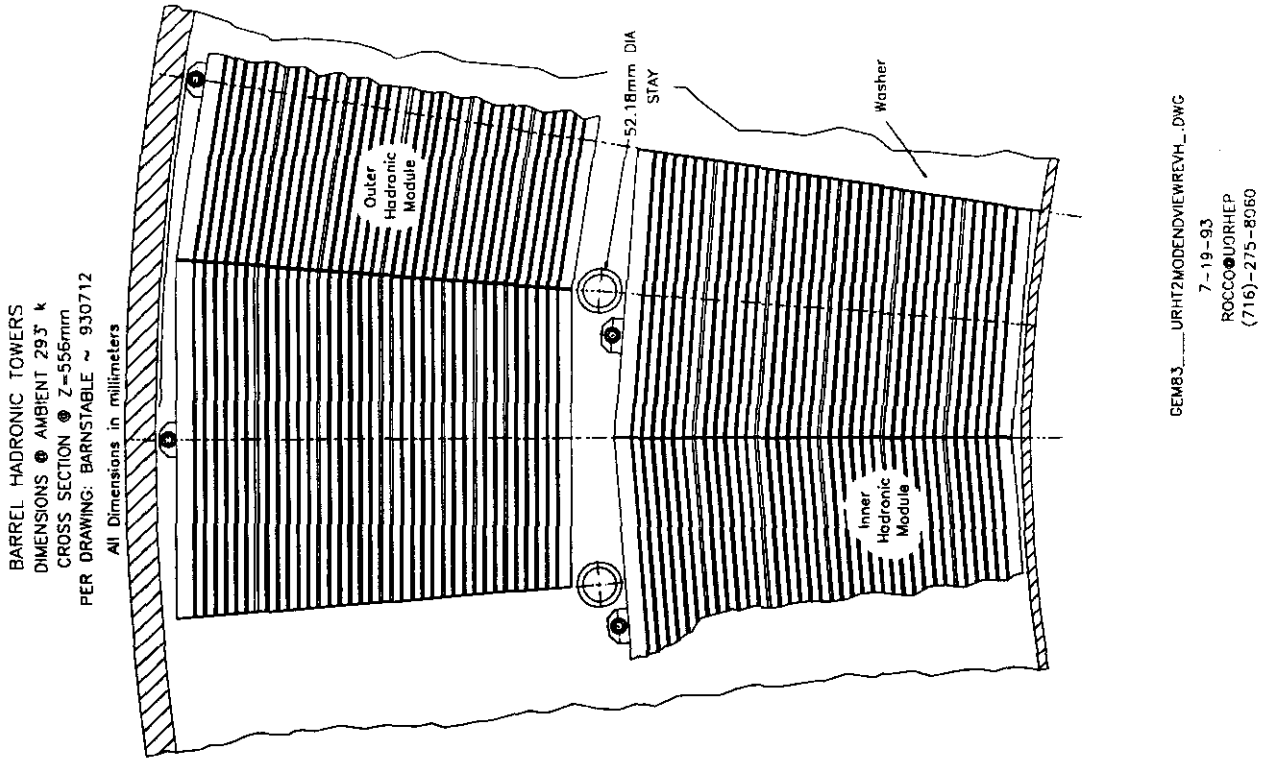

Figure 3.5: Endview of Inner Barrel hadronic modules

ratio (number of gaps in series) lies between 3:1 or 4:1, if one choses an absorber thickness of 9-10 mm. We have chosen an absorber thickness of 9 mm and a 3:1 ratio which implies that there are three gaps in series. Two such arrangements can be naturally set in parallel, and this is the unit we call one cell. It is sketched in Fig. 3.7 The modules in each layer consist of a total of 6 cells.

3.1.1.2.2 Absorber material Natural absorber materials for a hadronic calorimeter would be either copper or lead. However, copper (Z = 29) and krypton (Z = 36) are sufficiently similar so that there is hardly any e/mips suppression, and rough estimates predict an e/h value of 1.9. We therefore use lead as the primary absorber material, but use brass where both absorption and mechanical rigidity is required. A great advantage of brass is the fact that during cooldown its shrinkage is very similar to that of aluminum, the material selected for the overall GEM cryostat. Indeed, the relative shrinkage of aluminum (2024 or 6061) relative to free-machining brass is only 0.26 mm/m between room temperature and 77 K, while the same difference for aluminum to copper is 0.64 mm/m.

3.1.1.2.3 Absorber planes: There are two intrinsically different types of absorber material. Every sixth absorber is a ground plane. This is a solid brass sheet 9 mm thick, extending across the whole module, and rigidly tied to the endplates. Electrically a ground plane is tied to the signal ground of the readout cable leading to the amplifiers.

All other absorber planes are tile planes. A typical tile plane is shown in Fig. 3.8. It

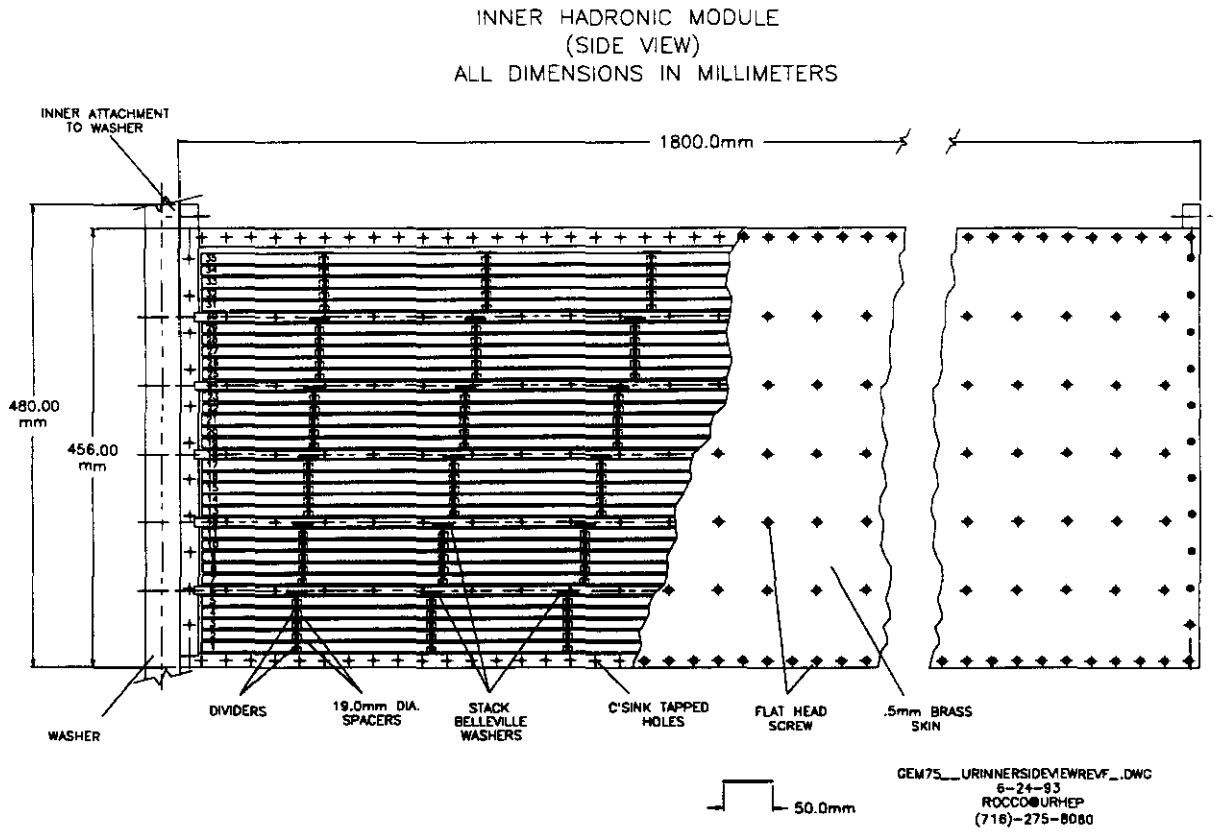

Figure 3.6: Sideview of Inner Barrel hadronic modules

consists of individual lead tiles, each corresponding to a single tower, separated by approximately 3mm gaps. On each side of the tiles, epoxied on (by using prepreg), is a 0.5 mm thick G-10 board which is copperclad on the outside. The cladding is subdivided into squares of the same size as a single tower, with only about 1.0 mm between each square. The individual squares are connected by a thin line of resistive ink, providing a resistance of a few MΩ. Thus all the pads are independent in pulse mode, but at the same voltage in DC mode. In the passive tile plane one of these pad structures is tied to HV, the other to ground. In the sense plane, both are tied to HV, and the tile itself is connected to the signal line which feeds the (capacitively coupled) pulse to the amplifier. These signal lines (not shown) have an impedance of $5 - 10\ \Omega$.

3.1.1.2.4 Electrical readout structure High energy electrons or photons will deposit a small fraction of their energy in the first layers of the hadronic calorimeter. One cell corresponds to about 11 X_0. The first two cells of the first hadronic module will be read out separately, and provide thus a "tail catcher" to the electromagnetic calorimeter in front. The next four cells of the first hadronic modules form the second readout group in the first hadronic layer. The second hadronic layer could either be read out by a single amplifier

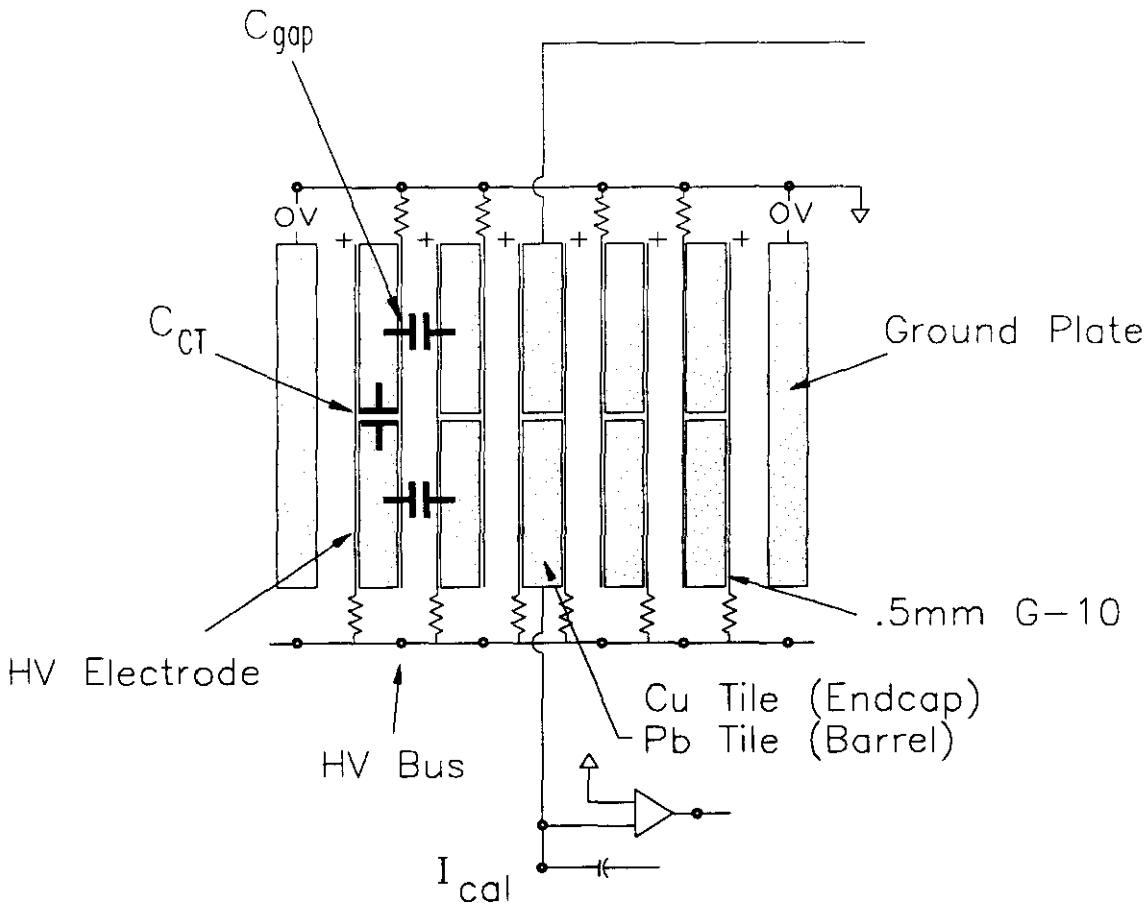

Figure 3.7: Electrostatic transformer for the barrel hadronic modules.

or again subdivided into two sections. Such a subdivision would improve the signal/noise ratio in this second hadronic layer and would allow (by adjusting the gains) possibly to compensate for the extra dead absorber material between the two layers. While no decision has been made for the real GEM detector, we propose to build half of the outer hadronic modules with a single preamplifier/tower, while the other half would have two preamplifiers in each tower. We would thus have two nearly independent half-detectors (one for positive and one for negative pseudorapidity) and could compare the two approaches.

The initial design of barrel hadronic modules by a group from Martin-Marietta has been

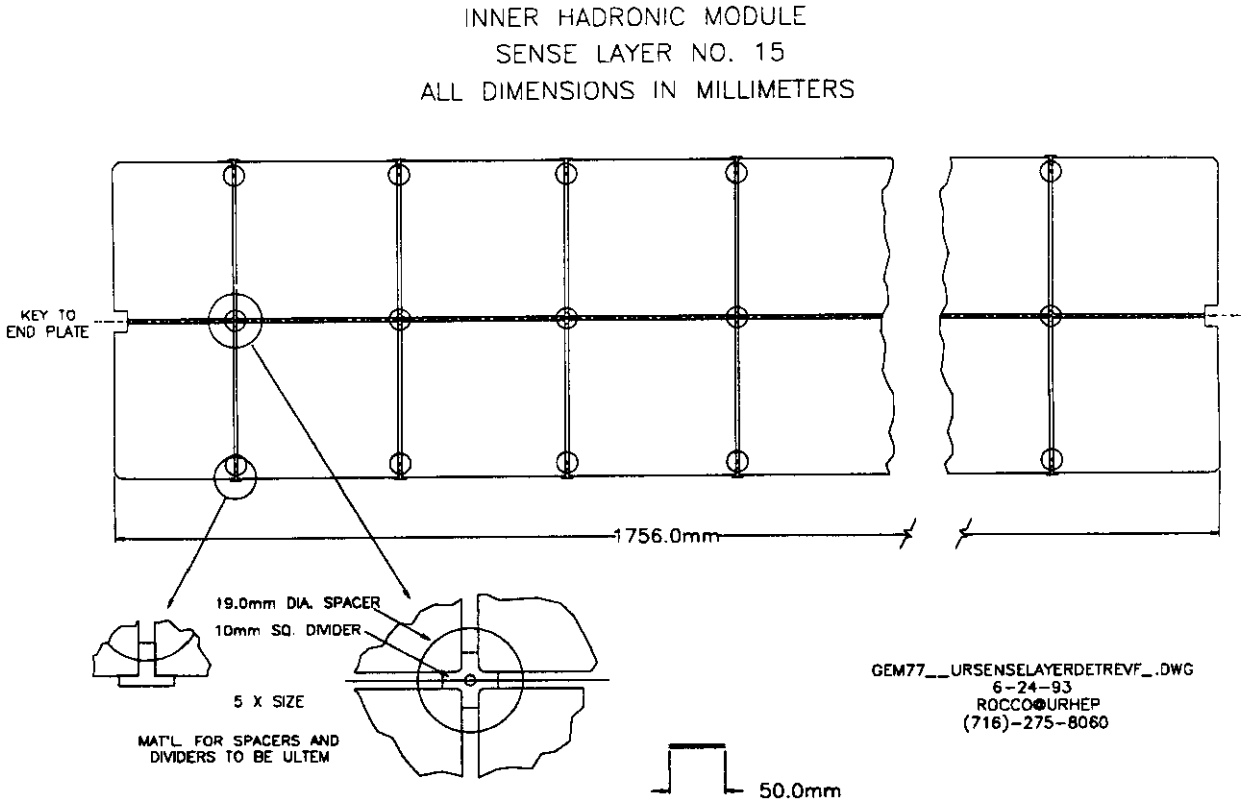

Figure 3.8: Tile plane for barrel hadronic calorimeter.

revised by U. of Rochester. This necessitated building a half-scale model of a single hadronic barrel module and subjecting it to stress and deformation tests. These tests have been completed and we have a design which promises to have negligible deflections (less than 0.3 mm) in any orientation. The note GEM-TN-93-311 [13] gives a detailed discussion of a preliminary design which has been improved since.

Various adhesives and prepreg layers from several manufacturers have been tested in order to determine the best adhesive to connect the individual lead or copper tiles to the supporting G-10 structure. Since all of these adhesives require curing at elevated temperatures, we have performed annealing tests of the special calcium-lead alloy which we plan to use as lead absorber. These tests are stil continuing as we are obtaining new adhesives and prepregs; the best adhesive is a compromise between the highest possible peel strength and a curing temperature which does not yet soften the lead (120° C is safe, 140° C is marginal, at 160° C the lead weakens intolerably).

We have tested many resistive inks which we plan to use to connect individual pads on the G-10 boards. These inks cure at a temperature at which copper-clad G-10 begins to oxydize if left in air. The final resistance is extremely sensitive to the exact curing temperature and duration. As a result of these tests, we have designed and built a gluing press for assembling individual absorber layers. We have also designed and are building a special oven for curing

the resistive ink. This oven will heat the 180 cm long and 20-40 cm wide G-10 boards in an argon atmosphere to prevent oxydization and discoloring of the copper. Exact temperature control and fast heating are critical, since the resistive inks require curing temperatures near the softening temperature of G-10 (170 C) and the final resistance is very sensitive to the curing cycle history.

We have begun purchasing component materials for the barrel hadronic modules. A large order for thin one-side copper-clad G-10 boards has gone out. We are negotiating with lead vendors, and have initiated discussions with vendors about other components.

3.1.1.3 Endcap HAD

The endcap hadronic modules cover the region from $\eta = 0.9$ to 2.5. Six different module structures are required. These modules are designated inner hadron A, B and C and outer hadronic A, B and C as shown in Fig. 3.1. Each module type weighs approximately 2.5 tons per module. Outer A surrounds the endcap monolithic electromagnetic calorimeter. Outer B and C follow outer A. This division is required by the structural stay that runs from the back of the endcap to the front cold wall. The front cold wall must be kept thin to prevent the degradation of the electromagnetic resolution. The three outer module types are constructed in 9° sectors while the three inner module types are constructed in 18° sectors. Hence in each end cap there are forty each of the outer modules types and 20 each of the inner module types.

The endcap calorimeter has a total depth of about 9 λ. This is sufficient to maintain good energy resolution up to the highest SSC energies. Although about 12 λ of absorber is required to shield the muon chambers, only about 9 λ need to be instrumented in order to measure the energy loss of the forward muons in the absorber to a level sufficient not to degrade the muon energy resolution.

The modules use copper as the absorber material because of its short absorption length and liquid argon as the ionization fluid. The absorber plates are 27 mm thick to reduce construction costs. Sampling fluctuations are not the dominant source of the resolution and thick plates can be used with only a small degradation of the resolution[7].

3.1.1.3.1 Cell structure Since short shaping times on the order of 100 ns will be used, the electrostatic transformer concept must be employed to provide adequate signal to noise. Although a single wide gap would provide the same signal to noise performance, such a gap would require a large operating voltage and might also present problems with ion buildup. A schematic of the cell structure is shown in Fig. 3.9.

The tower structure is etched on Kapton electrodes spaced between the ground plates and copper signal tiles. Using thin electrodes appreciably reduces the cross-talk between the towers as well as lowers the stray capacitance of the tower. A transformer ratio of four is used in the endcaps because of the signal is lower in argon than in krypton.

3.1.1.3.2 Module structure The outer hadron B module is shown in Fig. 3.10. The structure is supported by top and bottom plates that are bolted to the ground plates. This

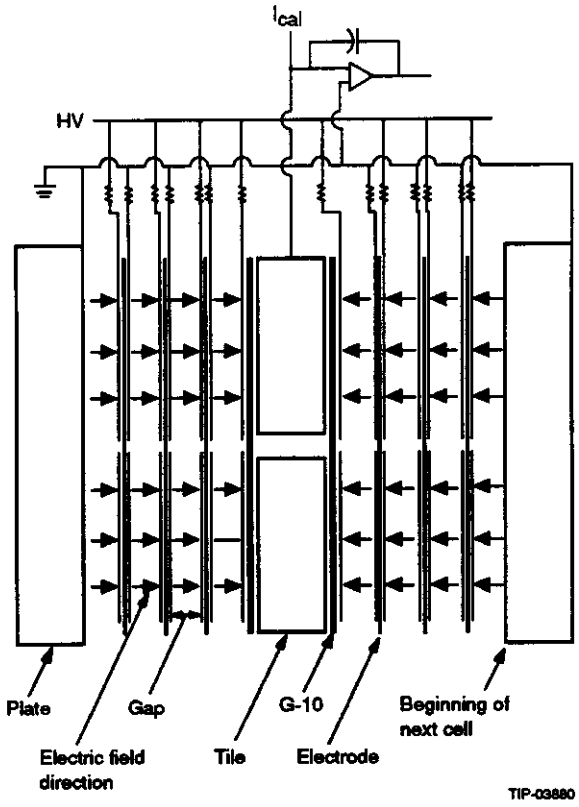

Figure 3.9: Electrostatic transformer for the endcap hadron modules showing the arrangement of the absorbers and electrodes.

arrangement forms a rigid truss for which finite element analysis shows the maximum deflection to be under a millimeter for the worst case of the top and bottom most modules. The tile layers are supported from the ground plates by G-10 rods. The Kapton electrodes are also supported from these G-10 rods. The ends of the modules are supported by keys mounted on the washers. The radial support is accomplished by bolting the endplates to the washers. Shoulder bolts are used on one end to provide for the differential thermal expansion between aluminum and copper. To minimize the noise contribution from the signal collection lines, the amplifiers are mounted on narrow mother boards that fit in pockets made in the ground plates. These ground plates also serve to carry the amplifier heat to the top plate which makes a good thermal conductor.

The tile layers are made by gluing the tiles between sheets of 0.5 mm G10. This produces a very rigid plane that can be easily handled during the module assembly. The tiles are spaced 4 mm apart to minimize the cross talk between towers while at the same time keeping cracks small.

Outer hadron A is preceded by an active massless gap that will be used to correct for the energy lost in the two cryostat walls between the barrel and the endcap. The first two cells of inner hadron A serve as a tail catcher for the electromagnetic section and are read out separately.

All modules are two tiles wide simplifying the signal collection hook up. Hence the ϕ

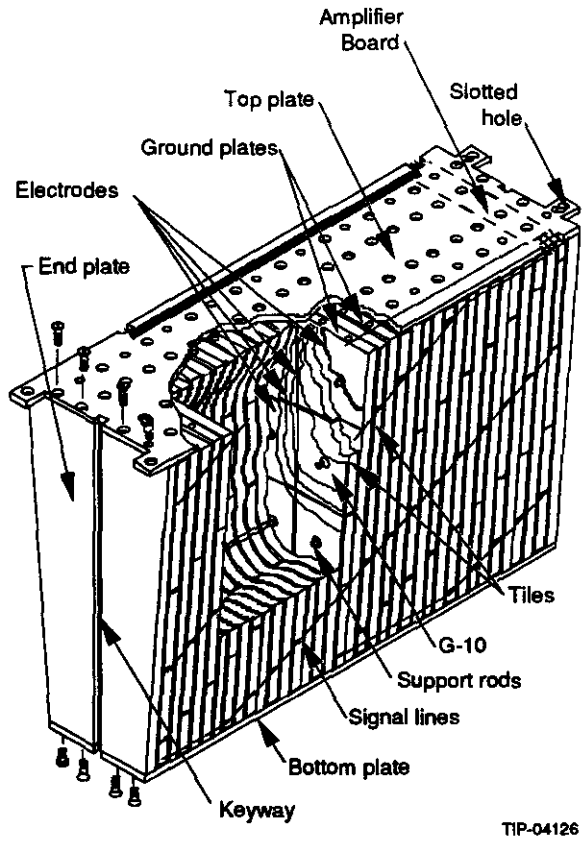

Figure 3.10: Outer Endcap Hadron Module.

segmentation is twice as large in the inner modules as in the outer modules. However since the inner modules are at a smaller radius than the outer, their tower widths are on average smaller than those of the outer modules.

3.1.1.4 SBC

Major parameters and the layout of the SBC design are given in the GEM TDR [1]. Figures 3.11, 3.12, 3.13, 3.14, and 3.15 show the layout of SBC modules to be tested and basic concepts of their design.

The SBC consists of separate modules which are easy to manufacture and test and which are later installed in the support tube to form the barrel. A typical module consists of eight layers of brass absorber and four layers of scintillating tiles uniformly spaced in the absorber. The number of scintillating layers was chosen from the results of MC simulation as well as from economical considerations. Scintillating light from the tiles is readout through wave length shifting fibers (WLSF) embedded in the tiles. WLSF are connected to PMT via clear transport fibers. Combining several fibers to one PMT readout channel, one obtains the required projective transverse segmentation which matches the segmentation in the hadronic part of the noble liquid calorimeter. Within one transverse tower all the scintillation layers are summed together providing a single longitudinal readout segment, though if it proves

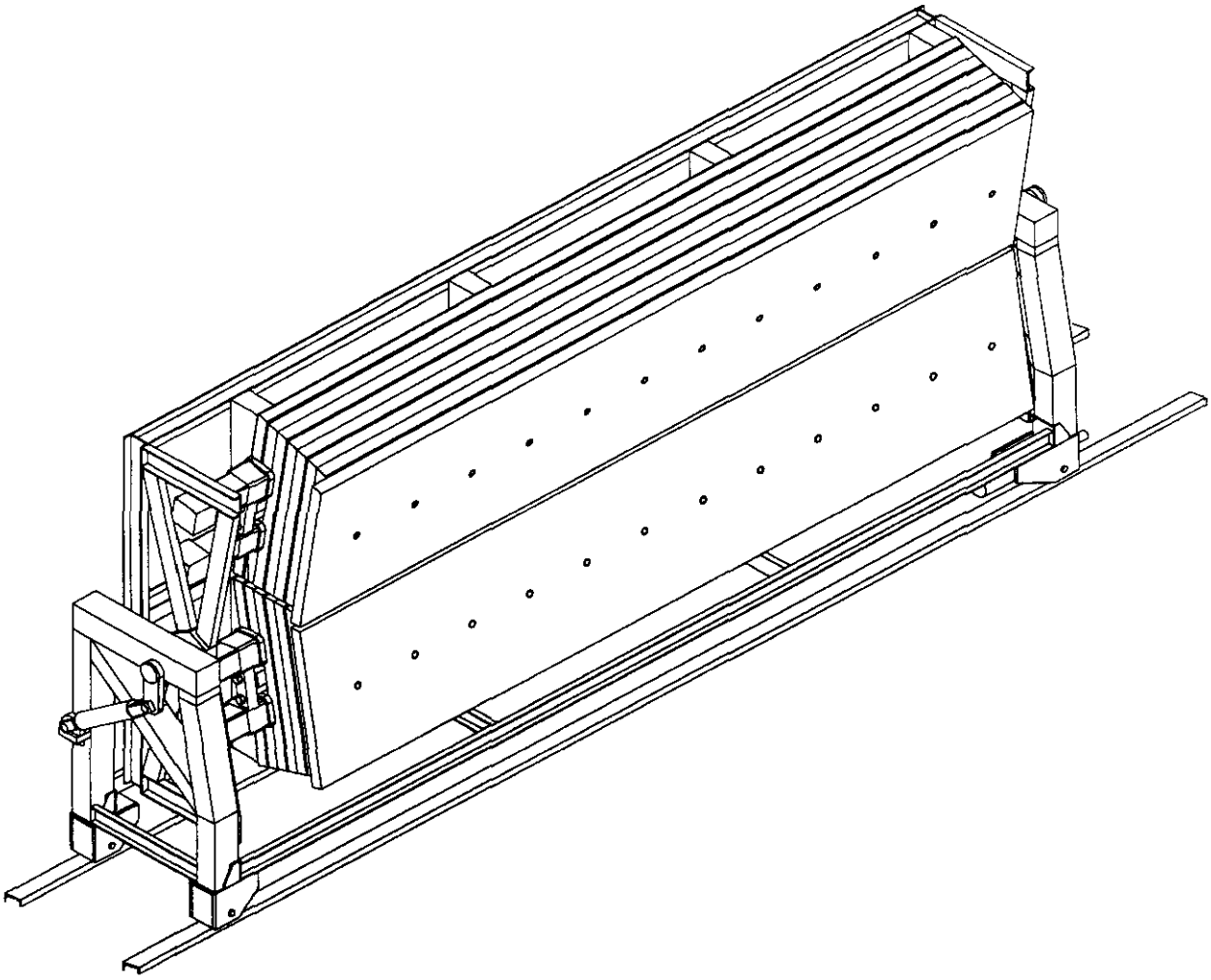

Figure 3.11: Scintillating Barrel Modules In The Fermi Test Stand

to be necessary, the readout can be rearranged flexibly into two and even four longitudinal readout segments.

Conceptual design of the SBC detector is close to completion. It is tightly coupled with the design of the Central Detector Support (CDS) structure, the noble liquid calorimeter and cable/communication services. R&D work is under way to determine basic light yield parameters of the tile/WLSF layout used in SBC; to study different PMTs and calibration/monitoring schemes; and to build several prototypes. Monte Carlo studies of GEM SBC system are summarized in GEM Technical Note GEM TN-93-349 [14].

3.1.1.5 Forward

The conceptual designs of two forward calorimeter options Liquid Argon Tubes (LAT) and Čerenkov Quartz Fiber (CQF) spaghetti are being developed by GEM Collaboration. Major features of these designs are determined by the conceptual requirements of GEM forward calorimetry: full crackless coverage of the available angular range between beam pipe and

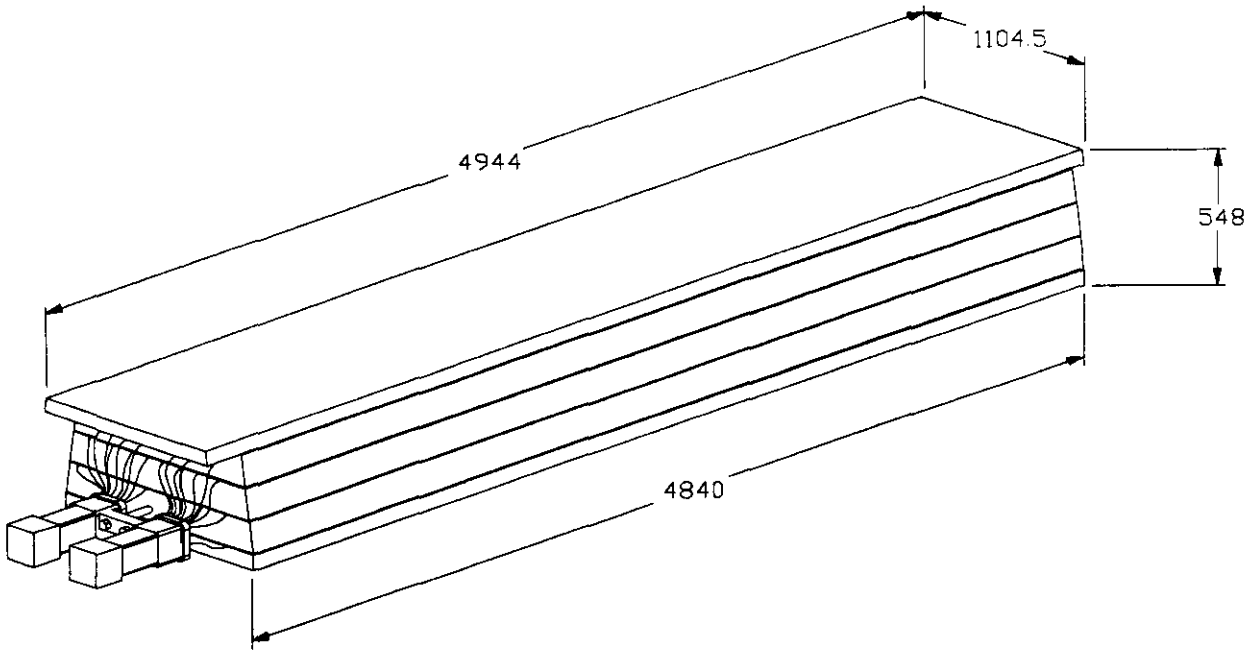

Figure 3.12: One Scintillating Barrel Module

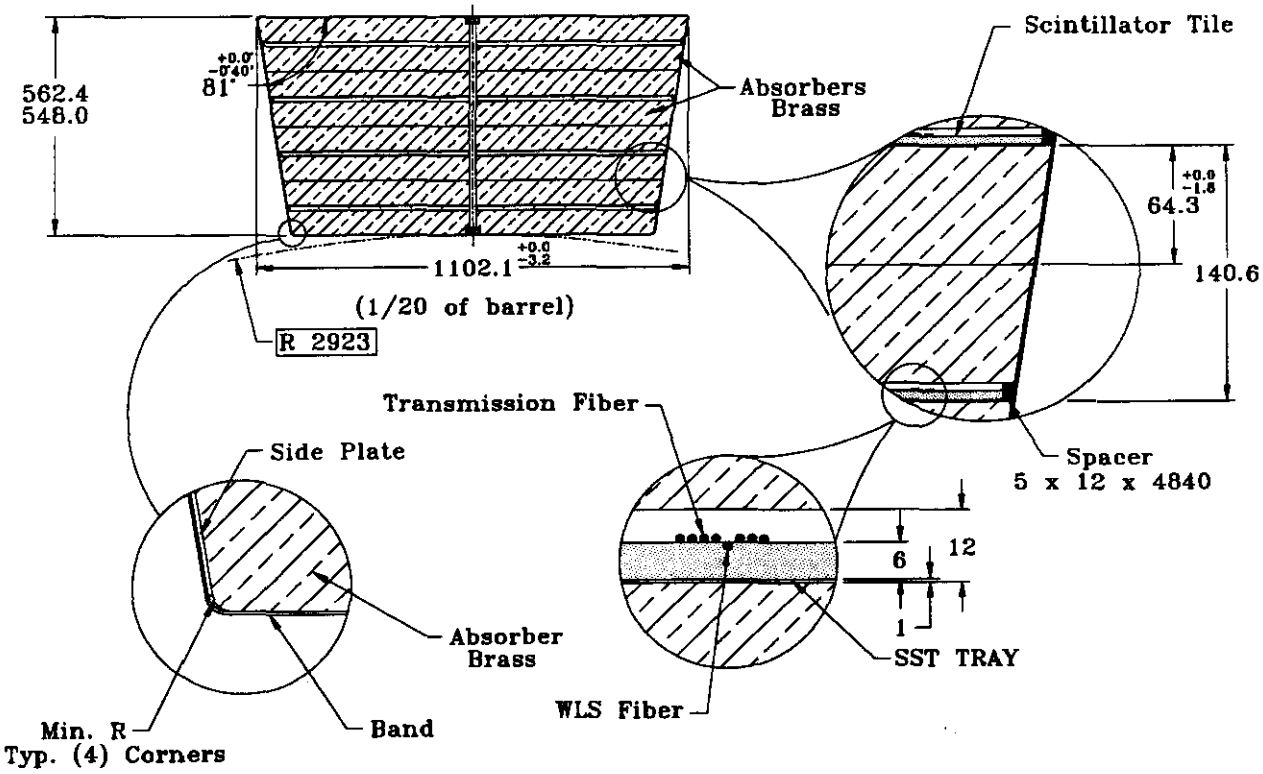

Figure 3.13: End View Detail Of Scintillating Barrel Module

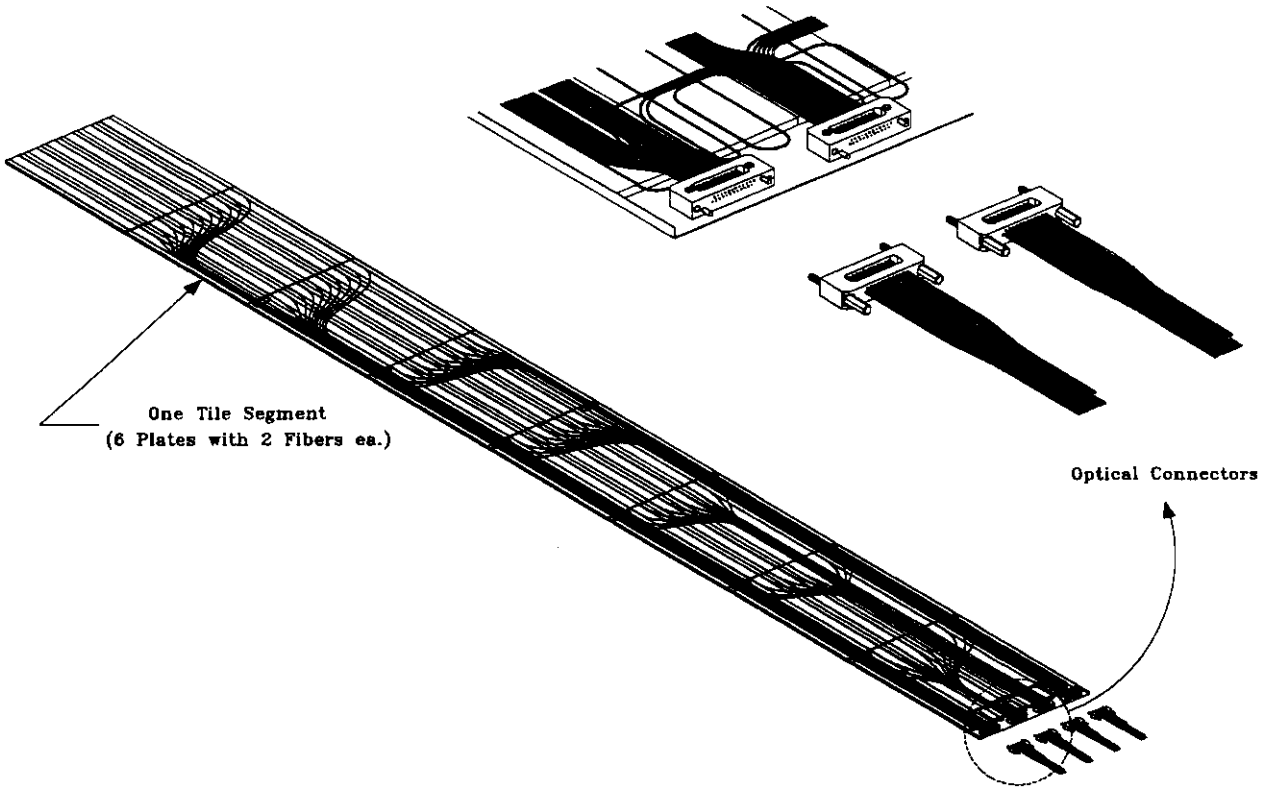

Figure 3.14: One Tile Layer

endcap calorimeter to provide missing transverse energy measurements and to shield the GEM muon system from excessive neutron background. These requirements imply that forward calorimeter is positioned relatively close to the intersection region at the distance of ~5 m. Radiation environment, assembly, access, integration with beam pipe and other issues are essential for the engineering development of the forward calorimeter system. Parallel with the engineering work, R&D studies are pursued to establish the performance of two proposed detection techniques LAT and CQF; they are concentrated on radiation damage effects, material studies as well as on the construction of several prototypes.

The noble liquid technology is inherently radiation hard. However due to the high ionization rate in the liquid, positive charges build up in the sampling gaps and can distort the signal. The theory has been worked out by the University of Arizona group (GEM TN-92-188 [15] and GEM TN-93-410 [16]) and the distortion can be avoided by designing a calorimeter with very narrow gaps. To this end the University of Arizona group has pioneered a novel electrode structure based on an absorber rod within a tube. A cross section of such rods in a matrix is shown in Fig. 3.16. The gap between the rod and tube is occupied by liquid argon and this gap may be as small as 100 μm across (compared to the conventional choice of 2 mm).

Arizona has built many such tubes in their labs and has run a number of bench tests. Starting in the Fall of '92 they designed and constructed a prototpe forward calorimeter module, the associated cryostat and cryogenics, and read-out electronics. This was taken

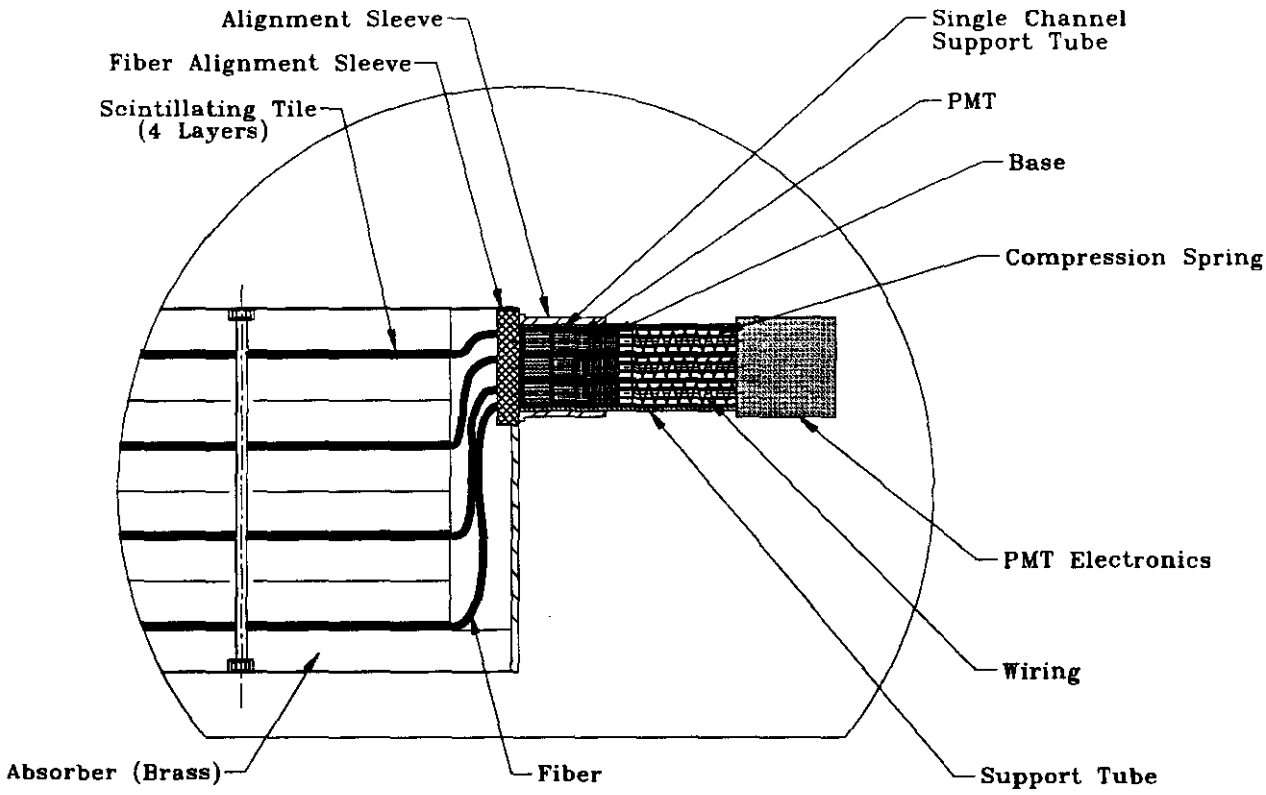

Figure 3.15: Scintillating Barrel Readout Assembly

to Brookhaven in the Summer of '93 for extensive beam tests at electron and pion energies of 2, 4, 6, and 8 GeV. Preliminary analysis of that data shows that the module worked exceedingly well. The energy resolution for electrons at 8 GeV is better than 13% and the position resolution is of order 2 mm. Lower energies show linearity of response to better than 5%. Fig. 3.17 shows the energy response of the prototype to 8 GeV electrons.

Arizona has sent their apparatus to CERN for beam tests at higher energies. The RD3 collaboration (liquid argon accordion EM calorimetry), a part of the ATLAS (LHC) R&D program, is interested in this technology, and is considering it for their forward calorimeter as well. They invited Arizona to use their beam parasitically while their cryostat is out of the beam for modifications in October and while RD6 (TRD straw tube tracker) is in the upstream part of the beam.

The quartz fiber technology is geometrically similar to spaghetti scintillator calorimeters. But Čerenkov light rather than scintillator light is read out by the phototubes. While there are no definitive measurements of the transmission of blue and UV light at SSC doses, quartz fibers are more likely to survive than other materials. Fairfield University has constructed several quartz (or plastic) fiber modules for exposure in test beams. Of order one photo-electron per GeV of deposited energy is observed and energy resolutions of order 25% for electrons at 10 GeV were seen at Brookhaven. Gorodetzky et al. [8] have built and tested

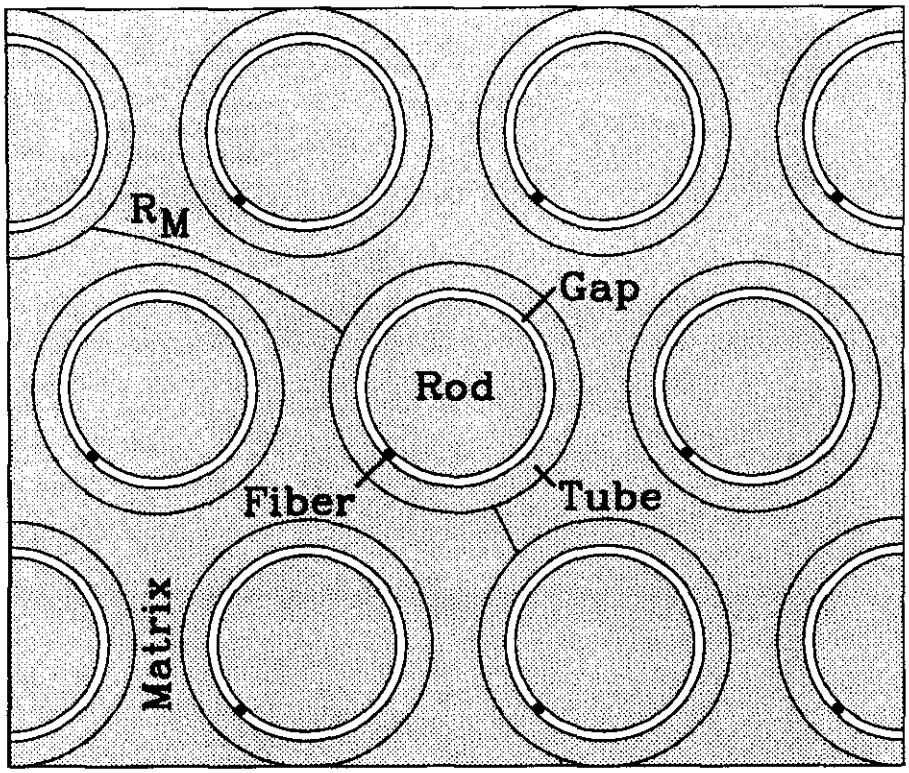

Figure 3.16: Cross section of GEM liquid argon forward calorimeter showing liquid argon Gap, fiber used as a spacer and the Moliere Radius - R_M.

several prototypes with fibers at 45 degrees to the incident beam. More light is collected at this angle and the central core of the shower is better sampled but this geometry is not appropriate for GEM forward calorimetry.

One of the options proposed for GEM Forward Calorimeter is Čerenkov Quartz Fiber (CQF) calorimeter (another GEM option is Liquid Argon Tubes calorimeter). This calorimeter will use thin parallel quartz fibers embedded in massive metal absorber (spaghetti scheme) to detect shower particles by Čerenkov light produced and propagated in quartz fibers. To insure uniformity and symmetric (Gaussian like) response of the calorimeter with hadronic jets, CQF calorimeter should have relatively high sampling frequency of fibers – ~20 fiber bundles per cm^2. To provide sufficient light yield the sampling fraction should be of the order of few percent.

3.1.2 Proposed Liquid R&D and Engineering in FY1994

The effort on the Liquid Ionization Calorimeter in the coming year will concentrate on the following areas. The preparation of the EM and hadronic modules for test at Fermi-

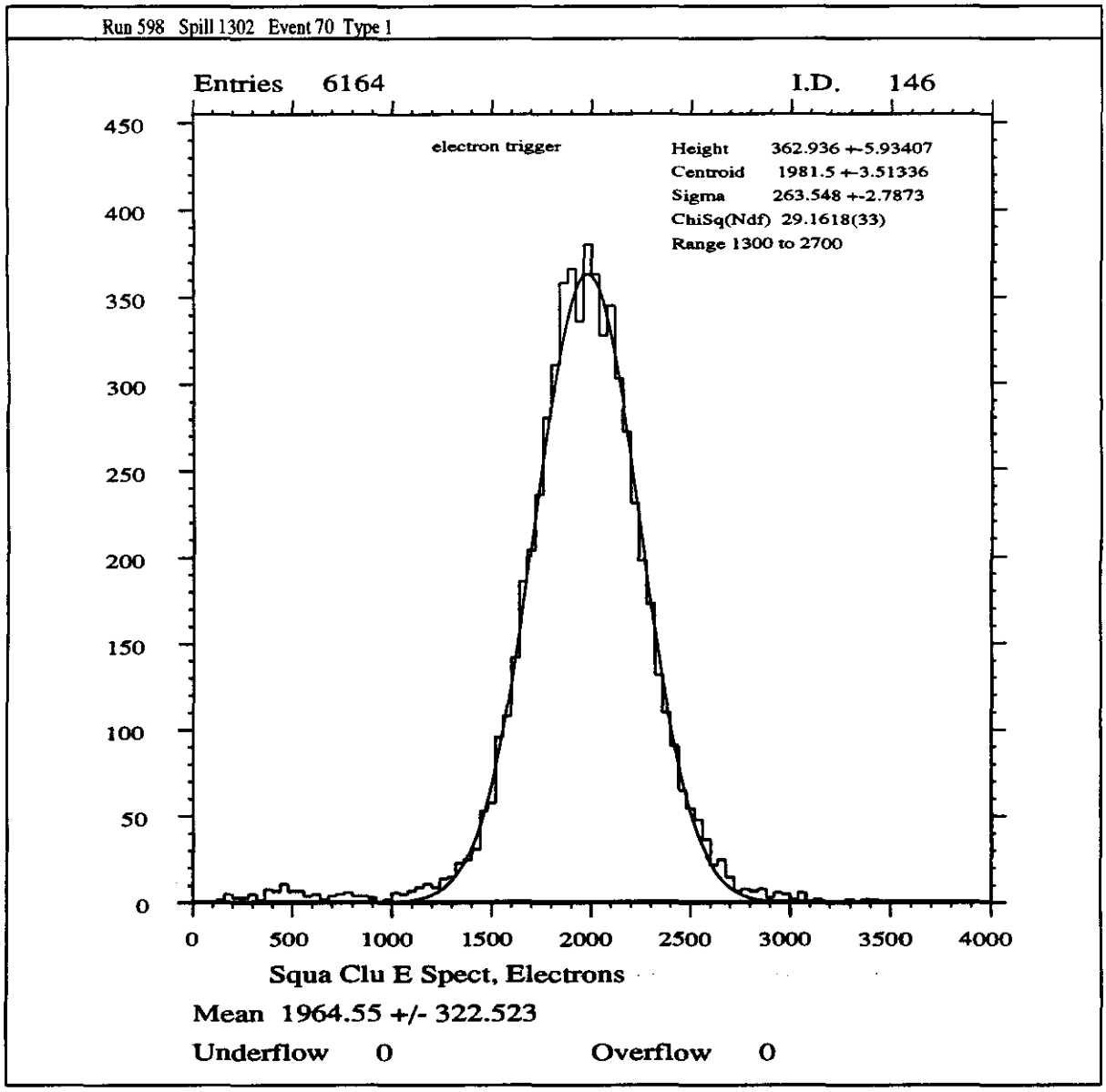

Figure 3.17: Response of forward liquid argon prototype to 8 GeV electrons at BNL

lab(FNAL)(detailed in Section 3.2), R & D activity needed to finalize the calorimeter design, engineering of the final calorimeter and preparation of the production and assembly facilities for the construction of the calorimeter. Below we give a summary of the main activities.

It is important to realize that these activities are highly interdependent and can not be completely separated. The activities are:

3.1.2.1 EM Prototype

We expect this activity to concentrate at BNL/Columbia-Nevis/Stony Brook. Some of the mechanical engineering of the module is presumed to be done at Martin Marietta. The engineering related to the bending machine, pressing of the boards, electrode design is being done at BNL. Pressing of the boards will be done either at Nevis or at an outside vendor and the assembly of the module is planned at BNL. The bending machine is being designed and will be constructed jointly by BNL and Nevis engineers.

We plan to test a small projective prototype EM calorimeter within our collaboration with RD3. The main goals are to test the performance of narrow strips in the first longitudinal layer of the calorimeter, to measure the constant term with the GEM design optimized for krypton, to measure the extent to which the massless gap compensates for the dead material of the cryostat, to measure the performance of long strips which would be orthogonal to the narrow strips, and to test the calibration system over a large dynamic range.

3.1.2.2 Hadronic Prototypes

The overall responsibility for the barrel hadronic will be with the U. of Rochester and the endcap hadronic at the U. of Washington. Most of the engineering of the module structure, mechanical integrity of the system is presumed to be done at Martin Marietta. The engineering and development of the bonding technique for the tile plates, readout strip lines and connections to high voltage will be done at the U. of Rochester and the U. of Washington. BNL will give engineering support needed to coordinate the effort.

3.1.2.2.1 Barrel The overall responsibility for these modules will lie with the University of Rochester. However, assembly of the modules will take place at Fermilab, and FNAL technicians will be used for manufacture of the G-10 boards. All the components supplied by outside vendors for the first 7 barrel hadronic modules will have been purchased and will arrive by late spring 1994. By that time we also will have hired 3-4 technicians for the assembly of modules. The area at FNAL where barrel hadronic modules will be assembled will have a clean room by summer of '94. The gluing press and oven, after being thoroughly tested at Rochester, will be installed at FNAL by fall of '94. About half of the G-10 for the first 7 modules will have been machined, and assembly of the individual absorber layers will be well underway around the same time. The first modules should be ready for testing by the end of 1994. We anticipate that the funding profile will force us to delay the production of the residual 7 modules into FY 95. The present plan is to build the first 7 modules using lead absorber, and the next 7 using copper as the absorber material. This will allow testing whether the hadron resolution of a lead-LKr calorimeter is indeed substantially better than can be achieved with copper.

3.1.2.2.2 Endcap We are beginning the construction of two of the three required Outer Hadron B Modules. The basic design is complete although there is a small amount of work to be done on the details of the support to the washers, in particular the specific size of the shoulder bolts required. The design has been optimized to take into account the dead material of the aluminum washers. This requires that the end plate and first tile layer

be made 1/2 the basic 27 mm thickness. This will compensate for the energy lost in the aluminum. The finite element analysis has been done to specify the fastener size for the absorber plates to the top and bottom plates. We are assembling an etching system to make the Kapton electrodes and G10 covers for the tile assemblies in house. The G10, copper and Kapton are on order. We are still investigating the glue to be used for the tile assemblies. We have two excellent candidates at present. Our goal is to minimize the cost. We also need to investigate the radiation hardness. We are starting a program to determine the effects of neutrons on the bond strength and shear strength of the glues under cryogenic conditions.

3.1.2.3 Forward Calorimeter:

U. of Arizona has the main responsibility for the construction of the liquid argon forward calorimeter, see section 3.1.4 and are part of the liquid calorimeter team.

3.1.2.4 Cryogenic Feedthroughs for Barrel and Endcap

The U. of Washington has designed the cryogenic feedthroughs to bring the large number of signals out of the cryostat. These feedthroughs are compact, robust and cost effective. It is our responsibility to finish the design and test it as well as fabricate the assemblies for the FNAL beam test cryostat.

The design is shown in Fig. 3.18. Special Inconel X750 feedthroughs have been designed that contain 480 signal pins each. Each signal pin is isolated from the Inconel by a ceramic spool. The ground is carried by the Inconel itself which reduces the pin count by a factor of two without seriously degrading the transmission performance of the 50 ohm signal lines. Two such feedthroughs are welded into stainless steel plates along with commercial high-voltage cryogenic feedthroughs and low-voltage cryogenic feedthroughs. The inner and outer plates are connected by a stainless steel bellows that isolates the assembly from the main vacuum. The design is sufficiently compact that the ends of the GEM barrel cryostat can handle the approximately 75000 signal and control lines required in the design. These feedthroughs will be used in the FNAL tests as a field test of their design. Prototypes will be evaluated soon.

As part of this system a stripline connector has been designed to mate with these feedthroughs. The ground connection is made using springs that engage the walls of the Inconel housing. This ground design keeps the inductance low as well as cutting the pin count by a factor of two. The connector parts are injection molded using a plastic called Vectra made by the Celanese Corporation The actual pin connectors are commercial items from Samtec. The stripline is made from Kapton printed circuit material. The heat load carried by the stripline to the liquid argon is about 7 mWatts per channel.

3.1.2.5 Material Selection

This involves certification of the materials that can be used in the calorimeter in the appropriate radiation environment without poisoning of the liquid. We expect to establish test cells at Arizona, BINP, BNL, Stony Brook, and SSCL. These groups will be responsible initially for this effort.

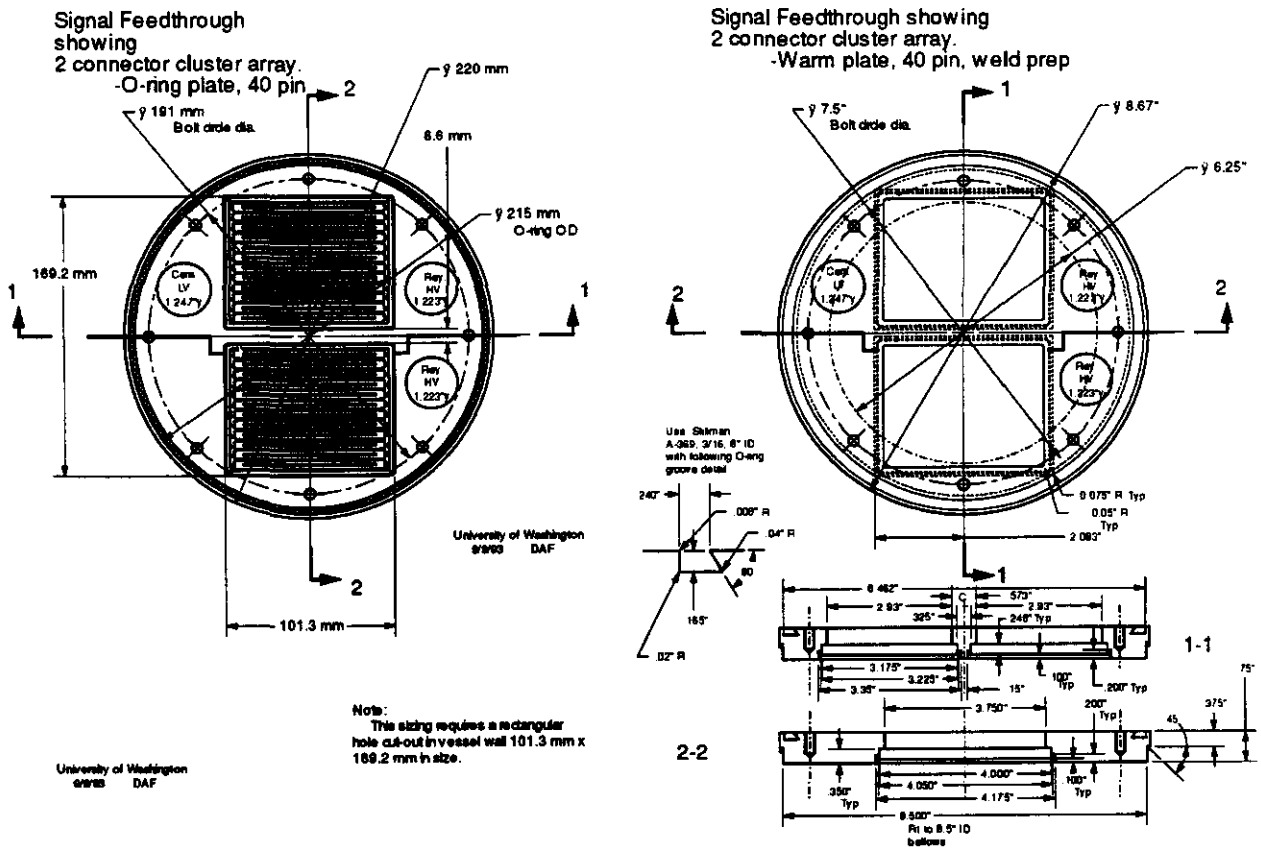

Figure 3.18: Feedthrough design

3.1.2.5.1 Arizona The technologies which are most likely to survive the intense radiation environment in which the GEM calorimeter will operate, for instance liquid argon and liquid krypton, could potentially be effected by the radiation induced break down of components, such as the insulation on the cables, immersed inside particularly in the forward direction. It is a concern that these components could be chemically altered after exposure to high intensity radiation and give off minute amounts of a "poison", which would attach the drifting signal electrons to massive ions — essentially killing the signal. We are gearing up to systematically answer the "engineering" questions concerning which substances are suitable for use in the forward calorimeter. In addition, the GEM krypton electromagnetic calorimeter presents new poisoning challenges where at least anecdotal information indicates that some substances known to be safe in liquid argon seem to poison liquid krypton.

Our plan for the following year is to irradiate calorimeter prototypes and potential construction materials with a high intensity beam of ionizing radiation in the actual environment in which it will be used at the SSC. Any released chemical poisons will be analyzed in situ using the FTIR and correlated with electron attachment by using a standard beta cell. The X-ray machine which will be used for this irradiation is capable of producing many times the dose rate expected at the standard SSC luminosity so that construction materials can be tested for poisoning in a reasonable time. A rate of 5000 Mrad per year (five to ten times the dose rate at a point near the inner most corner of a SSC forward calorimeter) is a reasonable

maximum deliverable X-ray intensity.

Often, the fabrication process and not only the building materials can contribute to the response of the calorimeter. For instance, freon, which is a powerful poison of liquid argon is frequently used in cleaning electronic components and could be present in arbitrary amounts inside the calorimeter. This has hampered previous systematic poisoning studies because of the impossibility of reproducing quantitative results when these results are dependent on the vaporization rate of chemicals used in the processing. The FTIR spectrometer should considerably reduce such systematic uncertainties. On the other hand, Kapton is a material generally considered safe for use in calorimeters but it has never been systematically tested after being irradiated. Kapton's long organic molecule is particularly susceptible to radiation damage and it could break down and release smaller molecules containing electronegative compounds into the liquid argon. Kapton, because of the current interest in it, will be the first material we test.

3.1.2.5.2 BINP (Novosibirsk) We propose to study the gamma irradiation of the materials used in the accordion structure at high gamma dose level(up to 100 Mrad). Towards this end we have performed the following test experiment.

Using our 2.4 MeV electron accelerator we have irradiated a structure containing 10 layers of Pb of 1 mm thickness with 0.3 mm Cu sheets in between. This structure was located in the iron box with 1 mm walls at the distance of 13 cm from the Ta converter upstream the beam after 8 mm of the stainless steel "flange". The geometry was chosen close to the possible cryostat design.

The dose levels were measured in each Pb layer. The results obtained after 1/2 hour exposition at the beam of the average power 8 kW are between 400-100 Krad depending on the depth.

The accelerator power can be increased up to 20 kW, and in this case a dose level of 100 Mrad can be collected during 10 days. It means that we have possibility of the high level irradiation and if necessary we can design the cryostat for the materials and preamplifiers boards test. We have experience in the measurements of the contaminations level in LKr using the laser or beta-source technology.

3.1.2.6 Liquid Calorimeter Engineering

The engineering work needed to design the final calorimeter was centered at Martin Marietta. We expect this successful effort to continue and work closely with the scientists and engineers who are producing prototypes. BNL will coordinate the engineering done at Martin Marietta, Nevis, Rochester, SSCL and Washington for the liquid calorimeter.

3.1.2.7 Integration and Assembly

This activity will be concentrated at the SSCL in close cooperation with BNL, Oak Ridge and Martin Marietta. The main activity here is to engineer and build the facilities needed for the assembly of the calorimeter and its installation in the experimental hall. This should include the development of the testing procedure that is needed before and during the installation period.

3.1.2.8 Electronics development

The electronic readout of the calorimeter is a vital part of the system and BNL/Columbia-Nevis/Arizona are deeply involved in this activity. However, the support is covered by R & D request by the Electronics, Trigger and DAQ Group and only the calibration and DAQ associated with the Fermilab test discussed in this request.

We would like to emphasize that the Liquid Calorimeter System is being built jointly by all the collaborating institutions. The initial named assignments are made in order to identify the main institutional responsibilities. There is a large degree of overlap among various components of the calorimeter and close cooperation is required to optimize the R & D effort as well as the money spent.

3.1.3 Proposed Scintillating R&D and Engineering Program

Though the technique of scintillating tiles with WLSF readout has been extensively developing in the last years by CDF and SDC collaborations [11], there are specific R&D issues of implementation of these techniques in GEM SBC detector. These issues are addressed in SBC R&D program which should precede the construction of prototype modules and the major construction of the whole SBC for GEM. The R&D program includes:

- Development of a uniform, reproducible and cost effective technique of tile/WLSF layout and coupling. GEM SBC design calls for relatively large light yield with few readout layers in a sampling calorimeter. This work with single tile prototypes concentrates on three aspects: measurement of absolute light yield (in p.e. per mip) in a controlled optical environment and comparison with Monte Carlo light transport simulations; search for the optimal (maximum yield) match of types of scintillating and WLSF materials, quality of the fiber grooves in the tiles and reflecting wrap; control of optical, machining and assembly parameters which determine the uniformity and reproducibility of the tile/WLSF readout.

- Development of calibration and monitoring (C&M) system. The proposed C&M scheme assumes that each tile (read out by two WLSF) receives a short stable and adjustable light signal from an optical distributor via thin quartz fibers which allows (with a number of reference measurements) calibration and monitoring the response of each tile in SBC. The plan includes the construction of several small prototypes which will verify the technical realization of this scheme. The C&M system should be later cross calibrated in a realistic calorimeter layout of noble liquid and SBC prototypes with the high energy test beam at FNAL.

- Study of PMT readout. A selection needs to be made of green extended PMTs with an optimal match to the WLSF spectral light yield, working in an axial magnetic field and complying with GEM SBC requirements of dynamic range and stability. Since PMTs comprise a considerable fraction of the SBC readout cost, the selection of cost effective devices is an important constraint in these studies.

- Development of readout and signal processing electronics. In order to match the relatively low gain PMT signals ($\sim 10^5$), the preamplifiers should have wide dynamic range, good output driving capabilities and sufficient bandwidth to preserve the speed of the scintillating technique. The present plan includes the modification of the preamplifier/shaper/driver scheme used in GEM noble liquid calorimetry to provide a uniform calorimeter readout. Several prototypes have to be built and tested with tile/WLSF test setup.

- Development of optical contacts. In addition to the technique of thermal splicing of WLS and clear fibers which was developed by the CDF and SDC collaborations, the multifold contact optical connectors and fiber bundles to couple fibers to PMTS will be used in the SBC. Various quality control devices have to be designed and built to control the uniformity, reproducibility and reliability of optical contacts.

- Longevity studies. Since the SBC has to operate in the GEM detector for 10-15 years (in a moderate radiation environment while the SSC is operating) the issue of optical longevity and response stability becomes important. These studies are aimed at accelerating the aging of scintillator tile/fiber assemblies with the methods which are known to produce mechanical aging (thermal and humidity cycling, radiation, atmosphere changes, chemical contacts) and observing optical aging by comparison with reference samples. As a result the extrapolated estimate of light yield response changes during the SBC life time period should be obtained.

- The mock-up of the end of an SBC module is to be built to develop a scheme for practical routing/assembly of fiber bundle connections with PMT assemblies and to minimize space needed for the PMTs and connections.

- Construction of four scintillator layer intermediate size prototype (two to four SBC readout towers) which will be tested in the Texas Test Rig (TTR) setup at SSCL with cosmic muons. This test will address the response uniformity of scintillating readout towers and tile to tile reproducibility of the light yield in an experimental environment with moderately large number of tiles.

- Problems of the assembly of five meter long layers of scintillating tiles will be addressed in the construction of the One Layer Prototype (OLP) with a tile size representing the GEM SBC θ-segmentation. A study of the variation of light yield for tiles with different dimensions and possible moderation of this variation will be studied with this prototype.

- Monte Carlo studies will be directed on the simulation of effects of slit and non-instrumented (dead) regions in the SBC module design. The effect of these regions on the physics performance of the GEM detector will be evaluated. Also the detection of muons and hadronic jets in the GEM calorimeter will be simulated in order to choose the optimal longitudinal readout segmentation of the SBC detector.

Presently (October, 1993) conceptual design of the SBC detector for GEM is close to completion. R&D work is under way to determine basic light yield parameters of tile/WLSF

layout used in SBC, to study different PMTs, calibration/monitoring schemes. Monte Carlo studies of GEM SBC system are summarized in GEM Technical Note GEM TN-93-349 [14].

Institutions participating in GEM SBC project and task assignment by institutions are listed below:

- ORNL : Engineering, readout electronics, coordination of R&D.
- Boston University : Readout electronics development, machining mechanical components for prototype construction. construction, SBC FNAL test integration.
- Fairfield University : Study of alternative methods of optical readout; high stability optical referencies for calibration/monitoring system.
- University of Iowa : PMT studies, development of Calibration and monitoring system, provides these components for various prototypes; QA equipment for PMT and C&M system components acceptance control.
- Louisiana State University : Tile studies - control of factors determining the uniformity and reproducibility of light yield; production/test of samples for longelivity studies; construction scintillation counters for One Layer Prototype cosmic muon test trigger.
- Memphis State University : measurement of optical properties of materials used in scintillation layer construction;
- Michigan State University : Development of equipment for the production and QA control of optical contacts - fiber splicing, optical connectors, fiber mirroring, fiber bundles, light mixers.
- University of Mississippi : Tile studies - measurement of absolute light yield (in p.e. per mip) in the controlled optical environments and comparison with Monte Carlo light transport simulations; construction and assembly of TTR prototype; provide coordinate measurement stand for One Layer Prototype; provide X-Y scanner and readout for Assembly/Test table; construction of module end mock up
- University of Tennessee : Tile studies - search for the optimal (maximum yield) match of types of scintillating and WLSF materials, quality of the fiber grooves in the tiles and reflecting wrap; production and assembly of One Layer Prototype; Monte Carlo studies; production and assembly of Assembly/Test tables.
- Texas A&M University : Study of tile/fiber longevity in aging environment (temperature, atmosphere, humidity, radiation).
- SSCL group : Operation of SBC prototype in TTR stand; construction, assembly, test and operation of cosmic muon stand at SSCL for module QA.

3.1.4 Proposed Forward Calorimeter R&D and Engineering Program

3.1.4.1 Liquid Argon Calorimeter R&D program

Since the proof of principle for this device has been established by the BNL and CERN beam tests, the main goals for the coming year are to optimize the design shown in Fig. 3.1. This shows a change from the TDR with the forward calorimeter separate from the endcap. The details of interfacing the calorimeter with the beam pipe need more work. Another design goal is have enough material to minimize the singles rate in the muon chambers near $\eta = 3$.

3.1.4.2 Positive Ion Buildup measurement

Positive ions build up in the gaps of noble liquid calorimeters under the high rate conditions of the SSC. In calculations, the effect is parameterized via the unknown positive ion mobility. But single positive argon ions may not be the only positive charge carriers in liquid argon. Some published work suggests that positive argon molecular ions also contribute with varying numbers of neutral argon atoms bound to an argon ion. At least one group measures a current due to positive charges in solid argon. This must surely be due to hole transport. So it is possible that liquid argon also supports hole transport. If two or more mechanisms contribute to the transport of positive charges in argon then a simple measurement of the positive ion mobility could be very misleading when applied to the build-up problem. We propose to construct a simple multicell calorimeter and to simulate the high rate conditions of the SSC in this calorimeter by using our DC high energy X-Ray machine to produce a constant background of ionization at rates in the same range as we will see at the SSC. We will then use a lower energy (25 kV) pulsed X-Ray machine (which we have arranged to borrow from Veljko Radeka at BNL) in order to simulate the passage of a high energy particle. The measurement is simple. We measure the size of the pulsed signal as a function of the level of DC background. Calculations suggest that the signal should be insensitive to the DC background up to some critical value and then the signal should fall quickly above this critical value. We will be able to sweep through this critical value. This measurement is very important for the detailed design of the endcap and forward calorimeters.

3.1.4.3 CQF Calorimeter R&D program

The most crucial requirement for the forward calorimeter in GEM SSC detector is extremely high radiation stability of the technique. Expected doses range up to 500 MRad and neutron fluxes up to 10^{15} per cm^2 per SSC year (at luminosity $10^{33}cm^{-2}s^{-1}$). Recent results obtained by CERN-Strasbourg group [8] show that for some modern types of quartz fibers, the Čerenkov response remains stable at the doses of 2-3 GRad and possibly even beyond that limit. Radiation damage effect studies of quartz fibers have been previously performed for reactor experiments and for waste management applications [12]. Such factors as high OH^- content and purity of quartz material are well established for radiation hard fibers. Considerable improvement of radiation properties of quartz fibers is believed to be connected with surface protection techniques - doped silica cladding with a radiation hard buffer. New

technology is available in US and in Russia to make hermetic metal buffers with copper or aluminum. Fibers with metal buffers are expected to be extremely robust and radiation hard.

A study of radiation damage of CQF will be performed by the irradiation of fiber samples with different sources : gammas, electron beam and reactor neutrons at the irradiation rates not considerably exceeding those anticipated in GEM forward calorimeter. The fiber samples will be 1-10 m long. The spectral transmission of irradiated fibers will be measured in the range of 200 - 600 nm and compared with that for non-irradiated reference fibers. Different types of quartz fibers will be tested including those with metal cladding. Self annealing and thermal annealing effects will be studied. Thermal annealing might be a practical thing which can be implemented in the forward calorimeter design and operation. Measurements of radiation effects with quartz fibers will be performed by the Texas A&M University and University of Tennessee groups. In parallel radiation studies with quartz fibers produced in Russia will be performed in Moscow by the ITEP and Kurchatov Institute groups.

In the scheme proposed for GEM CQF forward calorimeter all fibers are parallel to the colliding beam direction. As it was shown in [8] the light yield captured in the aperture of quartz fiber is maximum if particle producing Čerenkov light is crossing the fiber at an angle of 45-60° relative to fiber axis. Thus for the most of the particles in the hadronic or electromagnetic shower, the detection efficiency is not very favorable in the proposed fiber layout. In Monte-Carlo simulations [9] where these effects were taken into account, the light yield for electromagnetic showers in a copper absorber with the proposed fiber layout is $\sim$3 p.e./GeV. This Monte Carlo prediction can be tested with small prototype of 12×12×30 cm^3 size which is planned to be built at University of Tennessee and ORNL. This prototype will be than tested at ITEP (Moscow) with 1-6 GeV electrons from the ITEP 9 GeV PS to determine the light yield experimentally.

Quartz window PMTs for the small prototype test will be selected and prepared by the University of Iowa group. The spectral response of the PMT tube should be carefully selected because, according to [8], it can help to minimize the radiation damage effect which is minimal for quartz in the range near 400 nm.

A calibration and monitoring scheme will be prototyped by the Fairfield University group and also will be implemented for the small module to be tested at ITEP. In the proposed calibration scheme several additional fibers per readout cell having a $\subset$-shape are embedded in the calorimeter parallel to readout fibers. A light signal is injected into the calibration fibers from the back of the calorimeter through one end of the fiber, then propagates to the front of calorimeter, returns to another fiber end, which is bundled with regular readout fibers, and finally comes to PMT.

The proposed R&D program will be performed during FY'94 before the decision about the construction of a larger prototype for the FNAL beam test will be made.

3.2 Fermilab Beam Test Program

The main goals for the overall calorimeter test will be to verify the parameters of the design listed above. We want to map the EM response and the energy resolution to verify the goals

of the design both in the stochastic and constant terms. We want to verify the details of the shower shape so we can obtain π^0 rejection and pointing. We want to measure the response to hadrons: the energy resolution, the e/π response, and to determine the optimal weighting of the longitudinal layers. We want to map out the barrel/endcap transition region. We want to test the readout electronics in as close to the final GEM configuration as possible.

In addition, the purpose of SBC tests at FNAL is to verify experimentally the design concept of GEM calorimeter system in terms of hadron resolution, punchthrough and muon detection in the combined Noble liquid - SBC system. Particularly important will be to observe that the shape of the hadronic energy resolution is close to a Gaussian and that it does not have long tails which might affect the missing E_T measurements. The GEM calorimeter is longitudinally segmented. Such segmentation might further improve [2] the jet energy resolution if the appropriate calibration constants (or parameters) are found and applied. It is assumed that the calorimeter response will be optimized by the selection of the appropriate weighting scheme.

If the CQF technique is chosen for the forward calorimeter, it will be important to verify experimentally the linearity of the hadronic response over a wide energy range, measure the constant term in the energy resolution, determine the space reconstruction accuracy for hadronic showers and jets, the angular dependence of the response and and any transition effects in the region near the beam pipe.

We plan to test all of these aspects in the beam tests with the following more specific goals:

- Perform full-scale engineering studies of all calorimeter subsystems: mechanical, electronic and cryogenic;
- Achieve full system integration of the electromagnetic and hadronic cryogenic calorimetry, and of the external scintillating calorimetry;
- Carry out a full system test of the calorimeter readout and calibration systems;
- Measure the response of the scintillating calorimetry, and determine the reproducibility of its performance from module to module;
- Study the calorimeter's energy and spacial resolution up to the highest available energies for both electrons and hadrons; for electrons to be sensitive to the expected constant term of 0.4%;
- Investigate the calorimeter's single particle response in the vicinity of representative cracks;
- Study the calorimeter's response to single particles across the barrel to end cap transition region;
- Investigate the calorimeter's response to high energy muons;
- Study the pointing and timing performance for EM showers.

- Study linearity, energy and space resolution of Forward Calorimeter with hadron showers and jets; study effects of material in front of Forward Calorimeter as well as effects of beam pipe hole.

3.2.1 Noble Liquid Calorimeter Testing

To characterize the beam, the MWEST beamline will be instrumented with 50 μm pitch silicon strip detectors capable of tagging the momentum of incident particles to a precision of $\pm 0.2\%$. It will also be equipped with high energy electron identification, using the existing Čerenkov counter augmented by a synchrotron radiation detector to tag very high energy electrons (>200 GeV/c). A versatile calorimeter transporter will be constructed and mounted on the existing MWEST rail system. This transporter will provide for independent horizontal and vertical motions, as well as rotation and limited tilting ($\pm 4°$) capability. The test cryostat will be a double-walled, flanged stainless steel cylinder equipped with a thin ($\leq 0.15\ X_0$) upstream beam window. It will be loaded from one end using an insertion bridge.

Plans call for calorimeter testing using first LAr, and then LKr in the barrel calorimeter. To minimize the amount of LKr required for the second phase of the testing, the cryostat will contain separate bath boxes for the barrel and end cap calorimetry. A comprehensive program of Monte Carlo simulation will provide the critical link between the test beam results and the performance of the operational GEM calorimeter.

Fig. 3.19 displays a plan view of the test cryostat fully loaded. Indicated on the figure is the angular range over which beam testing is to be performed. This range allows a study of the barrel to end cap transition. In order to accomplish this there needs to be a correlation between the transverse and rotational motions to allow the fixed beam to simulate the intersection point for different η.

Figure 3.20 shows an end view of the cryostat as it would be positioned for studies of representative cracks in the barrel hadronic calorimetry; the coupling between the elevation and tilting motions needed to achieve focusing is indicated. We have designed a transporter to allow the needed movements of the cryostat as well as a scaffolding above the cryostat to hold the necessary services such as electronics, cryogenics controls and purification system. This can be seen in figure 3.21.

We plan to test two full-size (4 m long) 9° electromagnetic barrel wedges, each consisting of three readout layers. The barrel hadronic towers will also be full-size, split at 90° into two 2 m long modules, and employing two physical, but three readout, layers. To contain hadronic showers transversely, the inner layer of the hadron calorimetry will contain four modules, on each side of the 90° split. The outer three modules will be shifted in azimuth by 4.5° relative to the inner modules to minimize the consequence of cracks.

The end cap calorimetry will include prototype electromagnetic calorimetry and a total of 10 hadronic towers: 3 (each) outer hadronic A and B modules, and 2 (each) inner hadronic A and B modules. The outer end cap hadronic modules (in radius, relative to the GEM axis) are full-size, while those at larger η (in the GEM context) are special units truncated to fit within the test cryostat. Behind the test cryostat are two full-size wedges of the external scintillating calorimeter.

Our strategy allows great flexibility in the mix of modules included in a given load of the

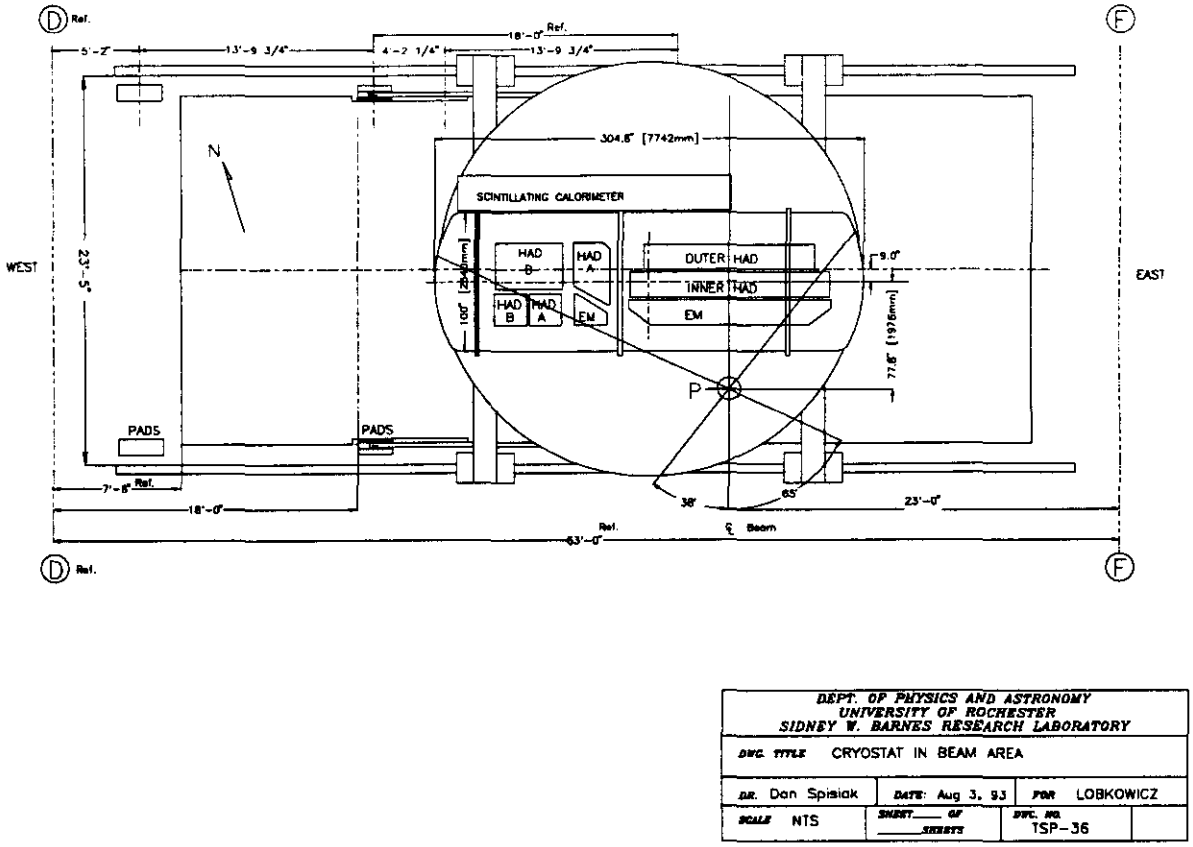

Figure 3.19: Fully loaded cryostat(dimensions in inches).

test cryostat. Options include starting with only one side of the barrel hadron calorimetry, thus postponing the study of the 90° crack, or delaying the installation of some of the end cap prototypes, thus postponing full investigation of the transition region. In particular, the initial round of testing may involve simulated end cap electromagnetic calorimetry, rather than a full-fledged (albeit truncated) prototype module. To accommodate these options, the test cryostat and transporter are being designed to accommodate multiple loads with minimum down time. It is anticipated that MWEST beam time will be available for other GEM test beam purposes during these transition periods.

The plan for the test beam calls for an 18° sector of the EM section. The prototype module will be constructed at BNL and assembled by August 1994. Once the module is assembled it will need to be wired and stuffed with electronics. The next step will be a full test of the module by pulser at liquid nitrogen temperatures. This program will be finished by November of 1994.

The sectors will be transferred to Fermilab for assembly in the cryostat. Upon arrival, the module will be tested by pulser at ambient temperature to search for any problems that might have occurred due to the transport. High voltage tests will also be performed.

Once installed in the cryostat, another test will be made with pulsers to check the in-

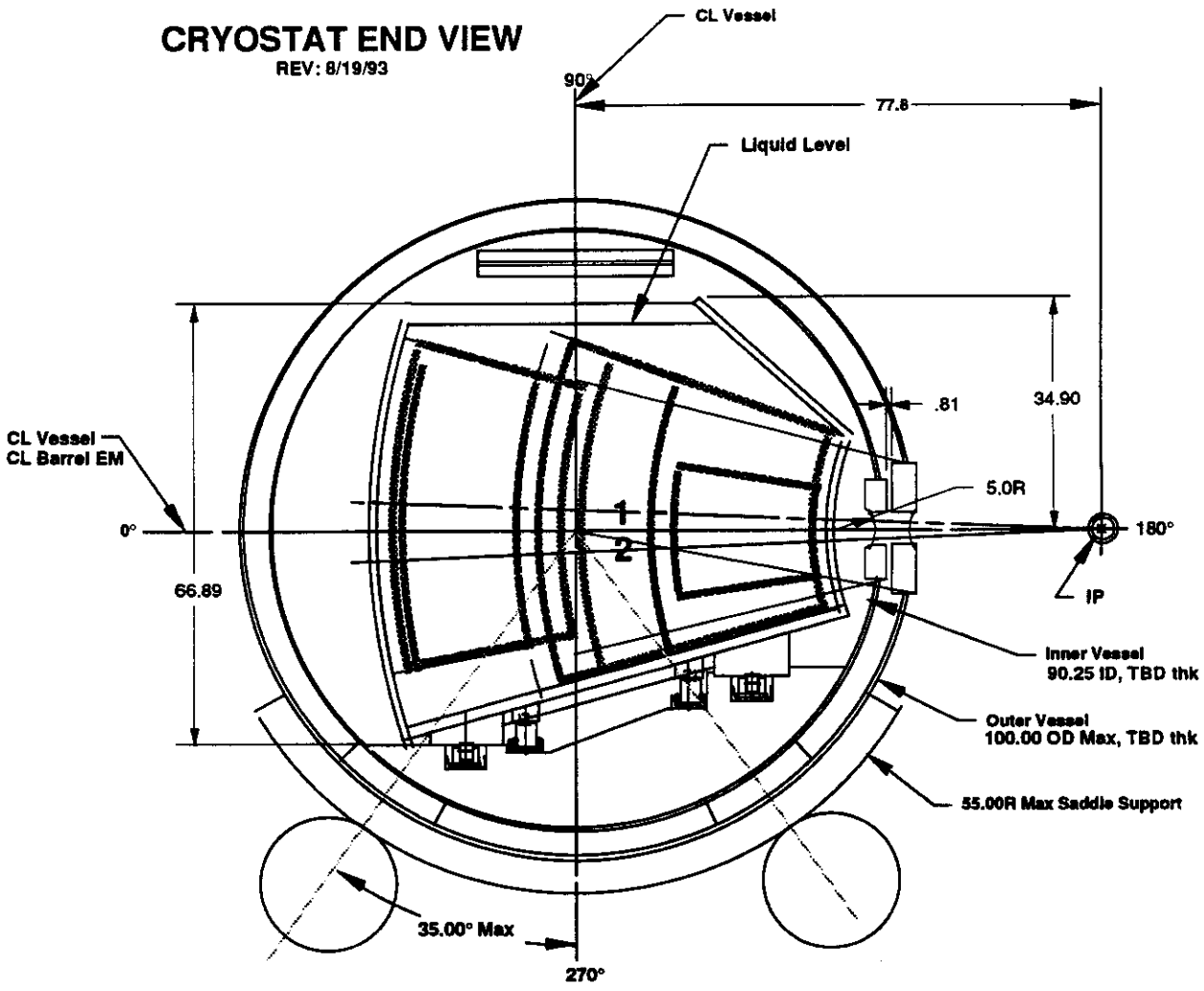

Figure 3.20: Endview of cryostat(dimensions in inches).

stallation procedure before the cool down. If all tests are satisfactory and the rest of the calorimeters are installed the sectors will be cooled and a last pass test will be made.

3.2.1.1 Evolution of Test Program

The test of the calorimeter module will start at the BNL site where the electronics will be tested before shipping. Here, we will require a fairly complete data acquisition system that can read a minimum of 500 channels and allow us to test the entire calorimeter in a timely fashion.

The calorimeter will then be transported to Fermilab. Since initially only a small part of the calorimeter will be read out (probably an array of 12×12 towers, or 433 channels), a calorimeter scan will involve moving cables when the beam is to be directed to regions with no readout boards. All the preamps and calibration hybrids will be already installed and tested. Track-and-hold digitization and will be used, the latter starting late in 1995.

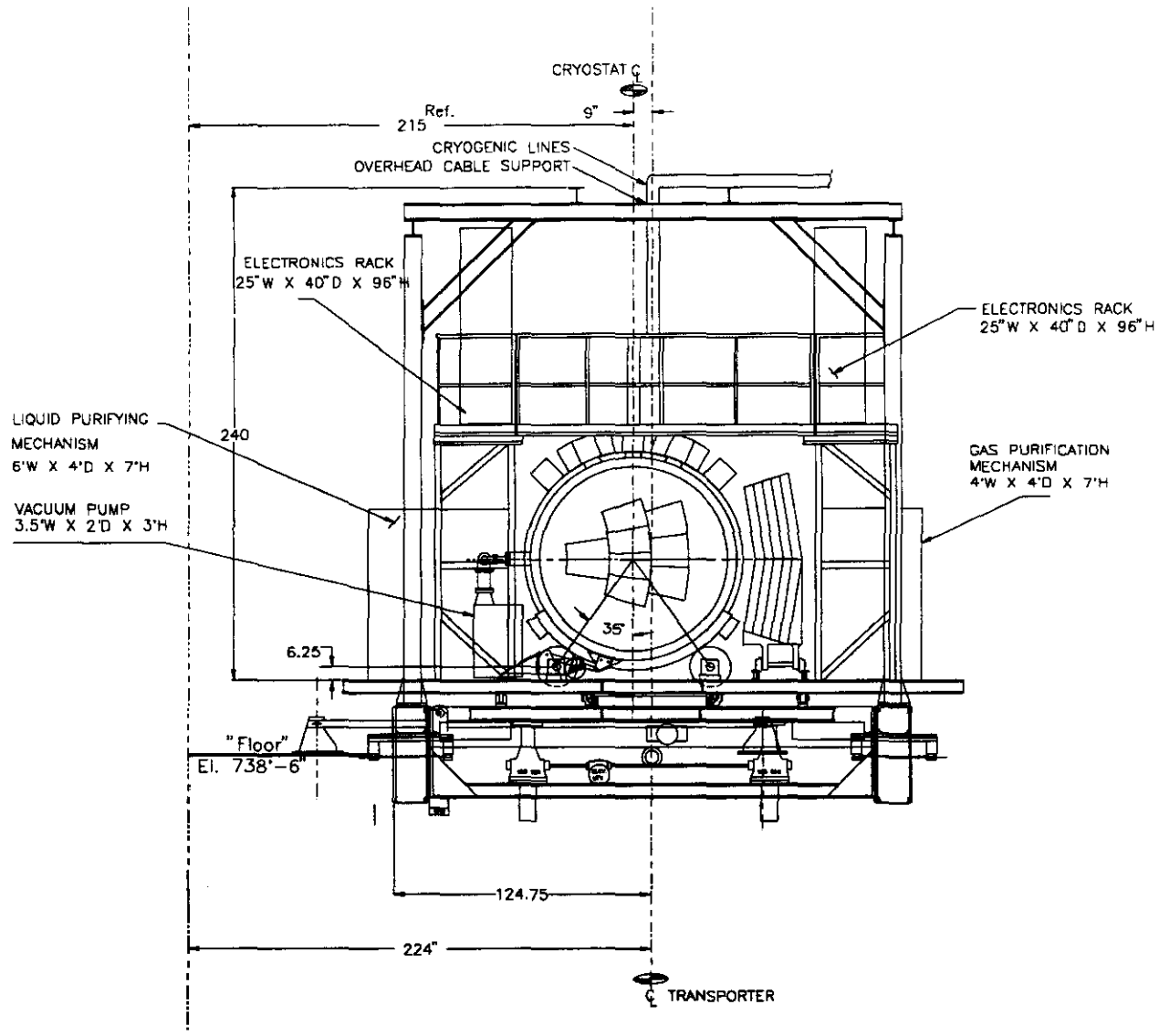

Figure 3.21: Elevation view of test beam cryostat showing the transporter, the structure holding electronics and other systems on top. (Dimensions in inches)

The second stage involves reading as many channels as we can, but at lower data acquisition rates. This type of readout will be geared towards studies such as coherent noise in a large scale and possibly to acquire data where events will be triggered. Thus it assumes that all the final GEM readout boards are present.

3.2.2 Cryostat

The test beam cryostat has been designed to allow easy implementation of the 18° calorimeter sector test. It consists of a pair of nested cylindrical vessels. The outer vessel provides insulating vacuum for the inner cold vessel. The cold vessel houses two containers that hold

the modules. These aluminium bath boxes mimic the GEM calorimeter vessels. The wall thickness of the bath boxes at the front of the electromagnetic modules matches that of the GEM calorimeter. In order to prevent showering upstream in the cylindrical vessel walls, thin windows are used. These windows accommodate the 8° that the vessel will roll on the transporter, as well as 100° about the nominal interaction point (about the transporter's vertical axis). The GEM module mounting scheme is used. The end walls in the region between the bath boxes match the thickness of the GEM calorimeter vessel head walls. The relative placement of the modules of the barrel with respect to endcap modules is also matched. Internal structural stays used in GEM are also built into the bath boxes.

We use bath boxes in the cryostat design in order to limit the amount of liquid krypton needed to affordable quantities. The bath box volume in excess of that needed for the modules is filled with excluder material to lower overall volume of krypton required. Two condensing coils, one for each bath box, are used. These are located at the top of the cylindrical vessel and allow the filling of either bath box with krypton, and both with liquid argon. The cool down, which will follow several warm gas purge and fill cycles, will require five days. Provision has been made to withdraw liquid from the bath boxes in order to purify it. The system planned allows for both liquid and gas phase purification. Feed-throughs which are pre-production prototypes of those planned for GEM will be used to pass signals through the cryostat.

The modules will be loaded into the bath boxes, using manipulator hardware developed for GEM, on a stand located outside the shielding wall. The bath boxes are then rolled into the cryostat vessels and locked down. The use of two bath boxes allows more flexible scheduling of module production.

The overall length of the cryostat is 305 inches, and its outer diameter is 100 inches.

3.2.3 Transporter

During the last 8 months U. of Rochester has designed a transporter which can move and rotate the test calorimeter modules inside their cryostat so that the MWEST beam (which has a fixed location and direction) can impinge on any one of the various modules to be tested. This design has undergone a detailed review at SSCL. The transporter allows the modules to be moved sidewise and up/down as well as rotated about a vertical axis and one horizontal axis. All motions are remotely controllable and positions can be read out to ± 1 mm.

The cryostat riding on top of the transporter and holding the actual modules is being designed by SSCL engineers; U. Rochester is coordinating the designs of the features external to the cryostat, such as cryogenic plumbing locations, electronics racks locations, cabling etc.

The EM calorimeter module to be tested at Fermilab during the 1995 fixed target run is a 18° sector of the GEM electromagnetic (EM) barrel calorimeter. Since the complete description of the device can be found in Chapter 5 of the GEM TDR [1], only a brief description is given here. See also section 3.1 for more details.

Although Monte Carlo calculations indicate the proposed design will meet the GEM bench mark requirements and extrapolation from other calorimeters support this conclusion, the beam tests will provide a direct check on their performance and design. We will also

measure their performance in liquid krypton and these results compared to those from the lead barrel modules in liquid krypton. We will also study and calibrate the barrel endcap transition region. We will use the results from measuring both the barrel and endcap modules in liquid krypton and in liquid argon to infer the correct weighting when the barrel modules are in liquid krypton and the endcap modules are in liquid argon. In addition the effects of the cracks between modules will be measured and calibrated. We also plan to make 7 barrel modules from lead tiles and 7 barrel modules from copper tiles to make a direct measurement of the difference in response.

3.2.4 Scintillating Barrel Modules

Two modules need to be produced for FNAL tests. They will cover an azimuthal angle of 36°. Larger azimuthal acceptance is needed to contain completely the hadronic showers within the desired 18° working region. Two modules will also allow a scan of the "dead region" between modules in order to study its effect on the energy resolution. According to the existing prototype construction plan (see Table 3.1), the SBC modules will be assembled in May-June 1995 and after acceptance tests will be transported to FNAL and installed on the support behind the noble liquid cryostat in August 1995 so that the combined calorimeter test can be started at the proposed time. Additional area at MWEST figure 3.22 near the calorimeter transporter will be required for loading modules Figure 3.23 on the support which can move in on the rails into its place on the transporter. The cost estimate of SBC prototype construction as well as the cost of R&D program outlined above is given in table 3.2.

The study of hadronic response of the combined noble liquid - SBC system should be performed with the hadron beam in the energy range 10 - 800 GeV (or highest possible energy) in order to study the energy dependence of the weighting coefficients. These measurements will require sufficient statistics in order to obtain enough events with late developing showers. To enhance the sample of events with late developing showers one can use in the trigger: the signal from the SBC itself or perhaps a counter positioned behind the SBC module which can measure the amount of energy escaping from the back of SBC. Data should also be taken with the muons of various energies in order to study the accuracy of measurement of catastrophic energy losses in calorimetry. Muons can be selected by a trigger based on the signals from an additional 5-10 λ small longitudinally segmented calorimeter positioned downstream behind the SBC modules. Prototype of the forward calorimeter described in the next section can be used for that.

It is assumed that data collected in the hadron and muon runs will be used for compilation of the data bank which will be used in more realistic simulation of hadronic jets in the GEM calorimetry. Measurements with the known hadron beam energy will allow the absolute energy scale calibration (for hadrons) provided that an adequate monitoring system will be installed and operational in these tests. The scheme of monitoring discussed in GEM TDR [1] with a distributed light source to each tile (via thin quartz fibers) will be implemented in these modules. Muon response of SBC modules also can be used for monitoring of the low side of the dynamic range of hadronic response.

Since the SBC modules in these tests will operate in a non-magnetic environment, regular green extended photocathode PMTs can be used, though it is very desirable to use the final

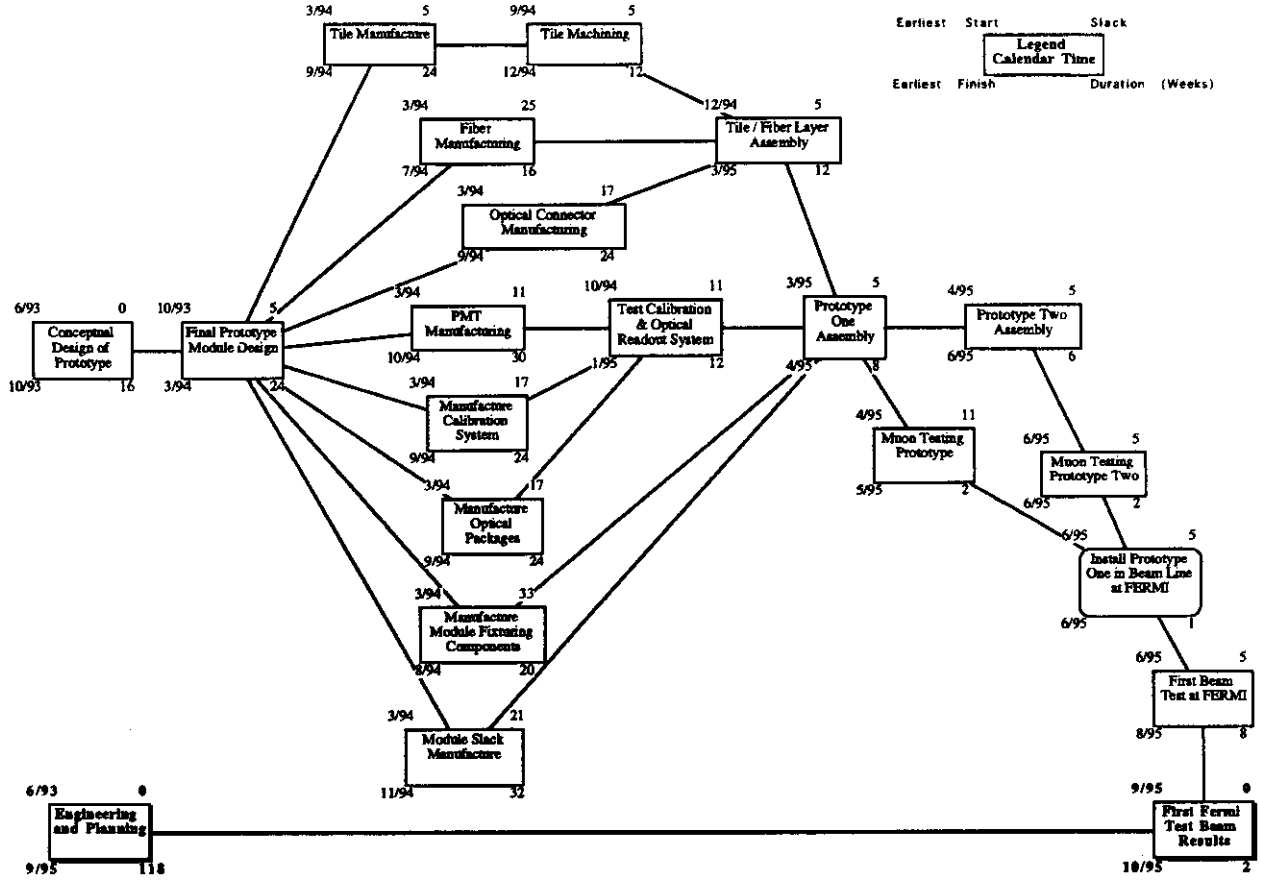

Table 3.1: Construction schedule of SBC prototype for FNAL tests

PMTs tolerant to the magnetic field , since the dynamic range, stability etc. of these could be different.

3.2.4.1 Quartz Fiber Forward Calorimeter Prototype

CQF is a relatively new technique in calorimetry and R&D efforts are required in order to verify light yield, radiation hardness, and to devise/test the calibration scheme. For the FNAL beam test a prototype of CQF hadron calorimeter based on spaghetti principle with thin 300μ core diameter quartz fibers embedded in the copper absorber is being planned, though the final decision on the construction of hadronic prototype for FNAL tests will be made only after the results of CQF R&D work will be available. According to present plans (Table 3.3) R&D studies will be performed in FY'94 in parallel with engineering development of CQF calorimeter concept. Construction of FNAL CQF prototype calorimeter will start in FY'95 and prototype will be available for FNAL beam tests in early FY'96.

A prototype shown in Figures 3.24 and 3.25 which is sufficiently large transversaly and longitudinaly to detect hadronic showers can be constructed for the FNAL beam tests.

The purpose of FNAL test of CQF is to study the performance of the device for the detection of hadrons and hadronic jets of very high energy. In the collider environment large

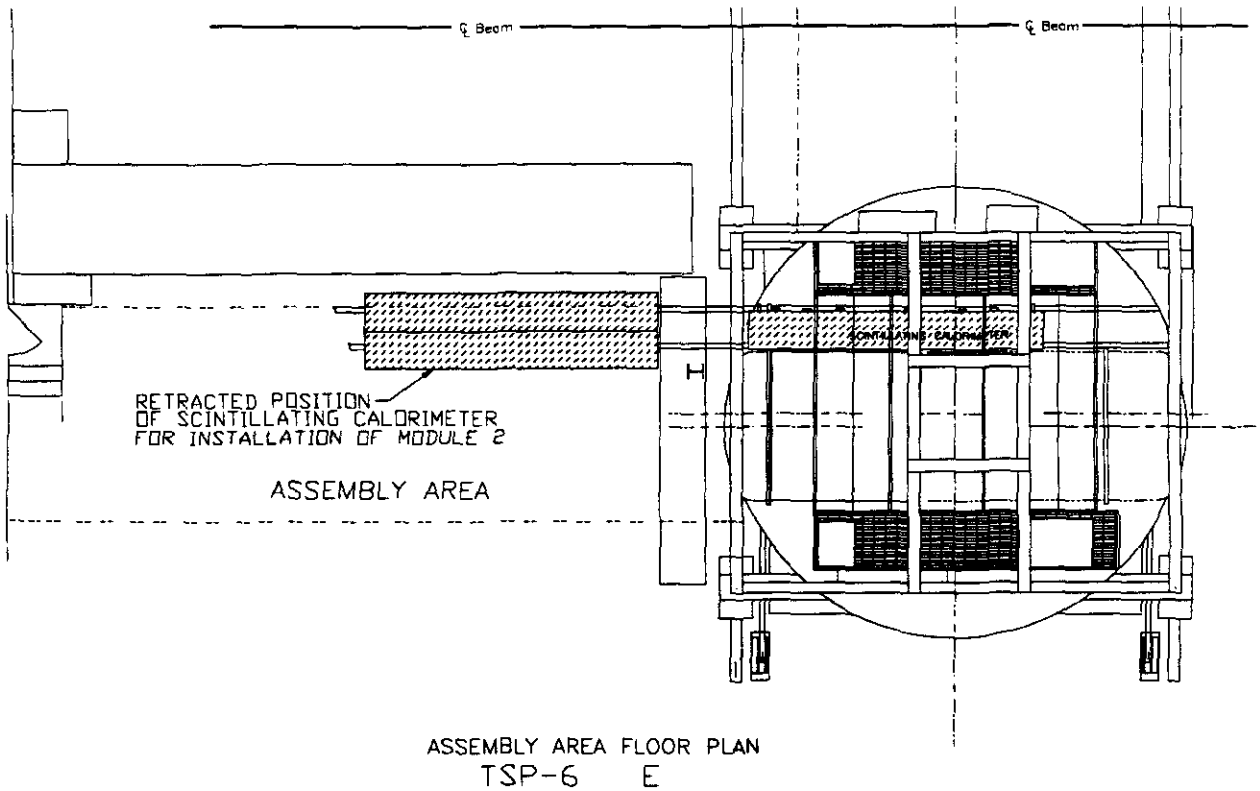

Figure 3.22: SBC Assembly Area Floor Plan in MWEST

p_T of interest (> 50 GeV/c) in the forward direction ($\theta < 0.1$ rad) can be only produced by hadrons and jets with the energy > 500 GeV and higher. This is the reason why forward calorimeter prototype should be studied and calibrated at the maximum available energies. For the forward calorimeter modest energy resolution (constant term 10%) is adequate but the response shape should be close to gaussian without significant tails. Objectives of the FNAL beam test of the quartz fiber prototype are the following:

- Measure light yield for electron and hadron showers;
- Test the linearity of hadronic response in the whole energy range;
- Study EM and hadron energy resolution;
- Study space resolution for electrons and hadrons showers;
- Study energy leakage effects and particularly leakage effects near the simulated collider beam pipe;
- Develop and test calibration and monitoring system;
- Study radiation induced effects in the CQF calorimeter.
- Study effects of dead material in front of CQF calorimeter.

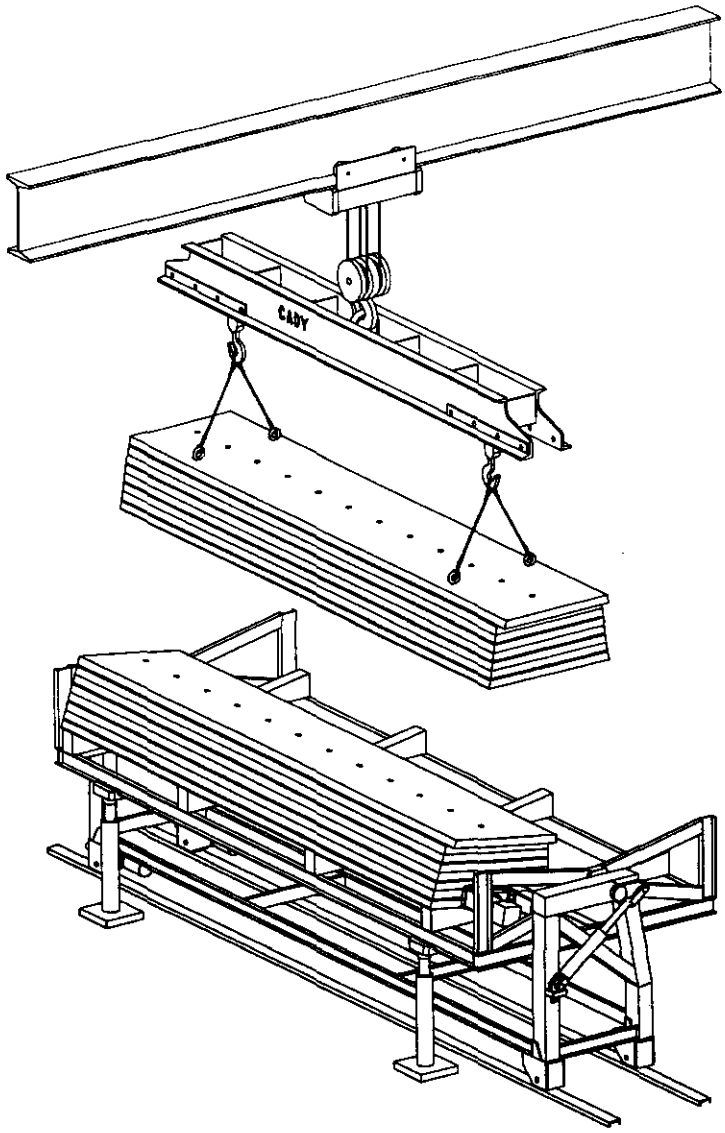

Figure 3.23: Loading SBC Modules on the Support

Proposed CQF calorimeter can have as low as 3-7% active sampling fraction of quartz fibers to provide required energy and space resolution. Though hadron part of GEM forward calorimeter is planned to be made out of tungsten, in this prototype copper absorber will be used for reasons of mechanical simplicity. It is assumed that copper absorber will be sufficient for the prove of principle of CQF detector and for tuning of Monte Carlo codes describing the calorimeter.

The forward calorimeter prototype should be deep enough to absorb highest particle energies in the beam test: 9 λ or 150 cm length of Cu absorber will be adequate. The transverse size of 50 $\times$ 36 cm^2 should be sufficient to absorb shower in the lateral direction (radius $< 1\lambda$) and to allow measurements at the angle up to 6° without essential energy leakage. The weight of the prototype is 2200 kg.

A. R & D Studies

	FY'94	FY'95	FY'96	Total
1. Tile Studies	$45,000	$30,000		$75,000
2. Calibration / Mon Prototype	$30,000	$12,000		$42,000
3. PMT Studies	$30,000			$30,000
4. Electronics Development	$30,000			$30,000
5. TTR Prototype	$60,000			$60,000
6. Opt. Connectors & Fiber Joints	$12,000			$12,000
7. One Layer Prot.	$65,000			$65,000
8. Module End Mock Up	$11,000			$11,000
9. Longevity Study	$25,000	$25,000		$50,000
10. Monte Carlo	$10,000	$10,000	$10,000	$30,000
11. Misc. + Intern. Travel	$55,000	$45,000	$25,000	$125,000
12. Personnel (Postdocs, Students)	$106,000	$200,000	$250,000	$556,000
Total	**$479,000**	**$322,000**	**$285,000**	**$1,086,000**

B. FNAL Prototype Construction

	FY'94	FY'95	FY'96	Total
1. Module Stacks		$249,000		$249,000
2. Tile Layers		$142,000		$142,000
3. Readout Electronics		$116,000		$116,000
4. Assembly			$50,000	$50,000
5. Test Structure		$53,000		$53,000
6. Transportation			$19,000	$19,000
7. Tile Assembly & Test Table	$60,000	$55,000		$115,000
8. Other QA Equipment	$40,000	$20,000		$60,000
9. Muon QA Stand	$70,000	$170,000		$240,000
10. Test Operation		$50,000	$100,000	$150,000
11. Engineering	$640,000	$640,000		$1,280,000
Total	**$810,000**	**$1,495,000**	**$169,000**	**$2,474,000**

Table 3.2: Cost Estimate of SBC Prototype Construction

The prototype module will be assembled as a stack of 2 mm thick copper sheets (width 50 cm, length 150 cm). Sheets will be bonded by low temperature foil soldering under pressure. Copper sheets will have machined grooves along the length of the sheets. The distance between grooves will be 2.3 mm and grooves should be large enough to accommodate 3 fibers with OD 360 μm each (core diameter 300 μm). The volume sampling fraction in this way will be 6.6% and average distance between fiber triplets will be 2.3 mm (which can be compared with $\sim$ 13 mm Moliere radius in Cu). Transverse segmentation will be arranged at the level of fiber grouping in front of the quartz window PMT. A front electromagnetic section will be created by pulling back every third fiber in each grove by $\sim$ 30 cm (as it is

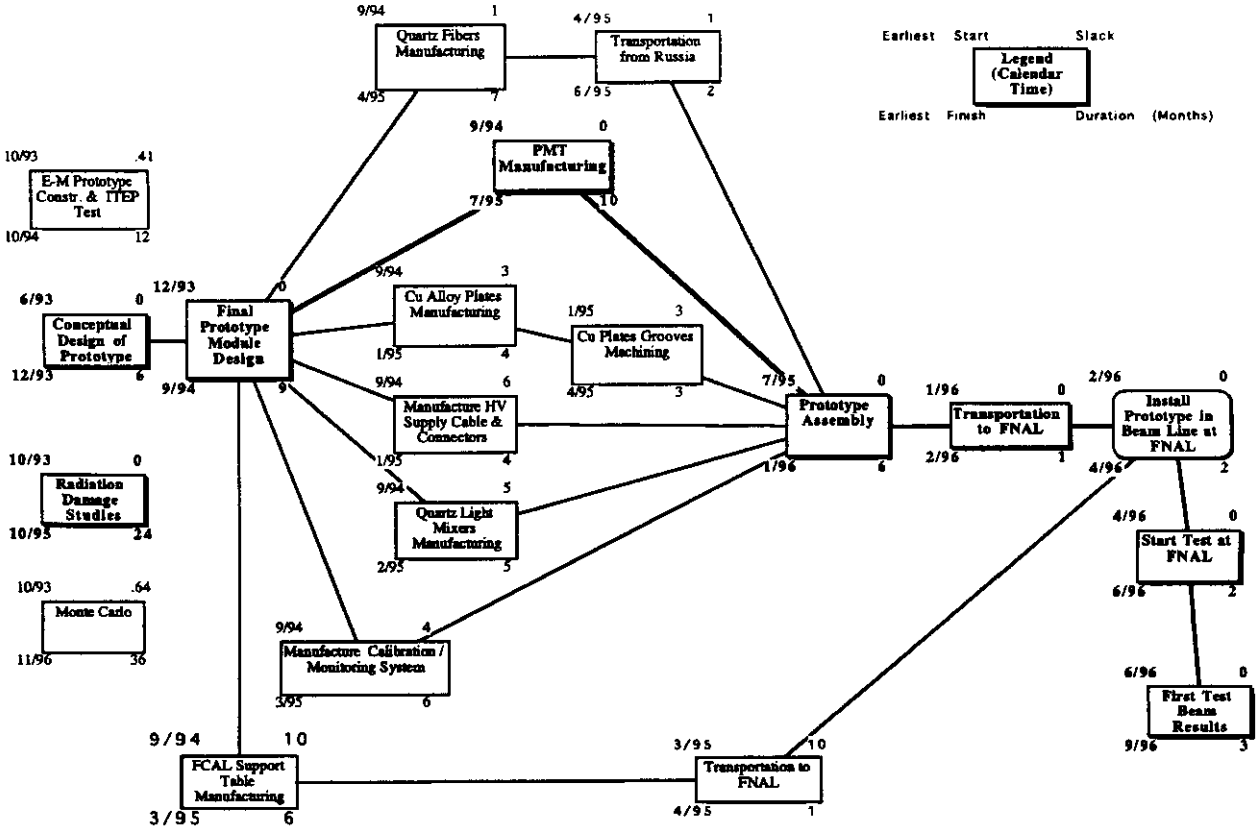

Table 3.3: R&D and FNAL Prototype Construction Schedule of Čerenkov Quartz Fiber Calorimeter Group

optimized by MC simulations) and reading out short and long fibers separately by two PMTs for each $\Delta r \times \Delta\phi$ cell. Information from these two readouts can be used for e/π correction in the detection of hadronic jets. In addition the effective longitudinal segmentation will allow improvement in the spacial accuracy of impact point reconstruction as it was shown by MC simulations of hadronic jets incident to the forward calorimeter at different angles between 0° and 6° [9]. Figure 3.24 gives the lateral size of the prototype module, outlines the region where fibers will be installed and shows the embedded projected beam pipe hole. The former feature will allow direct measurement of the behavior of hadronic showers in the region which is rather difficult to simulate and analyse by Monte Carlo.

In Fig. 3.25 transverse segmentation can be flexibly arranged by grouping QF in front of the readout PMT. The segmentation should be close to one in the GEM forward calorimeter and is the subject of further Monte-Carlo optimization. The total number of readout channels in the prototype will be around 140 (for both short and long fiber groups). There will be also a possibility to arrange three longitudinal sections by pulling each of three fibers in the groove to a different length. Advantages and disadvantages of this arrangement will be also studied later by Monte Carlo simulations.

It is anticipated that after the exposure to the test beam the absorber activation can be measured and resulting level can be scaled up in order to compare with simulations made by

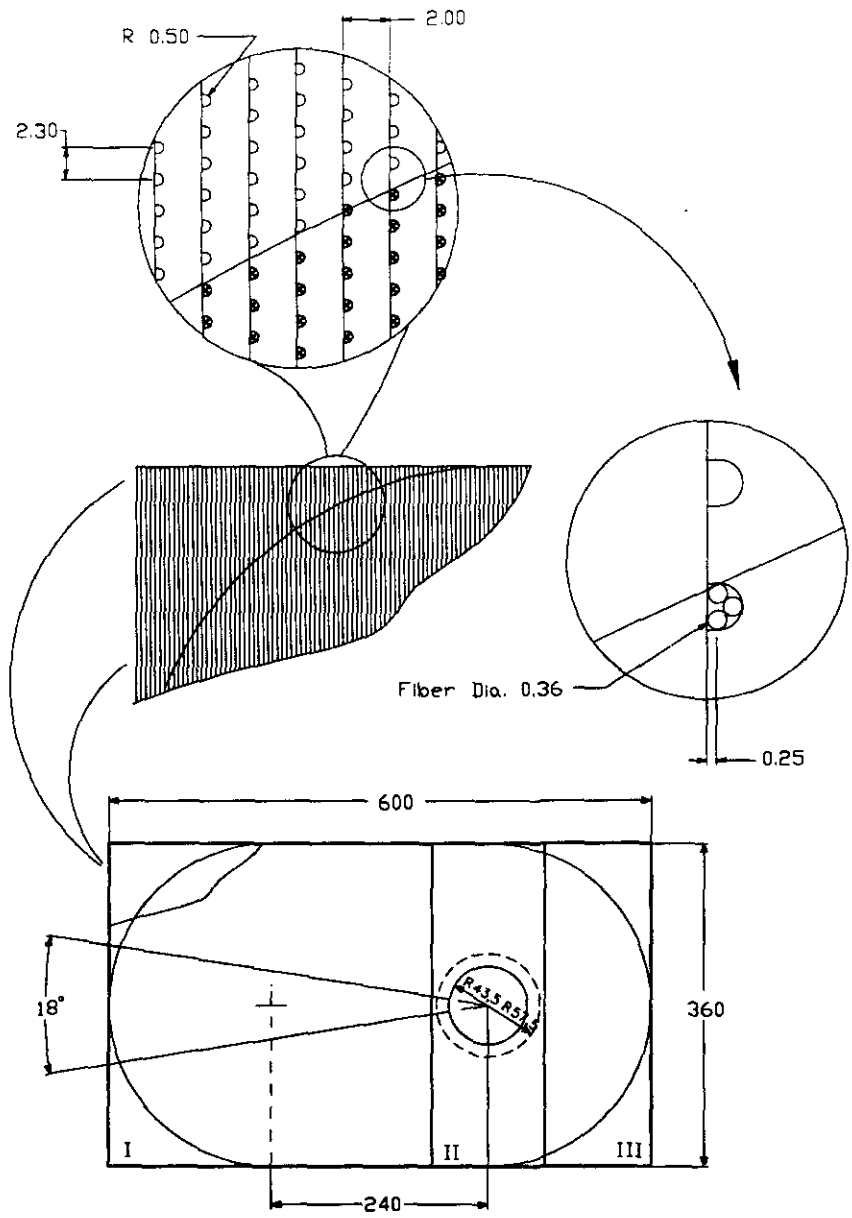

Figure 3.24: Basic Structure of the Forward Quartz Fiber Prototype Module for Fermilab Tests

activation codes [10]. Since the construction will allow splitting the module in the vertical plane, it will be also possible to measure activation "inside" the calorimeter absorber which will be particularly interesting for comparison with simulations.

The CQF prototype will be installed in the beam line on a separate support table which will allow rotation within ±6° and transverse movement in the horizontal plane. The CQF prototype on the test stand is shown in Fig. 3.26.

Table 3.4 gives the cost estimate of R&D work and CQF FC prototype construction for FNAL beam tests. It is expected that a significant part of the prototype manufacturing

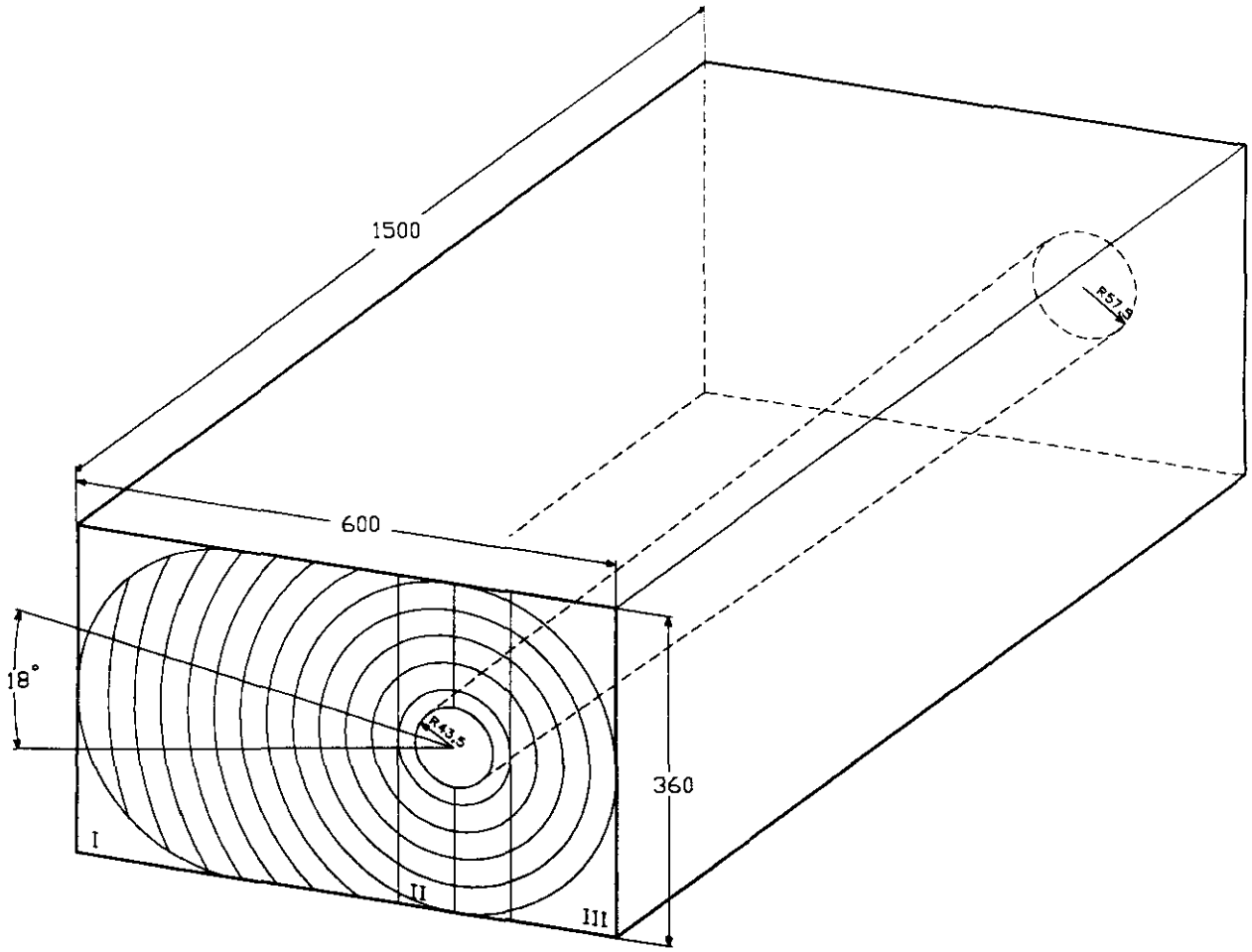

Figure 3.25: Forward Quartz Fiber Prototype Option with Simulated Beam Pipe

and assembly will be done by two Russian institutions (ITEP and Kurchatov Institute). It is also expected that radiation hard quartz fibers for the FNAL hadronic prototype will be produced in Russia. In this case ITEP and the Kurchatov Institute will cover 2/3 of the US market quartz fiber price which will be equivalent to the contribution of 480K US dollars from the Russian side. Under this arrangement, the cost of fibers used in Table 3.4 was assumed to be \$1.0 per meter.

Tasks assignments by institutions participating in CQF project are listed below:

- ORNL : Engineering, coordination of R&D.
- Fairfield University : Calibration system prototyping; calibration system assembly in beam tests prototypes.
- University of Iowa : Quartz window PMT selection and assembly for beam tests.
- University of Tennessee : construction of small EM prototype to be tested at ITEP; quartz fiber radiation damage studies with gamma source; Monte-Carlo simulations.

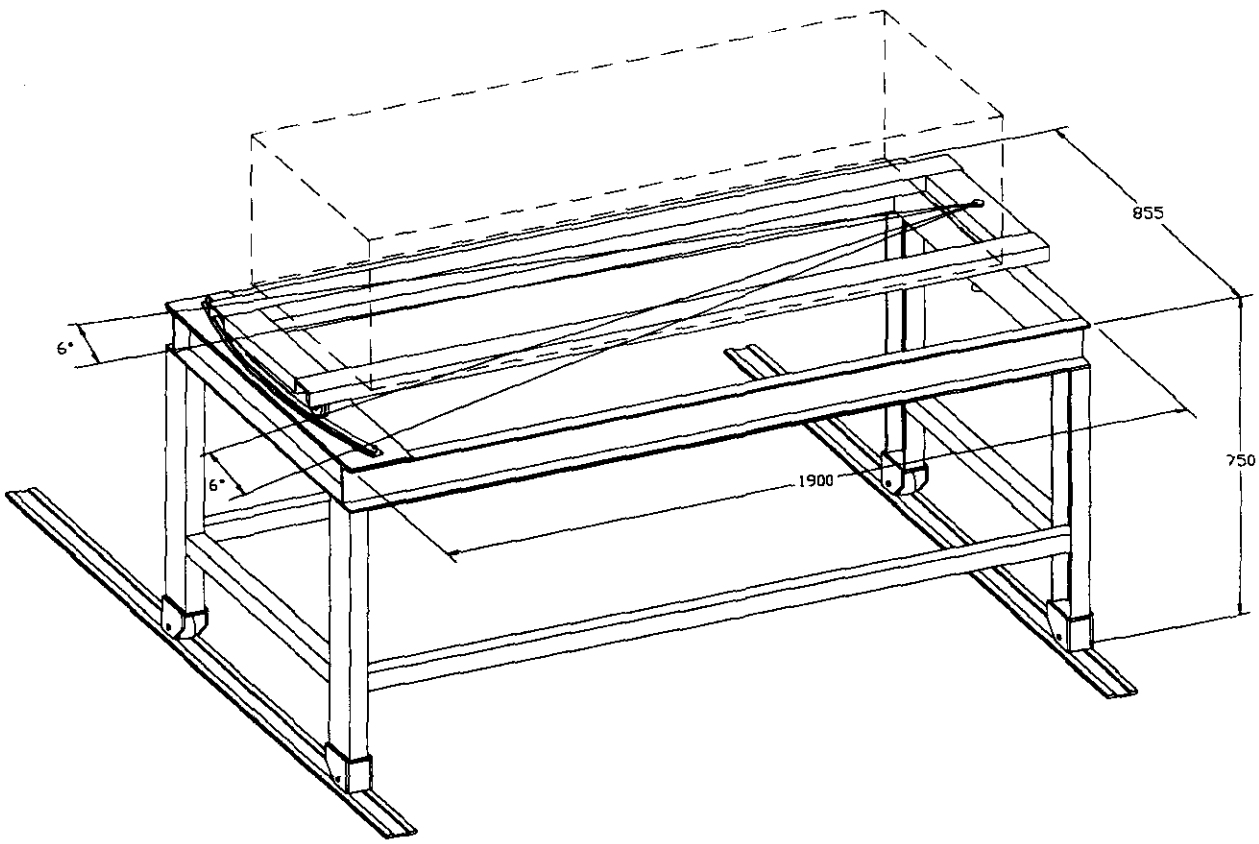

Figure 3.26: Quartz fiber prototype of the test stand.

- Texas A&M University : Radiation damage studies of quartz fibers with electron beam and reactor neutrons; Monte-Carlo simulations.
- ITEP and Kurchatov Institute (Moscow): Supply of radiation hard quartz fibers produced in Russian industry; radiation damage studies of these fibers; provide beam test facilities at ITEP to test small size prototype.

3.2.5 Electronic Readout

In the noble liquid section of calorimeter signals from the strip and square towers pass through three stages of amplification and shaping before they are digitized (see figure 3.27).

The induced charge on the readout electrodes is boosted by charge-sensitive preamplifiers located as close as possible to the physical module. These therefore operate at cryogenic temperatures. The output signals are carried by 50 Ω stripline cables up to a feedthrough connection at the wall of the cryostat.

When they exit the cryostat, the signals are boosted by differential line drivers and are sent via individually shielded twisted pair cables to shaper amplifiers. A shaping time of 40 ns will be used for the barrel EM module while the hadron signals will use a shaping time of 100 ns. Lastly, the signals are digitized and collected by the data acquisition system.

	Quantity	Units	Unit Cost	Cost	Cont.	Subtotal
1. Radiation Damage Studies						$65,000
2. E-M Prototype Constr. & Test	1	unit				$40,000
3. Calibration & Monitoring System	1	unit		$29,000	10%	$31,900
4. Quartz Fibers ***)	240000	meters	$1.00	$240,000		$240,000
5. Cu Alloy Plates	6400	lb.	$1.90	$12,160	7%	$13,011
6. Cu Plates Grooveing (labor included)	600	hrs.	$39.47	$23,682	10%	$26,050
7. PMT+ Bases	138	unit	$1,000	$138,000	5%	$144,900
8. Qaurtz Light Mixers	138	unit	$300	$41,400	11%	$45,954
9. FCAL Support Table	1	unit		$24,000	9%	$26,160
10. HV Supply, Cables & Connectors	1	unit	$11,000	$11,000	9%	$11,990
11. Transportation				$3,000		$3,000
12. Miscellaneous Items for Assembly	1	unit	$15,000	$15,000	13%	$16,950
13. Assembly, installation (labor included)	1020	hrs.	$20	$20,400	30%	$26,520
14. Monte Carlo				$30,000		$30,000
15. Misc. + Travel						$70,000
16. Design & Engineering				**		**
Total Cost						**$791,435**

** *Design & Engineering will be Provided by ORNL Engineering Group within GEM SBC project funding.*

***) *Russian price*

Table 3.4: Cost Estimate for Čerenkov Quartz Fiber Forward Calorimeter R&D and FNAL Prototype Construction

The number of readout channels in SBC and FC is considerably lower than in noble liquid calorimeter sections. For readout of SBC and FC a similar electronics scheme will be used with modifications necessary to adopt to the different sensitivity, dynamic range and shaping time.

3.2.5.1 Calibration

Instead of coping with the difficult task of accurately distributing analog signals of calorimeter-like waveforms throughout the detector, the calibration circuitry shown in Fig. 3.27 generates pulses *in situ* using a RC-network at the input of each preamplifier. An individual channel can be selected for calibration by appropriately biasing the *select* line. A *clock* signal with sharp rise time injects a known amount of current, I_{Cal}, into the preamplifier. Although the RC network does not reproduce the triangular shape of the calorimeter pulse, only the rising edge of the pulse needs to be reproduced with fidelity since the shaping time is short.

Calibration schemes of SBC and Čerenkov Quartz Fiber Forward Calorimeter are based

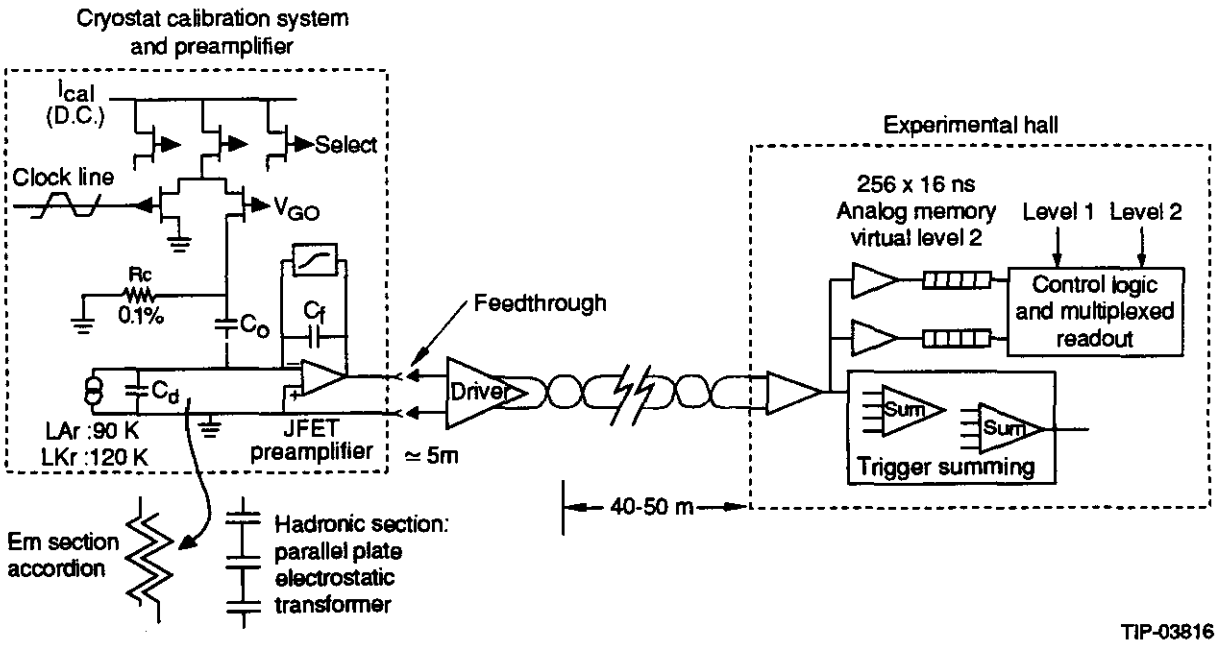

Figure 3.27: Electronic readout chain.

on the distribution of light signals from stable light source, cross monitored by reference devices, to the readout element of the calorimeter like tile, group of tiles or readout tower. Absolute calibration (conversion to GeV) should be obtained in FNAL beam test with optical calibration/monitoring system working in parallel. Cross check calibration between different readout towers can be also obtained with punch through muons, though they calibrate only the low end of dynamic range.

3.2.5.2 Electronics-Hardware

The electronics hybrids containing the preamplifier and the calibration circuits will be mounted on motherboards, along with the preamps and calibration hybrids. The motherboard provides DC power for these components, and also distributes calibration current and select signals. The preamplified signal will be available in multipin connectors on the motherboards. Lines carrying the current and select signals are not critical, but the clock line is an embedded 50 Ω transmission line. The clock signal is injected at one place in the motherboard, which means that a delay for each node must be determined and then implemented when calibrating.

3.2.5.3 Grounding and Power Requirements

To keep any external noise at a minimum, ground loops should be avoided at all cost. The cryostat itself should be connected to the electronics ground and should be isolated from the cryogenics and the transporter. This configuration was successfully implemented during the 1992 test beam at BNL, where the measured noise was mostly due to electronic thermal noise. In addition, the power for the electronics such as preamplifiers, shapers, and the DA

system should be isolated from regular power. This can be achieved by means of isolation transformers.

3.2.5.4 Front End Electronics

The readout electronics will be located in several places. Preamplifiers and calibration circuits will reside inside the cryostat and will operate at liquid krypton/argon temperatures. The connection between the motherboards and feedthroughs are made via 50 Ω stripline cables. Due to the arrangement of the test module inside the cryostat, (i.e. feedthroughs in one side), the cables from one of the halves will be different than the real GEM detector.

The junction boxes containing the line drivers will be mounted outside the cryostat and as close as possible to the feedthroughs. A short run from the feedthroughs to the junction box will be made using strip line cables similar to those inside. Outside the junction boxes, individually shielded twisted pair cables will be used to carry the signals to the shapers. These cables will be 40 m long, similar to that proposed for the GEM detector.

There are two options for housing the shapers. One is to use the same shapers modules used in the 1992 test run at BNL, and the other to use shapers in modules that will be used in the GEM experiment.

A module from the past test run contain 48 channels of shapers in a single Fastbus size board. Individual channels can also be turned on or off by computer control. Although the modules are housed in fastbus cards, a serial link protocol is used to program the modules, which allows them to be located far from the main Data Acquisition computer. In the second option the shapers will be mounted on $9U$ VME size modules.

In either case a sum of all signals handled by each board will be generated. The partial sums will be added together to generate the total energy signal.

3.2.5.5 Digitization Options

There are currently three different schemes in which data can be digitized before being stored on mass media.

1. Track and Hold plus conventional ADC. In this option a track and hold circuit is used to keep the information from the peak of the shaped signal for later digitization using conventional ADC's. In this option due to the required dynamic range, i.e. measure electrons of up to 150 GeV and noise at the level of 16 MeV a dual range ADC is required. Therefore the LeCroy 1885 ADC is the most adequate. In this mode of operation the time when the Hold signal is given to the T&H modules is critical. Given the shaping time the Hold signal should match the peak of the signal to within $\pm$2ns.

2. Multisample Data. In the later part of the test run in BNL the Zeus pipeline ADC was used to collect multiple sample data. The same electronics can no longer be used at Fermilab due to the dynamic range. To replace the Zeus pipeline we plan to build few modules that will house flash ADC's with 10-12 bit precision which can run at 40 MHz or synchronous with the accelerator RF signal. The digitizers will be housed in

VME boards. This will be used to digitize sum signals and in dedicated runs individual channels where most of the energy is deposited.

3. GEM electronics. At later stage of the test beam, GEM boards will become available in prototype form. The initial production might be restricted to 500 channels and enough to test a 12×12 tower configuration. At later stages more electronics may become available as more experience is gained in handling the modules. It is the current plan to house the modules in 9U VME boards with 36 channels per board. Each board will contain a summing circuit with the purpose to generate the sum signal corresponding to a trigger tower. The board will have an on board DSP for on-line data reduction.

3.2.5.6 Miscellaneous Electronics

The calorimeter test will require a small number of electronics channels that will be dedicated to the measurement of timing performance, so precision TDC modules—either CAMAC or Fastbus—are needed. CAMAC modules with 25ps/channel resolution such as the Phillips 7186, seem more appropriate. If a large number of channels is required the LeCroy 1875 TDC could be used.

The discriminator which will handle the total energy sums will be built by the University of Pittsburgh.

3.2.5.7 Calibration Procedure

The calibration of the calorimeter will permit a relative gain equalization of the electronic channels. Using the sum signal as a reference, individual channels are pulsed and read out using the normal readout channel. The calibration is automated and hence requires electronics modules which can be computer driven. In addition to activating the lines shown in Fig. 3.27, the differences in propagation time of the clock signal to different locations in the motherboard must be compensated for by the computer via a programmable precision delay generator.

The select lines can be activated by a CAMAC module such as an output register. The current sources can be set by a DAC with 12 bit precision or more. The clock in this case can be a free running pulser with appropriate delay inserted between the actual clock signal and the trigger. In the past run we used the Stanford Research System Model DG535 GPIB driven precision delay generator which has a stability of 5 pc and delay steps of 50 ps.

The calibration system should be able to select the channels to be calibrated, ramp the current source and obtain the gain for those channels, repeating the process for all channels.

A calibration run should generate a file with gains of each channel. We also anticipate making calibration runs in which data will be written to tape. This is most likely to happen when multiple sample data is taken for the purpose of understanding pulse shape in addition to the gain of each channel.

3.2.6 Data Throughput

At the start of the calorimeter module test we intend to connect a tower configuration of 12×12, or 432 channels, to the track-and-hold + fastbus electronics, similar to that used in the past run. With this conventional system we are confident that most of the readout problems can be worked out and will permit a good understanding of the calorimeter. If it is necessary to read other towers, the electronics can be rewired accordingly. We don't anticipate suppressing zeroes at this stage.

In the second stage, multiple sample data can be acquired using one of the schemes mentioned above.

Assuming a trigger mix rate of 100 events/s in the first case, the expected data rate from the EM section will be 86.4 kBytes/s, assuming 16 bit words. For the multiple sample date the number of samples is 10 so the rate could be as high as 870 kBytes/s. However, we can reduce the trigger rate as needed, if this is too high. In the last case we expect to acquire only 5 samples or a data rate of 432 kBytes/s. On top of this data from other detectors are read.

3.2.6.1 Possible DAQ System

In Fig. 3.28 we show a diagram of a possible first phase DAQ system for the calibration and data collection for the EM barrel module.

The system is basically that which was used during the 1992 test run at Brookhaven, different only in that the ADC's will be Fastbus rather than CAMAC-based. This system also handled the VME-based Zeus pipeline, and can easily accommodate the proposed new system from Nevis, which is also VME-based. Data is stored, on an event by event bases, on a high density 8 mm tape drive (not shown in the figure), which limits the overall bandwidth of the system to 512 kBytes/sec. If necessary, the system can be easily modified to store data corresponding to one full 20 sec spill on a memory buffer located in the crate, making it available to a Master VME system which can take care of event assembling and storing to tape.

The U. of Rochester has acquired a workstation which will act as the primary Data Acquisition (DAQ) computer. The design and adaptation of the software which will control the readout of all the GEM systems which will be tested at MWEST is underway, with one person full-time on the project.

3.2.7 Run Plan

We sketch the types of data runs required and how many events for each so as to determine how much beam time will be required. The run will have the following objectives:

1. Energy resolution:

   An energy scan will be made with electrons, π's, and μ's from 20 GeV to the highest available energy $\approx$ 600 GeV. While the precise energy points have not been determined, we will need of the order of 10 different energies for this scan. If we assume

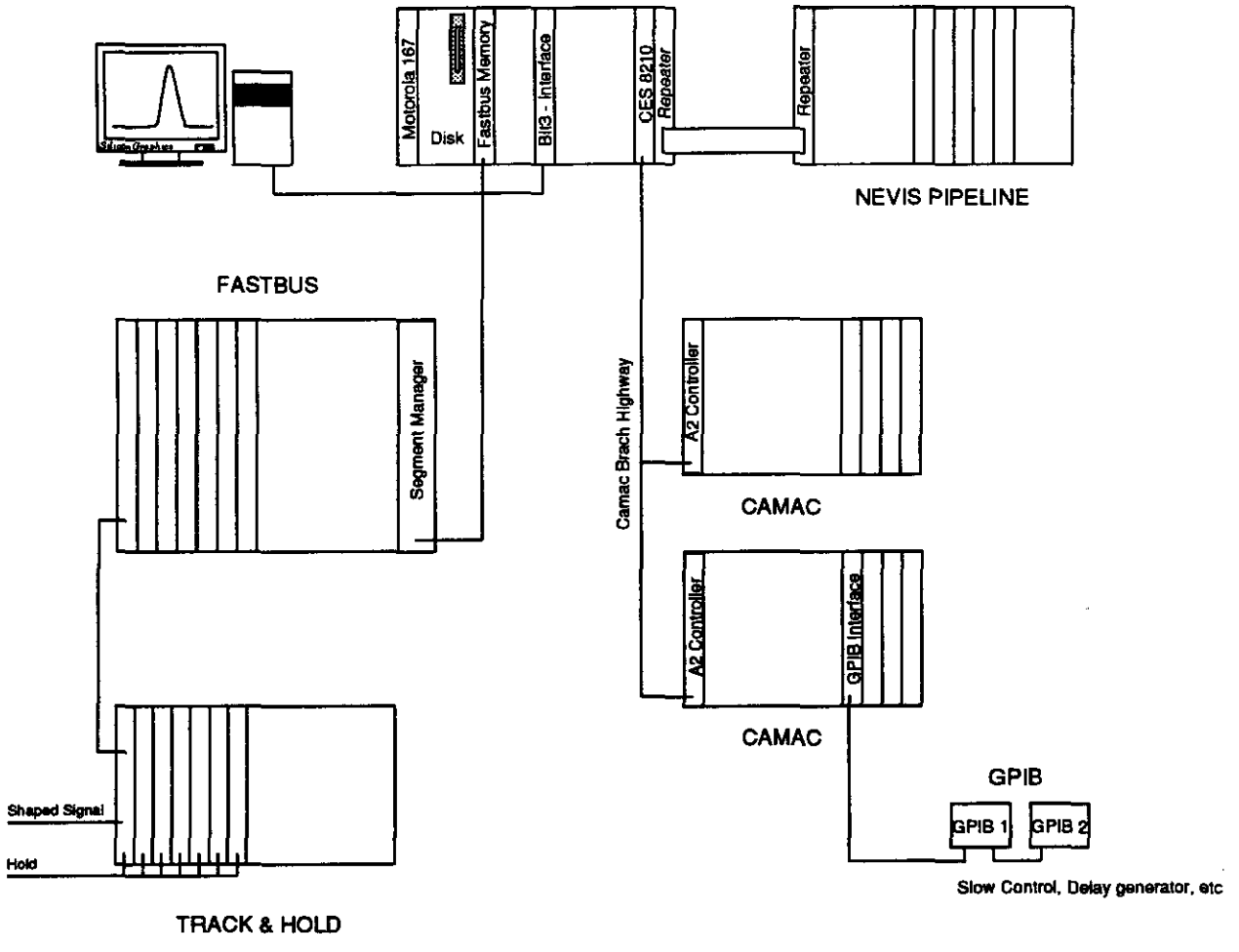

Figure 3.28: A Possible first-phase DAQ system for EM Barrel Calorimeter.

10^5 events for each particle type, we will accumulate $\approx 10^7$ events assuming the scan is done at two or three different positions in the calorimeter.

2. Electronics test: compare performance of a single sample at the peak to multi-sample electronics.

   The objective of this test will be to test an electronic chain as close to the final one as possible. We will have two readout chains available for the test. One consists of a standard track and hold followed by a 12-15 bit ADC (LeCroy dual range ADC's). The data on electrons for one of the energy scans will be taken with both systems adding an additional 10^6 events.

3. ϕ and η scan:

   The η scan is important for mapping both the EM and hadronic energy response. The ϕ scan is more important for calibrating the hadronic sections but can be used for studying the uniformity of the EM calorimeter in the ϕ direction.

   Data at a few selected energy values will be taken over a matrix of ϕ and η. We will need to take data at about 20 different ϕ and η positions in order to scan the calorimeter response. If we assume again a total of 10^5 events per particle species per point we will end up with $3 \times 10^5 \times 20 \times 4 = 2.4 \times 10^7$ events.

4. Pointing performance, Shower shape analysis, e/π rejection:

   These can be done from the same event sample we have for the η and ϕ scan.

5. Jet Resolution:

   We would like to take some π data when we have selected events where the beam had interacted in the nominal target position. The main objective is to find out what the effective resolution is for those π's relative to a single π. This is not the same as a jet but is as close as we can get to testing our jet resolution. A total of 10^7 interactions spread over different η and ϕ positions as well as different energies will be important.

6. SBC:

   The SBC needs some dedicated runs with muons to measure the uniformity of the response and a small amount of data with pions to verify the Monte Carlo. Otherwise, the data taking for hadrons entering the barrel will include the SBC.

7. CQF:

   Though for the study of CQF forward calorimeter prototype, dedicated beam runs will be required, we plan to use CQF calorimeter also as part of general setup in the combined exposures of calorimeter and the muon chamber systems, where CQF can serve as an additional active muon identifier.

Table 3.2.7 summarizes the run plan for the sector test. These would all (except electronics test) require the calorimeter to be the "prime user". Of the order of 10^8 events will be needed for a full study of the calorimeter. If we assume a data rate of 100 events/s and the Fermilab spill structure of 20 s on/40 s off - so we write an average of 30 events/s, and $10^8/30 = 3 \times 10^6$s. If we assume that we have 1/3 efficiency in data taking, we will need of the order of 10^7 s to take this data or $\approx$ 4 months.

3.2.8 Liquid Calorimeter Budget

Since the modules to be used in this test beam program are to be the actual modules of the GEM detector, some of the costs shown below include items that appear as part of the detector, as well as the incremental costs of building these modules.

These numbers have not been reviewed by the GEM Project Office and so have not been handled with the same ground rules. They are consequently provisional.

Table 3.5: Required statistics of beam tests to study the performance of the GEM calorimeter. Commissioning time period is not included.

Task	Particle type, beam energy	θ angle degree	Total No.of triggers	Comments
Electronics Test	(none)		1.0×10^6	
Energy scan	e's, π^-, μ 20-600 GeV	85	1.0×10^7	
η, ϕ scan	e's, π^-,μ 20-600 GeV	90-30	2.4×10^7	
Jet study	π^-,μ 20-600 GeV	90-30	1.0×10^7	Early Interaction
Muons	μ, 20-600 GeV	85	5.0×10^5	SBC alone
ϕ scan	μ, 20-600 GeV	85	2.0×10^5	9 ϕ points SBC alone
Angular scan	μ, 20-600 GeV	90-30	1.0×10^6	SBC alone
Energy scan	π, e, μ, 50-600 GeV	0	1.0×10^6	CQF
Angular scan	π, e, 50-600 GeV	1-6	1.0×10^6	CQF
Jet studies	π,p, 50-600 GeV	0	1.0×10^6	CQF
Scan near "beam pipe"	π,p,e, 50-600 GeV	0	6.0×10^5	CQF

Table 3.6: GEM Liquid Calorimeter Budget

	FY94	FY95	FY96	Total
Liquid Modules, Fixtures, Installation	\$4200k	\$4016k		\$8216k
Misc. Electronics	160	165	40	365
Test Cryostat	360	200	20	580
Loading Fixtures	30	62	0	92
Transporter	500	250	10	760
Vacuum Control System	100	100	0	200
Cryogenics	500	1527	100	2127
Engineering	1200	1200	2000	4400
Radiation Studies	200	200	200	600
Engineering R&D	150	150	300	600
RD3	150	100	30	280
Operations	100	100	300	500
Totals	7650	8070	3000	18720

Table 3.7: Number of channels per 9° sector of Electromagnetic Barrel Calorimeter.

	Qty.	Observations
Readout Channels	1512	using 6x6 segmentation
Motherboards	14	
Clock lines	28	02 per motherboard
Select lines	252	18 per motherboard
I_{cal} lines	28	02 per motherboard

Chapter 4

Muon Spectrometer

4.1 Abstract

The goal of the R&D and Engineering Program is to carry the design concept of the GEM Muon spectrometer into a fully engineering and integrated system ready for construction. The program outlined here will take roughly 3 years to execute and will involve work on the muon chamber design, alignment, chamber support structure, simulations and tests of performance, and general integration with the rest of the GEM detector. This program will be the central activity of the GEM Muon Group. The group consists of 26 institutions and over 100 scientists. All members are committed to participate in this program.

The GEM Muon Group

1. University of Arizona: K.A. Johns, Leigh, L. Shaver, J. Steinberg
2. Institute of High Energy Physics (IHEP), Beijing, China: Y.B. Chen, X.Z. Cui, W.X. Gu, Y.F. Gu, Y.N. Guo, T. Hu, Y.Z. Huang, Y.Y. Jiang, Y.F. Lai, J. Li, Z.G. Li, J.F. Lin, Z.A. Liu, C.S. Mao, Z.P. Mao, Q. Ouyang, H.Y. Sheng, M. Wang, Y.Y. Wang, D.M. Xi, J.W. Xi, Y.G. Xie, R.S. Xu, Y.L. Xu, C.S. Yu, B.Y. Zhang, C.C. Zhang, C.D. Zhang, D.H. Zhang, J.Q.Zhang, Q.J. Zhang, Y. Zhang, D.X. Zhao, J.W. Zhao, Z.M. Zhu, B.A. Zhuang
3. National Scientific and Educational Center of Particle and High Energy Physics, Minsk, Belarus: M. Baturitsky, S. Degtjarev, O. Dvornikov, I. Emeljanchik, A. Kurilin, A.Litomin, V. Mikhailov, V. Shuljak, N. Shumeiko, A. Solin, A. Soroko, V.Stepanets
4. Boston University: S.P. Ahlen, E. Hazen, J.T. Shank, G. Varner, J.S. Whitaker, B. Zhou
5. Brookhaven National Laboratory: M.S. Atiya, I.-H. Chiang, B. Gibbard, J.S. Haggerty, S. Kahn, S. McCorkle, M.J. Murtagh, P. O'Connor, L. Paffrath, V.A. Polychronakos, S. Protopopescu, G. Smith, J. Sondericker, D. Stephani, V. Tcherniatine, B. Yu

6. Brown University: M. Widgoff

7. California Institute of Technology: B.C. Barish, D. Burke, J. Hanson, H.B. Newman, X. Shi, H. Yamamoto, R.Y. Zhu

8. Carnegie Mellon University: R.M. Edelstein, A. Engler, T. Ferguson, R.W. Kraemer, M. Procario, J.R. Russ, H.Vogel

9. University of Colorado: B. Broomer, M. Christopf, E. Erdos, N. Krishna, J. Lee, U. Nauenberg G. Schultz, Q.V. Egeren

10. Charles Stark Draper Laboratories: F. Ayer, C. Elder, T. Hamilton, M. Hansberry, F. Nimblett, P. Sebelius, D.Sullivan, E. Womble

11. Universidad de Guanajuato, Mexico: A. Gonzales, L. Huanajvato, A. Morelos, G. Moreno, L. Villasenor

12. University of Houston: D. Hungerford, A. Lan, K. Lau, B.W. Mayes, L. Pinsky, J. Pyrlik, G. Mo, D. Parks

13. Lawrence Livermore National Laboratory: E. Ables, O. Alford, F.C. Belser, K. Bettencourt, R.M. Bionta, J. Clements, O.D.Fackler, M. Haro, F. Holdener, J. Horvath, C.V. Johnson III, G.J. Mauger, H.Olson, S. Pratuch, M. Roeben, K.A. Van Bibber, T.J. Wenaus, D. Wright, C.R.Wuest

14. Louisiana State University: R. Imlay, H.J. Kim, S. Kartik, C. Lyndon, R. McNeil, W. Metcalf

15. Massachusetts Institute of Technology: P. Burrows, W. Busza, R.J. Camille, Y.H. Chang, M. Chaniotakis, J. Feng, J.I.Friedman, E.D. Hafen, P. Haridas, J. Kelsey, H.W. Kendall, A. Korytov, P.Marston, J.V. Minervini, D.B.Montgomery, R.L.Myatt, L.S.Osborne, Z. Piec, I.R.D. Pillsbury, J. Pisera, A. Pless, S. Pourahimi, L. Rosenson, B. Smith, P.Sphicas, J.D. Sullivan, K. Sumorok, F.E. Taylor, R. Verdier, R.Vieira, B.Wadsworth

16. Michigan State University: M. Abolins, R. Brock, C. Bromberg, J. Huston, J. Linnemann, R. Miller, B. Pope, H. Weerts

17. Moscow State University, Russia: Yu.V. Fisyak, E.K. Shabalina, N.A. Sotnikova

18. State University of New York (SUNY) at Stony Brook: R. Engelmann, M.D. Marx, R.L. McCarthy, M.M. Mohammadi, M. Rijsenbeek, C.Yanagisawa

19. Oak Ridge National Laboratory: R. A. Todd

20. Princeton University: P.P. Denes, M.M. Ito, D.R. Marlow, E.J. Prebys, R.L. Wixted

21. Institute of Theoretical and Experimental Physics, Moscow, Russia: V. Balagura, S. Bojarinov, V. Chudakov, M. Danilov, V. Gavrilov, Yu. Gershtein, A. Golutvin, I. Korolko, S. Kuleshov, L. Laptin, P. Murat, A. Nikitin, A. Ostapchuk, V. Popov, F. Ratnikov, V. Rusinov, V.Shibaev, V. Stolin, I.Tikhomirov, V. Tchistilin

22. Joint institute for Nuclear Research, Dubna, Russia: A.V. Bannikov, L.S. Barabash, S.A. Baranov, D.A. Belosludtsev, V.N. Bychkov, A.S. Chvyrov, A.P. Dergunov, Yu.V. Ershov, V.N. Frolov, I.A.Golutvin, N.V. Gorbunov, Yu.A. Gornushkin, A.B. Ivanov, V.D. Kalagin, A.G.Karev, V.Yu. Karzhavin, M.Yu. Kazarinov, S.V. Khabarov, V.S. Khabarov, B.A.Khomenko, N.N. Khovansky, Yu.T. Kiryushin, O.N. Klimov, V.D. Kondrashov, V.M. Kotov, Z.V. Krumshtein, P.A. Kulinich, V.N. Lysiakov, A.L. Lyubin, A.V. Makhankov, V.L. Malyshev, I.M. Melnichenko, Y.P. Merekov, S.A. Movchan, A.A. Nozdrin, A.G.Olshevsky, V.V.Perelygin, V.D.Peshekhonov, Yu.P.Petukhov, D. Pose, T. Predo, V.P.Rashevsky, Yu.V.Sedykh, S.Yu.Selyunin, S.V.Sergeev, L.M. Smimov, D. A. Smolin, L.G. Tkachev, V.V. Tokmenin, L.S. Vertogradov, Y.B.Viktorov, A.V. Vishnevsky, V.S. Yamburenko, V.E. Zhiltsov

23. St. Petersburg Nuclear Physics Institute, Russia: V.M. Andreev, V. Astashin, N. Bondar, A. Denisov, O. Fedin, A. Golyash, V.Gratchev, M.Guriev, N.Isaev, M.Ishmukhametov, V.Ivochkin, S. Kalentarova, O.Kiselev, A.Krivshich, L.Lapina, P. Levtchenko, V.Maleev, M. Nesvizhevskaya, S. Patrichev, Yu. Platonov, O. Prokofiev, V. Razrnislovich, N. Sagidova, V.Sarantsev, A. Schetkovski, D. Seliverstov, A. Sergeev, V. Sknar, V.Scorobogatov, A.Srnirnov, E.Spiridenkov, V.Suvorov, I.Tkatch, G.Velichko, S.Voikov, Yu. Volkov, A. Vorobyov, Yu. Zhelarnkov

24. Simpson, Grumpertz, and Heger, Inc.: J. Antebi, M. Zarghamee, D. Dusenberry, R. Ojdrovic

25. Superconducting Super Collider Laboratory: Y. Bonushkin, P. Dingus, H. Fenker, Y. Fisyak, M.Gamble, V.Glebov, A.Gordeev, M. Harris, C. Johnson, C. Milner, G. Mitselmakher, A. Morelos, R. Shypit, F.Stocker, G.P. Yost, E. Zimmer-Nixdorf

26. Tsinghua University, Beijing: M. Cao, H.Y. Chen, Z.M. Chen, J.K. Deng, W.H. Gao, K.J. Kang, Y.P. Kuang, D.C.Li, Y.X. Li, L.S. Liu. Y.Q. Liu, W.Z. Luo, D.H. Nan, W.D. Ni, Y.G. Qian, J.L.Ren, R.C. Shang, K. Shen, B.X. Shi, K.R. Shi, J.Wang, J.J.Wang, J.M.Wang, Q.Wang, Y.M. Wang, K.L. Wen, S.D. Xu, Y.P. Yi, G.Z. Yu, Y. Zhao, H.Y. Zhou, S.J.Zhu

4.2 Overview of R&D Program

All key components of the GEM Muon System must be fully prototyped, engineered, and costed before construction of the system can begin. Since many of the attributes of the muon system design are driven by the chamber technology one of the main activities of the R&D program will be to develop the Cathode Strip Chamber design. By means of fabricating and testing a series of prototypes, key parameters of the design will be studied and engineering designs tested. In addition, the full engineering details leading to the "industrialization" of the chamber construction will be conducted with the goal of setting up a pilot factory and fabricating first production chambers in FY95.

Another important thrust of the program will be the design of the chamber support and alignment systems. The concept and performance of these two important subsystems will be tested by an alignment test-stand presently under construction at LLNL. The test stand will enable the notion of the "false-sagitta" alignment method to be validated using optical survey techniques.

All aspects of the R&D and Engineering Program will come together in the FNAL test beam effort. The beam will enable every critical part of the muon system to be tested simultaneously by using high energy muons which penetrate an alignment tower of the muon system composed of 6 full-scale barrel chambers. The muon trajectory will be reconstructed using information from the chambers and their alignment. In this manner the "false sagitta" of the muon tracks can be reconstructed with all sources of experimental error contributing. (Only the small degradation of the spatial resolution of the muon chambers from the Lorentz angle effect will not be included. This effect will be tested separately.)

The FNAL test program will be as complete as possible with in budgetary and time constraints. The goal of the program is to measure all relevant performance characteristics of the GEM Muon System design. Especially interesting will be the following investigations:

- By means of a high energy muon beam measure the total spatial resolution of the muon system. Separately evaluate the resolution error contribution of the cathode strip chambers and their alignment and calculate how these come together to determine the "false sagitta" of the muon track.
- Study the Lorentz angle effect for both the barrel and endcap configurations.
- Determine the time resolution of the muon trigger system and evaluate its implication for tagging the beam crossing of the event.
- Validate the performance of the electronics for both trigger (fast) and tracking (slow) systems under the working conditions of the test beam.
- Gain experience with the integrated performance of detectors, support system, alignment system, and chamber services.

4.2.1 Description of the GEM Muon Subsystem

Muons from pp collisions at the SSC provide signatures for a wide range of new physics processes. The topics that the GEM muon system can probe include: (1) Higgs particle searches up to 800 GeV/c^2, (2) High mass physics, such as searches for Z' and W' bosons, and (3) Heavy flavor physics involving muons in and near high P_T jets. Some of these processes are expected to be quite rare, and will require the highest luminosity which can be obtained at the SSC. The mission of the GEM muon system is to identify these muons, and to provide a precision measurement of their momentum over a wide range.

The GEM muon system [1] is designed to make high precision measurements of muons over the full kinematic range and up to the highest luminosities available at the SSC with little reliance on other subsystems. The muon system performance is complementary to the electron and photon capabilities of GEM in ability to measure trajectories of muons even inside jets, and by determining muon charge up to the kinematic limit of the SSC. To meet the physics goals of the GEM Muon Subsystem we have designed a system that will provide the following functionality and performance:

- Muon identification by requiring penetration through a thick calorimeter.
- Solid angle coverage from 9.75° to 84° with minimal gaps.
- P_T trigger in the range of 10 to 50 GeV/c.
- Beam crossing tag.
- Momentum resolution for 500 *GeV* P_T: 5% at $\eta = 0$; and 12% at $\eta = 2.5$.
- Low channel occupancy compatible with high luminosity operation.
- Correct charge assignment at 95% confidence for 6.5 TeV ($\eta = 0$) to 2.8 TeV ($\eta = 2.5$).
- Knowledge of beam position to better than 500 μm initially, but improving tou 200 μm as the Central Tracker - Muon System alignment becomes better known.

The layout of the GEM muon system is shown in figures 4.1 and 4.2. In order to accomplish the stringent resolution requirements the system is based on 3 superlayers of chambers embedded in a large magnetic volume. These superlayers provide a measurement of the trajectory sagitta which is given by:

$$s = 0.3BL^2/8P_T$$

The design utilizes a large lever arm, multiple layers of high precision chambers, and a novel alignment scheme to achieve the requisite precision. The contributions to the momentum measurement error are listed in Table 4.1.

Cathode strip chambers (CSC) based on proven MWPC technology will perform all the needed functions of the muon system. The chambers provide very high precision (75 μm) measurements over active areas approaching 5m^2. They are mechanically stable and can be fabricated out of industrially supplied high precision components, with minimal material for

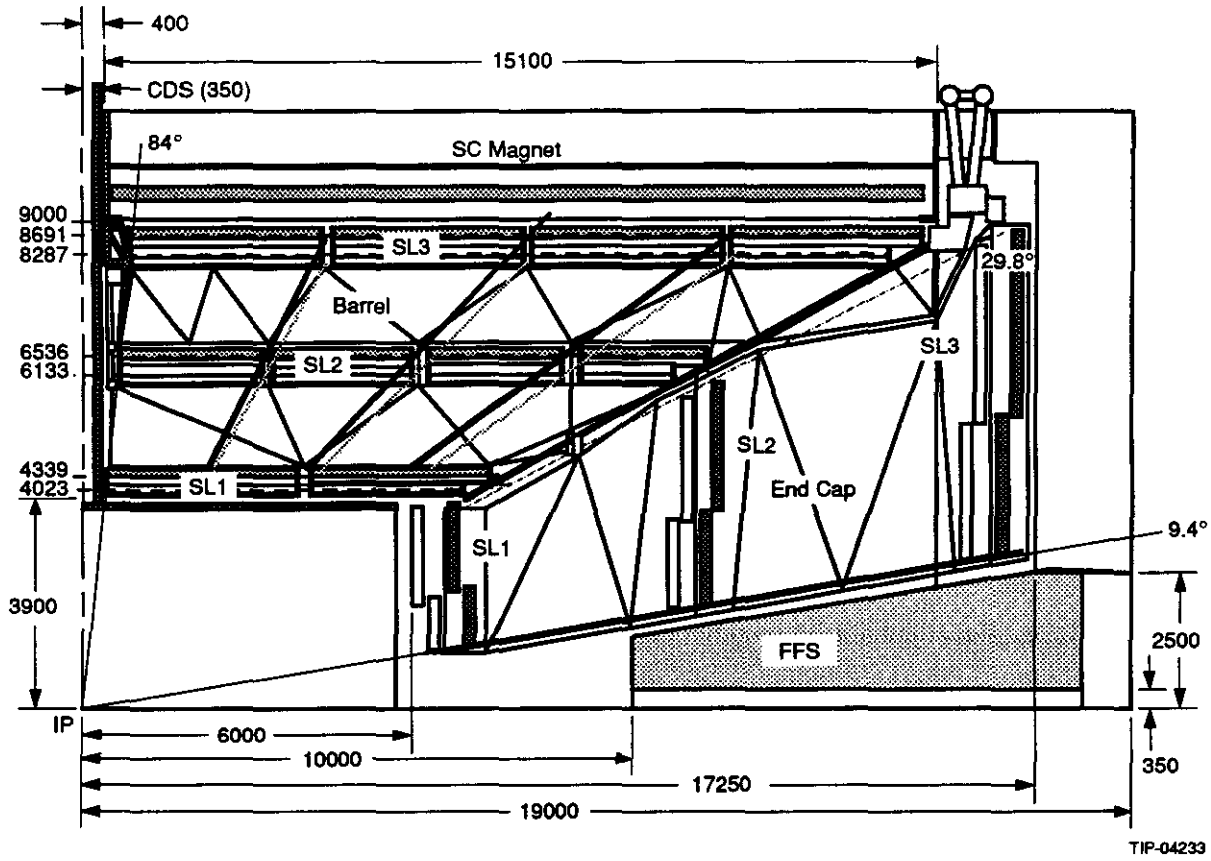

Figure 4.1: Overview of the GEM muon system shown in quadrant view

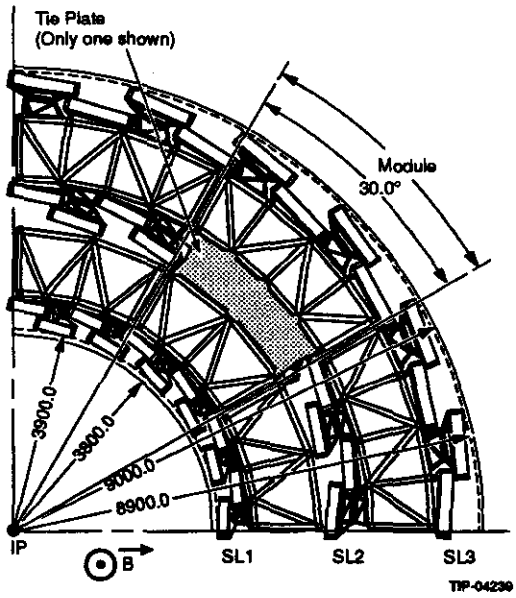

Figure 4.2: Endcap view of the GEM muon system from IP

Table 4.1: Contribution to the momentum measurement error

Error Source	Label	RMS μm
Intrinsic chamber measurement	σ_{ch}	75
Multiple scattering (p = 500GeV)	σ_{ms}	1
Strip-to-strip placement	$\sigma_{s/s}$	17
Layer-to-layer placement	$\sigma_{L/L}$	50
Fiducial placement	σ_{fid}	10
Sagitta error measurement accuracy	σ_{alg}	25
TOTAL	σ_{sag}	54

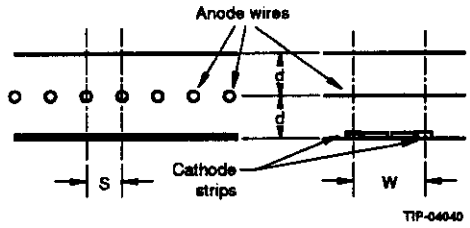

Figure 4.3: Schematic diagram of the Cathode Strip Chamber

multiple scattering, which contributes to the low momentum resolution performance. The chambers provide both a high precision measurement in the bend direction, as well as a coarser measurement in the non-bend direction achieved by summing groups of anode wires. In addition, the chamber provides timing information of sufficient quality to enable tagging the correct beam crossing. All these measurements are available on board the chamber to create a fast muon trigger. A schematic of the chamber showing the construction is given in figure 4.3.

The layout shown in figure 4.1 and 4.2 are those as presented in the TDR. There are distinct regions corresponding to the barrel ($0 < |\eta| < 1.3$) and endcaps ($1.3 < |\eta| < 2.5$). The barrel region is constructed of rectangular chambers while the ends are trapezoidal. The chambers are supported by a truss work structure that provides stability minimizing material while allowing access.

To achieve the requisite tolerances the positions of the CSC sensing elements must be known to higher precision than the measurement error as indicated in Table 4.1. To accomplish this we have proposed a novel alignment scheme that directly estimates and removes chamber misalignments, rather than attempting to position and hold extremely tight tolerances on chamber placement. This is realized by a projective alignment system that utilizes straight line monitors on the edges of projective chamber towers. These monitors directly measure misalignment contributions to the particle sagitta. Figure 4.4 indicates the contributions to sagitta measurements before and after correction.

Since the writing of the TDR in April 1993 we have endeavored to optimize the Muon System design and better integrate it with the rest of the GEM detector. Under consideration

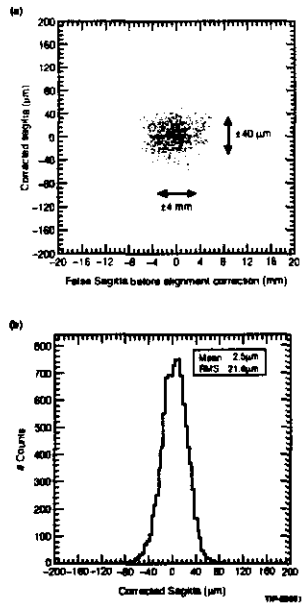

Figure 4.4: Attenuation of statistically distributed alignment errors by monitor correction

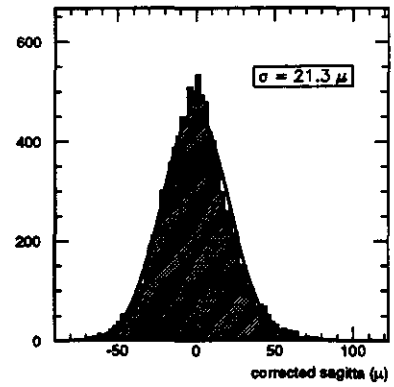

Figure 4.5: Residuals expected from axial/projective alignment scheme

are a completely monolithic chamber support structure [17], which has better stability and integrates the barrel and end regions and decreases the gap between these regions, and a new singled chamber layout in the barrel, which reduces the overall number and type of chambers with somewhat improved performance. Further improvement in the angle coverage of the system may be gained by a new scheme to align chambers in the barrel region along the beam direction by utilizing stretched axial wires [18]. This effectively increases the size of the projective tower, reduces sensitivity to rotational errors, and obviates the need for projective alignment gaps between chambers in the middle layer [19]. Figure 4.5 shows the residuals expected from this axial/projective scheme.

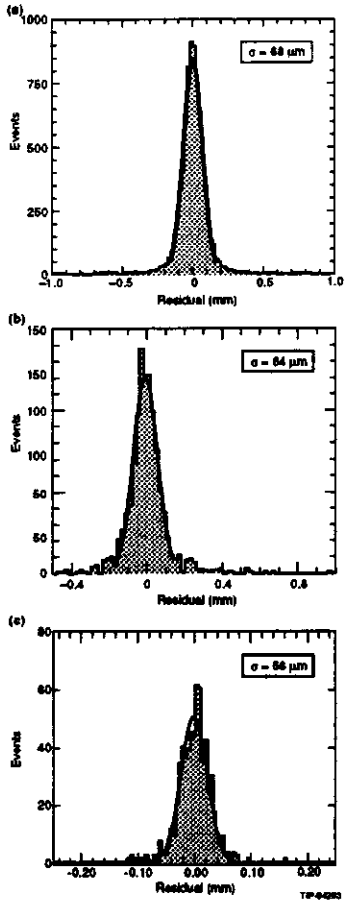

Figure 4.6: The single layer spatial resolution obtained at the TTR

4.3 Pre-FNAL R&D Program

In the R&D program the electrical and mechanical aspects of the CSC design will be developed with the economical mass production of some 1400 chambers in mind. Furthermore, the design of the chamber support and alignment systems will be worked out in detail. Important objectives of this phase of the R&D program will be the construction and testing of a full-scale barrel chamber prototype and the design and fabrication of the Alignment Test Stand (ATS). The ATS will allow full lever arm tests to be made of the chamber alignment system.

Many of the elements of the GEM muon system are based on well-established technologies but in our system must be applied and optimized to achieve unprecedented performance over very large areas. Some have already been tested in the GEM R&D program, yet much remains to be done in proving system performance.

The CSC technology was selected after an extensive program of R&D where a number of different chamber technologies were tested at the Texas Test Rig(TTR). Four different CSC chambers ranging up to 2 m^2 in area were tested and all provided better than the 75 μm per plane resolution (see figure 4.6). The spatial resolution of the order of 80 μm has

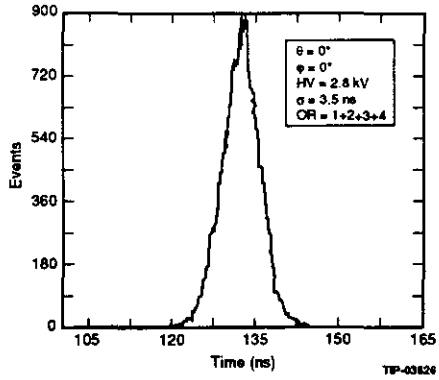

Figure 4.7: Timing resolution: "OR" of four CSC chamber layers

been achieved at Dubna [20] for 3.0 m × 0.3 m CSC prototype. In addition several smaller chambers have been tested elsewhere, providing critical information on timing capabilities (see figure 4.7) and on performance in a magnetic field. These chambers were equipped with prototype electronics that performed most of the needed functions of the final system, although not in an integrated fashion. It is expected that a full-size 6-layer prototype chamber (1.1 m × 3.0 m) equipped with prototype anode and cathode electronics will be tested by the end of 1993 at the TTR. Other prototypes of both the barrel and endcap chambers will be constructed and tested during the 3 year period.

The alignment system, critical for achieving the required performance of the GEM muon system, has been extensively studied in simulations. The optical straightness monitors and stretched wire monitors, which comprise the key measurement elements of the axial/projective scheme have been independently tested with prototype hardware and their expected performance verified (see figures 4.8 and 4.9). For study the chamber alignment as an integrated system the Alignment Test Stand (ATS) will be constructed. This will be a test bed to verify different aspects of the alignment system over the full lever arm of the three superlayer design.

4.3.1 Chamber Design

The design of the CSC will be further developed during FY94 to prepare for their pilot mass production to start in FY95. This work will involve the determination of the mechanical and electrical parameters of the chamber construction which meet the tight mechanical tolerances and operational stability requirements of the GEM muon system. Consideration will be given to the industrialization of the design, where a major element will be the development of techniques for mass production of large panels, chamber frames, and large volume anode wire winding.

To check specific aspects of the design several small prototype chambers as well as a full-scale endcap chamber and several full-scale barrel chambers will be constructed. A special emphasis will be placed on the fabrication and testing of full-scale barrel and endcap chamber prototypes. Experience has repeatedly shown that it is only in the successful demonstration with full scale prototypes completely instrumented that the actual chamber concept will be

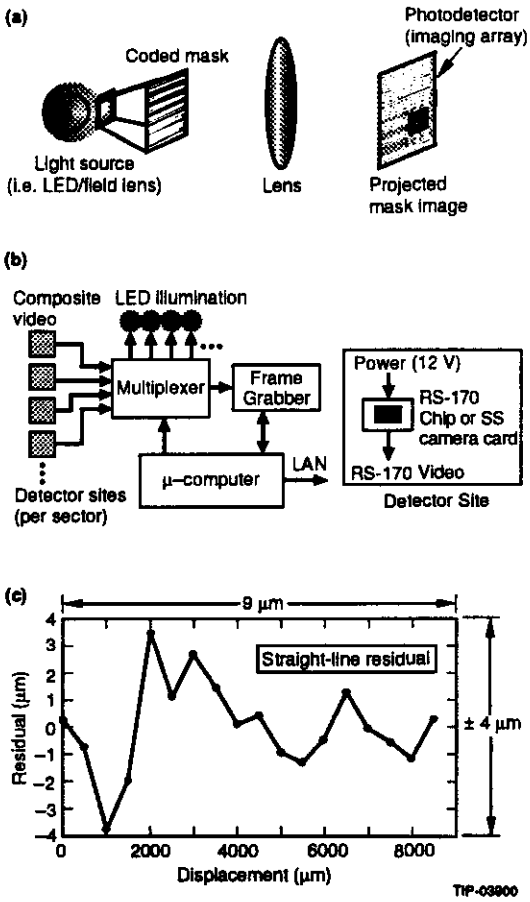

Figure 4.8: Wide-range video straightness monitors

proven.

The chamber prototyping is divided into a series of generations to mark the evolution of the engineering design. The generations are as follows: "Generation -1" are chambers built to study certain specific aspects of the design, "Generation 0" are those built according to the state of the engineering design in FY93-94, and "Generation 1" are the chambers which are fully engineered, tested, and constructed by mass-production techniques.

Figure 4.10 shows the most recent engineering design of a typical barrel chamber.

1. Final engineering and evaluation of full-size prototypes for mass production:

   (a) "Generation-1" prototype of a BARREL outer layer chamber: 3.0 m by 1.1 m – six 10 mm gaps;

   (b) "Generation-0" prototype of an ENDCAP middle layer trapezoidal chamber: approximately 2.2 m by 0.9 m – six 8 mm gaps.

   (c) "Generation-0" BARREL prototype 0.4 m × 0.4m × 6 for Lorentz angle studies.

   (d) "Generation-0" ENDCAP prototype 0.4 m × 0.4m × 8 for Lorentz angle studies.

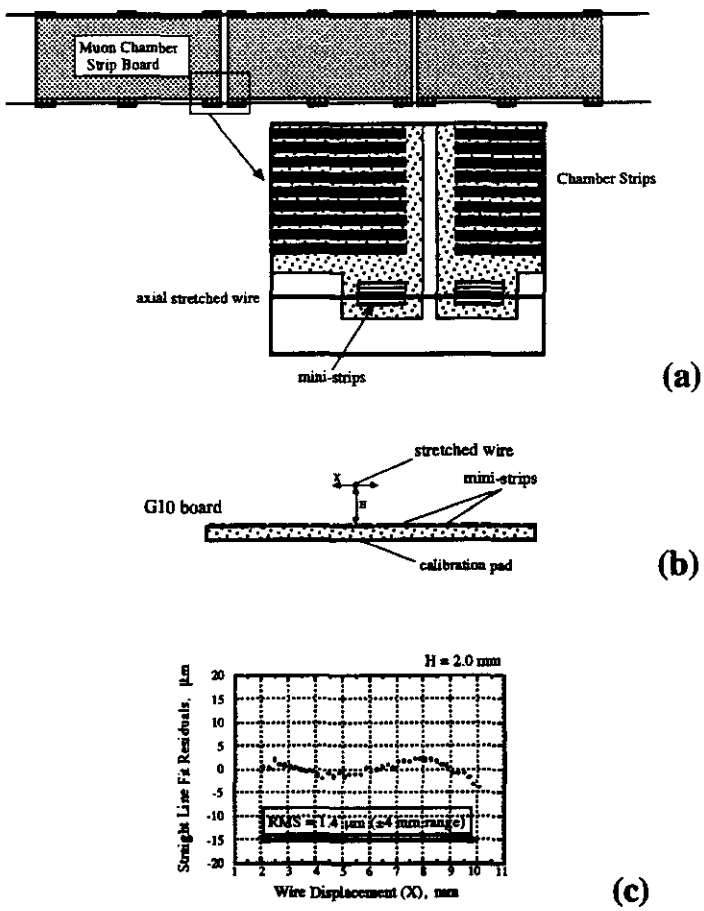

Figure 4.9: Stretched wire straightness monitor

2. Construction of the 6 full-size ("Generation-1") chambers needed for the FNAL test program. These will be typical full size barrel chambers of the three superlayers, each consisting of 6 internal layers, and will be outfitted with the necessary alignment fixtures. [The "Generation-1" design can be mass produced.]

3. Engineering drawings of chambers needed for mass production.

The following is a schedule of the chamber prototype program.

The readout electronics will be developed in concert with the design of the CSCs. We have initiated an electronics design where the entire front-end for both the precision cathode and the anode readouts and a significant fraction of the trigger logic reside on PC boards mounted directly on the chambers. The precision cathode readout electronics must employ a low-noise front-end with a high degree of noise immunity. This is essential in order for the system to achieve the desired resolution by interpolation of small analog signals. The readout and trigger schemes have a high degree of integration and modest amounts of cabling and interconnects. This layout will minimize the cost and complexity of the system. It is our plan to test prototype electronics on real chambers thereby providing a validation of the chamber electrical design, as well as the design of the electronics for the chambers.

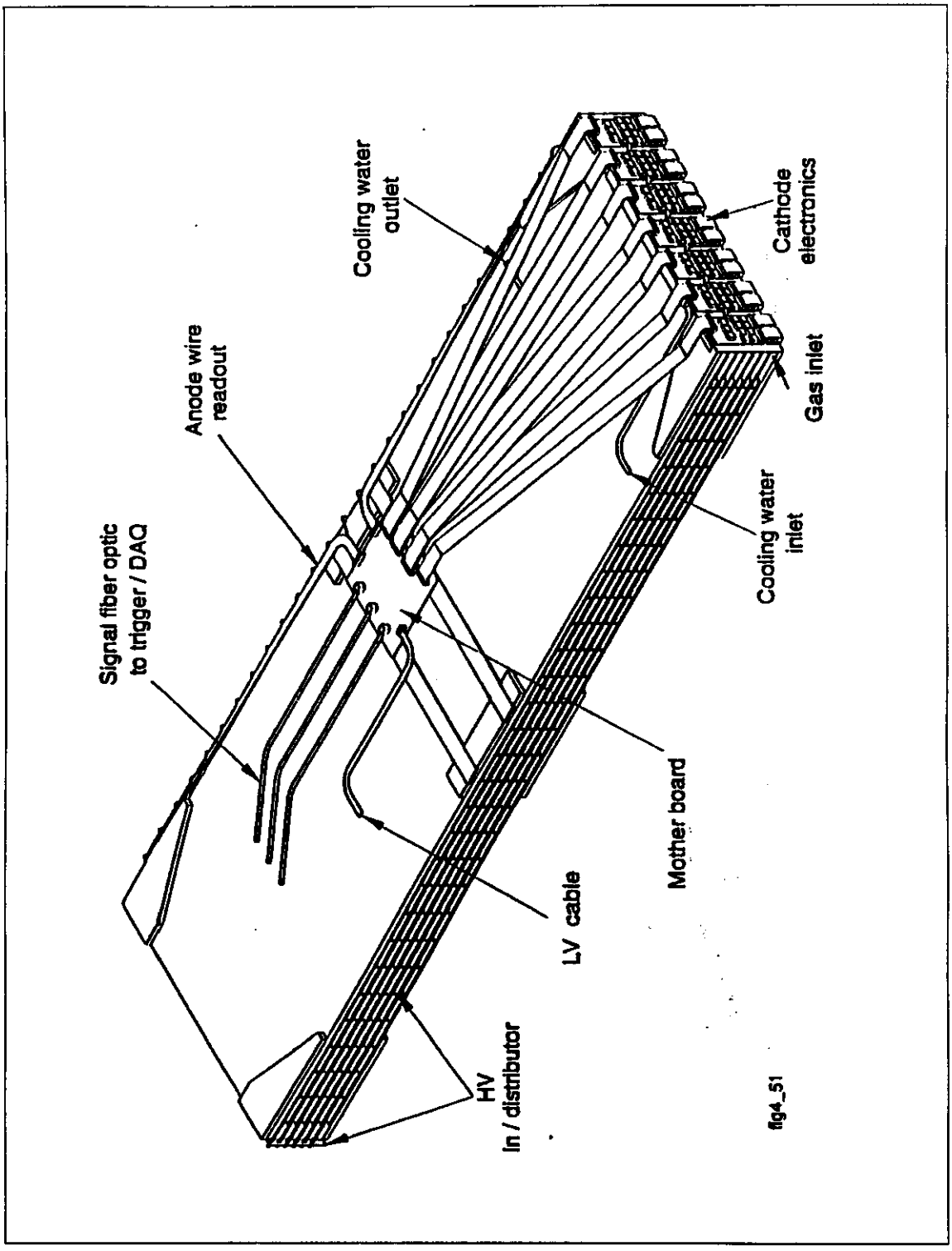

Figure 4.10: Design of a typical barrel chamber

In this way solutions to ground loops, shielding, feedback, and electronics layout will be co-developed with the chamber design.

4.3.2 Pre-FNAL Chamber Testing

An active testing program will be necessary in order to evaluate the CSC performance as the prototyping and engineering design evolves. This work will involve testing the various CSC prototypes with cosmic rays (at the Texas Test Rig) and at various available accelerator beams (BNL, RD5, ITEP, and PNPI). The use of cosmic rays, and the muon and hadron beams available at RD5-CERN, ITEP at Moscow, and PNPI at St. Petersburg comprises a flexible and powerful attack of the various R&D questions in the period before the FNAL test.

The RD5-CERN beam program deserves special mention. Elements of the GEM Muon Group are also members of the RD5 Collaboration. They have exploited the beam opportunities at CERN to extensively test an early prototype GEM endcap chamber. The RD5 program is an opportunity to work out test procedures which can be applied on a more extensive scale in the sector test proposed for FNAL.

The RD5 test data are presently being evaluated, but a preliminary analysis has yielded important verification of the chamber resolution and infra-layer alignment. Key properties, such as spatial and temporal resolution, of later generations of CSCs incorporating engineering features needed for mass production will be measured in the beam. The proposed RD5 test program will permit the optimization of spatial resolution vs. other chamber parameters, and the determination of the HV plateau, noise immunity, gas mixtures, L-angle correction, alignment, and timing characteristics.

In addition, the CERN beam will allow a systematic study of hadron punch-through as a function of calorimeter depth to be performed, as well as determination of the behavior of a cathode strip chamber in the presence of muon-associated backgrounds. Early results indicate that the hadron punchthrough probability is somewhat larger than GEANT-based calculations would indicate. These tests will be extended and refined in further measurements during the summer of 1994.

1. Critical parameters of CSC production prototype performance:

   (a) Spatial resolution of cathode readout.

   (b) Timing performance vs. gas, anode-cathode gap.

   (c) Lorentz angle compensation for barrel and endcap chambers.

   (d) Wire - strip angle correction for endcap chambers.

   (e) Optimization of gas mixture.

   (f) Optimization of chamber operation region in terms of high voltage, gas.

   (g) Double track resolution.

   (h) Pattern recognition and trigger capabilities.

(i) Electronics operation in accelerator noise environment.

2. Determine the operating stability of CSCs with respect to gas mixture, temperature, pressure, and ambient noise.
3. Measure the chamber sensitivity to neutrons.
4. Measure the muon-associated background.
5. Measure hadron punch-through.
6. Software development for CSC evaluation:
   (a) computer controlled calibration for standard CSC electronics;
   (b) on-line monitoring;
   (c) off-line software for CSC data processing.

4.3.3 Chamber Industrialization

The primary effort of constructing the GEM muon system will be the fabrication of approximately 1400 chambers which make up the three superlayers of the barrel and endcaps regions. It is estimated that the cost of fabrication of the muon chambers will be about 1/2 of the total cost of the system and will require several chamber production factories to manufacture the chambers in the time frame needed for the experiment.

To initiate the chamber construction process both the development of tooling and the setting up of a chamber pilot factory are necessary in the pre-FNAL period. The tooling needed will be wire winding machines, masks for cathode panel fabrication, alignment jigs, production survey techniques for cathode panel alignment, etc. The design and construction of the tooling will be integrated into a chamber pilot factory where all aspects of parts production, and scheduling needed for an efficient operation will be worked out. The development of chamber production tooling and pilot factory will be a collaborative effort among the institutions of the GEM muon system. It is anticipated that the site for the chamber pilot factory will be chosen in the third quarter of 1994.

4.3.4 Alignment Technology

The detailed design of the chamber precision alignment system will be developed and analyzed. Emphasis will be placed on the evaluation of sensors, integration of alignment systems with the chosen technologies, and testing of the alignment system. The design will be documented in terms of drawings and specifications which will be used for the prototype of the alignment system.

The alignment of the individual layers of cathode boards in a chamber is an important engineering issue and key to achieving the desired performance of the chamber modules. For this task it has been proposed to employ penetrating X-rays to orient the individual chamber layers. Tests at PNPI will be performed to certify the efficacy of this idea.

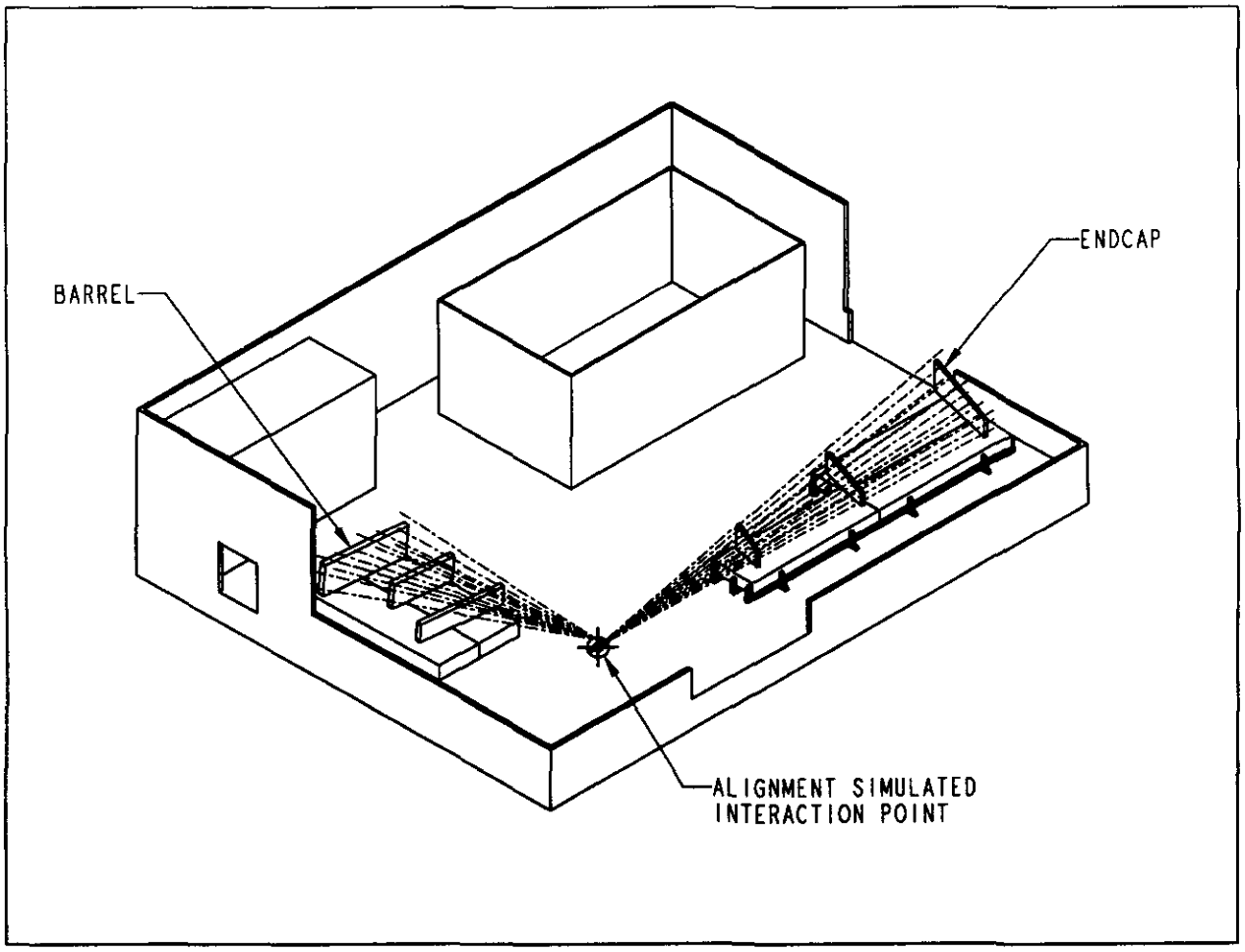

Figure 4.11: Alignment Test Stand

To validate the concept of the sagitta correction function measured by the projective/axial alignment method, the basis of all proposed GEM alignment schemes, the Alignment Test Stand (ATS) will be commissioned at LLNL. The ATS will consist of six mock chambers, arranged in two towers consisting of three chambers each, representing the three superlayers of the barrel and endcaps. (See figure 4.11) Each of the mock chambers will be instrumented with positioning actuators to place the chambers within the few millimeters dynamic range of the alignment fixtures. A series of tests will be conducted whereby the alignment system will be checked against a precise external alignment system for a realistic path length with standard chambers. It is envisioned that the ATS will be the prototype for the alignment system to be used in the Fermilab test program.

Deliverables:

- Develop and evaluate alignment technologies.
- Integrate alignment system with chamber design and support structure.
- Design and construction of ATS.

- Demonstrate proof-of-principle of chamber alignment with ATS.
- Global alignment evaluation.
- Simulate operation of complete system.
- Industrialization of fabrication of alignment sensors and associated hardware.
- Test the X-ray alignment method of aligning separate layers within a chamber module.

4.3.5 Chamber Support Structure and System Integration

The muon chambers must be supported on a stable platform in order to achieve the spatial resolution needed for the high momentum measurement. During the pre-FNAL test beam period work on the design of the support system will be undertaken. The design put forward in the TDR was based on separate barrel and endcap structures. The barrel structure was further partitioned into sectors which were fabricated separately, then installed in the GEM magnet and tied together to form a rigid platform for the chambers. Structural and vibrational analyses indicated that the design met the stability standard need for the GEM system.

Subsequent to the TDR, this design concept has been modified somewhat to obtain a more efficient structure. The new deign is founded on a simple network of diaphragms and reticulated shell structures. This allows for the development of an extremely sparse truss work resulting in good longitudinal and torsional stiffness, while reducing material at the the middle superlayer [17]. In this design the barrel and endcaps are tied together to form a monolith. As a consequence the amount of material in the structure is reduced over the original design by nearly 50%.

The engineering effort on the support structure during the 3 years described in this program will be applied to developing the details of the design, performing structural analyses under various loading and vibrational excitations, work out assembly procedures, and analyze costing and construction schedules.

The final design of the muon system must be integrated with the central tracker, calorimeter, and the magnet. The utilities needed for the operation of the muon system will be designed and integrated with the chambers and the rest of GEM. These include the chamber gas system, the HV and LV systems, water cooling of the CSC electronics, local and global alignment systems. The routing of gas system tubing, manifolds, gas leak monitors, gas purity monitors, gas purification and recirculation system should be specified.

Although it is impractical to construct a sector of the support structure for the FNAL test, key elements of the design will be incorporated. For example, it is envisioned that the actual interface hardware needed to attach the chambers to the support structure will be employed in the test. Furthermore, elements of the ATS will be included in the chamber support structure of the FNAL sector test. Therefore, the beam test program will be an opportunity to verify many critical aspects of the design.

4.4 FNAL Beam Program

The test beam program for the muon subsystem will be conducted in two phases. In Phase I small chambers of the barrel and endcap designs will be tested in a magnetic field. In addition a detail study of a full-scale barrel chamber will be conducted. In Phase II the performance of a sector of the barrel region will be tested. It is proposed that the GEM test beam program use the FNAL MWEST beam. Figure 4.12 shows a plan view of the MWEST experimental area and the placement of the GEM Muon System Test Sector in the area. By design the muon test sector is furthest downstream from the other GEM subsystems which will allow isolation of the muon setup from other upstream detector systems by using shielding blocks. Additionally, this isolation will allow chamber tests using pure muons if required. It is expected that personnel can have access to the muon system when proper shielding is in place.

4.4.1 Magnetic Field Studies

4.4.1.1 Phase Ia - Barrel Configuration

Preliminary tests of the CSC chamber resolution in a magnetic field in the barrel chamber configuration are planned for FY94 using the RD5-CERN beam. At Fermilab we will extend these important studies by measuring the behavior of a CSC in both the barrel and endcap configurations. The FNAL beam will allow an important and related study to be conducted of the backgrounds which accompany a high energy muon on the downstream side of an absorber.

In figure 4.13 we show the configuration of the chamber and absorber in the large dipole magnet in MWEST. Two interaction-lengths of Cu are placed in front of a small CSC chamber (0.4 m $\times$ 0.4 m $\times$ 6-planes). The chamber will be mounted on a manipulator which can both tip and rotate to simulate the angles of both the muons and the magnetic field which will exist in the SSC detector. This manipulator will also accommodate a number of Central Tracker detector elements which can also be positioned to have beam particles intercept them at the appropriate angles.

The tests in the large dipole magnet are summarized below:

1. Measure associated backgrounds of 500 GeV muon, and the absorber distance dependence
2. Θ angle dependence of resolution.
3. Lorentz force effects and their mitigation.
4. Rate capabilities.
5. Electronics Evaluation.

A full size barrel chamber will not fit inside the MWEST dipole magnet, however, with its mirror-plates removed, the fringe field of the magnet is significant beyond the plane of the coils. This option may be exercised if tests of a full size chamber in a magnetic field are deemed essential.

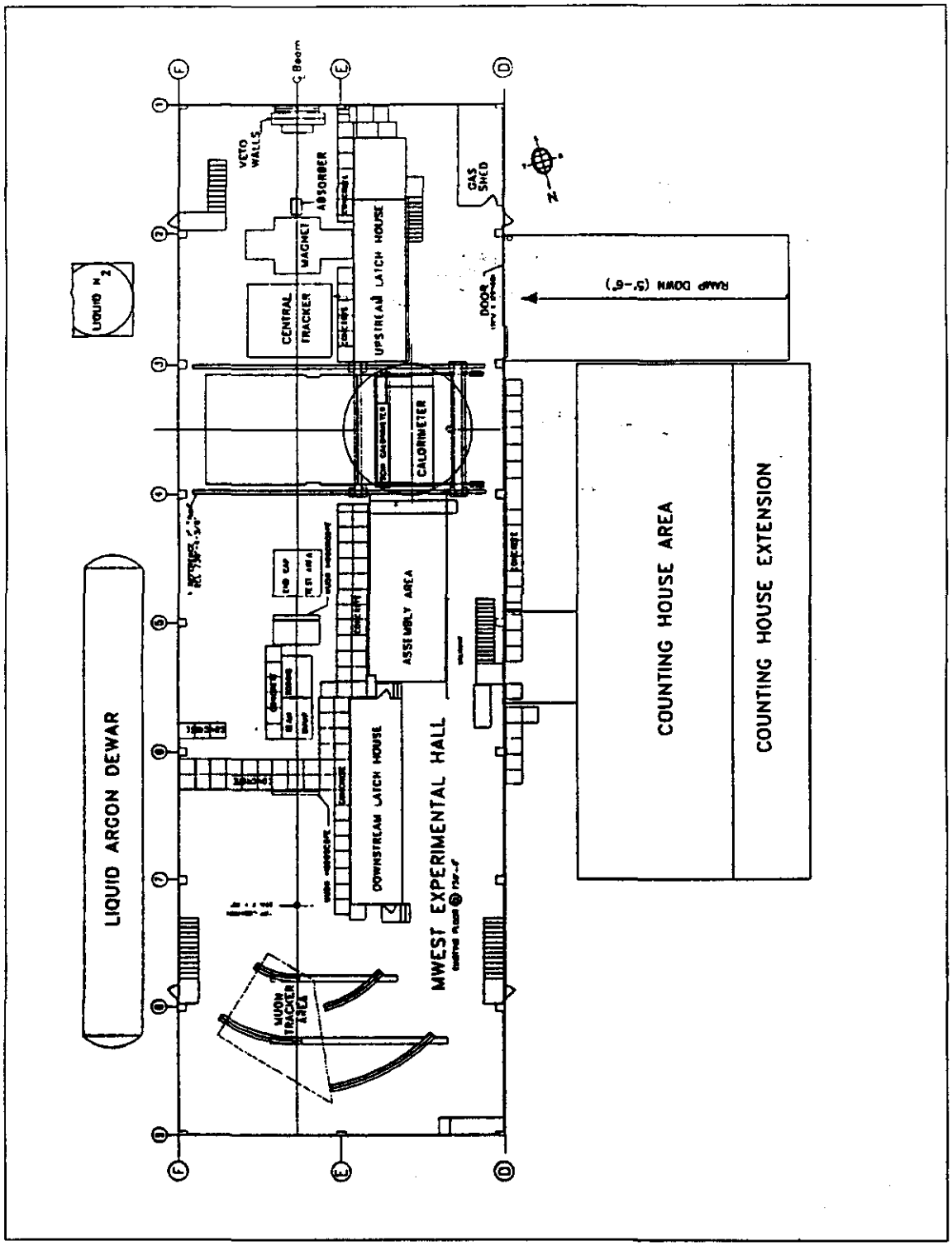

Figure 4.12: Plan view of the muon system sector in the MWEST area

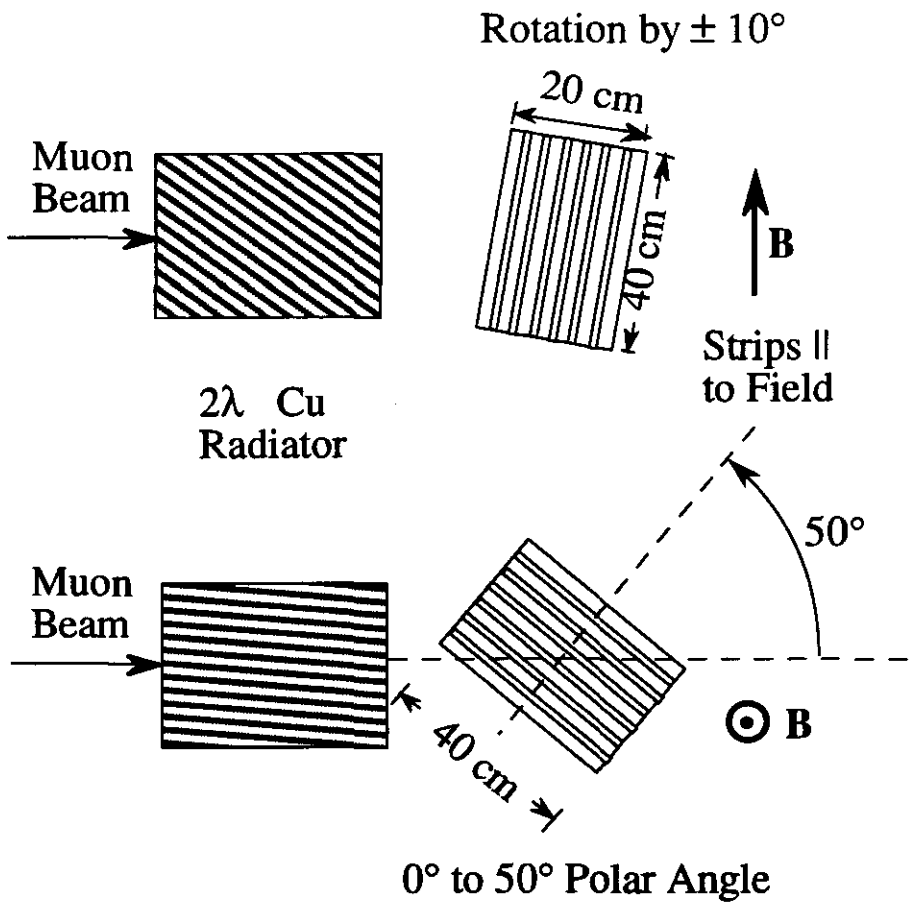

Figure 4.13: Configuration for tests of barrel-type chambers in a magnetic field.

4.4.1.2 Phase Ib - Endcap Configuration

A magnetic field parallel to the beam is required to test the configuration of the chambers in the endcap. A small C-magnet (or H- magnet) with a 30 cm gap, 30 cm diameter poles and a 2 m spacing of the flux returns would be appropriate for these tests. Such a magnet, sketched in figure 4.14, can easily be moved in and out of the beam, so holes in the poles will be unnecessary, and will allow scanning of a reasonably large (1 m × 3 m) endcap style chamber.

4.4.2 Phase II - Tests of Full-scale Barrel Sector

4.4.2.1 Overview

The Muon Test Sector is a reduced version of a section of the GEM Detector "barrel." Simplifications include the reduction of the number of θ and ϕ segments to an absolute minimum, while maintaining enough of the final design to thoroughly test the essential features of the GEM muon system, as described above. In essence, the test sector consists of a barrel alignment tower comprised of 6 full-scale cathode strip chambers aligned projectively.

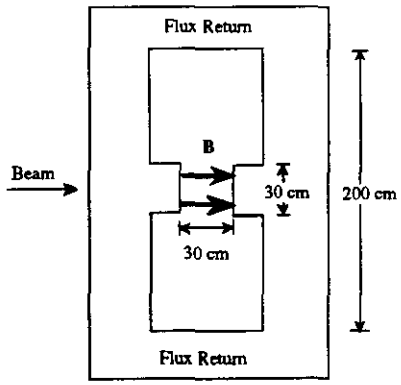

Figure 4.14: Magnet for testing endcap chambers.

Table 4.2: Sector Test Cathode Strip Chamber Physical Parameters.

Superlayer	Chamber Width (m)	Chamber Length (m)	Chamber Mass (kg)	Quantity for Test Sector	Superlayer Mass (kg)
Inner	0.853	3.540	155	1	
Middle	1.370	3.540	223	2	
Outer	1.370	3.540	223	3	
TOTALS				6	*xxx*

However,the implementation of this basic alignment concept in the practical design of the GEM muon system will probably involve several additional features which at the present time are under study. For example, in order to reduce the number of chambers in the barrel we are considering a 24-36-48 ϕ segmentation for superlayers 1-2-3, respectively. This has the consequence of 2-3-4 ϕ chamber match. Another feature under consideration is an axial-projective alignment scheme, where projective alignment paths penetrate the barrel system at 90 and 30 degrees with axial alignment in between. A similar scheme is envisioned for the endcaps. In this manner the θ gaps between chambers can be reduced.

The goal of the sector test is to validate as many of these features of the system as possible. Therefore, the test not only involves checking how well full-scale chambers perform under realistic beam conditions, but also how well they can be aligned with the axial-projective scheme over the operative dimensions of the barrel system. The fundamental false-sagitta method can be checked with only three chambers, but the addition features in the practical GEM layout will require 6 chambers overlapping in both ϕ and θ. The setup for 6 chambers is shown schematically in figure 4.15. The chamber dimensions and other relevant parameters are listed in table 4.2.

Under extreme financial exigency the sector test could be scaled back to the essential 3 chamber projectively aligned, but many important features of the system, such as the axial-projective alignment scheme, would go untested. In this situation we would probably not initiate a chamber pilot factory so production chambers would not be used.

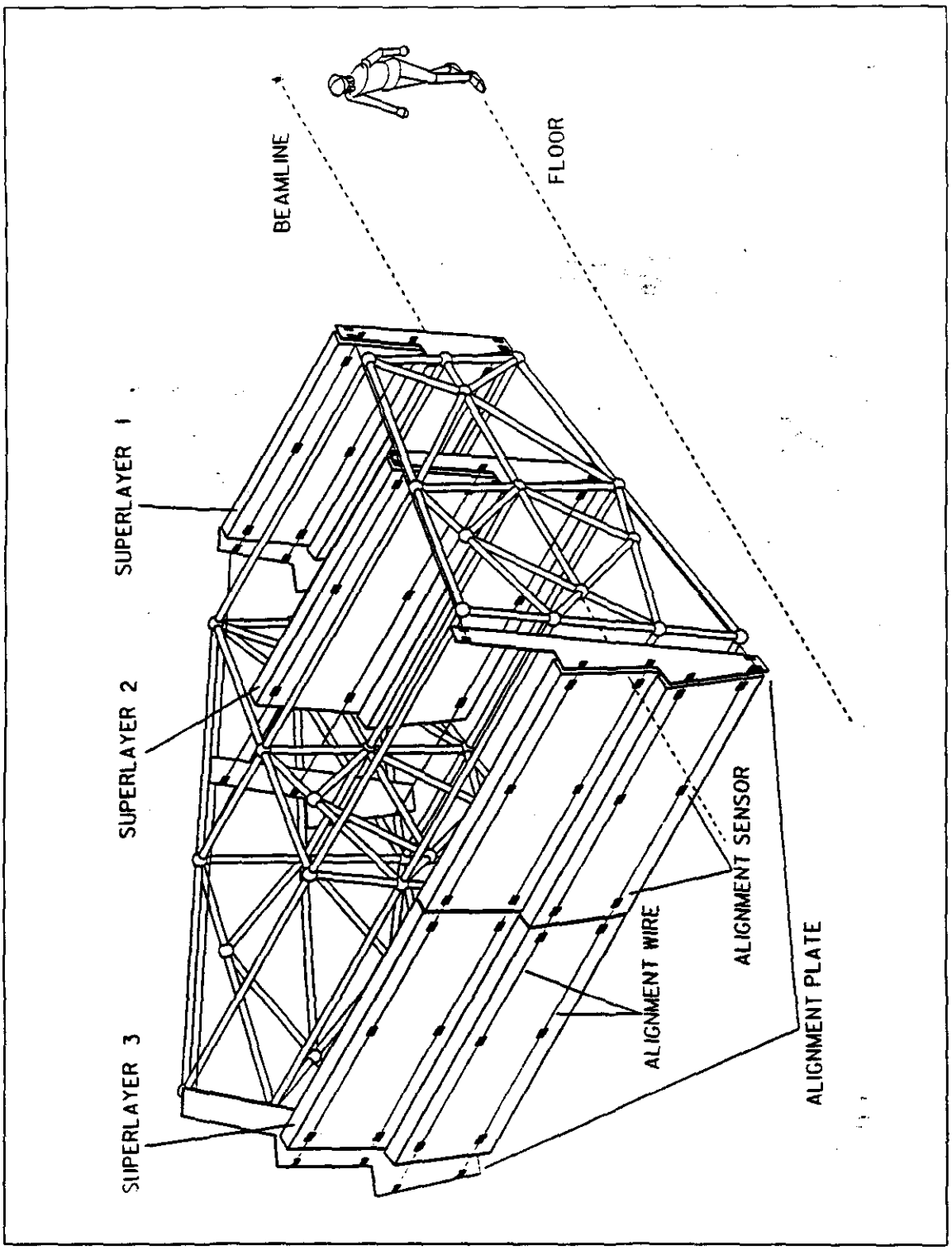

Figure 4.15: Configuration of the muon test sector

The precision of the CSC muon system for GEM relies on its ability to accurately measure a track's sagitta. In particular, a straight track (infinite momentum in a 0.8T magnetic field) should yield a sagitta of zero within errors. Any systematic point-to-point distortions in the sagitta measurement will result in a worsening of the momentum resolution. Since the chambers are not rigid nor immobile, an alignment system has been designed that has a primary sensitivity to movement which affects the sagitta measurement; absolute locations being a secondary concern. To achieve the GEM momentum resolution goals errors in the sagitta which are not removed by the alignment system must be less than 25 microns. The sector test at Fermilab, although not in a magnetic field, will confirm that the combination of support framework, chamber mounting hardware, alignment hardware, electronics and chamber services are compatible with the precision requirements of GEM.

The chambers for the sector test will be designed to be as close to the final CSC chamber for the GEM Muon System as possible. However, there will likely be design changes as we gain experience with the CSCs in the test beam program. Therefore, we will employ the minimal number of chambers needed to address all the required performance goals. At this time the CSC package exists as a conceptual design and a number of first order engineering prototypes are under construction. The sector test will be an opportunity to test all of these engineering concepts.

The goals of the sector tests are summarized below:

- Measure the sagitta correction with high energy muon tracks from a beam-simulated interaction region.
- Perform integrated test of chambers, support structure, alignment, and services.
- Determine the time resolution of the muon chamber anode electronics over the full sensitive area of a chamber.
- Verify that the chamber electronics works in the large scale needed to completely instrument three full-scale barrel chambers.
- Investigate trigger electronics prototypes.
- Test a completely functioning GEM sector with the central tracker, calorimeter, and muon subsystems all operating simultaneously.

4.4.2.2 Test Configurations

There are two geometrical directions which must be tested to verify that the alignment system can adequately remove distortions. The first configuration, shown in figure 4.16a, shows how the sector can be scanned about a horizontal axis which tests the sagitta resolution in ϕ. The second scan, shown in figure 4.16b, tests the behavior of the system in θ.

The chamber overlap regions will provide vital alignment information, effectively linking together chambers into a locally and globally aligned system. Straight line muon tracks (single tracks in the test beam program and single or double tracks in the GEM detector) that pass through overlap regions can be used to link separate chambers by virtue of the precision

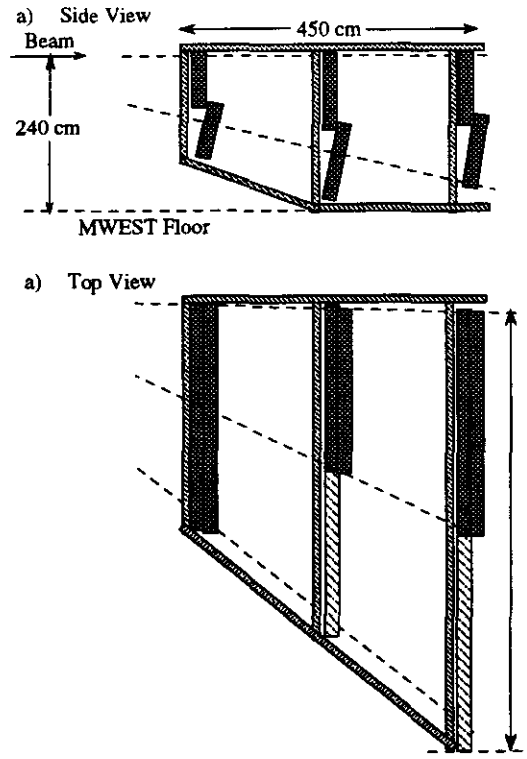

Figure 4.16: Muon sector scan in ϕ and θ achieved by a) vertical rotation by 15° and b) horizontal rotation by 38°.

track fitting afforded by CSCs. Muon tracks incident over the entire test beam system will provide a measure of system performance taking into account the effects of extraneous material such as support structures, electronics, services, and alignment hardware. Because a large amount of material exists in the CSC edges and overlap regions, extensive testing will be done in these areas using energetic muons.

Six chambers will be installed in a sector framework, shown in figure 4.15, which closely approximates the barrel support structure, and incorporates the chamber mounting hardware, alignment hardware, and chamber services. The sector framework will be attached to a transporter which can rotate the sector both vertically (ϕ) and horizontally (θ) to project high momentum tracks through the chambers at the angles expected at the SSC. This will allow a test of the muon trigger scheme which uses the chamber signals to select high momentum tracks.

To allow studies of the chambers while the beam is in use by the calorimeter and central tracker subsystems we will install a large area muon halo trigger system. This system uses the two walls of scintillators from E706/672 shown in figure 4.17. Although muon halo tracks are of unknown momentum and therefore are not appropriate for precision measurements they are a continuous source of particles whenever the primary target is being hit. This will allow a tune-up of the electronics and alignment systems prior to the tests in the muon beam.

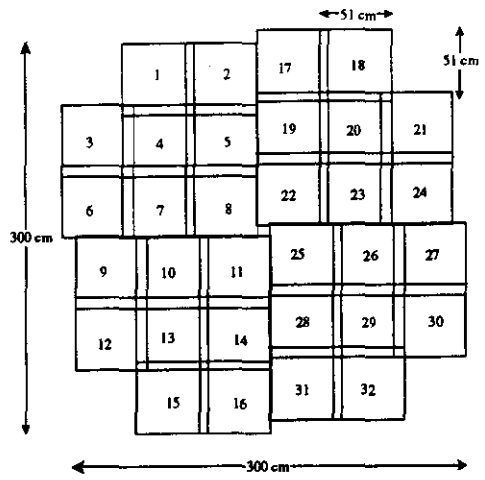

Figure 4.17: Two 32-element scintillator arrays for muon halo triggering.

4.4.2.3 Alignment System for Sector Test

The muon chambers will be aligned by means of both projective as well as axial alignment devices. Projective alignment monitors will be located at the outer corners of the chamber support frame. These monitors will precisely locate an alignment plate which will be used to align the chambers mounted between the projective paths. At the present time, two (three) chambers will be tied together by means of this precise alignment plate. To properly test the proposed axial alignment system in the GEM baseline design, at least two chambers in a superlayer are required in θ.

Under consideration at this writing is a SL1:SL2:SL3 = 24:36:48 ϕ segmentation scheme. The essential features of this system can be simulated by attaching alignment plates to the chamber tower and redirecting the alignment lines of sight without constructing more chambers. The performance of the system in the ϕ overlap region can be measured by sweeping the beam through the overlap region.

4.4.2.4 Transporter for Sector Test

Beam steering at the MWEST site will not be available and so we will have to provide a transporter system to move test sector in both the ϕ and θ directions across the beam. This assumes a primary beam incident on the test sector. In the event that the inner GEM detectors are installed, a fixed target will likely be placed at the simulated IP in order to generate events similar to those expected in the actual SSC environment. Under these conditions the transporter would simply place the muon test sector in its proper location with respect to the inner GEM detectors and the IP.

The concept for the support frame transporter is shown in figure 4.18. The transporter provides for translation of the muon test sector along floor-mounted rails transverse to the beam direction. Additionally, there is the ability to rotate the test sector in θ and ϕ, in order to place particular regions of the sector into the beam as discussed earlier. The transporter has the capability to locate the muon sector globally to well within the GEM tolerance of 1

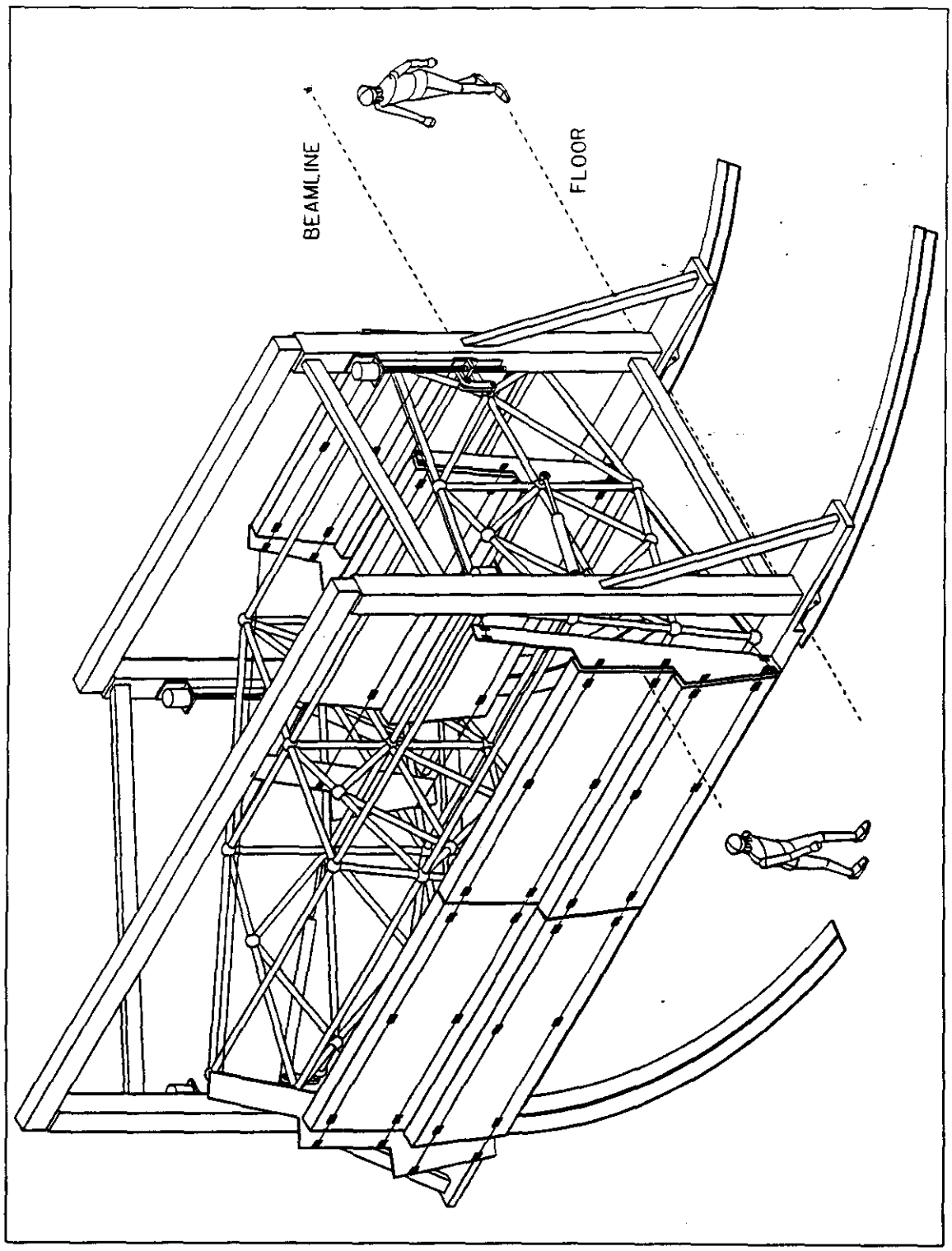

Figure 4.18: Muon transporter

cm with respect to the IP radially and 3 cm in the axial (Z) direction. A key element of the transport system is the ability to maintain the muon chamber local alignment tolerances (a few mm in X and Y and a few milliradians rotation in all directions) through the use of a support structure that is rigid under the expected extremes of the transporter motion.

4.4.3 Muon Gas System

During the FNAL Beam Test two gas systems will be used. First a small, simple open gas distribution will be used to test the small CSCs in Phase I. This will be similar to the existing TTR gas system, but simpler because it will be designed only for nonflammable gases. The second system will be designed for the muon sector test and will be produced as a prototype of the GEM muon gas system. This will be reliable, cost effective and meet performance requirements. It will provide gas flow rates up to 2.5 m^3/day mixed from three or four components with very high grade purity. Because of the relatively large gas flow rate and the high cost of CF_4 the large gas system will be recirculating.

The gas system will maintain gas purity during all period of operation comparable to that available from the commercial suppliers as "ultra pure" or "electronics" grade, i.e., with all contaminants certified to be in the few parts-per-million (ppm) range. A gas cleaning capability will maintain concentrations of O_2 and H_2O at the level of a few ppm. In addition, in order to avoid wire aging problems the gas system should be designed from "good" materials and will remove all hydrocarbon contamination that may cause polymerization on the CSC wires. The gas composition will be continuously controlled and monitored on-line with a 1% accuracy. The gas purity will be continuously monitored on-line at the level of a few ppm using gas analyzers. The large gas system will maintain an internal CSC pressure of 0.5 Torr above atmospheric pressure. The pressure difference from atmospheric pressure will be controlled on-line with high precision because the chamber surface is large and additional pressure can easily burst the chamber.

The large gas system will be used later on during the SSC Beam Test, and as a part of dedicated surface facilities located at the IR-5 for assembly and testing of the muon system, and at factories as well. This requires that the design and fabrication of the large gas system be modular on portable panels and standard racks.

4.4.4 Muon Electronics

One of the major goals of the muon FNAL Beam Test program is to test full-scale CSC prototypes with pre-production front-end electronics. In particular, we will seek to demonstrate that mixed-signal chamber-mounted electronics will operate properly in an accelerator environment. The test will also serve to validate our approach to electronic shielding and thermal management.

The details of the electronic implementation may be found in sections 7.2.2 and 7.7 of the GEM Technical Design Report and in Chapter 7 of this document. The purpose of this section is to outline the general design of the muon electronics and trigger for the FNAL Beam Test.

The muon CSC chambers will be read out using chamber-mounted cathode and anode

front-end processing chains. The cathode chain will consist of a low noise preamplifier, a fast and slow shaper, a sampling circuit, and a multiplexed ADC. In the current design cathode electronics consist of 96-channel front-end readout boards. Each 96-channel board services 16 cathode strips on each of the six layers that comprise a CSC chamber. Calibration of the cathode chain will be achieved using a set of precisely matched capacitors that couple a test pulse to each channel's input. An arbitrary pattern of channels can be programmed with a set of on chip switches and a control shift register. The anode chain will consist of a low noise preamplifier optimized for timing considerations, a shaper, a constant-fraction discriminator, and a DAQ readout controller. The discriminator provides a digital signal for the formation of the beam crossing time from all six measurement layers. In the current design anode electronics consist of 96-channel front-end readout boards. Digital signals from the cathode and anode front-end readout boards will be collected on a per-chamber basis by readout motherboard and transmitted off detector via optical fiber.

There will be about 5500 cathode and about 1400 anode electronics channels connected with 8 motherboards in the FNAL Beam Test. Most of electronics will be installed on the sector prototype but some of the electronics will be installed on a small CSC chamber in order to test the performance of the electronics in a magnetic field.

The GEM Level 1 muon trigger will be highly integrated with the cathode and anode readout chains. This will simplify the design and reduce system costs. The part of the trigger located on the chamber motherboard will be used to form a local charged track (LCT) segment. The forming of an LCT signal requires hit patterns corresponding to good tracks through the chamber. The cathode LCT signals correspond to track segments and will be formed by imposing a four-out-of-six majority logic requirement on the discriminated outputs of the strips from all six layers lying within a small angular range. In addition to the track segments, the signals from the local chamber encoder include an identification of the anode grouping responsible for the generated trigger. The signals from three superlayers will be brought together to a single location on a board housed in crate located in the electronics room. The trigger will be formed by loading the encoded LCT addresses from the three superlayers into memory cells. Selection of triggers using either the $\Delta\phi$ or the sagitta method will be made by downloading appropriate cell contents and by requiring either two-out-of-two or three-out-of-three matches within a column.

In the FNAL beam test the Level 1 muon trigger will be implemented only to the extent necessary to demonstrate that it will be possible to extract trigger signals that are sufficiently well timed to ensure tagging of the bunch crossing. Such a demonstration will be made using prototype versions of the anode preamplifiers and timing discriminators. The raw signals from these discriminators will then be recorded using commercial pipeline TDC's for analysis off-line.

4.4.5 Muon DAQ, On-line and Slow control

The muon DAQ subsystem will be located in a single VME crate. This VME crate will contain Event Data Collector (EDC) boards, a MVME-167 processor, trigger related module and some modules needed for CSC electronics calibration. The EDC boards will collect digital information from the on-chamber motherboards via optical fiber links to the EDC

memory. The data from EDC memory will be read out by the MVME-167 processor or transmitted to the Event Builder depending on the DAQ mode of operation (see Chapter 6 for details). In the initial phase of the FNAL Beam Test program, the muon DAQ subsystem will work in an independent data taking mode controlled from a dedicated muon workstation. In the final phase of the FNAL Beam Test program the data taking will be integrated and controlled by the GEM Global Control System. In the independent data taking mode the muon DAQ subsystem will work via an event builder or (in "fallback" option, see Chapter 6) will use existing PRDAQ [21] software, developed for the TTR. In both cases the muon DAQ subsystem will be debugged and tested at the TTR before the FNAL Beam Test.

The muon subsystem on-line and off-line software for individual CSC chambers in the FNAL Beam Test will be an upgraded version of the TTR software developed during the CSC chamber evaluation R&D Program. It will accumulate all experience in CSC calibration and data analysis from the 1992–1995 tests. The on-line software for the muon alignment system will be developed during the ATS R&D program. A full set of data from three chamber superlayers and alignment system will be available for the first time at the FNAL Beam Test. In order to develop software for the muon system precision tests full GEANT simulation of the muon sector including digitization and data structure simulation will be performed. The muon on-line and off-line software will accommodate as much as possible GEM software standards in Operating System, Languages, Databases, Graphic Interfaces etc.

The components of the muon subsystem that will be monitored and/or controlled by the Slow Control System during the FNAL Beam Test are:

- Chambers
- Alignment system
- Gas system
- Transporter position
- High voltage system
- Low voltage system

Most of the subsystems listed above are unique to the muon system, although high-voltage and low-voltage systems can be the same for the all subdetectors. Each control subsystem will have its own sensors and interfaces but all subsystems will be furnished with EPICS crates (EPICS is the system that has been selected for the GEM global control system). Each control subsystem will be supported by the same or similar EPICS-based software. The interfaces and drivers for most of the muon subsystems should be developed during R&D before the FNAL beam test.

In the initial phase of the FNAL Beam Test program the muon slow control subsystem will work in independent mode and will be controlled from a dedicated muon workstation. In the final phase of the FNAL Beam Test program the muon slow control subsystem will work in integrated mode as a part of the GEM Global Control System.

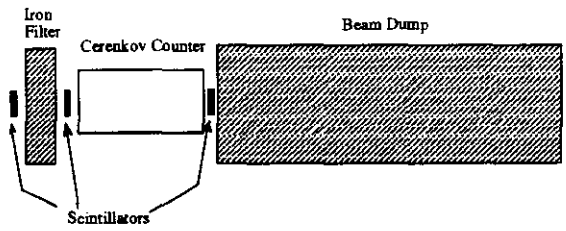

Figure 4.19: Beam dump and muon tagging system

4.5 Data Collection

4.5.1 Beam Requirements

The ideal beam for most of our chamber tests is an energetic (up to 500 GeV) muon beam with an intensity of at least 100 Hz. Since pion beams of 1 MHz (up to 10MHz) are standard for the MW-beam at 500 GeV, with a hadron filter inserted upstream followed by a momentum reselection, a clean muon beam of sufficient intensity should be readily available. Also we plan on a muon tagging system behind the CSC test stand consisting of a beam dump followed by a small Čerenkov counter and scintillators as shown in figure 4.19. This would also allow us to use a pion beam and trigger on the muon component in the beam. The pion beam may also be used for very high rate running and for commissioning the sector.

4.5.2 Run Plan

The run plan is broken down into two phases. The objectives of the first phase are to study the operation of small prototype barrel and endcap chambers in a magnetic field and to perform a complete scan of a full-scale barrel chamber. Of particular interest is the Lorentz angle smearing of the spatial resolution and the chamber operation in the presence of muon-associated backgrounds in a magnetic field. The second phase is devoted to the "false sagitta" measurement and thus will test the entire concept of the chamber-alignment system of GEM. The objectives of the various phases of the program are summarized in the table below.

Phase Ia - Tests in Large Dipole Magnet

- Beam: 200 to 500 GeV, 100Hz < flux < 50kHz
- Tuning with Beam: 1 week
- Data with Beam: 2 weeks
- Particle Type: muons, or pions for Lorentz Angle Studies; muons, or pions for Resolution, Rates, Electronics Studies; muons for Muon Associated Backgrounds

Phase Ib- Tests with Magnetic Field Parallel to Beam

- Beam: 200 to 500 GeV, 100Hz < flux < 50kHz
- Tuning with Beam: 1 week
- Data with Beam: 1 weeks
- Particle Type: muons

Phase II - Barrel Sector Tests

- Beam: 200 to 500 GeV, 100Hz < flux < 50kHz
- Tuning with Beam: 2 weeks
- Data with Beam: 4 weeks scheduled in two sessions:
- 1 week tuning/2 weeks data, with 3 week break to reconfigure the tower between sessions.
- Particle Type: muons

In the nature of a test beam program considerable flexibility is built into the program. We expect to guide the program as we gain experience.

4.6 Budget, Commitments and Schedule for R&D and Engineering Program

4.6.1 Budget

The R&D and Engineering budget for FY94 - FY96 will cover work needed to complete the engineering design of the GEM muon system and to prepare for the FNAL Test beam and conduct the test beam program itself. The scope of effort will be work to complete the engineering design of the CSCs, setup the pilot factory and operate it for 1 year, perform the alignment R&D (ATS), engineering of the chamber support structure, development of the trigger, and integration of the system with GEM. The costs assume that GEM will be commissioned by 2002.

4.6.2 Institutional Commitments for R&D Program and Task Coordinators

The GEM Muon R&D and Engineering Program will require the efforts of all members of the muon collaboration. The program is broken down into 9 major tasks. For each task a number of institutions will contribute and will be guided by a Task Coordinator. The overall coordination of the tasks will be conducted by the muon steering committee, which at present is chaired by the muon system manager.

Table 4.3: Summary R&D Budget FY94 - FY96:

	Task	FY94	FY95	FY96	Sum
1.	Chambers: R&D and construction	$ 800k	$ 800k	$ 500k	$ 2100k
2.	Chambers: Performance evaluation TTR, RD5 and other	$ 200k	$ 150k	$ 50k	$ 400k
3.	Muon Trigger	$ 40k	$ 30k	$ 30k	$ 100k
4.	Alignment/ATS	$ 450k	$ 300k	$ 200k	$ 950k
5.	Electronics Evaluation	$ 80k	$ 70k	$ 60k	$ 210k
6.	Simulations	$ 50k	$ 50k	$ 50k	$ 150k
7.	Tooling for chamber production	$ 300k	$ 400k	$ 300k	$ 1000k
8.	Pilot Chamber Factory	$ 0k	$ 0k	$ 570k	$ 570k
9.	Engineering	$ 600k	$ 720k	$ 1700k	$ 3020k
10.	FNAL test planning	$ 80k	$ 80k	$ 40k	$ 200k
11.	FNAL Test Beam Program	$ 1300k	$ 1300k	$ 400k	$ 3000k
	Total	$ 3900k	$ 3900k	$ 3900k	$ 11700k

4.6.3 Schedule for R&D and Engineering Program

The schedule for the R&D and Engineering Program is driven by goal to fully test "Generation 1" chambers in the FNAL test beam (FY96). In order to meet this goal the essential chamber engineering must be completed before that date as well as the development and validation of the essential alignment concepts. The schedules are shown in figures 4.20 and 4.21.

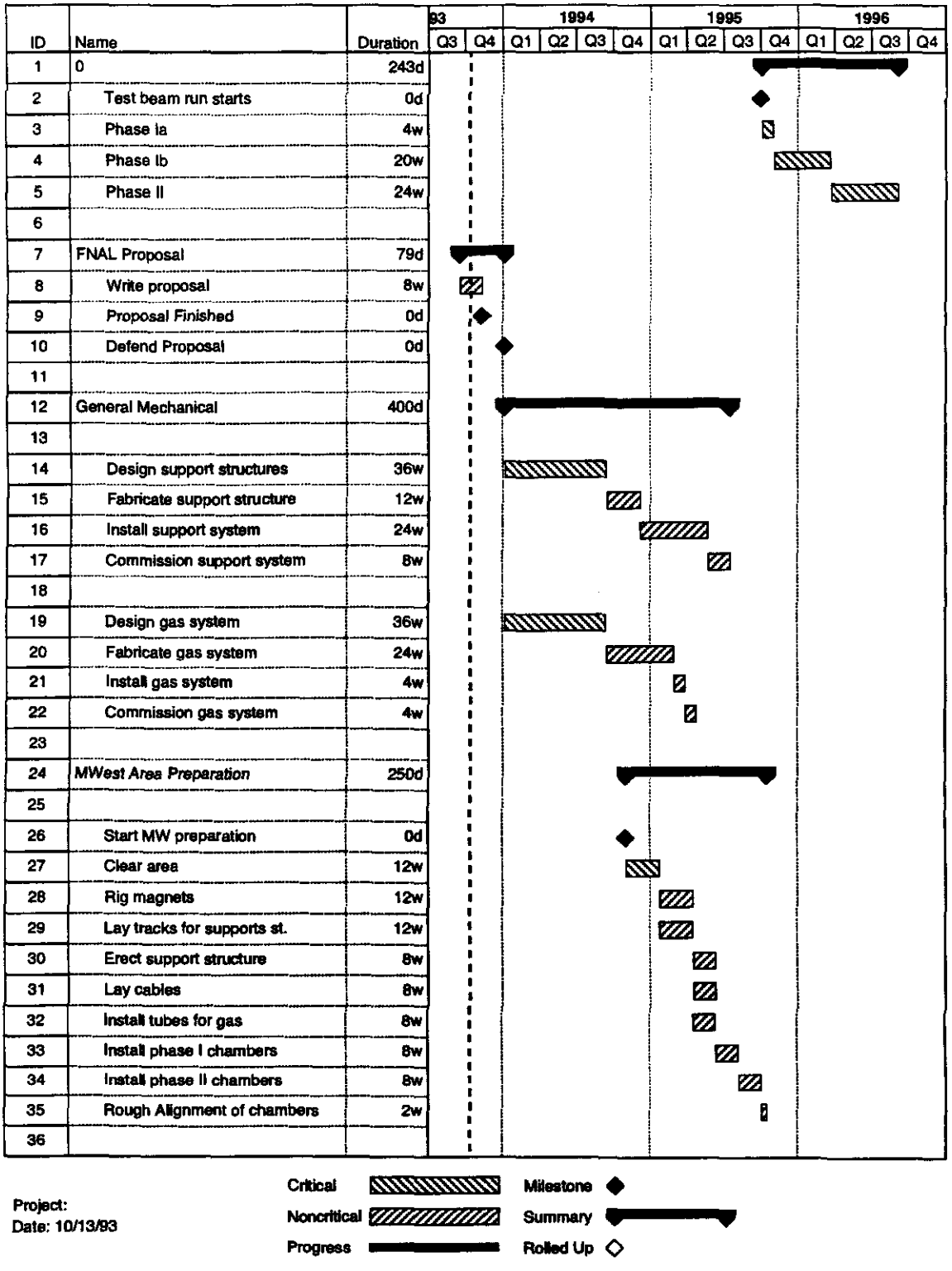

Figure 4.20: Schedule for R&D and Engineering Program

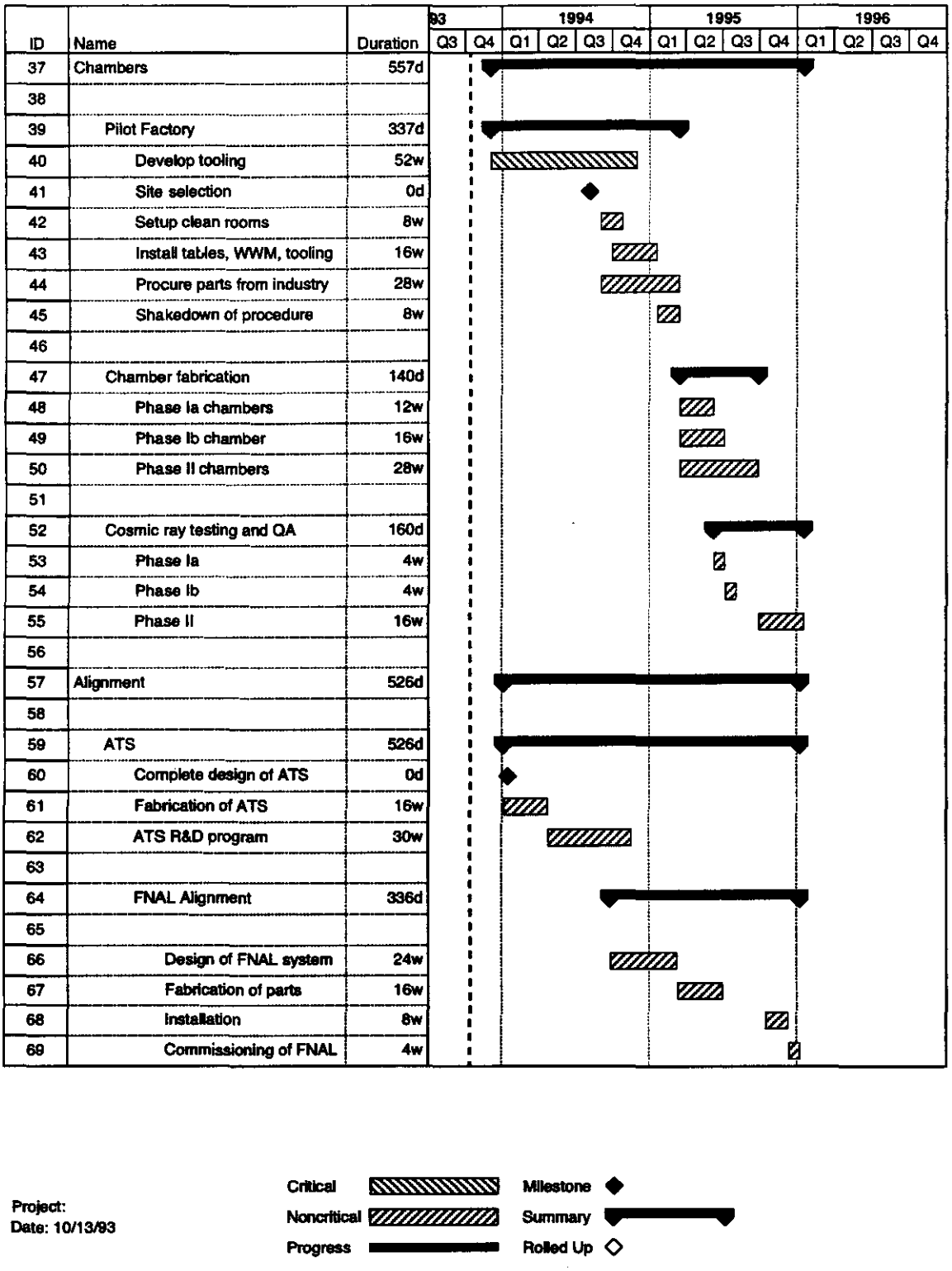

ID	Name	Duration
37	Chambers	557d
38		
39	Pilot Factory	337d
40	Develop tooling	52w
41	Site selection	0d
42	Setup clean rooms	8w
43	Install tables, WWM, tooling	16w
44	Procure parts from industry	28w
45	Shakedown of procedure	8w
46		
47	Chamber fabrication	140d
48	Phase Ia chambers	12w
49	Phase Ib chamber	16w
50	Phase II chambers	28w
51		
52	Cosmic ray testing and QA	160d
53	Phase Ia	4w
54	Phase Ib	4w
55	Phase II	16w
56		
57	Alignment	526d
58		
59	ATS	526d
60	Complete design of ATS	0d
61	Fabrication of ATS	16w
62	ATS R&D program	30w
63		
64	FNAL Alignment	336d
65		
66	Design of FNAL system	24w
67	Fabrication of parts	16w
68	Installation	8w
69	Commissioning of FNAL	4w

Figure 4.21: Schedule for R&D and Engineering Program

Table 4.4: Personal and Institutional Responsibilities

	Task	Task Coordinator	Institution Involved
1.	Cathode Strip Chamber Technology R&D and Engineering:	G.Mitselmakher	BNL, BU, CIT, IHEP, JINR, LLNL, MIT, MSU, PNPI, SSCL, UoC, UoH
2.	Chamber Performance Evaluation:	G.Mitselmakher	BNL, Brown, BU, CMU, ITEP, JINR, LSU, MSU, PNPI, SSCL, SUNY-SB, UoC, UT
3.	Muon Trigger:	M.Atiya	BNL, ITEP, PU, SSCL
4.	Alignment Technology R&D:	J.Paradiso C.Wuest	CIT, CSDL, ITEP, LLNL, MIT, PNPI, SSCL, Tsinghua University
5.	Electronics Evaluation:	D.Marlow V.Polychronakos	BNL, BSU-Minsk, BU, JINR, ORNL, PNPI, PU, UoC, UoH
6.	Simulations:	R.McNeil	IHEP, ITEP, LLNL, LSU, MIT, Moscow S.U., SSCL SUNY-SB, UoA, UoC
7.	Chamber Production:	TBD	
7.1	Development of Tooling for chamber production:		LLNL, UoC, UoH, SSCL
7.2	Pilot Factory Setup:		TBD, Interested parties: BNL, BU, CIT, CSDL, IHEP, JINR, LLNL, MIT, PNPI, UoC, UoH
7.3	Pilot Chamber Production:		determined by Task 7.2
8.	Engineering:	M.Marx	CSDL, LLNL, SG&H, SSCL, SUNY-SB
9.	FNAL Test Beam Program:		
9.1	Planning and support for FNAL	C.Bromberg	CMU, MSU, SSCL
9.2	FNAL Test Beam Program:		Muon Group

Chapter 5

Central Tracker

5.1. Introduction and Overview

We are proposing a three year (1994, 1995 and 1996) R & D Program for the GEM Central Tracker. This tracker consists of a silicon microstrip (SM) inner tracker and an interpolating cathode pad chamber (IPC) outer tracker. The geometrical arrangement of the Central Tracker is shown in Figures 5.1-1 and 5.1-2. The performance design goals of the tracker are given in Table 5.1-1. A detailed description of the Central Tracker can be found in the GEM Technical Design Report (April 30, 1993).

Table 5.1-1: Design Parameters for the Central Tracker

Outer Radius	90 cm
Length	350 cm
Rapidity Coverage	$\|\eta\| \leq 2.5$
Magnetic Field	0.8 T
Occupancy	
at $L = 10^{33}\,cm^{-2}sec^{-1}$	$\leq 1\%$
at $L = 10^{34}\,cm^{-2}sec^{-1}$	$\leq 10\%$
Charge separation at 95% c.l.	$p \leq 600 GeV / c$
Momentum Resolution	
at high momenta (measurement limited)	$\Delta p / p^2 \sim (1.2) \times 10^{-3}$ (GeV / c)$^{-1}$
at low momenta (multiple scattering limited)	$\Delta p / p \sim 3.5\%$
Vertex Resolution	
along beam direction	$\delta z \sim 1$ mm
impact parameter	$\delta b \sim 25\ \mu m$ above 10 GeV/c

The Central Tracker R & D Program naturally divides into five components, i.e. work on the mechanical aspects and the electronics of both the silicon and the IPC detectors, and the test beam program. These are described in sections 2 to 6 of this proposal. The purpose of this R & D program is to understand the technical issues and the conceptual design of the detector sufficiently so that at the end of this program the detailed engineering design can be rapidly completed and the construction of the detector can be started.

The Central Tracker R & D program has been well underway for the past two years (1992 and 1993). Small scale prototypes of the IPC's were tested in a beam at the Indiana University Cyclotron in 1992 to verify the basic operating parameters. A full scale prototype of the barrel IPC's was tested in a three-week run in a Brookhaven test beam in July 1993, where the chamber demonstrated the required performance. We are planning another test beam run in late 1994 with full size barrel and endcap IPC chambers as well as some 18 cm long silicon microstrip prototypes.

The culmination of the R & D program will be the 18 Degree Sector Test at Fermilab, which we anticipate will take place from mid 1995 to mid 1996. Portions of all of the detector components of GEM will participate in this test in approximately the same geometrical layout as they will occupy in the final GEM detector. In the first half year of this test we expect each detector component to be tested and comissioned independently. In the second half year they will operate in an integrated mode, i.e. readout the same test beam particle in all of the detector components simultaneously so that the response of all of the components of the GEM detector can be studied in an integrated way.

For the Central Tracker part of this test we plan to implement an 18° azimuthal sector of both the silicon and IPC full length barrel detectors and an 18° azimuthal sector of one of the endcaps of both the silicon and the IPC detectors. The layout of this test set-up is shown in Figures 5.1-3 to 5.1-5. At this time we expect to have the final design versions of both the silicon and the IPC readout electronics implemented for all of the channels of this test setup. However if funding or time do not allow this we will instrument only selected portions of the 18° sector.

All members of the GEM Central Tracker group are committed to participate in this R&D program. This group at the present consists of fifteen institutions and over 100 scientists, as listed in Table 5.1-2. The management of the Central Tracker project and the technical design is performed by the Central Tracker Steering Committee which consists of C. Baltay, J.E. Brau, D. Lee, S.C. Lee, K. Morgan, J. Musser, and T. Thompson. The chairman of the Steering Committee is C. Baltay. The chief engineer of the Central Tracker Project is T. Thompson, and budgeting support is provided by H. Pretty. The personal and institutional responsibilities in this program are summarized in Table 5.1-3.

Table 5.1-2: Membership of the Central Tracker Group

Academia Sinica, Taiwan, R.O.C.
A. Antos, Y.C. Chen, T.L. Chu, M. Huang, S.C. Lee, A. Sumarokov, P.K. Teng, M.J. Wang, P. Yeh

Brookhaven
P. O'Connor, V. Radeka, G. Smith, B. Yu

Indiana University
C. Bender, C. Bower, M. Gebhard, R. Heinz, S. Mufson, J. Musser, J. Pitts

Los Alamos
R. Barber, J.G. Boissevain, M. Brooks, D. Brown, M. Cafferty, B. Cooke, K. Fuller,, S.F. Hahn, J. Hanlow, C. Johnson, J. Kapustinsky, W.W. Kinnison, D.M. Lee, R. Martin, G.B. Mills, R. Prael, G.H. Sanders, W.E. Sondheim, T. Thompson, J. VanAnne, L. Waters, B. Weinstein,

Moscow State University
G. Bashindzhagyan, Y. Fisyak, D. Karmanov, E. Kuznetsov, A. Larichev, M. Merkin, A. Savin, A. Voronin, V. Zhukov

Nanjing University
E. Chen, D. Gao, M. Qi, D.X. Xie, N.G. Yao, Z.W. Zhang

Oak Ridge National Laboratory
C. Britton, K. Read

Rutgers University
P. Jacques, M. Kalelkar, R.J. Plano, P. Stamer

SSCL
S. Blumberg, H. Fenker, K. Morgan, R. Shypit, J. Thomas

University of Albany
M.S. Alam, I.J. Kim, B. Neman, J. O'Neill, H. Severini, C.R. Sun, L. Zhichao

University of Michigan
D Kouba, D. Levin, J. Mann, S. McKee, G. Tarle

University of Oregon
A. Arodzero, J.E. Brau, R.E. Frey, D. Gao, R.T. Kollipara, N. Sinev, D. Strom, X. Yang

University of Pittsburgh

E. Engels, P.F. Shepard

Vanderbilt University

R.S. Panvini, T.W. Reeves, S. Rousakov, J.P. Venuti

Yale University

C. Baltay, M.B. Barakat, R. Ben-David, W. Emmet, S. Manly, D. Pilon, S. Sen, J. Sinnott, J. Turk, E. Wolin

Central Tracker Steering Committee

C. Baltay (Chairman), J. Brau, D. Lee, S.C. Lee, K. Morgan, J. Musser, T. Thompson

Table 5.1-3 Personal and Institutional Responsibilities

Area of Effort	Person Responsible	Institution Involved
Silicon Detector	D. Lee, J. Brau	Los Alamos Nat. Lab., U. of Oregon, U. of Pittsburgh,, Vanderbilt U. Taiwan, Moscow State
-Mechanical	T. Thompson	
-Electronics	S. Hahn	
Pad Chambers	J. Musser, C. Baltay J. Thomas	Brookhaven Nat. Lab., Los Alamos Nat. Lab. SSC Laboratory Yale U., Indiana U. U. of Michigan, Rutgers U., Taiwan
-Mechanical	W. Emmet	
-Electronics	J. Musser, P. O'Connor	
Integration into GEM	K. Morgan, T. Thompson	All
Simulations	S. McKee	All
Beam Tests	K. Morgan	All
Budgets	H. Pretty	All

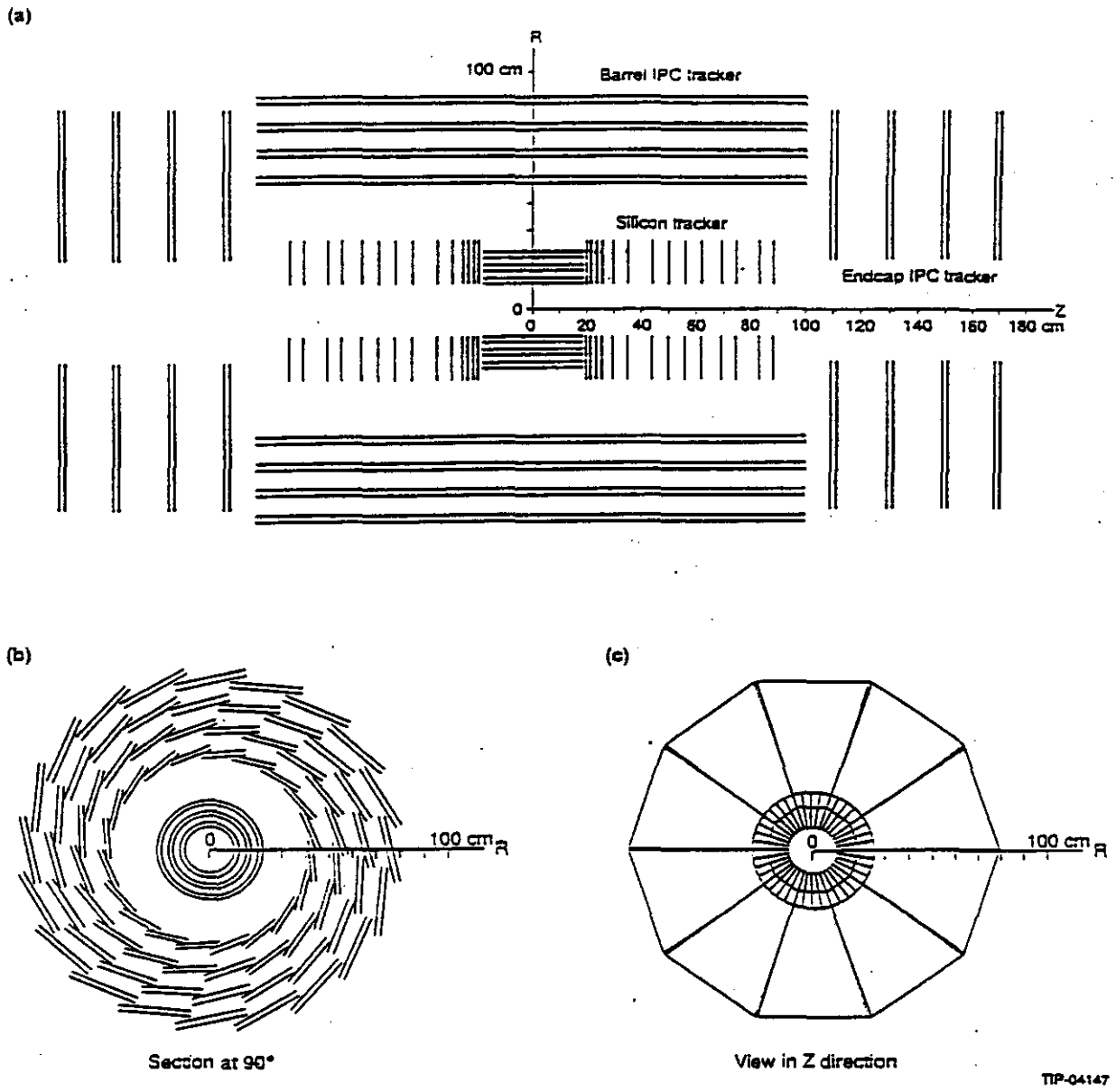

Figure 5.1-1: Schematic layout of the detector elements in the GEM central tracker. (a) Side view of the tracker. (b) End view of barrel section. (c) End view showing forward sectors of IPC and silicon rings.

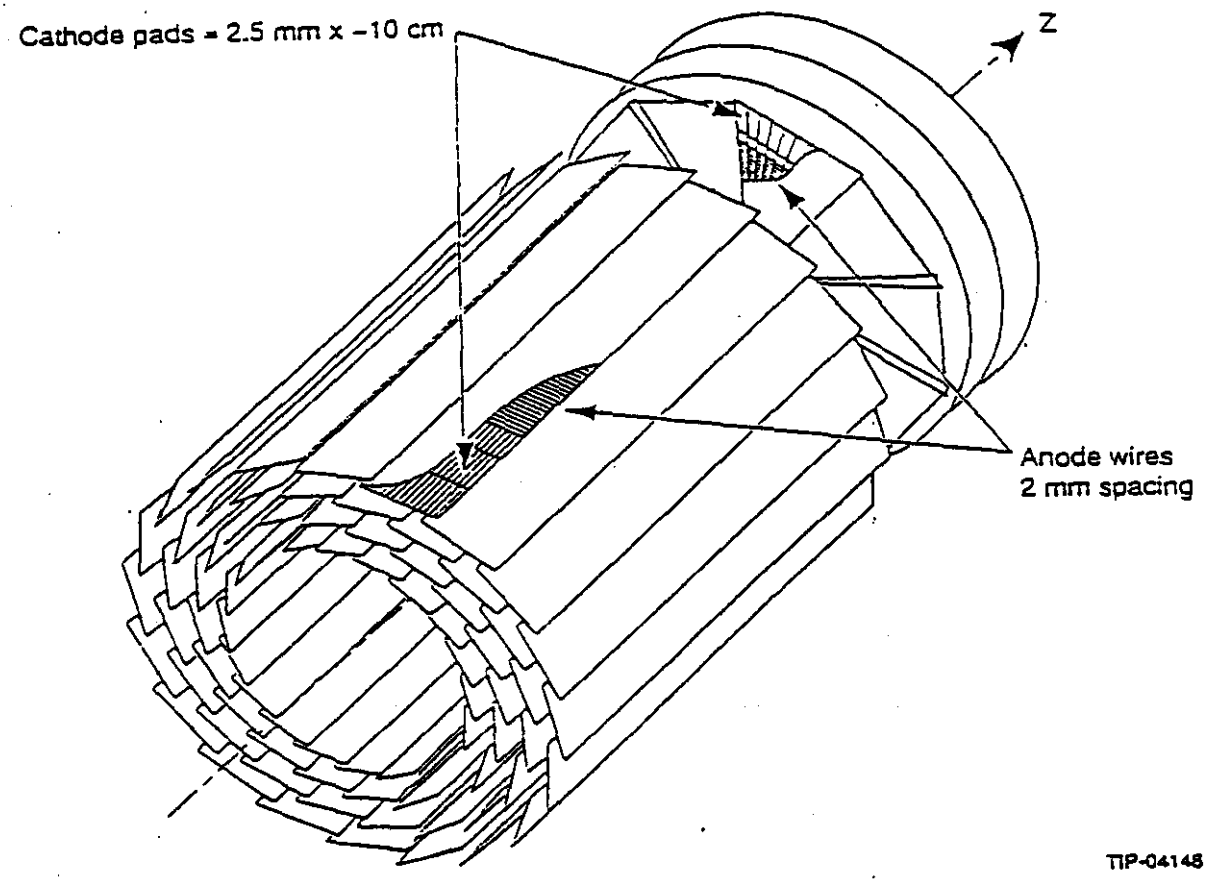

Figure 5.1-2: Schematic layout of the detector elements in the GEM interpolating pad chambers.

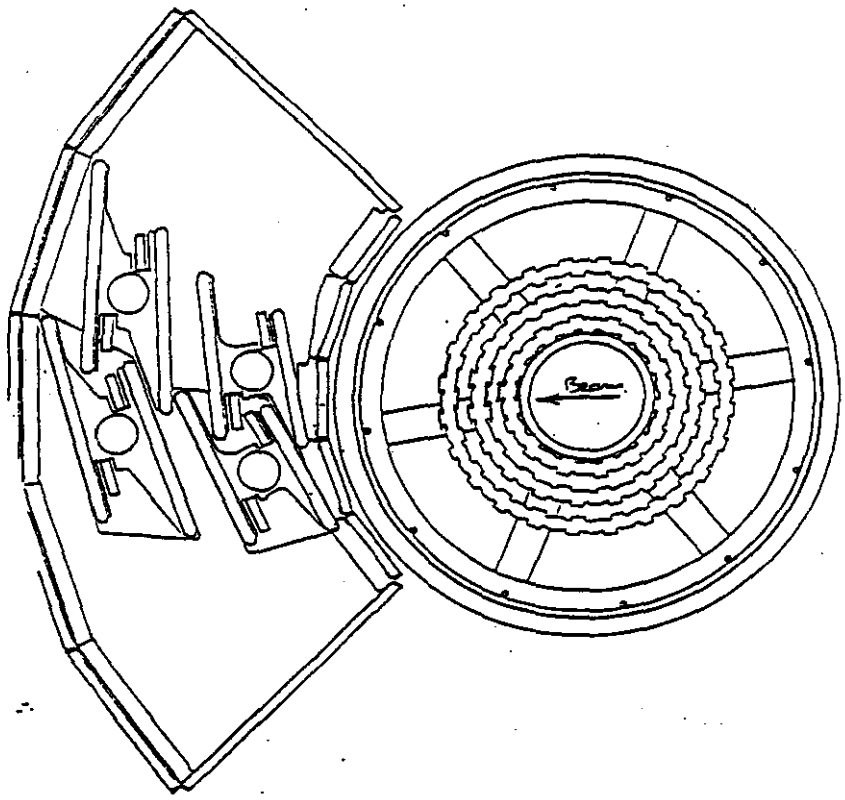

Figure 5.1-3: Arrangement of the detector elements in the η=0 plane of the 18° sector prototype.

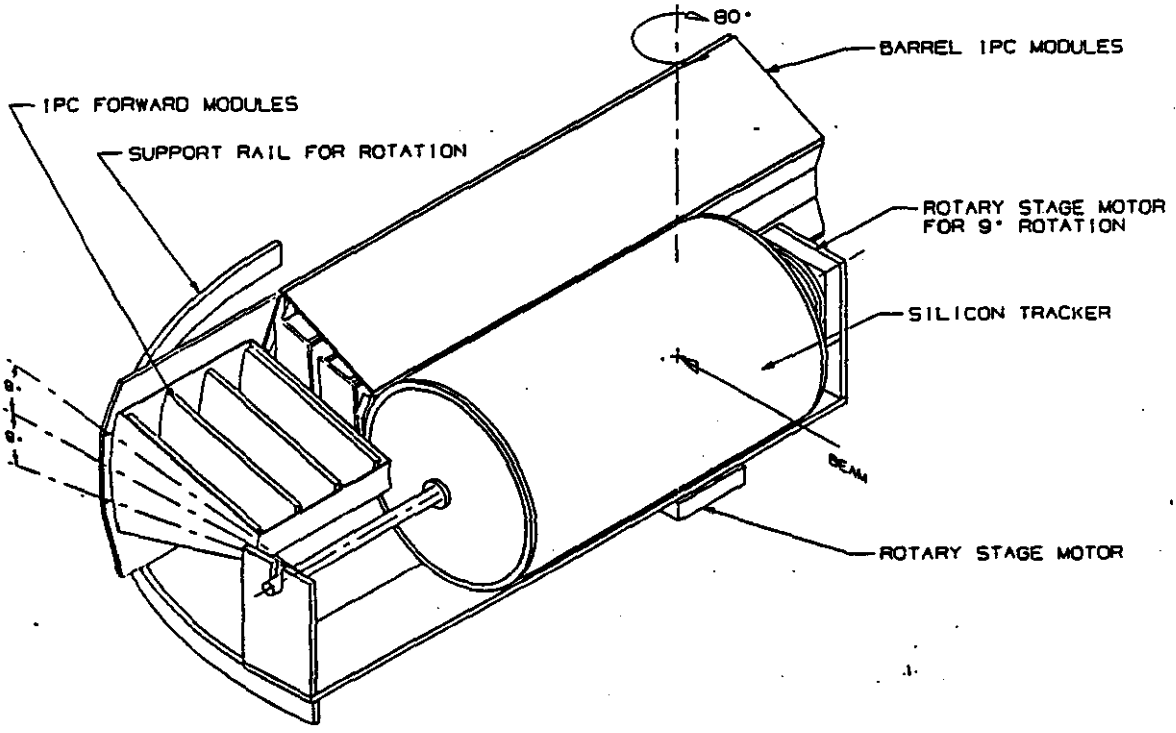

Figure 5.1-4(a): Isometric view of the Central Tracker 18° Sector Prototype

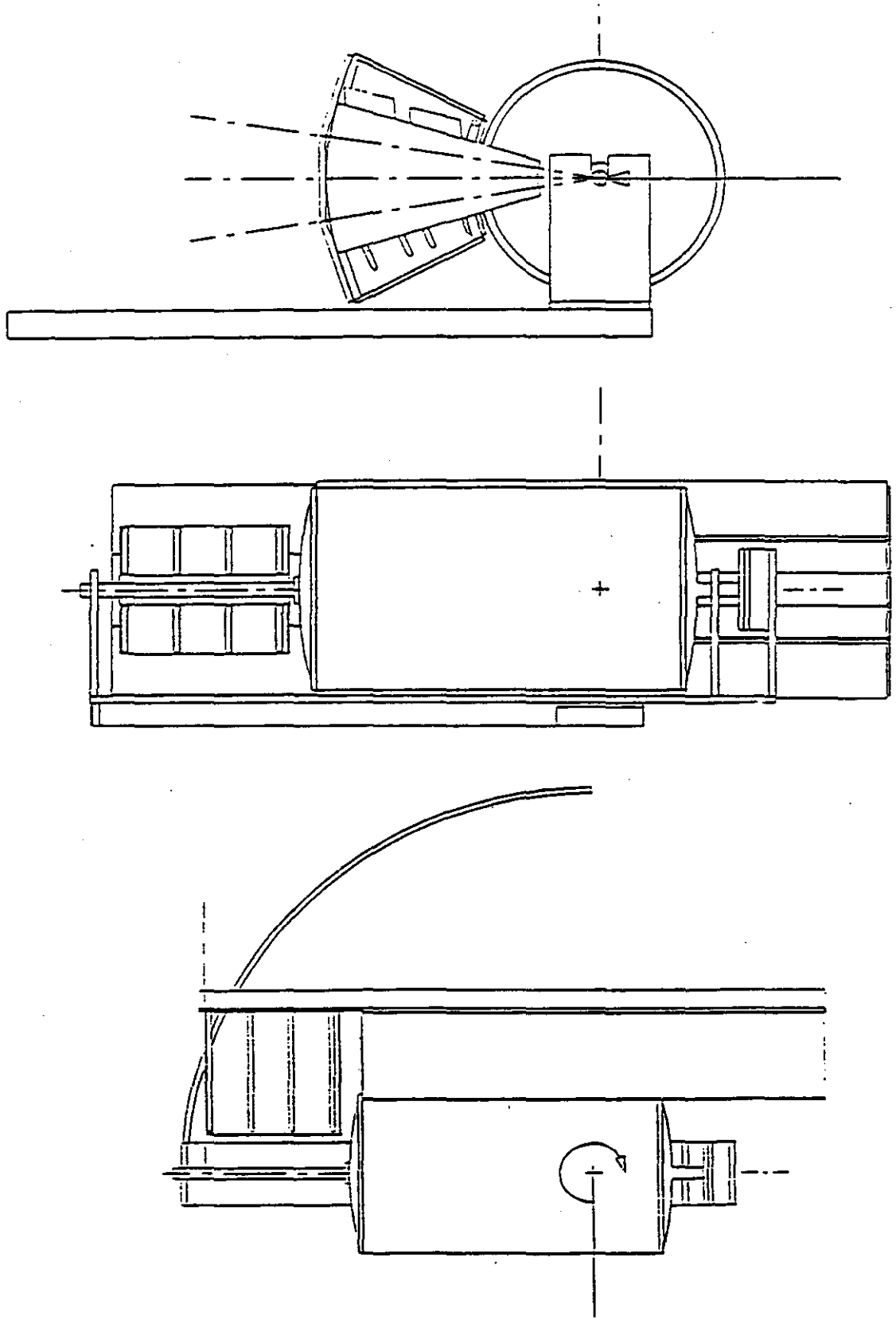

Figure 5.1-4(b): End, side and top views of the Central Tracker 18° Sector Prototype

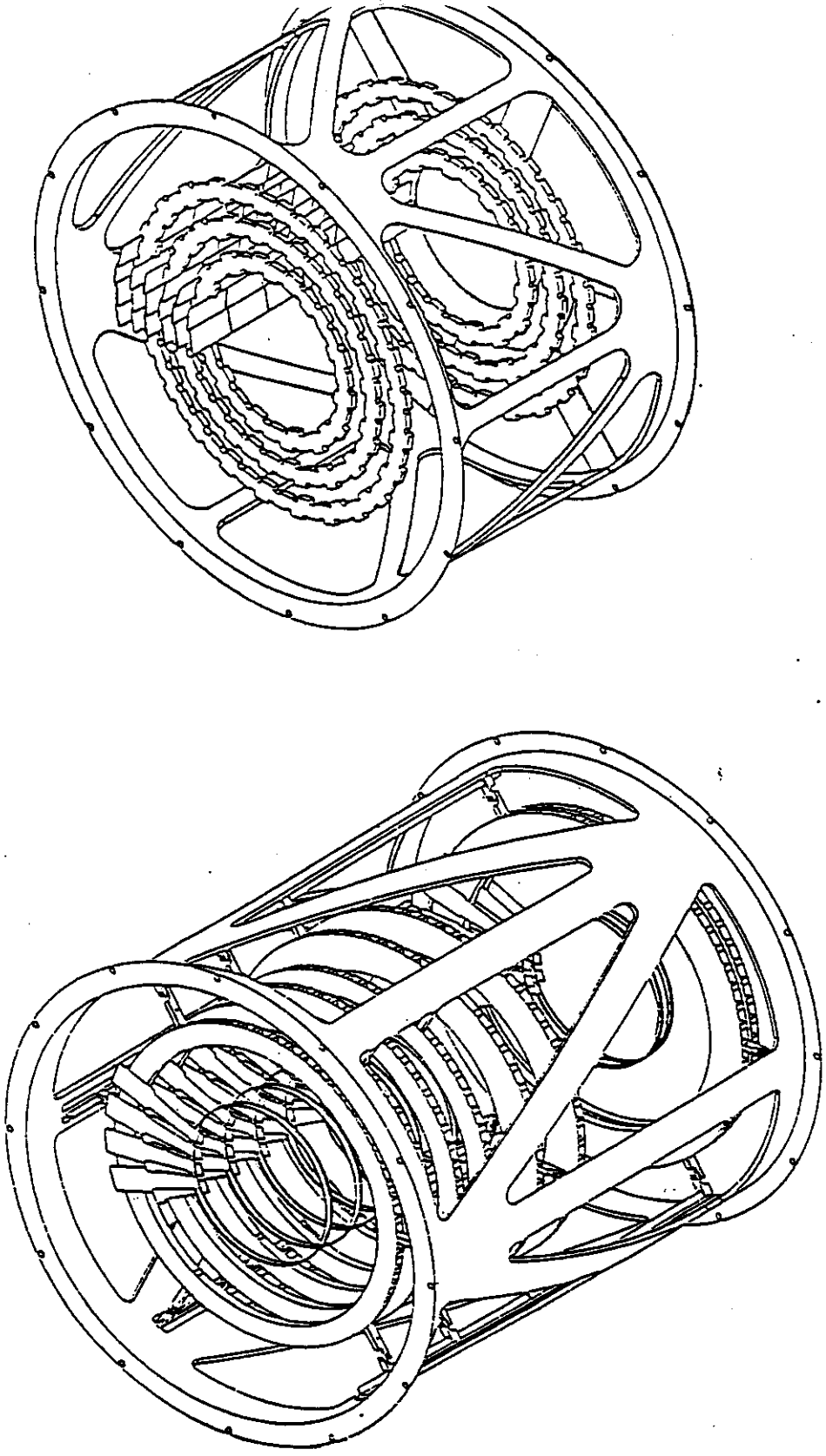

Figure 5.1-5: Isometric views of the silicon part of the 18° sector prototype for a) the barrel part and b) for the end cap part.

5.2. Silicon Detector R&D

The physics goals of the GEM detector have placed some very severe design restrictions on the Silicon Tracking System (STS). The Silicon Tracking System must have high resolution, high stability, high tracking efficiency, and as low a radiation length as possible. To satisfy these requirements we have initiated an important R&D program to address these central issues. The ultimate goal of the R&D program is to allow construction to begin on the GEM Central Tracker in 1996. The immediate focus is to prepare prototypes for the Fermilab test beam in 1996 that test the critical components of the system. The 18 degree sector test at Fermilab will be a full system test, designed to verify that the complete STS will satisfy all of the design requirements.

The design parameters for the STS are set by physics requirements of resolution, occupancy, and speed. The critical performance parameter of the tracker is the spatial resolution of 15 microns per layer in the azimuthal direction derived jointly from the momentum resolution and impact parameter resolution requirements. The resolution requirements translate into a stability requirement of 10 microns for the mechanical structures. Physics simulations show that a 10 micron stability is needed to preserve the ability to find secondary vertices. To achieve the highest efficiency for detecting electrons and photons we must minimize electron bremsstrahlung and photon conversions. This implies a low mass silicon tracker that is still sturdy enough to be stable to 10 microns. Low occupancy and high track finding efficiency require a fast low noise amplifier. However, satisfying these requirements with an 18 cm long strip detector coupled to the amplifier and maintaining low power is a formidable task. These issues are the focus of the Silicon Tracking System R&D program.

5.2.1. Microstrip Detector Design

The silicon microstrip detector R&D plan combines detector fabrication and testing with detailed simulation followed by a two step beam test plan for 1994 and 1995-96

The key issues being addressed for the microstrip detectors are:

- basic detector response
- multi-strip response (intra- and inter- charge coupling)
- strip length dependence
- minimization of microstrip capacitance
- reduction of microstrip resistance
- effect of 0.8 Tesla magnetic field on detector response

- effect of radiation on detector performance
- detector/electronics coupling

Many of these effects are being studied in the laboratory with very fast amplifiers with nanosecond resolution mounted on a few strips. Studies of the time-structure of induced currents correlated with simulation studies will lead to a full understanding of detector performance and optimization.

The test beam plans for 1994 and 1995-6 involve a two step process to achieve GEM requirements. In 1994 a single 18 cm ladder (back-to-back detectors) will be beam tested to confirm choices made in the laboratory R&D phase. It is critical that the GEM prototype front end electronics are included in this test. The preamplifier-comparator chip will be included, but a beam-test specific readout system will be developed for the back end of the electronics chain.

The 1995 test will be much more inclusive and larger as described below.

The R&D effort to investigate the issues enumerated above has begun with the assembly of a number of tools and resources to address them.

(1.) Detector fabrication is focused on a few sources. Existing studies of laser induced pulses show that the time needed to collect the charge from a track or laser pulse is primarily dependent on the resistivity of the strips. Figure 5.2.1-1 illustrates this trend, as the lower set of curves show a significant slowing of charge collection for strip resistances of 50 Ω/cm. We have had detectors fabricated by Hamamatsu with different strip widths and thicknesses to measure to what extent the resistance of the strips can be decreased. Increasing the strip width will increase the strip capacitance which is undesirable. The optimum strip width for GEM detectors will be determined.

(2.) The Santa Cruz code PULSE for the simulation of the signals from silicon strip detectors was obtained from the Santa Cruz group. This code includes the effects of Landau fluctuations and the drift of electrons and holes in the electric and magnetic fields inside the detectors. It has been modified for single-sided detectors and for the deposition of charge from alpha particles.

To date, the code has been used to study the following issues:

- the difference in time-walk between different timing algorithms: one algorithm based on the time of threshold crossing for the early charge collection and one based on using the peaking time of the charge collection. While the peaking time gives a very good time for uniform charge deposition, this study found that the Landau

fluctuations and the detailed pulse formation in adjacent strips for shared charged rendered the threshold algorithm more robust. Figure 5.2.1-2 illustrates this.

- the effect of detector tilt on microstrip response and charge sharing: the finite width of the detectors alone causes incident high momentum particles to pass through the detectors at angles of up to nearly ten degrees. In addition, there are mechanical motivations to tilt the detectors slightly, increasing the crossing angle for stiff tracks. Such crossing angles result in a sharing of charge between neighboring strips, and a weakening of the separation between signal and noise. These effects have been studied and have demanded a minimization of the tilt angle.

- the response of silicon detectors to alpha particles: alpha particles penetrate the detectors about 25 microns before coming to rest. This energy deposition so close to the surface creates a quite different response compared to a minimum ionizing particle passing through the detector. Quantitative understanding has been possible with the PULSE code.

- Lorentz drift studies of the electrons and holes in the detectors and studies of the relative importance of each to signal formation: due to the 0.8 Tesla magnetic field within the GEM tracking volume the charges experience an E x B drift. For the single sided detectors of GEM, the holes contribute about 80% of the response and therefore the approximately 1.5° Lorentz angle of the holes dominates the larger angle for electrons.

(3.) An infrared (1.06 micron) laser system has been established to study the attenuation and dispersion of signals on silicon strips. By using laser light to excite transitions from the valence band to the conduction band of the silicon detectors it is possible to simulate the passage of charged particles. The infrared diode laser produces pulses of 1 ns FWHM. The advantage of using the laser over charged particles is that the tracks produced by the laser do not have the Landau fluctuations associated with charged particles, making it possible to measure the response averaged over many pulses. Figure 5.2.1-3 displays the typical response of a microstrip detector to the infrared laser pulse after amplification of the signal with a fast, current sensitive Hewlett-Packard amplifier. To study dispersion we can pulse the detectors at different distances from the end of the strip detectors and determine how the observed signal evolves with strip length. Figure 5.2.1-4 presents a first preliminary measurement of the signal versus the distance the laser probe is located from the end of the strip for a few strips adjacent to the principal strip. Such studies have only just begun.

An important element of the microstrip detector R&D, as described above, is the characterization of strip resistances and capacitances. Results are presented in Table 5.2-1. These measurements of strip resistance are based on single-sided detectors manufactured by Hamamatsu for GEM

with several different strip widths on a single wafer. The strips on the detector are divided equally into groups with widths of 8 μm, 28μm, and 38 μm. The resistances of several of each of these types of strips were measured. Also a few strips with widths of 6 μm were placed on the detector, but only one ran the full length of the detector, so only one full measurement was possible. These results are consistent with a strip height of about 1 μm for the wider strips assuming a conductivity of pure aluminum. It also suggests that 30 Ω/cm is possible for strips of about 10 μm width and 20 Ω/cm for strips of about 14 μm width.

Table 5.2-1: Measured strip resistance as a function of strip width

width(μm)	R(Ω/cm)	ρ(Ω/cm x μm-width
38	7.4	280
28	10.1	284
18	15.8	284
8	40.1	321
6	70.0	420

(4.) Strip capacitance is also very important, perhaps more so, and is coupled directly to the effort to reduce strip resistance. In microstrip detectors with 50 μm pitch the strip capacitance is typically 1-2 pF/cm, depending on strip width. The capacitance is primarily due to the coupling to neighboring strips. If a bipolar amplifier is used, the noise, in terms of electrons detected by the amplifier is given by:

$$Q_n^2 = 2e\frac{I_C\tau}{\beta} + 2\frac{(kT)^2}{eI_C\tau}C^2$$

where τ is the shaping time of the amplifier, I_C is the collector current and C is the sum of detector and input capacitances. If the second term dominates then the noise is proportional to the input capacitance. If the collector current is increased to give the minimum noise (at the cost of increased power consumption), then the noise only depends on the square root of the capacitance. In either case it is desirable to minimize the capacitance. Calculations of strip capacitance have been compared to measurements for a series of strip configurations. The aluminum strip width and p^+ layer width can be varied independently. Table 5.2-2 presents these results. The capacitance is the total effective strip capacitance. A recent study found an increase in capacitance of about 50% after irradiation at the levels expected at the SSC. We plan to study the behavior of our prototypes before and after irradiation. We will also study what changes in fabrication techniques can be made in order to minimize the capacitance increase with radiation.

Table 5.2-2: Measurements and calculations of strip capacitance

w_{Al}(μm)	wp^{+}(μm)	C measured	C calculated	Comments
8	12	1.04	1.06	measured at Oregon
18	12	1.2	1.20	"
28	12	1.47	1.50	"
38	12	1.85	1.97	"
10	10	1.03	1.00	measured at Santa Cruz
20	20	1.31	1.30	"
30	30	1.79	1.66	"

5.2.2. Silicon Tracker Mechanical Design

To develop a full-scale STS for insertion into the SSC beamline by the year 2002 it will be necessary to test a prototype at the Fermi beamline in 1996. The test should focus on the high risk elements that are critical to the success of the STS program.

The design goal for STS stability has always been considered a critical item. The goal is to achieve a relative positional stability of approximately 10 microns between any detector elements. This difficult task is compounded due to the fact that the central and forward regions have to maintain this relative positional stability on separate mounting platforms.

To address the mechanical and physics issues it will be necessary to test an 18 degree sector of the Central Tracking System. To assess the performance and stability of the CTS it is necessary to pivot the tracker in the beamline in order to expose it to the full range of detector operation at the SSC. The Fermi test beam proposal is shown in Figure 5.2.2-1. The proposed detector is a fraction of the total detector proposed for the SSC, but is enough to meet the goals at a minimum cost.

The primary goals for the mechanical stability portion of the Fermi STS test are;

- Verify the stability of the superlayer components
- Verify stability between superlayer components
- Validate the optical metrology systems capability
- Investigate the effects of temperature and moisture on stability of the superlayer components

There are other additional difficulties which could be classified as evolutionary development efforts for which the Fermi test beam will provide a convenient opportunity to assess our design progress. The targets for these efforts are;

- Ladder construction technique
- Cooling system design margin
- Fabrication issues on structural components
- Cabling and utility routing issues
- Gas system design

To meet the development goals of the Fermi test scheduled for 1996 it will be essential to carry out in-depth R&D during 1994 to 1996. This work will focus on structures, ladders, alignment, and ancillary issues such as cooling and gas systems.

5.2.2.1. Structure

5.2.2.1.1. Structure Design and Assembly

To measure the stability of the STS it will be necessary to build the central and forward region support frames which carry the superlayers. This is to ensure that mechanically the structures behave the same as the actual final structure. The boundary conditions are going to be changed to reflect the fact that only a small portion of the silicon will be in place (non uniform heating). The distortion of the structure will be different than in the final configuration, however we will have the opportunity to assess our capability of predicting structural distortions which is the real issue. In addition, the long term stability (on order of one day) should not be altered with the different boundary conditions. This will enable us to assess the effects of variable ambient conditions on the long term stability of the tracker. The proposed support frame structure is shown in Figure 5.2.2-2.

The cooling rings which are used to hold the ladder assemblies will be installed on a support web in the central region of the detector as shown in Figure 5.2.2-3. It is important that full-scale rings and webs be fabricated in the same manner as the final SSC version since the structure will not behave the same if partial rings and webs are used. The modest extra expense incurred in building full rather than partial rings and webs is small in comparison with the knowledge gained by studying the real device.

The forward region will only use six of the fourteen forward planar arrays. We propose that full rings be mounted into the support frame as shown in Figure 5.2.2-4, following the same philosophy as used in the central region.

5.2.1.2. Radiation Hardness

The materials initially baselined for the CTS are believed to be suitable for the final SSC version of the tracker. Prototype radiation hardness testing will need to be done to validate material susceptibility to radiation environments anticipated at the SSCL. As the design has evolved, and the materials availability and cost have been closely factored into the design, the selection of final materials is similar but not identical to what we originally thought.

5.2.2.2. Ladder

The ladder development during the next two years is essential to the overall success of the program. Several issues, notably ladder fabrication and assembly, will need to be resolved within the scope of the R&D Program. The proposed central region ladder is shown in Figure 5.2.2-5.

The design requirements for the ladder assembly must meet numerous physics, mechanical and electrical specifications. The physics requirements of dimensional stability and low radiation length demand maximum structural efficiency of low radiation length stiffeners. Heat loads from the Multi-Chip-Module (MCM) mounted on the ladders will have to be extracted in a manner that minimizes the detector temperature and deflection, and still meet the MCM thermal specifications. Near the end of its expected lifetime the irradiated detector will require a suppressed operating temperature to lower the leakage current to acceptable levels. Proper selection of materials and structural placement will be required to minimize thermal induced strains.

Thermo-mechanical analysis will be required to develop an optimized design, which will be followed by prototype testing. Mechanical tests will verify structural stability, thermal deformation, MCM heat extraction and silicon detector thermal gradients.

5.2.2.2.1. Ladder Assembly

Strip alignment and assembly specifications require the development of a fast, precision assembly technique. Incorporated into the ladder assembly process will be high speed optical mapping of thousands of detector fiducials to record strip locations. Ladder assembly processes will be developed and tested to verify that prototypes comply to the specifications. Throughout each step of the assembly process, probe tests of the detectors will be done to ensure minimal degradation of the performance of the detectors.

5.2.2.2.2. Detector TAB Bonding

The immense number of channel connections that will have to be wire bonded will require the development of an affordable, reliable, high speed bonding technique. The detector specifications are at the leading edge of Tape Automated Bonding (TAB) technology, which is a commercial process currently being investigated. Development of fine pitch TAB tape and bonding techniques will be prototyped and tested. Probe testing of prototype detectors before and after TAB application will verify that the process does not degrade the silicon detector performance.

5.2.2.2.3. Radiation Hardness

The adhesives used in the assembly will need thorough evaluation under radiation environments similar to those expected at the SSCL. The next two years will be used to test potential adhesives which provide the necessary thermal-mechanical behavior to meet the design objectives. Adhesives and structural materials that are selected will have to be compatible with the detectors, electronics, coolant and the radiation environment. Compatibility and radiation testing of all components will be conducted.

5.2.2.3. Cooling System

The cooling system design must meet several challenging requirements: extract the heat generated in the MCM's, cool the detector down to the range of 0° to -10°C, maintain a stable operating temperature, have a minimum radiation length, and be compatible with the electronics and radiation environment. Both liquid convection (water/methanol) and evaporative phase change (butane) systems will be designed and tested. Systems studies will evaluate the trade-offs of each system against the design specifications. Thermal and fluid flow analysis will be done to establish the optimum design parameters for each system. The cooling system must be capable of removing the heat of over 2,000 individual MCM's while maintaining the ICs within specific temperature limits. Where possible, high thermal conductivity substrates and adhesives will be selected to keep the temperature drop acceptably low through locally high heat flux regions. The coolant fluids selected will have to operate as low as -10°C and still have efficient thermal transfer properties. Dimensional stability specifications require the system to provide a narrow operating temperature range to minimize the detector distortions. Detector subassembly thermal analysis will lead to establishing the maximum acceptable cooling system thermal drifts.

Prototypes will be built and tested to verify predicted thermal gradients, thermal stability, heat transfer coefficients, fluid flow rates and system pressure drops. A complete barrel superlayer prototype will be tested to demonstrate both mechanical and thermal stability under duplicated operating conditions.

5.2.2.4. Alignment and Optical Monitoring

The alignment and optical monitoring systems are additional key R&D areas in the overall CTS program. The R&D in this area must ensure that we are able to meet the 10 micron stability requirement. Two areas need development: the first is the stability measurement system and the second is the optical monitoring system.

The stability system is currently under development by SDC and the bulk of this work will be directly applicable to the GEM program. The R&D undertaken by GEM will mainly consist of tools which will be unique to the GEM size platform.

GEM will initially lead the development effort for the optical monitoring system. The effort will consist of developing a fiber-optic probe head which will be used to measure the relative distortion of a superlayer in-situ. This effort will culminate in a working system which will monitor real time displacements of the detector components. The R&D will focus on optimization of the parameters for producing a lightweight, durable and radiation hard piece of equipment.

Prototypes will be built and tested to verify predicted displacement resolution. A complete barrel superlayer prototype with fiber optic displacement sensors will be tested to measure both mechanical and thermal stability under duplicated operating conditions.

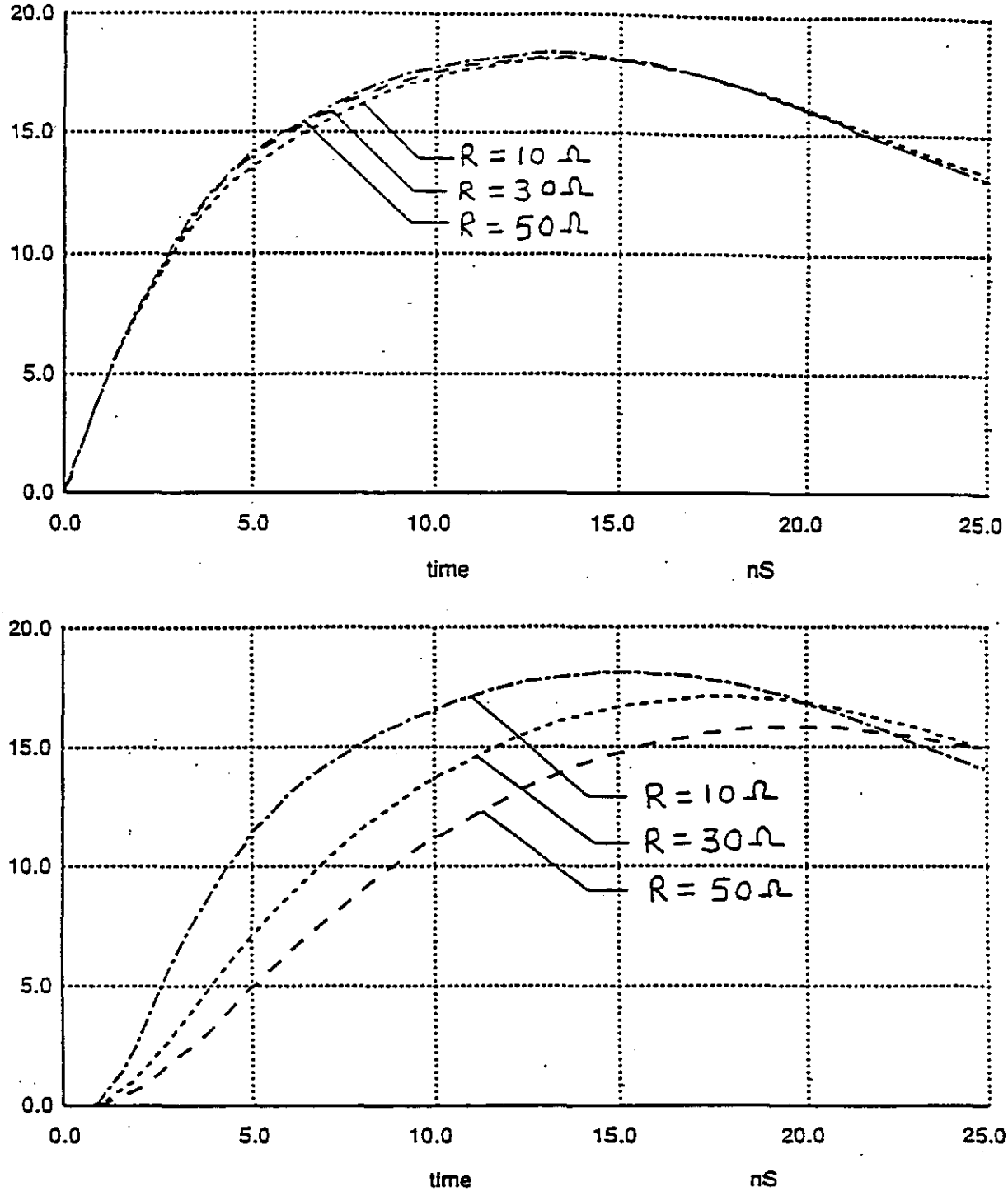

Figure 5.2.1-1 Calculated GEM preamplifier output waveforms as a function of strip resistance. The upper curves show the waveforms for 10 Ω/cm, 30 Ω/cm, and 50 Ω/cm where the charge is deposited at the end of the strip nearest the preamplifier. These curves show little dependence on strip resistance, as is expected. The lower curves show the waveforms for these strip resistances where the charge is deposited at the far end of the microstrip, 18 centimeters from the preamplifier. Here the effect of strip resistance is clear.

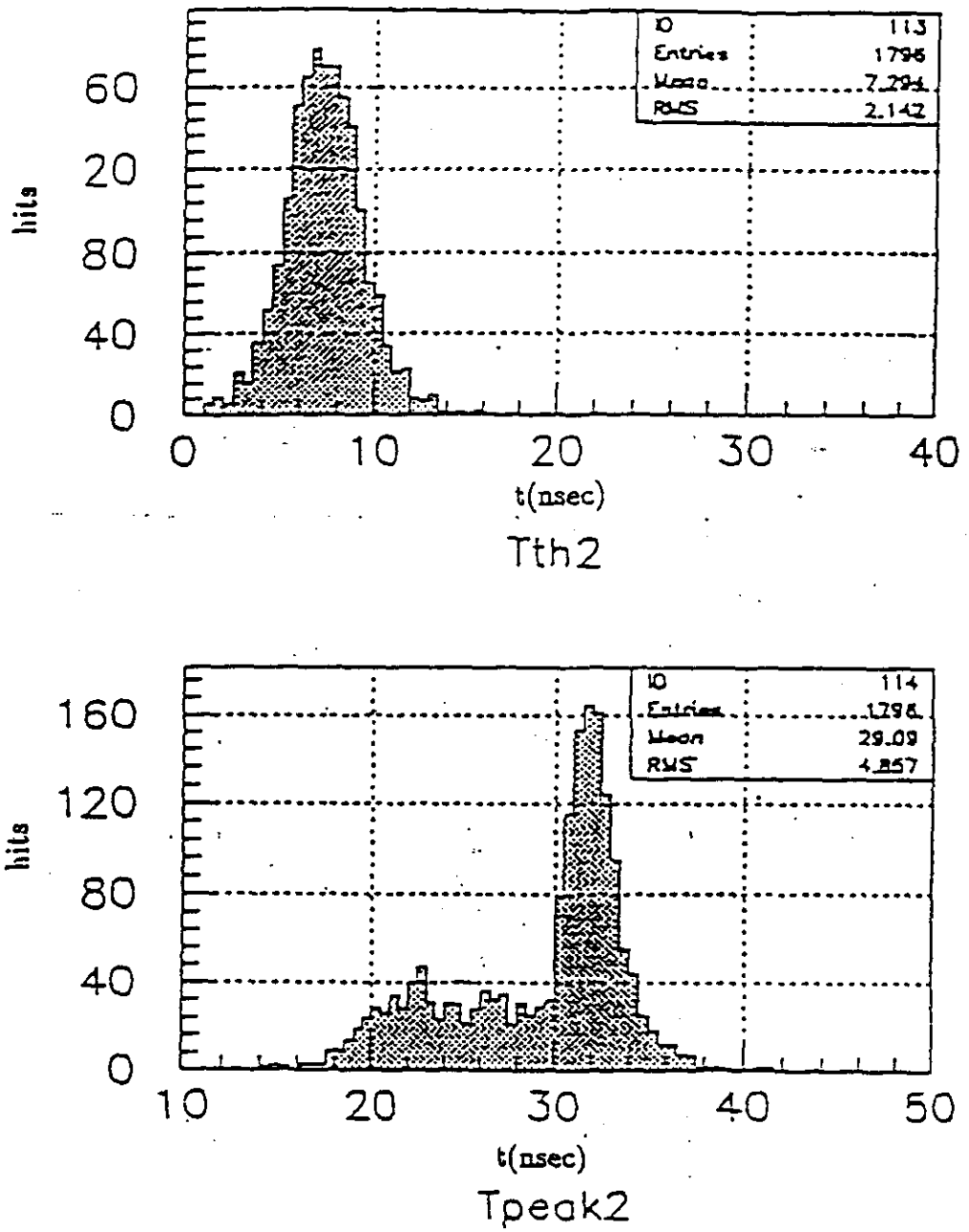

Figure 5.2.1-2. Timing of hits in microstrip detectors for two different time algorithms. The microstrip responses have been convoluted with a simulation of the preamplifier response having a 20 nanosecond shaping time. The upper figure results from using the time of threshold crossing with the threshold set to 1/4 mip. The lower figure results from using the peaking time of the convoluted pulse. 1000 particle crossings were simulated with 1796 hits (average 1.8 strips per crossing).

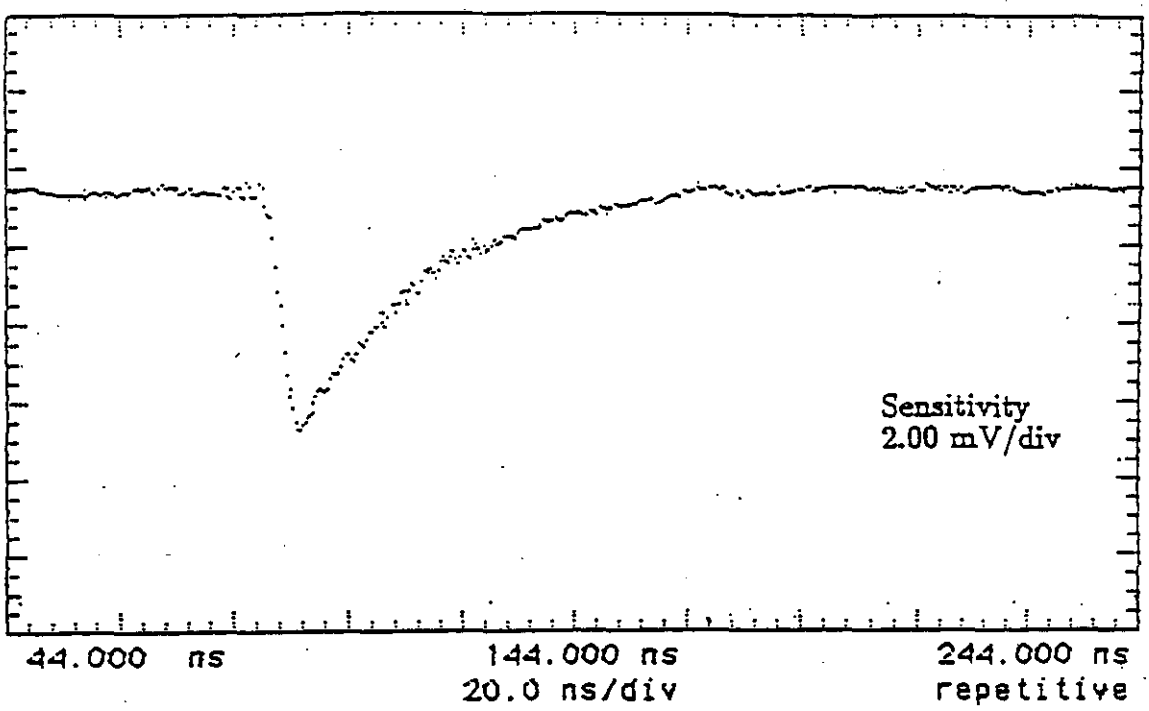

Figure 5.2.1-3. Measured average response over an 18 centimeter microstrip to the 1.06 μm laser pulse. The laser pulse has been located at the far end of the 18 centimeter strip from the fast current sensitive Hewlett-Packard preamplifier.

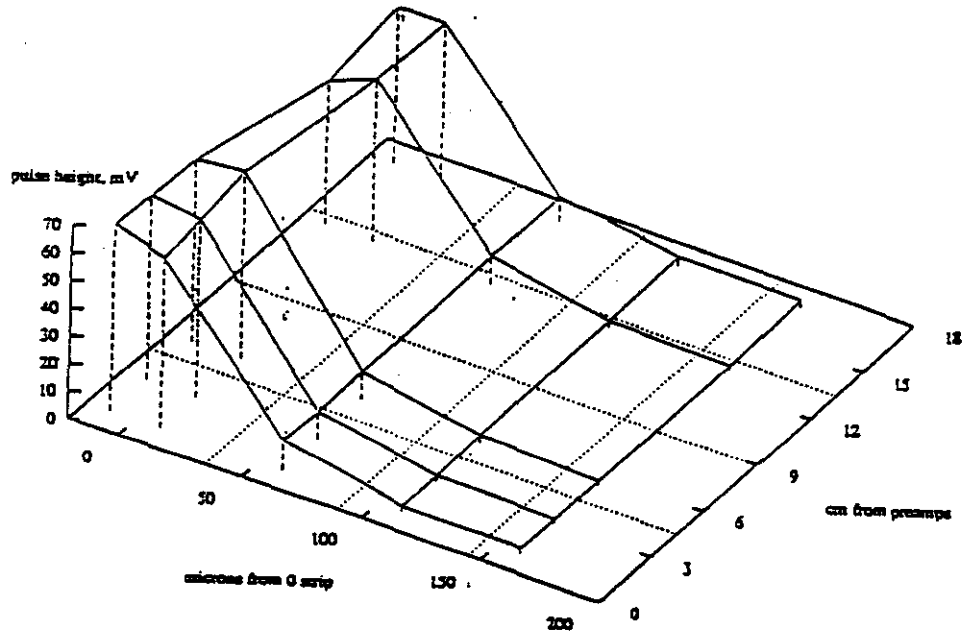

Figure 5.2.1-4. Response of charge sensitive preamplifiers to 1.06 μm laser pulse versus distance along the 18 centimeter strip for several adjacent strips.

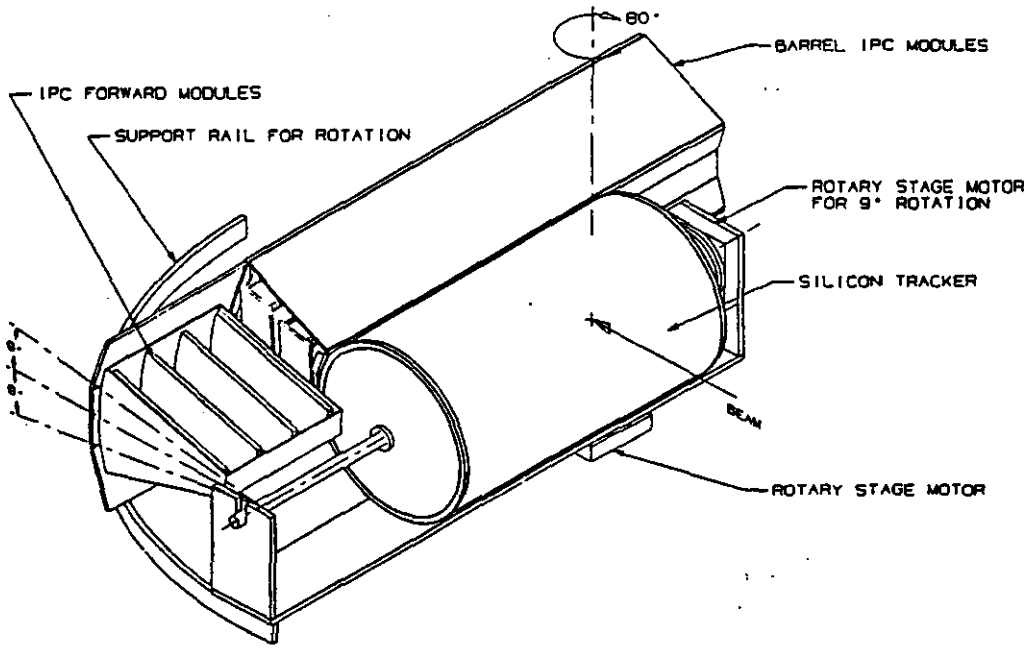

Figure 5.2.2-1: Central Tracker prototype for the 18° Sector Test at Fermilab.

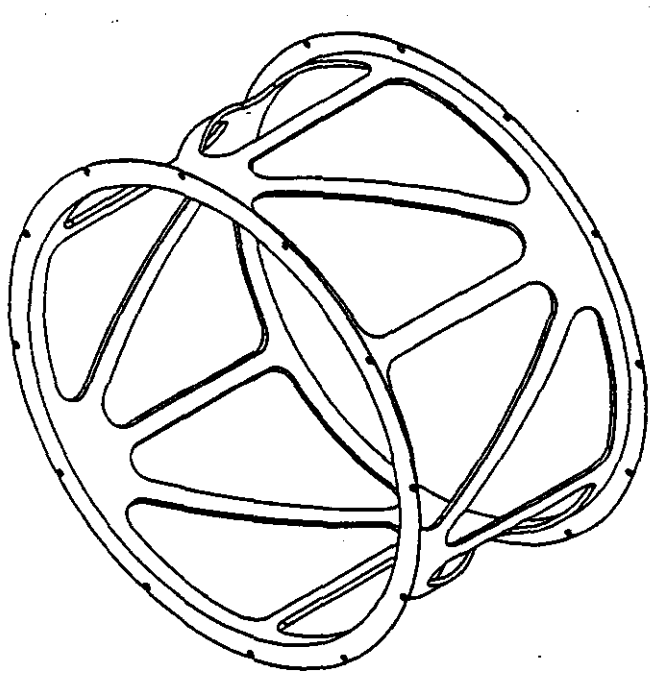

Figure 5.2.2-2: Proposed support frame structure for the barrel region of the silicon detector.

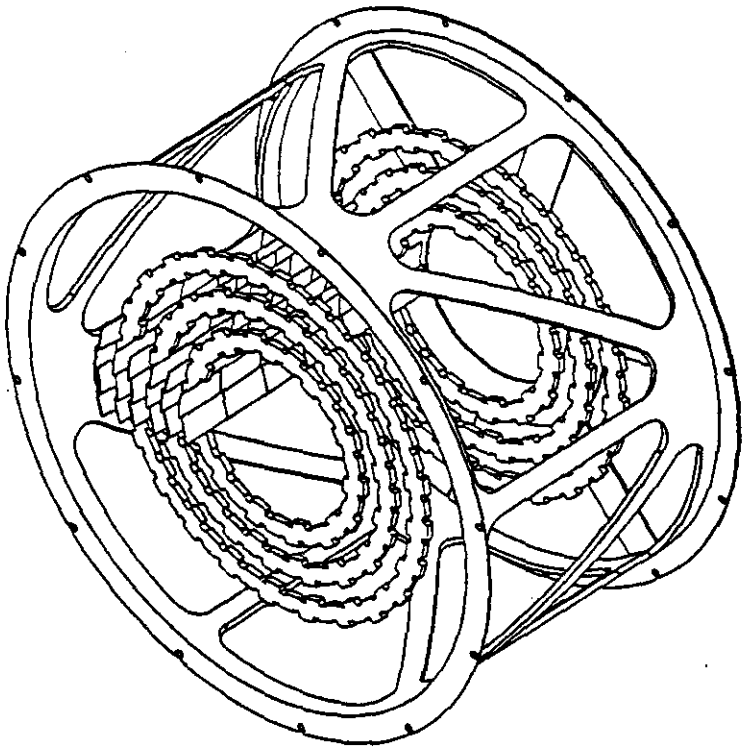

Figure 5.2.2-3: Barrel region of silicon prototype.

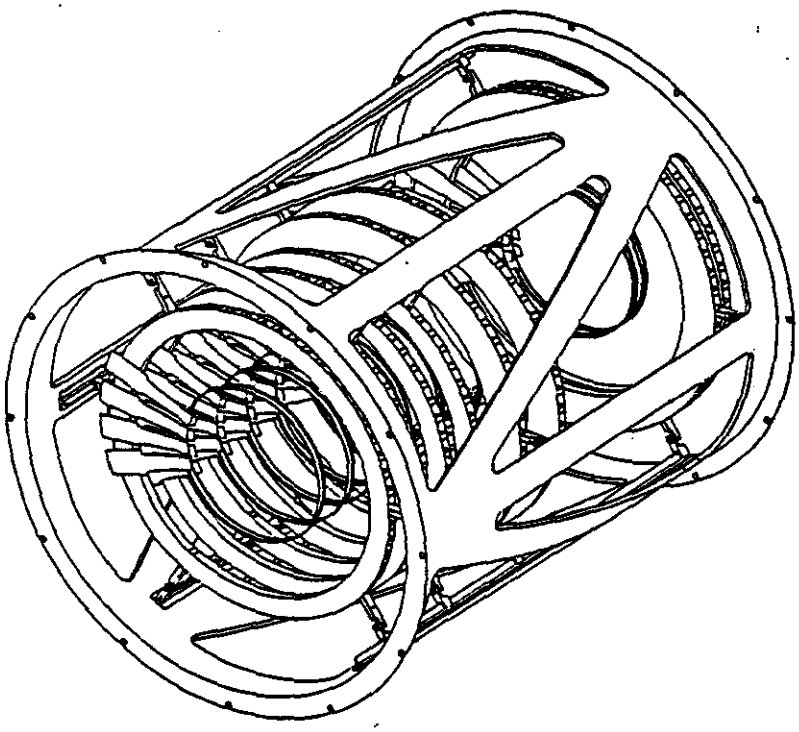

Figure 5.2.2-4: Forward region of silicon prototype.

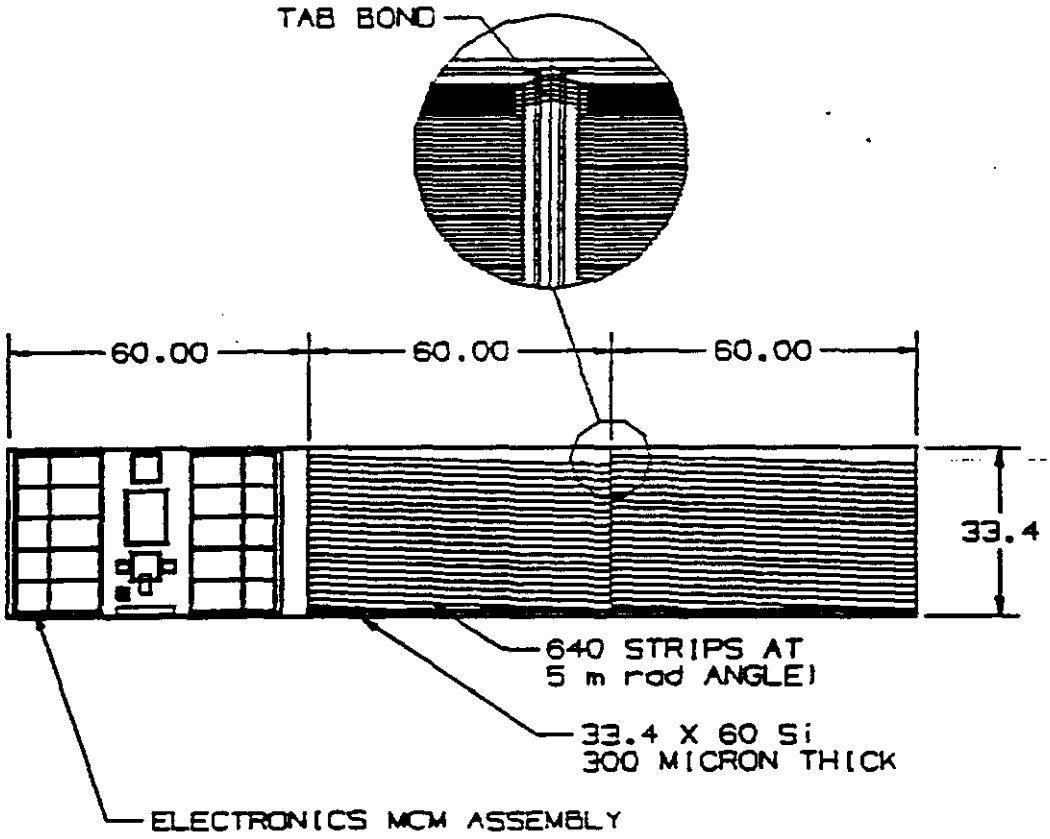

Figure 5.2.2-5: The proposed central region ladder for the silicon detector.

5.3. IPC System R & D

The IPC system R&D program is a comprehensive multi-year plan whose primary goals are the development of barrel and endcap chambers, support structure, and readout electronics for the GEM outer tracker. Starting with small chambers, in which the basic IPC concept is proven to work, larger and more suitable chambers will be constructed, with the final pre-production prototypes expected to meet all the requirements for operation at 10^{34} luminosity. In the following sections we outline our development program in each of these areas.

5.3.1. IPC Chamber R & D

The development of IPC chambers for GEM will proceed through three stages. The first stage, which is largely complete, involves addressing through simulations a number of performance issues which arise from the unique characteristics of the tracking environment at the SSC, such as the effects of a high beam crossing rate, track density, and radiation levels. In addition, a set of basic operating parameters for the IPC chambers, such as gas composition, chamber dimensions, gain, etc., which optimize the performance of the system were determined using tests conducted on small scale chamber prototypes. Some of the key results of these studies, including the measured position resolution of an IPC prototype using fast gas and electronics, are presented in section 5.3.1.2 of this document. Further tests on these small prototypes will be conducted through 1993, with the primary goal of implementing a full readout system prototype. The next stage of the IPC R&D program, which is now underway, involves the fabrication of full scale prototype chambers, incorporating the results of the initial prototype studies including optimal cathode layout, wire spacing, and other chamber parameters into the mechanical design. The first full size barrel chambers have been constructed, and were the subject of a test beam run at BNL in July 1993. Some preliminary results of this beam test are presented in section 5.3.1.2. The key issues which will be addressed in the future beam tests involve the performance of full scale IPCs in a high rate environment. Multi-track resolution will be measured as well as single track resolution in the presence of a high rate background. During this time period the readout electronics development will progress to the point where a prototype readout system can be fabricated. The final stage of the IPC R&D program involves the integration of this front end electronics with a full scale IPC chamber. The IPC R&D program will culminate in the 18 degree sector test at FNAL, described in section 5.7.

5.3.1.1. Progress to Date

5.3.1.1.1. Drift Velocity and Lorentz Angle Measurements.

Because of the high beam crossing rate at the SSC, a fill gas with a high electron drift velocity and a small Lorentz angle is required for the GEM outer tracker. Mixtures of freon-14 (CF_4) and carbon dioxide (CO_2) exhibit both of these characteristics. A test chamber was built

to measure these properties and has been used to test different ratios of these gases to find the proper optimization for the GEM IPCs.

Figure 5.3.1-1 is a sketch of the chamber built to conduct these gas studies. An electromagnet was provided by the Indiana University Cyclotron Facility (IUCF) to generate a uniform magnetic field of 0.8 Tesla. A nitrogen laser (337 nm) was focused with two cylindrical fused silica lenses to provide a region of localized ionization within the drift region of the chamber. A MWPC with cathode strip readout was located adjacent to the drift region, and separated from it by a grounded mesh. The straight cathode strips were 4 mm in width on a 5 mm pitch, and were separated from the anode wires by a distance of 8 mm. The position was determined by a centroid finding method similar to that used in the prototype IPCs, and described below. The laser was used to generate ionization at three known positions, and the differences in times and measured centroid positions were then used to determine the Lorentz angle and drift velocity. Based on these measurements and the requirements on the IPCs, a nominal mixture of 62% CF_4, 38% CO_2 has been chosen for tests of the prototype IPCs.

5.3.1.1.2. IPC Prototype X-ray Studies

Small scale prototype IPCs have been designed and built to study the performance of these devices for the GEM outer tracker. The initial set of tests were conducted using an x-ray source as the primary ionization source. Figure 5.3.1-2 shows a 3-dimensional assembly drawing of this chamber design. The anode wire size and spacing, the anode-cathode separation, and the cathode pitch and pad length are all taken from the GEM baseline design for the outer tracker.

The preamplifiers and shaping amplifiers used in these studies were designed by our collaborators at Brookhaven National Laboratory and have the fast response times required in this application. The total gain of the front end amplifiers is 10 mv/fC, and the shaper has a peaking time of 30 ns.

Most of the x-ray tests to date have been done using a Philips-Norelco 3 kW x-ray generator. Both Copper (8 keV K-line) and Tungsten (8.4 and 9.7 keV L-lines) x-ray tubes have been used in our tests. Our best position resolution measurements have been obtained using the low energy (2 keV) Bremstrahlung photons from the Tungsten tube. Note that 2 keV is the expected energy loss of a minimum ionizing singly charged particle passing through the prototype IPC when it is filled with the baseline gas mixture. A 2 cm thick brass collimator with a 25 μm wide slit was used to localize the x-ray beam and facilitate the measurements of the position resolution of the chamber.

Figure 5.3.1-3 shows the measured gain vs high voltage for a prototype IPC and a gas mixture of 62% CF_4 38% CO_2. We have assumed an ionization yield of one electron-ion pair created for 34.3 eV of energy deposited in the gas.

The energy resolution measured on the anode and the position resolution vs gain is shown in Figure 5.3.1-4 for the prototype IPC. The minimum in the position resolution curve determines the optimum operating voltage for this gas mixture. There is a relationship between energy resolution and position resolution, because the dominant contribution to energy resolution degradation, electron recombination, also affects the position resolution. Therefore, we show the measured FWHM energy resolution as a benchmark against which to compare other gas mixtures and detector designs with known energy resolution.

Due to the high beam crossing rate at the SSC, the chambers must be capable of clearing the ions generated in the chamber between events to avoid the buildup of space charge around the anode wires. We have estimated that a peak flux of 10^4 tracks per second per square mm will occur in the innermost IPC layers during SSC operation at ultra-high luminosity (10^{34} $cm^{-2}s^{-1}$). We have measured the chamber response to Tungsten L x-rays as a function of x-ray intensity to determine the effects of space charge on chamber gain. The x-rays were transmitted through a 1 mm diameter, 6 cm long stainless steel collimator, ensuring that a uniform ionization region is produced. The chamber gain was determined to be independent of x-ray intensity to fluxes several times higher than that expected at the SSC during ultra-high luminosity operation. Further space charge studies are planned in the test beam phase of this program.

5.3.1.1.3. IPC Prototype Muon Telescope Studies

A multi-element telescope, consisting of four IPC chambers contained within the bore of a 0.8 T magnet, were used to track cosmic ray muons, and thereby determine the performance of the small scale IPC prototypes for throughgoing minimum ionizing particles. Tests were conducted both with and without a magnetic field, and the results are shown in Figure 5.3.1-5.

This figure shows the measured single chamber resolution vs. the angle of the track relative to the pads, and illustrates the expected degradation of resolution for non-normally incident tracks. Also shown is the effect of a magnetic field, which is to shift the optimal angle off normal incidence. These tests demonstrate that IPC chambers, with compensation for the Lorenz angle of the chamber gas, can operate in a magnetic field of 0.8 T without degradation in position resolution.

5.3.1.1.4. Development of Full Size Chambers

A full scale design for the barrel chambers was developed in late 1992 and early 1993. 1/6 scale barrel chambers were subsequent constructed, and these too gave acceptable resolution

in source tests at BNL. Except for being 1/6 the length of a full scale chamber, these chambers are identical to the full scale chambers.

As the next step, a full scale prototype barrel chamber was installed and tested in a BNL test beam (July, 1993). The chamber also had 10 cm X 2.5 mm pads, 2 mm gap, 2 mm wire spacing, 20 micron wires, G-10 substrates, aluminum foil cathodes (Al is acceptable at low rates; Cu is required at 10^{34} luminosity), and was operated with a fast gas (50/50 CF4/CO2) .

Figure 5.3.1-6 shows a layout of a full scale IPC chamber. Overall mechanical strength is provided by a composite structure consisting of a NOMEX honeycomb core with 2 layer G-10 cathode printed circuit boards acting as laminate skins. The PC boards have the readout pad structure etched onto them, while traces underneath the pads connect them to connector traces on the PC board edges. The wire tension (50 grams, the wires are strung transverse to the long dimension of the chamber) is held solely by the honeycomb composite structure. Both sides of the honeycomb composite have cathode pads, so one module consists of 2 chambers.

In the construction sequence G-10 high voltage wire support rails are glued along the long edges of the composite structure, and the wires are soldered and glued down. G-10 cathode rails glued on top of the HV rails supports the Al (later Cu) coated mylar cathodes. Finally, G-10 gas window support rails are glued on top of the Cathode rails, and Al coated mylar gas windows are glued on. The latter also act as electrostatic shields. Current limiting resistors and isolation capacitors are soldered along all the long edges of the chambers.

The ends of the modules are machined PET polyester gas plenums into which gas supply and return fittings are glued. Both the cathode windows and gas support windows are glued onto the gas plenums.

In GEM the chamber modules are mounted as doublets, with 2 modules bonded together in a truss-like structure, with a carbon fiber support tube supplying the longitudinal stiffness. Thus each doublet consists of 2 modules, or 4 chambers.

The most important future improvement to the chamber design is to replace the G-10 with Astroquartz, a higher modulus material with better thermal, mechanical, and water absorption properties. Numerous other minor improvements (better HV distribution system, lower mass gas plenums, etc.) are planned.

5.3.1.2. BNL Test Beam Results

The GEM requirements are that the IPC chambers achieve better than 50 micron resolution. Source and cosmic ray tests with small chambers gave acceptable resolution, but the BNL test beam was required to convincingly measure the resolution of the full scale chambers.

A full size barrel prototype interpolating pad chamber (IPC) for the GEM tracker was exposed to a beam of 9 GeV pions at BNL in July 1993. The pad chamber had two pad planes separated by 2.54 cm with stereo angles of +/-50 mRad. The position of the tracks was measured by 3 planes of silicon measuring the x direction and one plane measuring y. (See Figure 5.3.1-7.) The tracks were projected into the pad chamber with an accuracy of about 12 μm, this uncertainty coming mostly from multiple scattering. The position and orientation of each plane of silicon and IPCs was measured using the data tracks to an accuracy of about 5 μm in x and about 1 mRad in xy. The coordinate measurement was carried out using a function due to Mathieson which parametrizes the electrostatics of the chamber. The position in the IPC layer was compared with the projected position from the silicon and the residuals gave a measure of the resolution. Figure 5.3.1-8 shows our results. The resolution ranged from 40 - 50 μm. The multiple scattering projection error of 12μ has not yet been corrected for in Figure 5.3.1-7; the actual resolution will be slightly better. Using both layers to form a y measurement (the direction along the pads) and comparing that with the y value measured in the silicon gives a second coordinate resolution of about 840 μm as shown in Figure 5.3.1-9, in agreement with that expected from the resolution measured in x.

5.3.1.3. Future Plans

After the 1993 BNL test beam, we will continue to refine the barrel chamber design, and will build additional 1/6 and full scale chambers. Monte Carlo studies will determine optimum pad sizes, placement, channel counts, etc. Progress towards the choice of final materials will be made. Further, construction techniques suitable for large scale production of the IPC chambers will be developed.

During this period the design and construction of prototype endcap chambers will begin as well. Where possible design efforts will take advantage of lessons learned from the barrel prototypes, however, the endcap chambers have some unique problems compared to the barrel chambers.

The previous two efforts will lead to subsystem and 18 degree sector tests at FNAL in 1995 and 1996.

After the FNAL tests, the last refinements of the barrel and endcap chamber design will be performed. Choice of final materials and manufacturing strategies will be made, manufacturing sites will be chosen, and production of the final chambers will begin.

5.3.2. IPC Detector Supporting Systems

Several supporting systems are required as part of the GEM IPC detector and they must be designed and tested in much the same way as the detectors themselves. Two of these systems, gas and electronics cooling, are described here and a proposal for further studies is included.

5.3.2.1. IPC Detector Gas System

5.3.2.1.1. Summary of Results from Beam Tests at BNL

The beam tests at Brookhaven National Laboratory (BNL) afforded the opportunity to test the feasibility and reliability of the gas system prototype. The gas system was designed to provide recirculating or single-pass flow of ultra pure CO_2CF_4 gas to up to three prototype pad chambers during the BNL tests. Recirculating flow of the ionization gas will be required because discarding this gas is prohibitively expensive. The requirement for recirculating flow dictated the need for a gas cleaning or "scrubbing" capability, which was designed into the system in the spring of 1993.

During the tests at BNL the system mass flow rate, pressures at 5 locations, and temperatures at 4 locations were continuously monitored and recorded by a data acquisition system. The gas purity was continuously monitored on line during running using CO_2 and H_2O (moisture) gas analyzers. Also, grab samples were obtained and analyzed using Fourier Transform Infrared (FTIR) techniques.

During the BNL tests all goals were met during actual operation of a prototype IPC chamber installed in an operating beam under controlled experimental conditions in both recirculating and straight through operation. These included successfully demonstrating the feasibility and reliability of a continuous recirculating system, maintenance of gas purity comparable to that supplied by the gas companies as "ultra pure" or "electronics" grade, and controlled operation of the IPC at an internal pressure of 0.5 Torr above atmospheric pressure to cause only outward leakage, if any.

5.3.2.2. IPC Detector Cooling System

5.3.2.2.1. Cooling System Requirements and Design

The IPC detector electronics cooling system for GEM has been designed to fulfill IPC requirements of 36 kW total electronics heat generation, dimensional and positional stability in the range 25 μm to 100 μm, low vibration, low risk of water leakage, and low radiation length. The baseline cooling concept selected is a "leakless" chilled water cooling system. Future studies must consider the force and vibration levels associated with the water flow, corrosion in the aluminum cooling channels, modeling of heat transfer from the multichip modules and other powered components, and the design, operation and control of the leakless system. The IPC electronics cooling system will be prototyped to confirm its performance.

The IPC electronics water cooling system consists of two unconnected loops, one containing high-purity demineralized water for cooling the electronics, and one containing house mixed chilled water. Considering the electronics cooling loop that runs through the Central Tracker first, it will be a leakless cooling system consisting of redundant vacuum pumps to pull demineralized water up into the system and into a level controlled reservoir to a vacuum pressure of from 400 mbar to 600 mbar (which corresponds to working liquid heights of from 6 m to 4 m, respectively. Thus, if any leaks occur, they will only admit $C0_2$ and not release water, as long as the vacuum pumps are functioning. Redundant water pumps will be used to circulate water in the electronics cooling loop. The total inventory of recirculating demineralized water in the IPC tracker will be about 20 l. Figure 5.3.2-1 shows a schematic of the water cooling system. Not indicated are the vacuum pumps at the top of the loop, which pull a vacuum over the water reservoir, and the water reservoir at the bottom of the loop.

The house water loop shown to the right in Figure 5.3.2-1 will direct house water through a 40 kW refrigeration unit. The house water loop flow will pass through a heat exchanger coupled to the electronics cooling loop, which will serve to remove the IPC heat load.

Most of the IPC electronics cooling system will be located in the mechanical room planned for the GEM utilities shaft. Total water flow to the IPC tracker will be on the order of 86 l/min, but the flow in the individual IPC cooling passages will be laminar with a temperature rise of about 5° C and a pressure drop of about 12 kPa.

5.3.2.2.2. Proposed Cooling System Studies

It is proposed to design and fabricate a prototype IPC electronics cooling system to investigate cooling effectiveness and validate the concepts of leakless systems. A test fixture will be designed that can allow repositioning of the simulated (or actual electronics if available) heat load on actual IPC cooling passages. Repositioning is desirable to investigate the effects of

varying system pressure associated with the gravitational head on water vaporization (and possible vapor lock). A computer based data acquisition system will monitor the controlled water mass flow rate, as well as cooling channel ΔT and temperatures of the electronics. System pressures and vibration will also be measured and recorded. The test bed will allow check-out of flow distribution quality, flow connections, and other mechanical details required for SSC IPC cooling system construction.

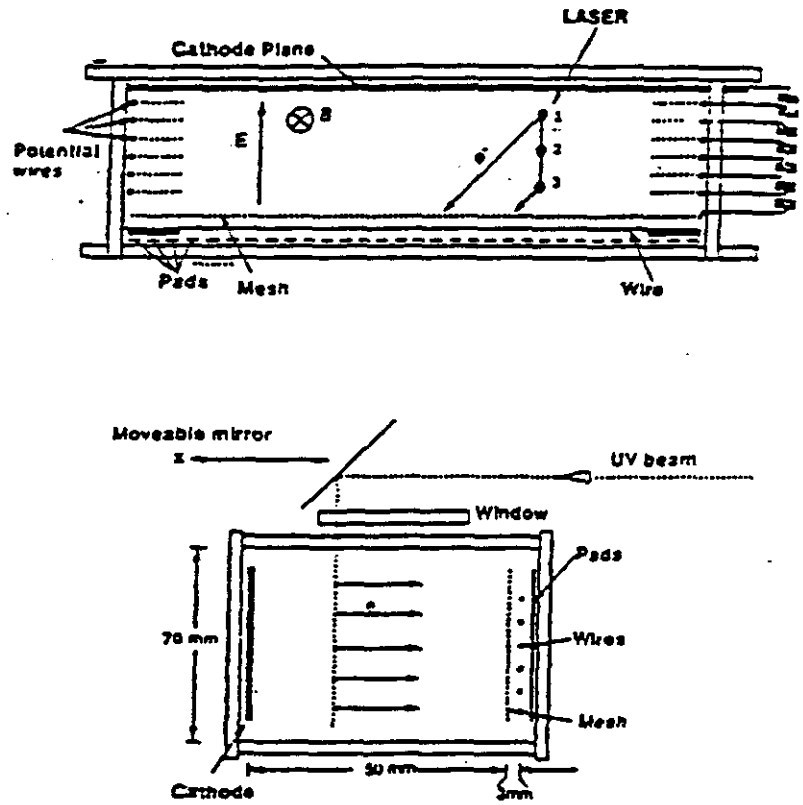

Figure 5.3.1-1: Sketch of the chamber built to conduct gas studies.

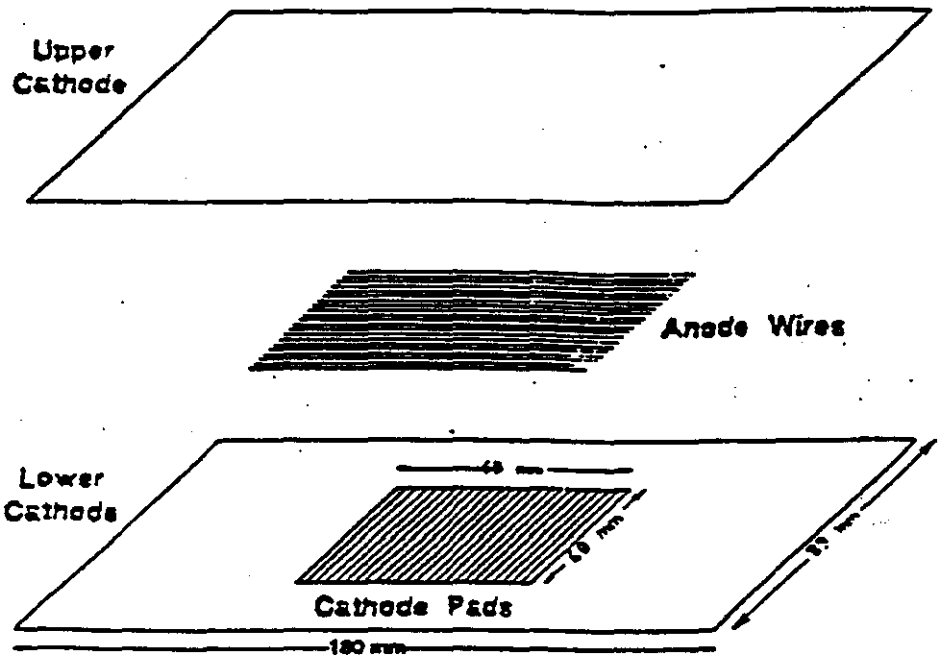

Figure 3
IPC Prototype

Figure 5.3.1-2: 3-Dimensional assembly drawing of IPC chamber design.

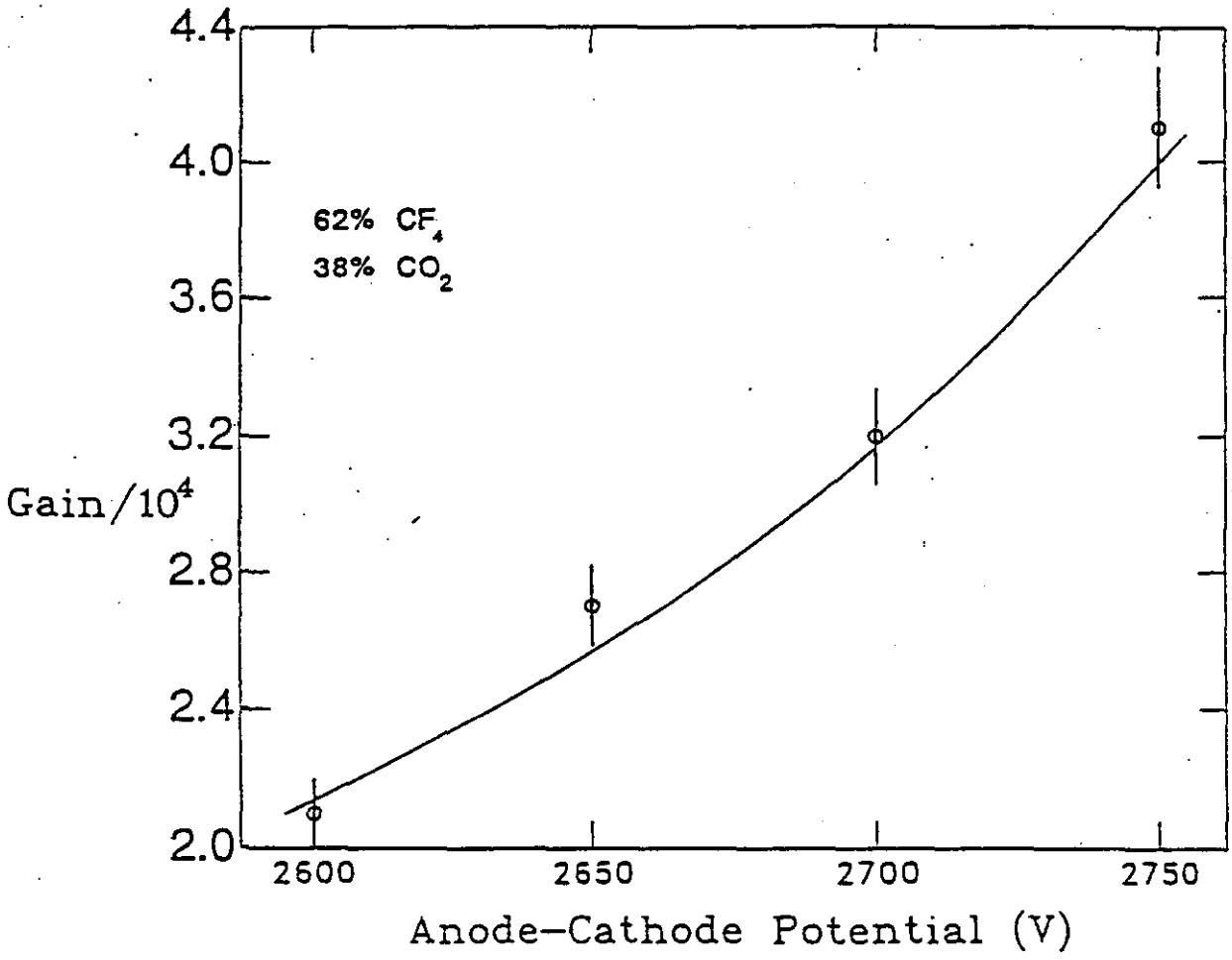

Figure 5.3.1-3: Measured gain vs. high voltage for a prototype IPC and a gas mixture of 62% CF_4, 38% CO_2.

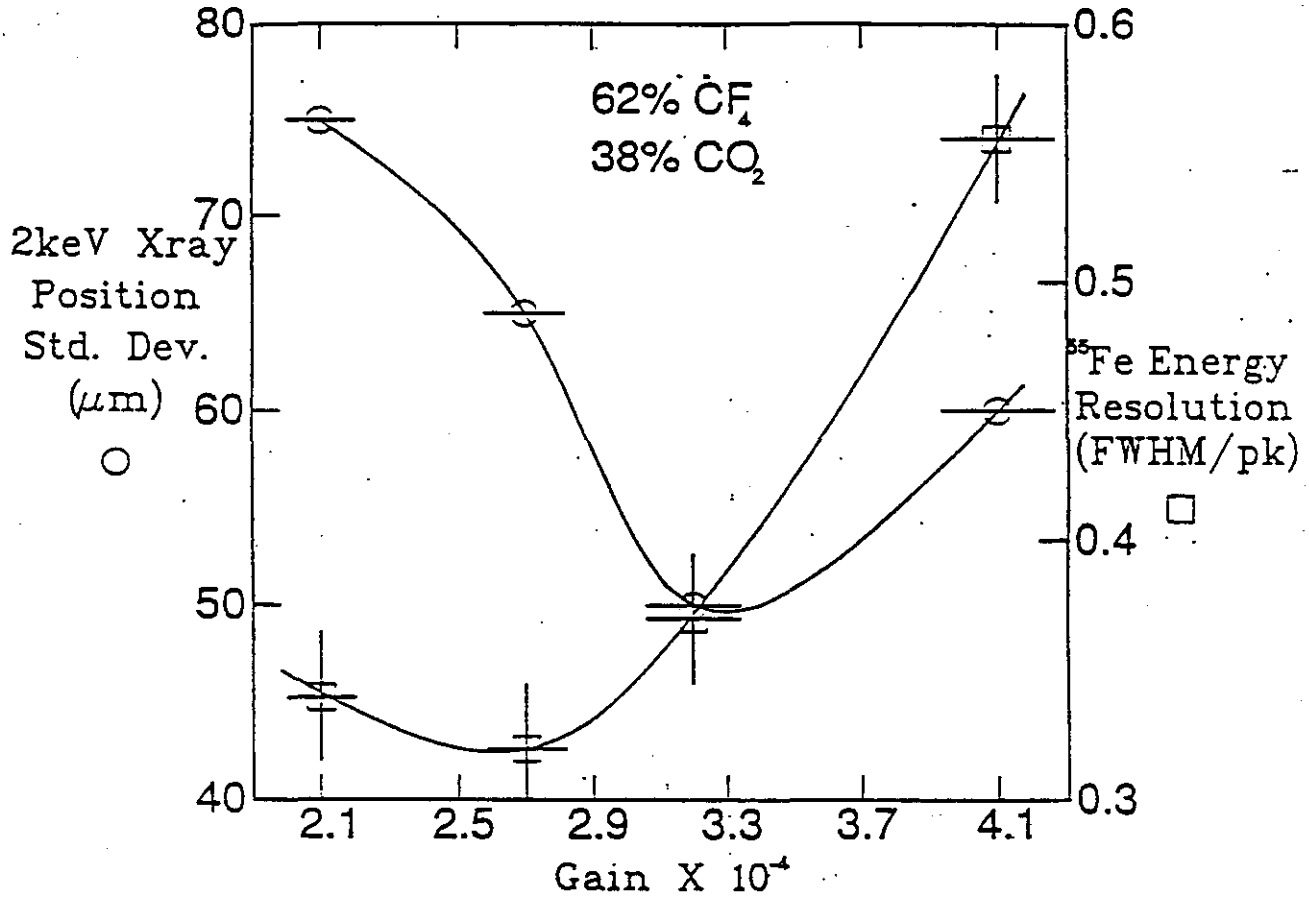

Figure 5.3.1-4: The energy resolution measured on the anode and the position resolution vs. gain for the prototype IPC.

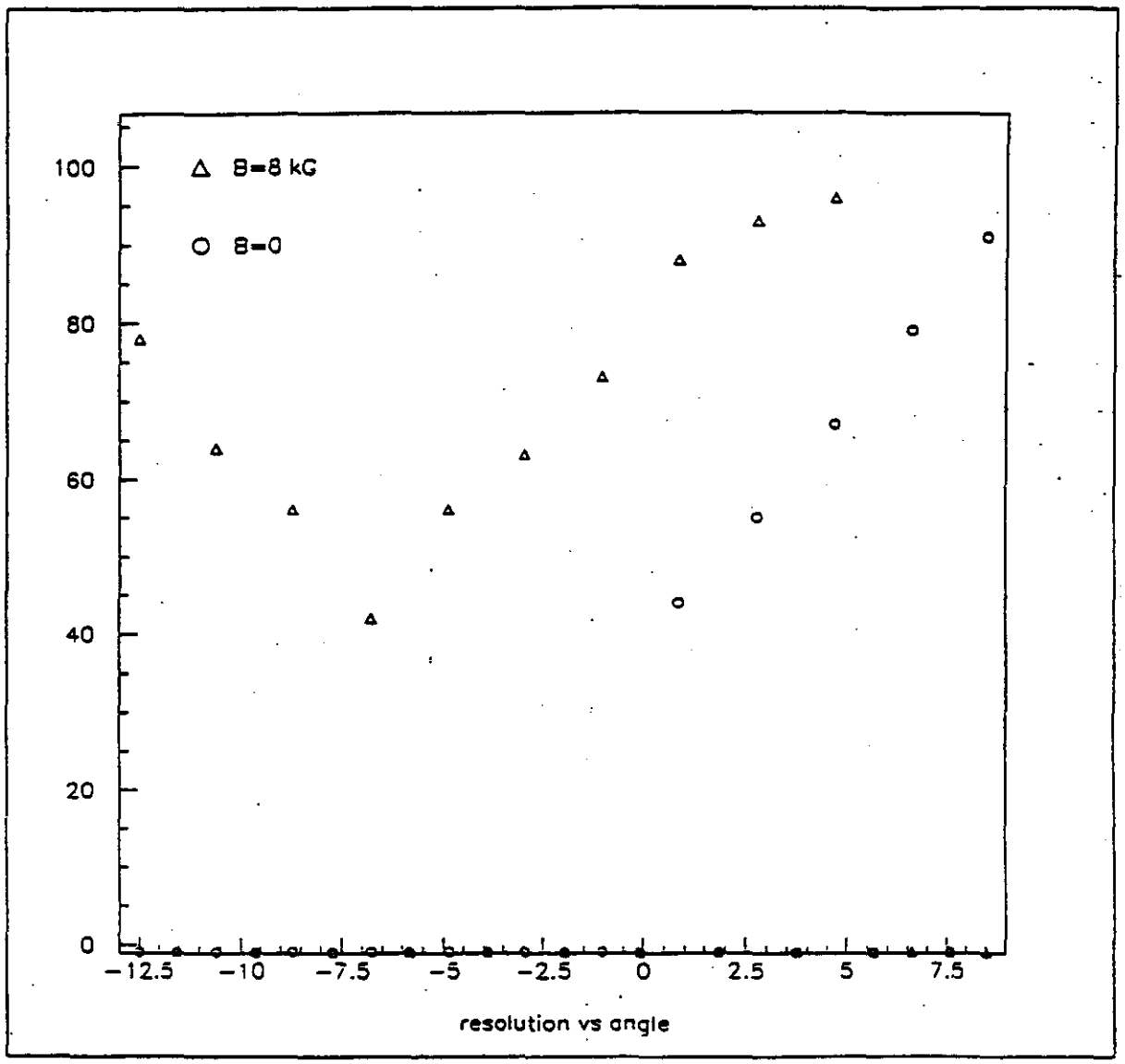

Figure 5.3.1-5: IPC prototype muon telescope tests conducted with and without a magnetic field.

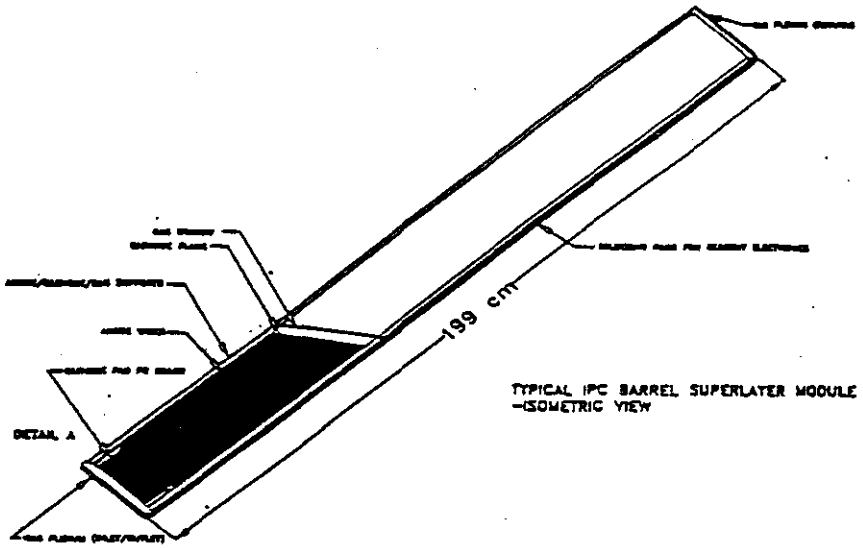

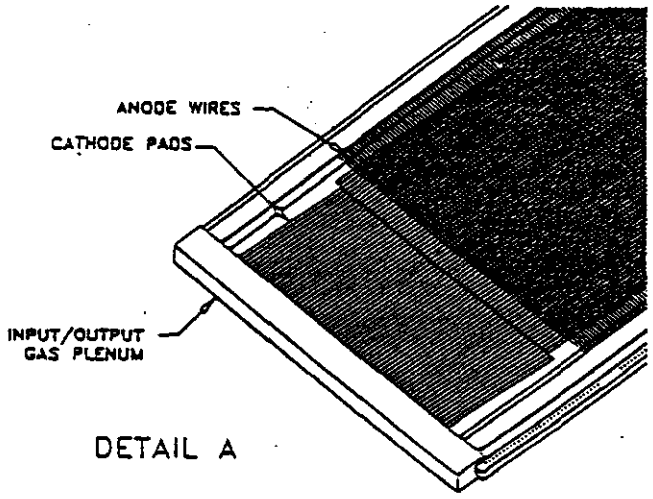

Figure 5.3.1-6: Full scale IPC chamber and detail.

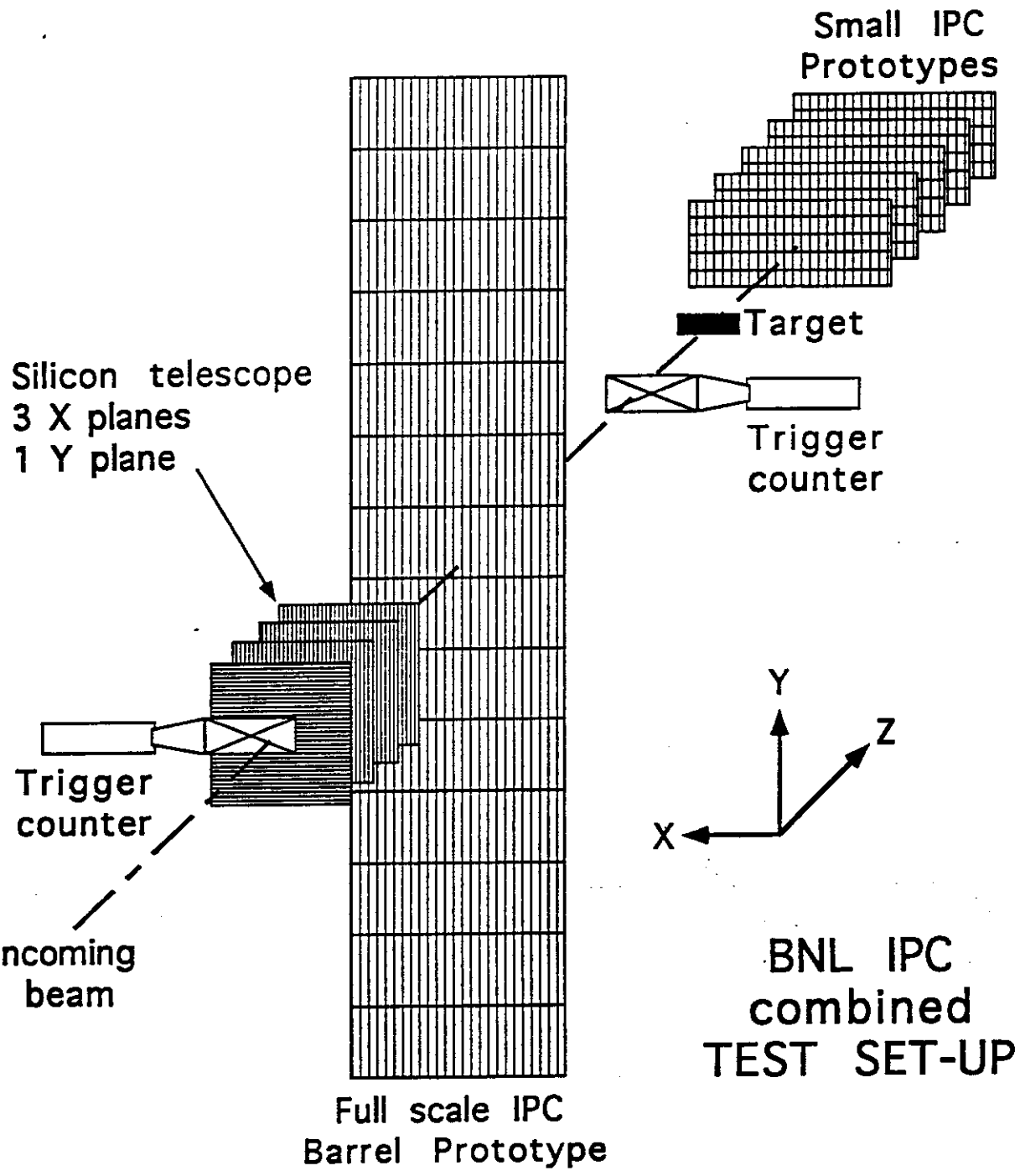

Figure 5.3.1-7: BNL combined test setup.

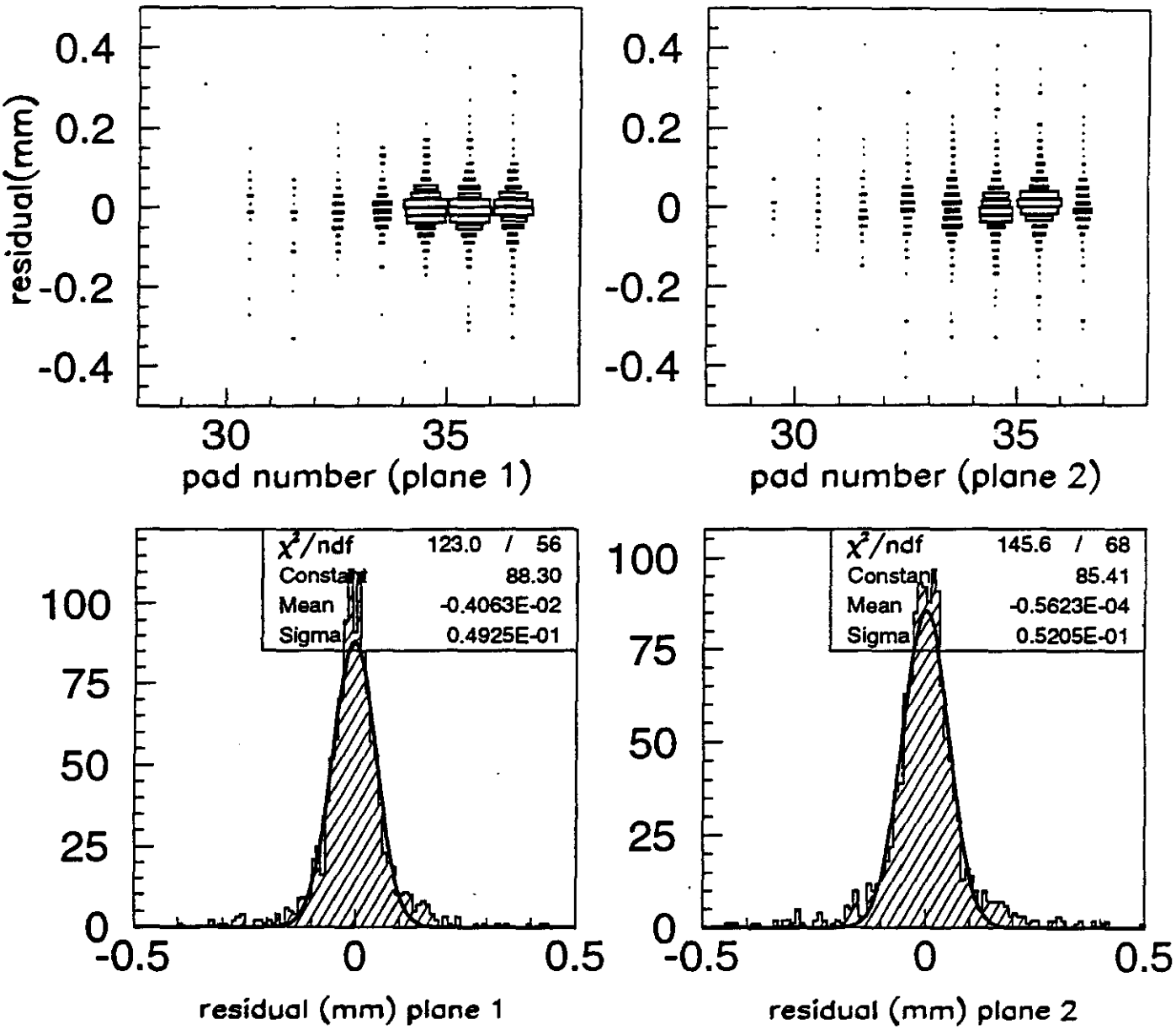

Figure 5.3.1-8: "Box Plots" (top) showing the residual distributions for several pads and (bottom) the overall residual distributions for both of the IPC planes. These distributions were fit by Gaussian distributions as shown. It is the width of such a distribution which we take as the measure of chamber resolution.

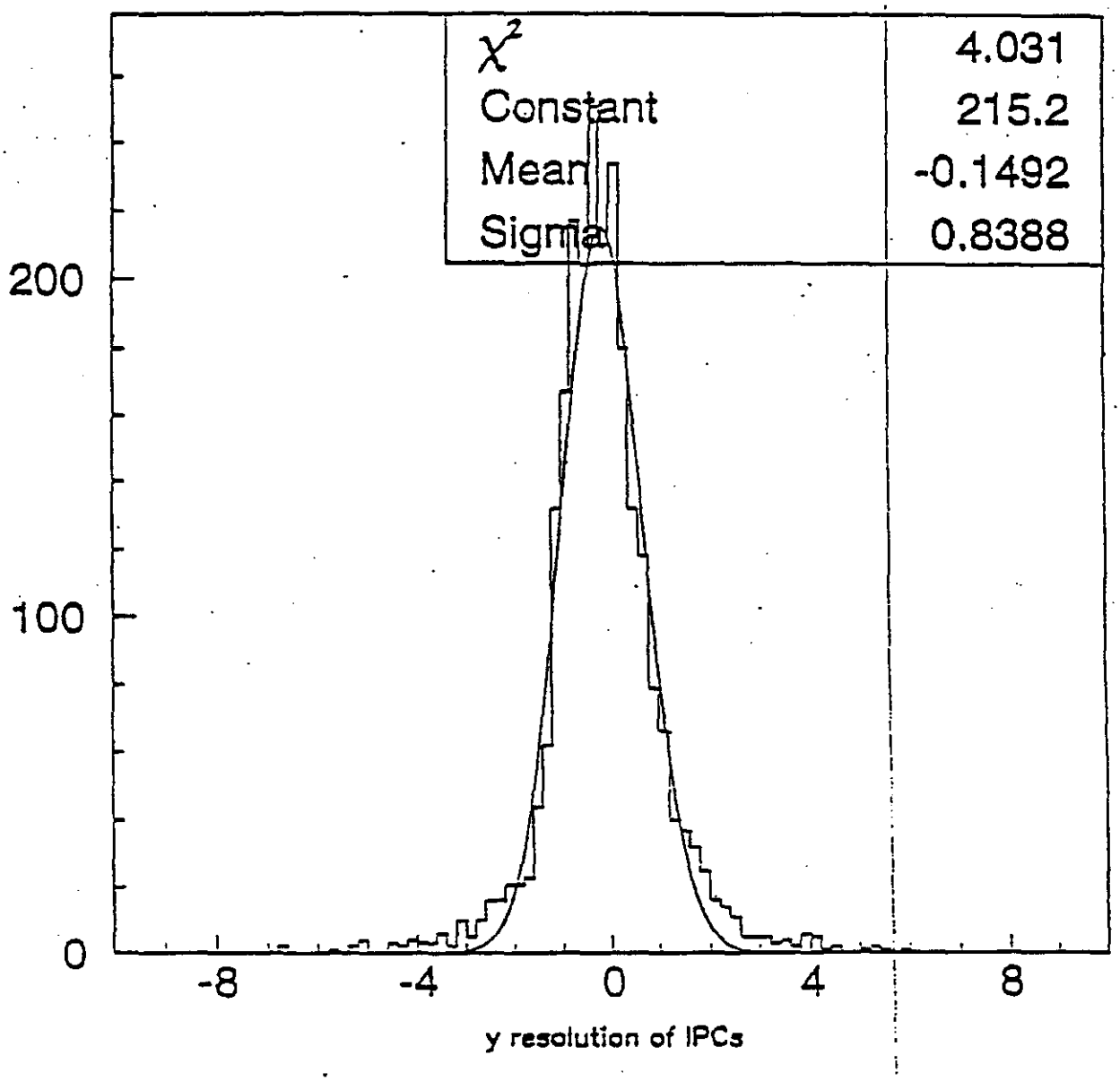
χ²
4.031
Constant
215.2
Mean
-0.1492
Sigma
0.8388
200
100
0
-8
-4
0
4
8
y resolution of IPCs

Figure 5.3.1-9

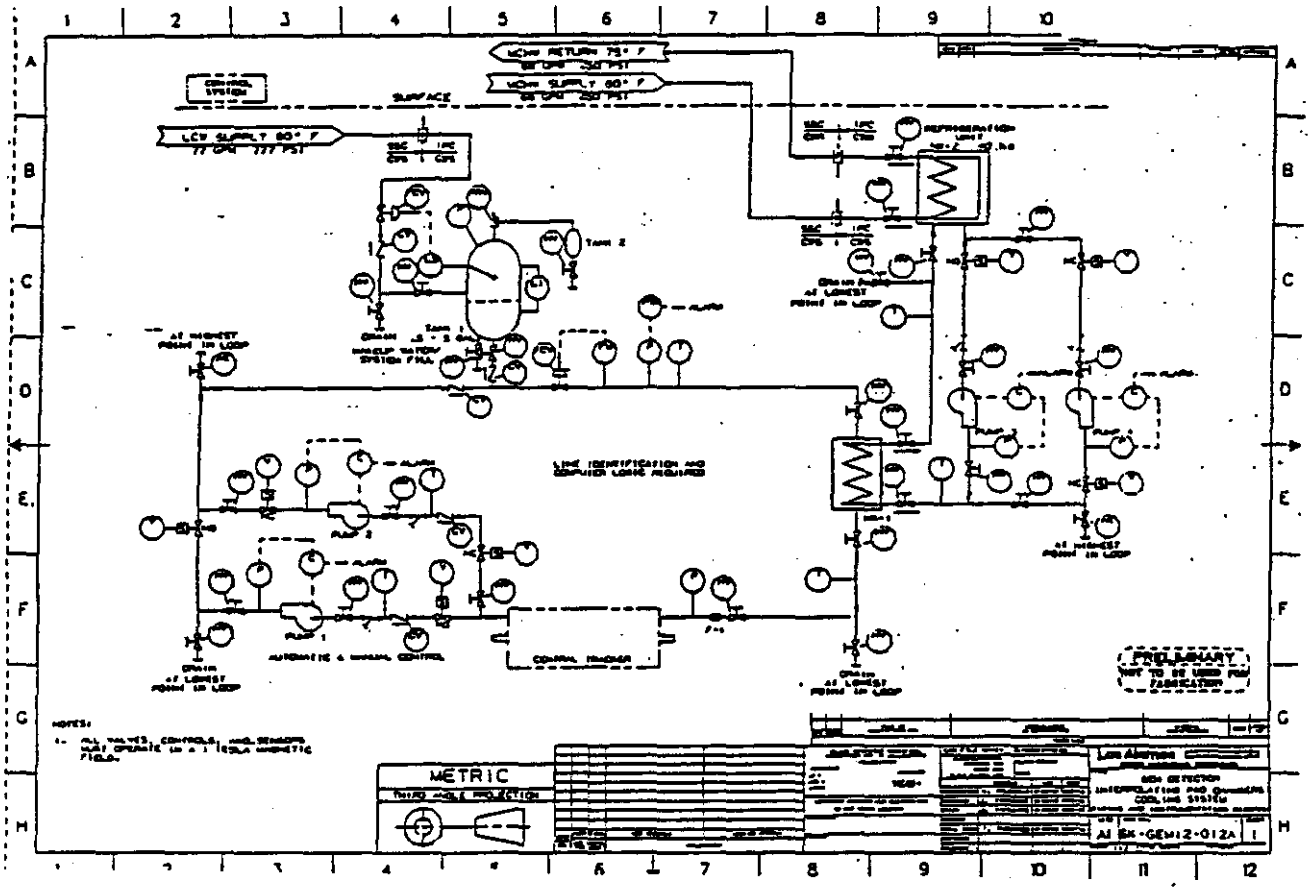

Figure 5.3.2-1: Cooling system for the interpolating pad chambers.

5.4. Silicon Tracker Electronics R&D

5.4.1. Scope of Work

This proposed silicon tracker electronics R&D effort is to design, fabricate and test a prototype system to be used to verify the functional requirements and operation of the electronic designs for a future silicon tracker. The prototype is complete enough to demonstrate the operation of the electronics in a high rate beam environment, and will provide a testbed to investigate possible design improvements. The prototype design follows the GEM TDR design as closely as possible.

5.4.2. Design Requirements and Specifications

The prototype design requirements are necessarily different from those of the future collider, and there will be sensible engineering decisions to balance the cost and schedule of the R&D effort against a design and setup that are representative of future collider operations. The design specifications of the prototype should reflect most of the crucial operational parameters as anticipated for the SSC, and still be flexible enough to realize the design within budget and schedule. Some of the most critical parameters include the per-channel power consumption, beam crossing time, data compression and readout data bit-rate, radiation hardness, and the signal to noise ratio of the front-end circuits.

On the other hand, the specific packaging technology of the electronics, command and control, power distribution and cabling are to be optimized for the prototype so that the setup yields a useful database for further improvements without undue cost and schedule constraints.

5.4.3. Approaches

The components of the electronics prototype setup and the development plan for each are described below.

5.4.3.1. Analog Front-End

A single-channel bipolar chip using a semi-custom tile-array process has been produced and is being evaluated for its performance. The design was optimized for low noise (2200 electrons ENC) and low power (1.2mW) operation with extra long (18cm) strip detectors, and has a fast (less than 4ns) logic output. An improved design with full-custom, 64-channel layout should be ready for fabrication during FY'94, and a set of fully tested chips will be available for Multi-Chip Module fabrication in 1995.

5.4.3.2. Digital Data Processors

The VHDL(VHSIC Hardware Description Language)-based top-down design of the logic chips to process event pulses from the analog chip has started, and the specifications for the main chip are already defined. Based on an event-driven data storage and a simple compression architecture to exploit the expected low occupancy, the chip design will consume minimum power per channel. The test beam version of the chip will most likely use a FIFO memory instead of the data-driven memory. Full Register Transfer Level design of the chip will be available for synthesis and target foundry layout for FY95 fabrication. The chips will be tested and delivered for MCM production in 1995.

5.4.3.3. Multi-Chip Module

The Multi-Chip Module (MCM) for the prototype is ideally fabricated using an HDI (High Density Interconnect by Texas Instruments) process, but its high non-recoverable expense (NRE) might prevent us from using such technology. Extremely high circuit density and thermal issues, however, need to be addressed, and a low-cost alternative may not be adequate. The MCM design will be finalized as the bipolar and CMOS chips are fabricated and tested, so there is some breathing room before we settle on a technology. Lower cost alternatives to the HDI process which satisfy the goals of the test beam will be explored.

5.4.3.4. Clock Distribution, Cabling, Fiber Optics, Power Supplies

Off-the-shelf chips and conventional hybrid technologies are available for clock distribution circuits, and only minor effort is needed to produce prototypes. However, the cables including TAB lead frames for MCM-to-detector interconnects still require state-of-the-art design and fabrication to handle fast signals with very high interconnect density. Fiber optics (LEDs and optical fibers) design and fabrication may be by-passed entirely if we can rely on a British effort to develop a low-mass, low-power system that can handle better than 100MBPS data transmission rate. Power supplies will be regular laboratory units with GPIB controls for currents and voltages.

5.4.3.5. Test and Operations Stations

The test stations are to be developed along with the development of the VLSI chips. The chip tests are done on an automated test station, which can be easily converted to different tasks as necessary to save capital investments. The same test stations are also to be used in test and operations of the MCM ladders and tracker assembly as well.

5.4.4. Issues and Solutions

There are several major R&D issues to be resolved in the electronics. First is the issue of noise and time-walk of the analog chip operating with the long (16 -18cm) strip detectors. While the design will be optimized for the two requirements given the power, the prototype design will favor a slightly higher power consumption rate than optimum since the cooling requirements may not be as stringent as expected in future colliders. The problem due to interference from the logic pulses generated in the level discriminator and the digital VLSI chips to the preamplifier front-end will also have to be worked out without incurring additional costs in development.

The second involves the VHDL-based design of the digital chips which will have to be optimized for the most efficient use of the chip areas. The VHDL-based design makes it possible for the development of the chips to be more flexible in mapping the design into different target foundries, but may also introduce inefficiency in die area usage. The use of MOSIS service and possibly others to produce the chips will require extra effort to optimize the layout. The storage and compression architectures are also areas for further research to arrive at the best possible solutions.

Multi-chip module production is the third major issue. The HDI process mentioned earlier is the best option in dealing with the tremendous circuit layout density and heat dissipation requirements, but the NRE is quite high (in the neighborhood of $0.5M) for prototype production. It will be a difficult choice between conventional fabrication alternatives, which might not meet the ultimate design requirements, and the costly but ideally suited HDI technology. Further commercialization of the HDI may lower the NRE in the future and the slight lag of the MCM design phase from the VLSI chip development will allow us to monitor market developments before commiting to a process.

Radiation hardness is one of the most demanding requirements imposed on the silicon tracker systems. The designs of the integrated circuits are centered around that issue and its verification will be a goal of this effort.

5.4.5. Deliverables and Milestones

Our goal is to deliver the necessary front-end electronics for an 18 degree sector test of the GEM silicon tracker in time for a test beam run in late 1995. This includes the development of the necessary VLSI electronics, Multi-Chip Module, fiber optic data link, and the assembly and testing of those components. A proposed schedule is attached to this document.

5.5. IPC Electronics R&D

5.5.1. Scope of Work

The IPC electronics system R&D program includes work needed to verify that the rather novel approach taken to the readout of the IPC system, dictated by the SSC tracker environment, is viable; to develop the custom rad-hard integrated circuits used in the IPC readout system, as well as the very high density packaging of the front end components needed in this application; and finally, to fully develop all critical aspects of the overall system design, such as power and signal distribution, calibration, and the connections to the chamber and cooling systems.

5.5.2. IPC Electronics Design

The approach followed in the IPC readout system is somewhat unusual, in that neither a peak sensing circuit nor a gated integrator is used to obtain the induced charge on the cathode pads. Instead, after the induced signals are amplified and shaped, with a peaking time for the shaped signal of 25 ns, the shaped signals are sampled at 16 ns intervals. These samples are stored in analog form in a switched capacitor array until the receipt of a trigger. At that time, the samples of interest are digitized, zero suppressed, and transmitted off the detector through a fiber optic link. For each pad with valid data, 3 to 4 samples are transmitted on each event. These correspond to a presample, which allows the baseline to be subtracted from subsequent samples, and the samples which span the shaped pulse. Because the time development of the signals on pads with induced signals from the same avalanche is identical (in the absence of shaping time variations in the electronics), each of the samples from a set of adjacent pads can be used to obtain an independent position measurement.

The basic components of the IPC readout architecture are illustrated in Figure 5.5.2-1. Each of these components is described briefly below.

5.5.2.1. Pre-amp/Shaper

The signals from the IPC cathode pads are input to preamp/shaping amplifier circuits, eight of which are contained on a single die. The gain of the preamp/shaper is 10 V/pC, and the nominal peaking time of the shaped output is 25 ns. The position resolution of the IPC system will be determined to a large extent by the signal to noise ratio of the readout chain, which is dominated by the noise contribution from the front end preamplifier transistor. As designed, the signal to noise performance of the amplifier is 2000 electrons for an input capacitance equal to the maximum expected in the IPC system. This noise figure has been verified on small scale prototypes, and will allow the 50 micron position resolution design goal of the IPC system to be met.

5.5.2.2 Analog Memory

The amplified signals from the shaper are input to an analog memory element, consisting of a switched capacitor array capable of simultaneous read and write operations. The inputs are sampled at the 60 Mhz SSC bunch crossing rate. The analog memory is packaged 16 channels to a chip, and includes a 16 to 1 analog multiplexer at the output. The readout of the analog memory takes place through an amplifier on each channel having a settling time of 500 ns, which provides the input to the multiplexer. We are now in the process of evaluating the first rad-hard analog memory prototypes, developed to meet the 2 Mrad ionizing radiation dose requirement for the IPC front end electronics.

5.5.2.3. FADC

The digitization of the sampled waveforms is accomplished using an 8 bit FADC. A rad hard FADC developed by Harris in the same CMOS process employed by us in the development of the amplifier and analog memory devices is commercially available, and meets our needs.

5.5.2.4 .Readout Controller

Control of the analog memory write address generation and readout sequencing is handled by the readout controller. The analog memory itself is used to buffer data prior to readout, and the controller contains a status array containing the locations of memory locations awaiting readout. These locations are protected from being overwritten by the controller, allowing essentially deadtimeless operation. The readout controller also contains an internal buffer, used for building the output data packets. Finally, it provides the interface to the clock, trigger, slow control, and calibration inputs. Each readout controller services 128 pad channels, and has a dedicated output data link.

5.5.2.5.Data Link

The data packets built by the readout controller are serialized, and output on a 60 Mhz bandwidth LED/fiber optic link. The approach used by the IPC system for the data link will be identical to that used by the Silicon Tracker, and it is expected that most of the development work for this component will be performed by that group.

5.5.3. IPC Electronics Development

The development of the IPC readout electronics will take place through three major stages, corresponding roughly to the major IPC test beam milestones. During FY 92/93, both lab tests and a test beam run at BNL were conducted on IPC chambers instrumented with fast preamplifier and shaper hybrids having the same essential characteristics as the final ASIC implementation. These amplifiers were read out through a commercial integrating ADC system.

This allowed the basic operating parameters of the IPC chambers to be determined, as well as their performance. The next stage of IPC electronics development involves the fabrication of a readout board employing rad-hard custom ASIC prototypes of the amplifier and analog memories, driven by a Field Programmable Gate Array (FPGA) based readout controller, as well as the continued testing and development of ASICs. The custom IC development will proceed through three protoype fabrication runs prior to a pre-production run, and these chips will be evaluated using both bench testing and on-chamber tests at each stage of their development. These tests will include studies of the performance of the devices as a function of radiation dose levels. In the second and third prototype fabrication runs full functionality will be achieved on these ASICS by adding capabilities such as pole zero compensation to the shaper, and an output multiplexer and bi-range output to the analog memory.

The first prototype readout board, the design of which is now complete, is shown in Figure 5.5.3-1. This board contains all the functionality of the production board, with the exception of the fiber optic link, which is replaced on this prototype with a FERA-bus connection. The rad-hard components from the first ASIC prototype fabrication run are being used on this board, as well as the Harris rad-hard FADC, and a rad-hard analog multiplexer. Bench testing of this board will begin in September 1993, followed shortly by chamber tests. It is expected that sufficient channels of this prototype will be fabricated to instrument one IPC chamber (approximately 1000 channels). This readout electronics will be used for the 1994 BNL beam test. Finally, a preproduction prototype of the final readout system, shown schematically in Figure 5.5.3-2, will be developed and used for the 1995 FNAL beam test. In addition to the ASIC development, the major development items required to move from the readout prototype now under development to the production version are packaging, migration of the readout controller to a rad-hard gate array, and development of the fiber link. Development of high density packaging of the front end electronics is underway. Several options are being explored, including standard hybrid fabrication, as well as more exotic Multi-Chip Module technologies. In order to fully instrument an IPC chamber, a requirement for the FNAL tests, a solution to the packaging problem must be in place. The present readout controller design, implemented on a Xilinx FPGA, will require modification to optimize its performance on the final gate array architecture. It is likely that this work could be deferred until after the FNAL beam test without serious risk to the development program. In addition to the major development items listed here, the design of the power distribution, cooling, and shielding systems, which should be identical to that used in the final system, must be completed prior to the FNAL test.

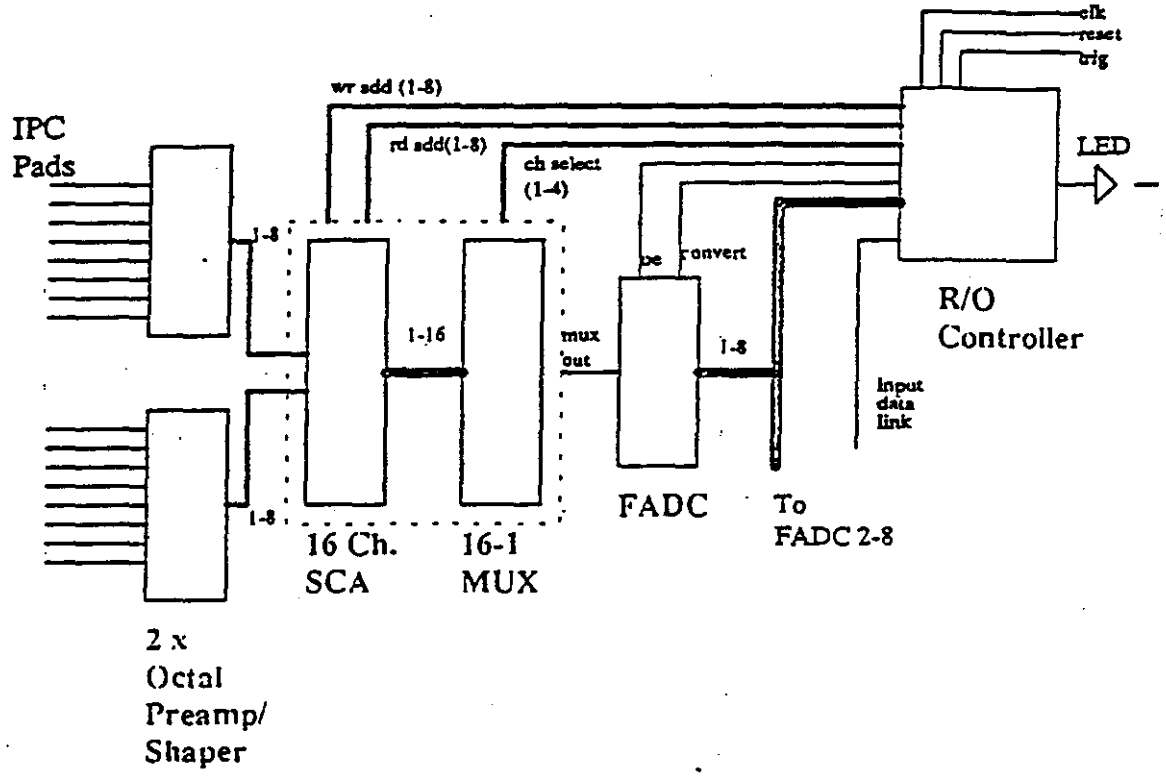

Figure 5.5.2-1: Basic components of the IPC readout architecture.

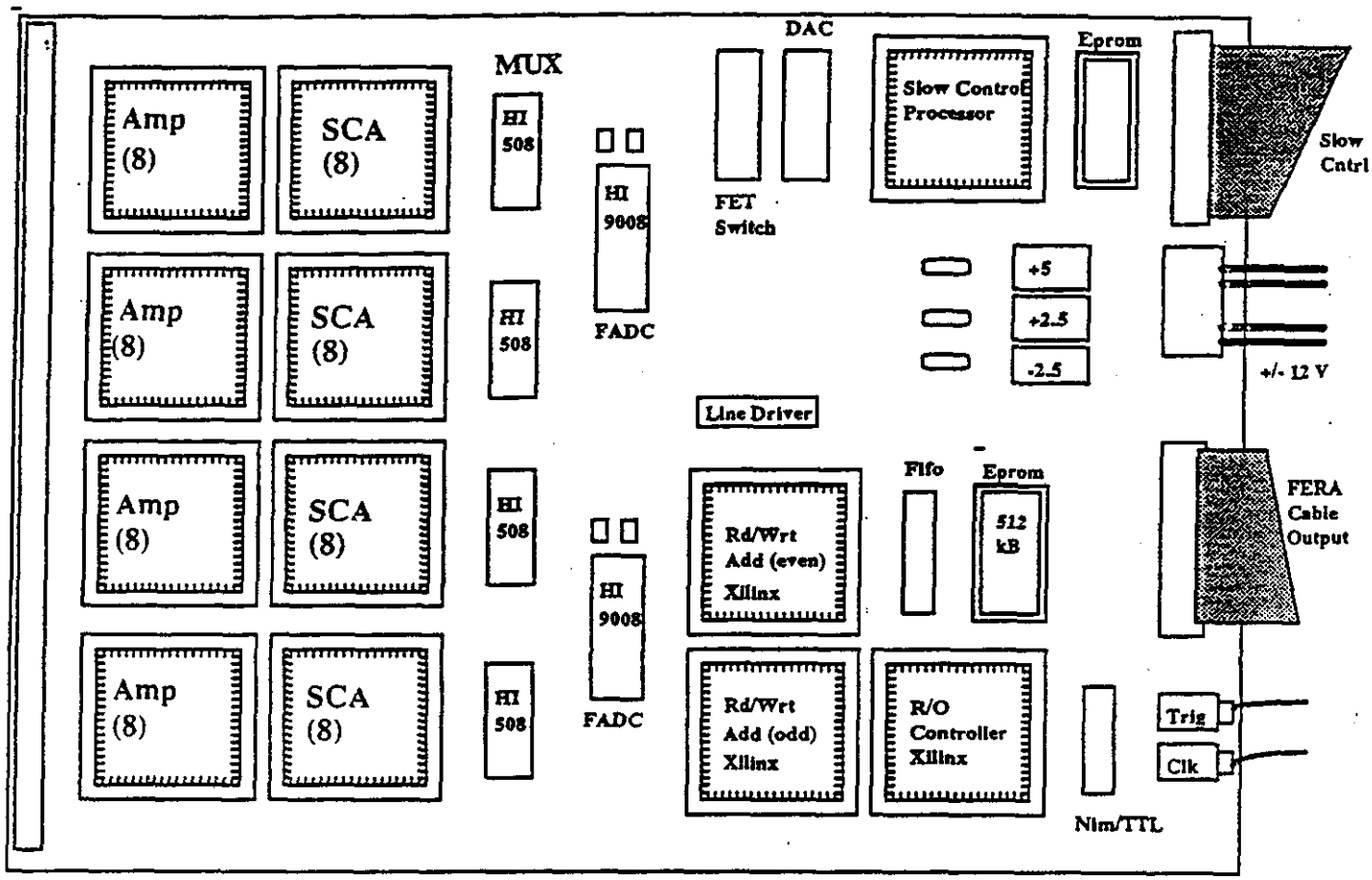

Figure 5.5.3-1: The first prototype readout board.

Figure 5.5.3-2: Schematic preproduction prototype of the final readout system.

5.6. Test Beam Program

5.6.1. Overview

The test beam program for the Central Tracker has been developed to answer questions about the performance capabilities of the detectors in a logical and sequential fashion. This program began in the summer of 1992 using small IPC prototypes. The goals of these early tests were to find stable operating conditions under which the chambers would achieve the required resolution of 50 μm, to explore the Lorentz angles of different gas mixtures and to gain experience operating Interpolating Pad Chambers. In the absence of available test beams, those first tests were carried out with cosmic rays using a magnet at Indiana University.

Testing in beams from accelerators has begun with a beam test at Brookhaven in July 1993. This test was designed to measure the single particle resolution as a function of position on a full scale barrel IPC prototype. Approximately 70 channels of an early version of IPC electronics were available for this test. We used an external Silicon telescope to define precise trajectories of the particles. In another test in parallel using smaller IPC prototypes we began to study the two track resolution.

In beam tests in 1994 we plan to continue the IPC two track resolution studies begun in 1993 and we plan to measure resolution as a function of variation in the phi and theta angles of incoming particles. There will be a full scale End Cap IPC available for resolution studies and we will for the first time test GEM Silicon prototypes. For these tests we should have about 1000 channels of IPC electronics which are one stage closer to final design, with the ADC's integrated on the preamplifier chips. For the Silicon tests, we will study the effects of incident particle position and angle on efficiency and time resolution in the 18 cm ladders. GEM-specific microstrip detectors and preamplifiers will be used to verify performance prior to fabrication of the components for the 1995 sector test. Upon completion of the 1994 tests there will remain a few unanswered questions about Central Tracker performance. These questions, which must be resolved for both the IPC and the Silicon components of the tracker, are 1) the high rate performance, 2) detector and electronics performance in a magnetic field, and 3) the overall integrity of the final designs for the various systems: electronics, gas, mechanical support structures, and cooling. The Fermilab tests, scheduled to begin in 1995 in MWest will provide the opportunity to complete our testing goals.

The Central Tracker beam test program is summarized in Tables 5.6.1 and 5.6.2.

Table 5.6.1

GEM Central Tracker

Silicon Test Beam Needs 1994 - 1996

Time	Goals	Beam Parameters	Required Beam Time
1994	Efficiency and time resolution of 18 cm ladders as a function of incident position and angles with GEM bipolar electroncis.	Ionizing particles ≥ 10 GeV/c. Well collimated beam.	3 months
1995	Rate capabilities	Secondary beam with 5 x 10^8 particles/s spread over 30 x 30 cm^2	2 weeks
early 1996	Magnetic field tests	Ionizing particle beam, ≥ 10 GeV/c in a vertical field ~ 0.8 T	2 weeks
late 1996	Performance studies of detectors and electronics and Systems Tests: gas, cooling, mechanics, etc. of final design, with final electronics.	Ionizing particles ≥50 GeV/c and tagged electrons. Rate: a few hundred particles/s. Well collimated beam with position measurement.	3 - 6 months

Table 5.6.2

GEM Central Tracker

Interpolating Pad Chamber Test Beam Needs 1994 - 1996

Time	Goals	Beam Parameters	Required Beam Time
1994	Resolution scan over the full surface of the prototype, angular resolution studies, two track studies	Ionizing particles ≥10 GeV, a few hundred particles/s. Well collimated beam with position measurement.	3 months
1995	Rate capabilities	Secondary beam, 5 x 10^8 particles/s spread over 30 X 30 cm^2	2 weeks
early 1996	Magnetic field tests	Ionizing particles, ≥ 10 GeV/c in a vertical field ~ 0.8 T	2 weeks
late 1996	Performance studies of detectors and electronics and Systems Tests: gas, cooling, mechanics, etc. of final design with final electronics	Ionizing particles ≥ 50 GeV/c and tagged electrons. Rate: a few hundred particles/s. Well collimated beam with position measurement.	3 - 6 months

5.6.2. Beam Tests at FNAL

5.6.2.1. FNAL Test Beam Goals

The Central Tracker team expects to conduct three independent sets of tests at Fermilab. These are the high rate tests, tests in a magnetic field, and the 18 degree sector test. Each of these tests will require a dedicated test set-up with detectors, electronics and support systems; however where possible, we will reuse equipment from previous beam tests; for example part of the 1994 Silicon prototype will be used for the high rate test and part in the magnetic field measurements. The high rate test will also require its own data acquisition system as it will operate in a different physical location from the rest of the GEM tests.

A) The high rate tests will be conducted in a primary beam line independently of the general GEM test beam program at FNAL. The goals of these tests are:

- Demonstrate reliable operation of IPC's at 10^{33} and 10^{34} cm^{-2} s^{-1}
- Demonstrate required resolution in IPC's at high rates
- Demonstrate Silicon performance at 10^{33} cm^{-2} s^{-1}
- Evaluate Silicon performance at 10^{34} cm^{-2} s^{-1}.

B) The magnetic field tests will be conducted in the dipole magnet located upstream in the MWest test area. The goals of the magnetic field tests are:

- Verify the effects of the magnetic field on the IPC resolution
- Verify Silicon response in the magnetic field
- Evaluate the performance of all detector mounted electronics in the magnetic field.

C) The 18 degree sector tests are considerably more extensive than the other two tests. They will be conducted in the beam line at MWest with the Central Tracker components located in front of the calorimeter. The goals for these tests are:

- Demonstrate combined tracking performance of IPC and Silicon systems
- Study overlap regions from barrel to end caps in both Silicon and IPC's
- Systems checks for all service systems in IPC's and Silicon
- Provide track information to other GEM subsystems
- Study the effect of the material in the tracker on the calorimeter response

These last goals fall into two main categories. Listed first are the goals which are internal to the tracker. Tests to acheive these goals will be undertaken early in the running period when the various subsystems are operating mostly independently. Once the subsystems have satisfied their individual goals, the tracker will participate in the overall integrated GEM 18 degree sector test by providing tracking information to the calorimeter and muon systems.

5.6.2.2. High Rate Tests

The high rate tests will be conducted in the MW6 Pre-target area. This is a primary beam line which can supply a maximum beam rate of 10^{11} particles per second and a mimimum of a few x 10^7. A rate of about 5 x 10^8 spread uniformly over 30 x 30 cm^2 is required to simulate the effects of operating the tracker at a luminosity of 10^{34} cm^{-2} s^{-1}. Another feature of the MW6 Pre-target area which makes it a candidate for these tests is an existing enlarged area between the shielding walls sufficiently large to accomodate the necessary equipment. Figure 5.6-1 shows the available space along the beam line and in the direction transverse to the beam. It is presently undecided whether we will use a silicon telescope, as is indicated in the Figure, or a set of three additional IPC chambers to provide the external definition of the tracks. Since this test is not located in the immediate MWest vicinity, it will also require a dedicated data acquisition system. The equipment required for this test is very similar to the IPC set-up used in the Brookhaven test beam in 1993 and it is possible that some of the test set-up from BNL could be reused in this measurement. The Silicon components are similar to the set-up we plan to use in our beam tests in 1994 and we expect to reuse that set-up as well. We will study the resolution while investigating the effects of voltage sag due to current draw and any saturation effects in the IPC's. We estimate that two weeks of running will provide all the data needed to determine the performance of the IPC's and Silicon at high rate.

5.6.2.3.Tests in the Magnet at MWest

At MWest we will be able to study the effects of a magnetic field on chamber resolution, on Silicon efficiency, and on the response of the electronics of both IPC's and Silicon. These studies can be conducted jointly with the muon group using a common mechanical manipulator inside the dipole magnet. The aperture in the magnet is 90 cm high, 125 cm wide and 165 cm along the beam. Figure 5.6-2 shows A) the dimensions of the aperture, and B) the configuration of 5 IPC prototypes arrayed to study resolution as a function of variation in the phi angle in the magnetic field. With the vertical field will be able to explore the response of the barrel IPC prototypes using devices similar to the small IPC prototypes which were used in the multi-track study in the 1993 BNL test. In addition to chamber resolution and Lorentz angle studies, we can also check the expected Lorentz angle effects in the Silicon and any effects on the various electronic components. In these tests we expect to use the common GEM data acquisition system. Several weeks of operating in the magnet should be sufficient to measure the responses of the detectors in the field.

5.6.2.4. The 18 Degree Sector Test at Fermilab

The Central Tracker group plans to build a major prototype of the GEM Central Tracker for the 18 degree sector test at Fermilab in 1995-96. This prototype will demonstrate the feasibility of most aspects of the Central Tracker, building on the experience gained from the 1993 and 1994 beam test results as well as the other research and development work within the collaboration. For the system level tests to be useful, the prototype must contain a representative subset of final prototypes with final design services.

There are two major phases of the 18 degree sector test in the MWest area at Fermilab that correspond to two modes of operation. The first is a stand alone mode which will serve as a final check on all tracker subsystems before construction of production modules begins. In this mode we will demonstrate the integrity of the mechanical design of the tracker at the system level. This will include mechanical stability and all operational aspects of the system, including detectors, electronics, and cooling, thus validating the entire concept prior to full fabrication. In addition, we will evaluate the effects of overlapping IPC chambers and the effects of the transition zones between end caps and barrels in both IPCs and Silicon. The second mode of operation is an integrated mode where the tracker will operate in concert with the other GEM subsystem prototypes in approximately the configuration that will exist in GEM. In addition to providing track information to the other GEM subsystems for use in determining their performance, we will also study the effects of the material in the tracker on the calorimeter response, and to some degree, the coordinated response of the GEM subsystems. It is important to note that the same physical apparatus will be used in both these modes of operation. Figure 5.6-3 shows the layout in MWest with the tracker between the forward dipole and the calorimeter.

The configuration planned for the test has been developed to include the possibility of testing the important performance issues. For example, tracking through overlapping chambers must be demonstrated and multiple chambers in azimuth will be deployed for this purpose. Additionally, the overlap region between the barrel tracker and the endcap tracker is an important area; engineering choices in this overlap region can have a significant impact on the tracker performance. An endcap will be deployed and the tracking through this interface region will be studied.

From a mechanical engineering viewpoint the Fermilab prototype test will assess the components to see if their performance meets the stringent requirements for stability. Due to the tight timeframe and cost constraints of the Fermilab prototype, alternative construction methods are being planned for the major structural suppport components used in the Silicon Tracking System. The use of Metal Matrix Composites (MMC) was planned for the GEM Silicon Tracking space frame, which supports all of the critical detector elements. The Fermilab test will substitute cynate-ester/graphite composites for the MMC. The use of advanced polymer

composites in key areas could not be attempted without the testbed provided by the Fermilab prototype testing. If the planned changes prove to meet the stringent stability requirements these cost saving components will be incorporated into the baseline for the Tracker.

The planned layout is illustrated in Figures 5.1.3 to 5.1.5. The full silicon barrel support structure is deployed with silicon ladders covering the 18 degree sector. Eighteen silicon ladders are installed in the barrel, two in the inner radius and three in each of the second through fifth radii and four at the sixth radius. Eight Interpolating Pad Chambers are deployed in the barrel as shown. With these detectors, the full barrel length is covered over the 18 degree sector of azimuth. The endcap region is illustrated in Figure 5.1.5. Twenty-four of the forward silicon ladders are installed, with three in each of eight longitudinal layers. Four forward IPCs are installed. This configuration allows all overlap issues to be addressed.

The plan is to install electronics for all channels in these detectors, totalling 103,148 channels. The breakdown of these between the various subsystems is given in Table 5.6-3.

Table 5.6-3

GEM Central Tracker Prototype Channel Count

Subsystem	Units	Channels
Barrel Silicon	18 ladders: 2 x 18 cm long each 2560 channels/ladder	46,080
Endcap Silicon	3 ladders/disk 8 disks 1280 channels/ladder	30,720
Barrel IPCs	8 modules (2 chambers each) (1280 channels/chamber)	20,480
Endcap IPCs	4 modules (2 chambers each) (1280 channels/chamber)	10,240

The support structure must be articulated to allow the prototype to be scanned through the beam in both theta and phi. This support structure will be constructed such that a rotation around the vertical corresponds to motion in the pseudorapidity direction of the final GEM detector, or movement from barrel to endcap and back. Rotation about the azimuth is effected by tilting the apparatus about a horizontal axis perpendicular to the incident beam. The mover support is illustrated in Figure 5.6-4. This structure is capable of rotating the system over 90 degrees about the vertical, to permit beam studies from the far forward region (corresponding to a pseudorapity of 2.5) to the central region (pseudorapidity of zero) and beyond. The mover support can rotate

the apparatus forward or backward by 8 degrees to move the beam in azimuth through the detector units.

An important aspect of the test from the tracker perspective will be the integration of response with the calorimeter and the muon system. Initial tracking measurements in a stand-alone mode will demonstrate tracking capabilities, but measurements of electrons and muons, for example, require the coordinated operation. Electron measurements in the tracker and the calorimeter will establish important performance levels for electron/gamma separation, and operation of the tracker, calorimeter, and the muon system in a muon beam will test the GEM-wide muon identification capability.

5.6.2.5. Run Plan

Table 5.6-4 presents a run plan for the FNAL tests.

Table 5.6-4

GEM Central Tracker

FNAL Run Plan

Tests	Required Beam Time	Required Prime User Time	Beam Parameters
Rate capabilities	**2 weeks**	**2 weeks**	Secondary beam, ionizing particles, 5×10^8 particles/s spread over 30 X 30 cm^2
Studies @ 10^{33} equivalent	1 week	1 week	
Studies @ 10^{34} equivalent	1 week	1 week	
Magnetic field tests	**2 weeks**	**2 weeks**	Ionizing particles, ≥ 10 GeV/c in a uniform field ~ 0.8 T
Lorentz angle studies	1 week	1 week	
Silicon detector and electronics effects	1 week	1 week	
Performance studies	**8 - 16 weeks**	**2 - 4 weeks**	Ionizing particles ≥ 50 GeV/c and tagged electrons. Rate: a few hundred particles/s. Well collimated beam with position measurement.
IPC + Silicon performance	4 - 8 weeks	1 - 2 weeks	
Response to electrons	2 - 4 weeks	0.5 - 1 week	
Overlap studies	1 - 2 weeks	0.25 - 0.5 wk	
Effects of material	1 - 2 weeks	0.25 - 0.5 wk	
Systems Tests	**4 - 8 weeks**	**1 - 2 weeks**	Ionizing particles ≥ 50 GeV/c and tagged electrons. Rate: a few hundred particles/s. Well collimated beam with position measurement.
Stability studies	2 - 4 weeks	0.5 - 1 wk	
Gas studies	1 - 2 weeks	0.25 - 0.5 wk	
cooling studies	1 - 2 weeks	0.25 - 0.5 wk	

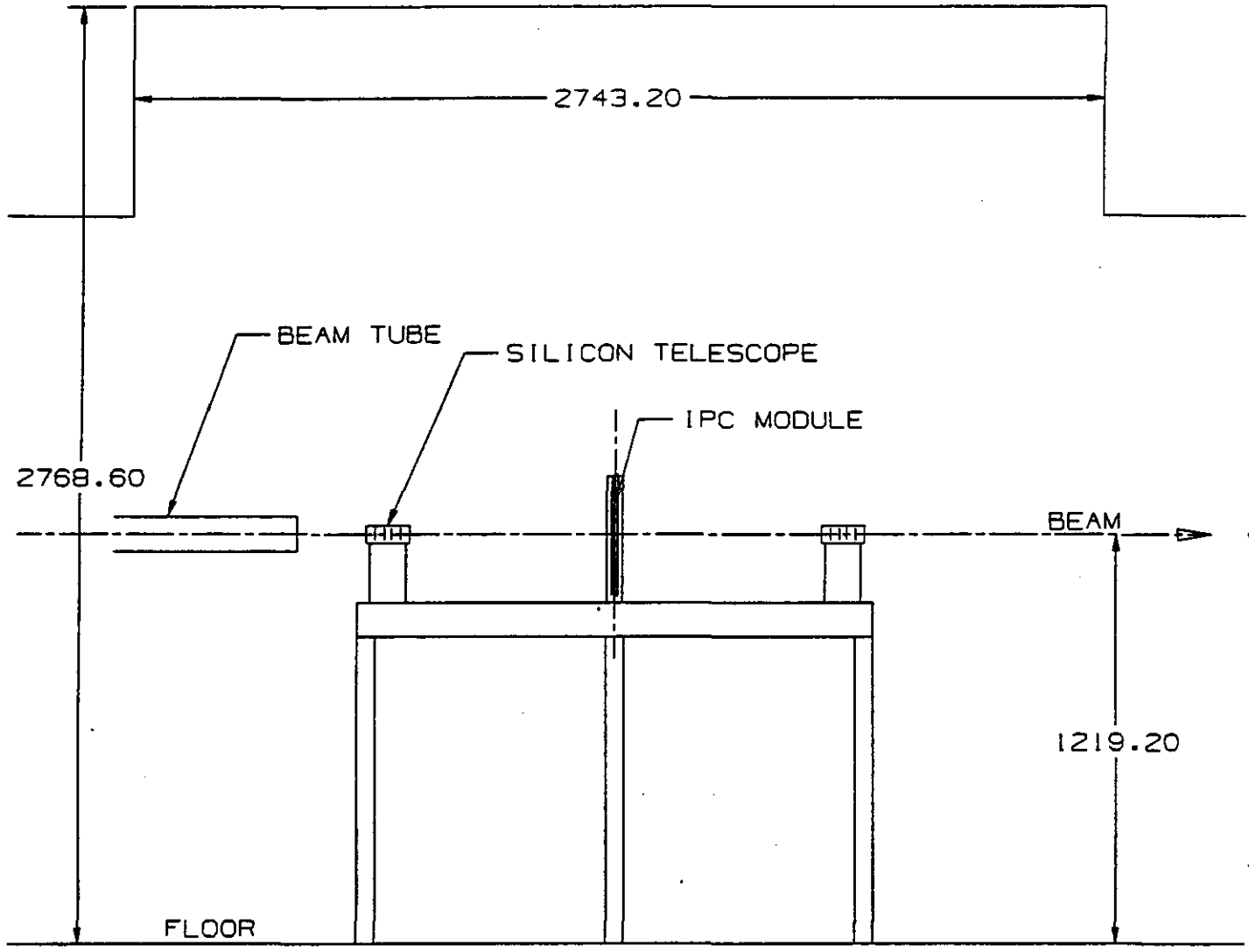

Figure 5.6-1: Central tracker high rate test area in MW6 Pre-target beam line.

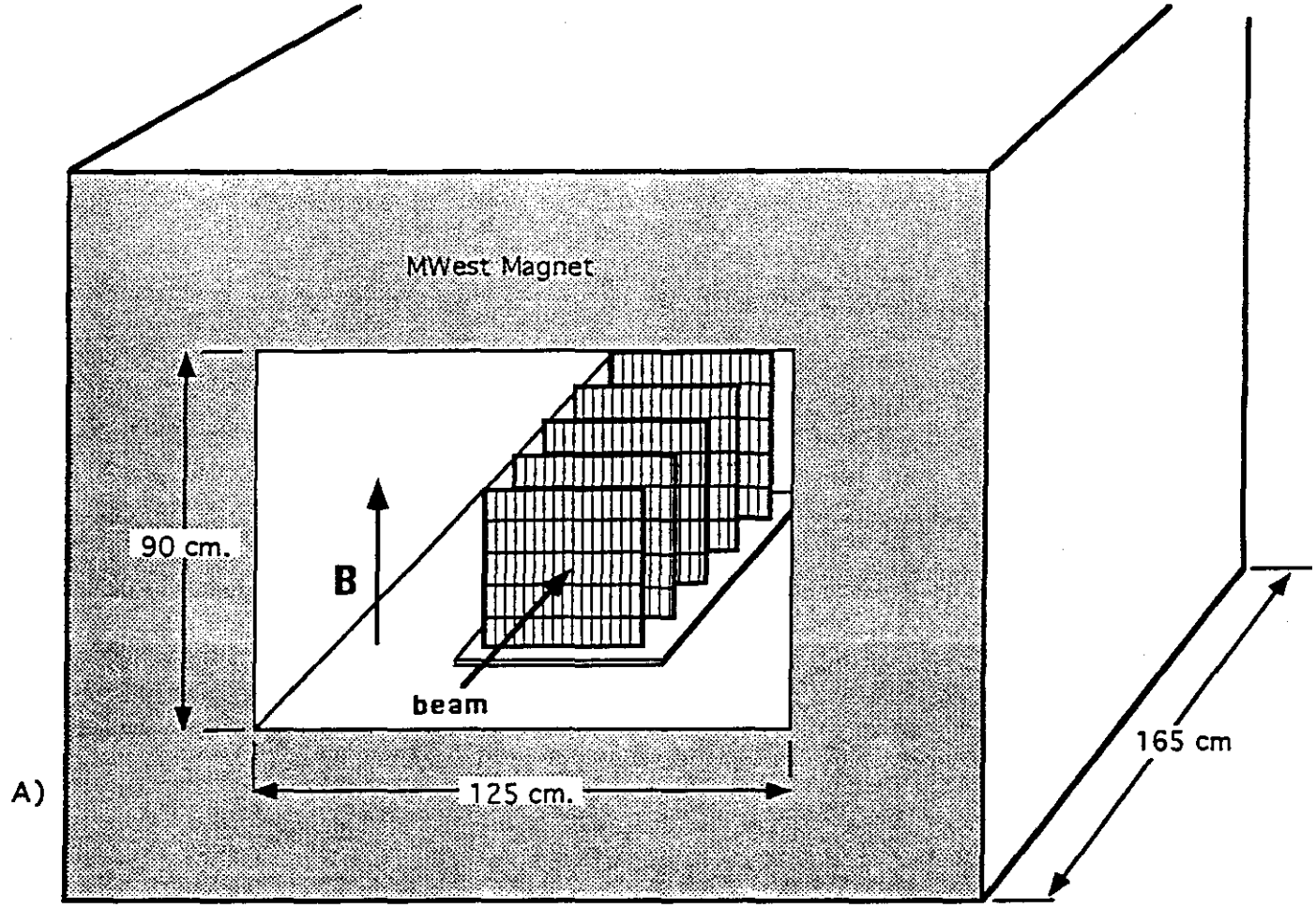

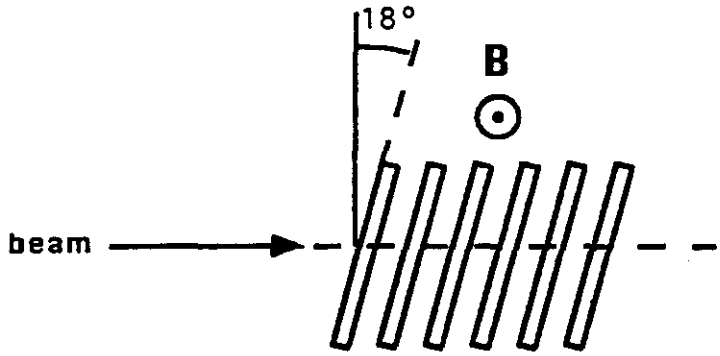

Figure 5.6-2: A) Schematic drawing of the MWest magnet with IPC prototypes inside showing the relationship between the B-field and the beam directions and B) a plan view of 5 IPC prototypes in the magnetic field with an 18 degree variation in the phi angle of the chambners.

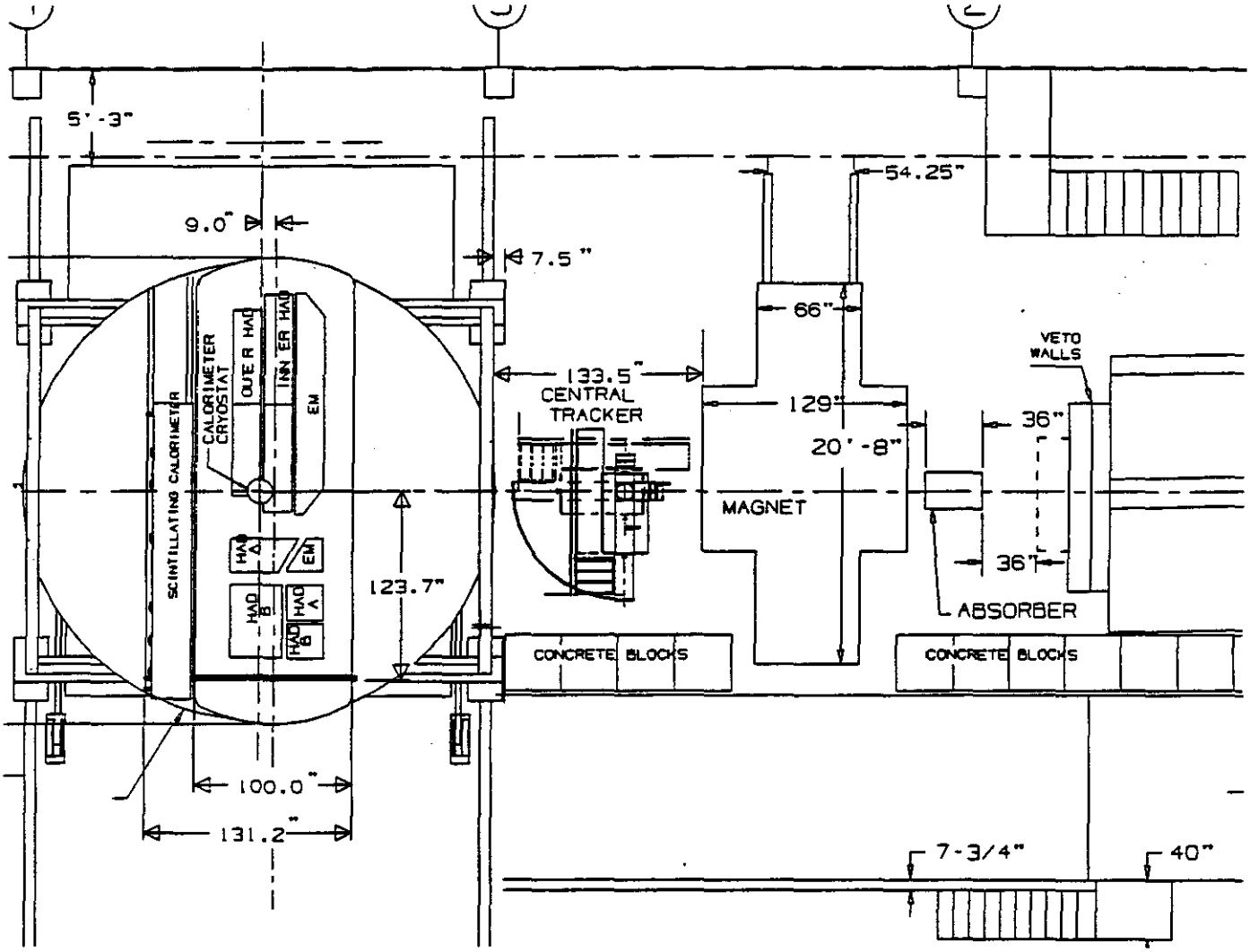

Figure 5.6-3: Partial configuration of the GEM subsystems in MWest showing the tracker located between the calorimeter and the magnet. The beam enters the area from the right side of the drawing.

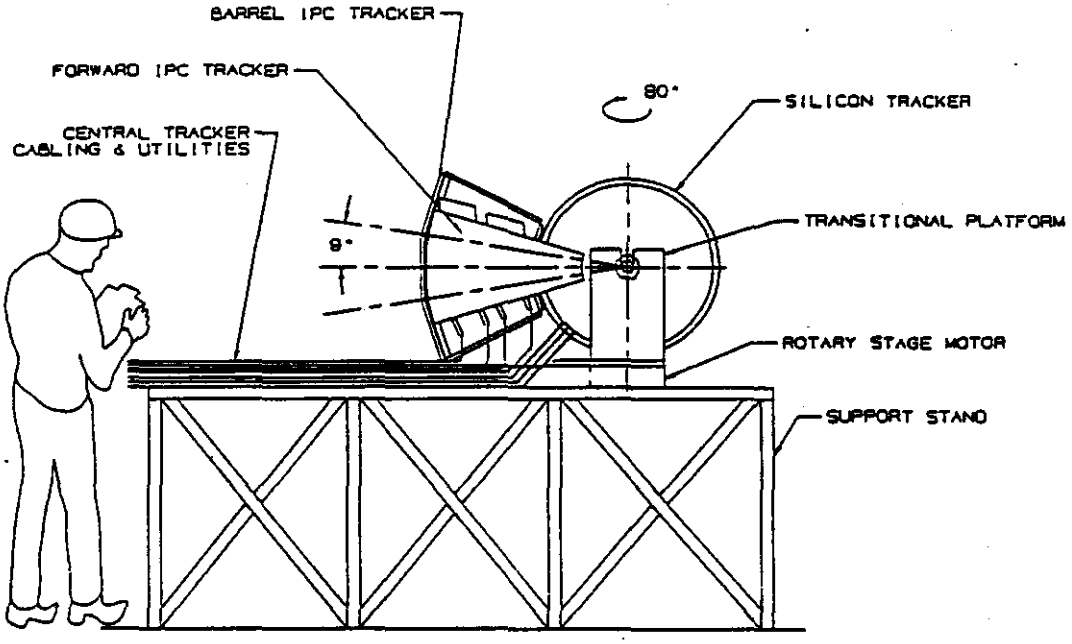

Figure 5.6-4: Central Tracker 18 degree sector test prototype support structure.

5.7. Schedule and Budget

The overall schedule for this proposed R & D program is shown in Table 5.7-1 and the budget required is shown in Table 5.7-2.

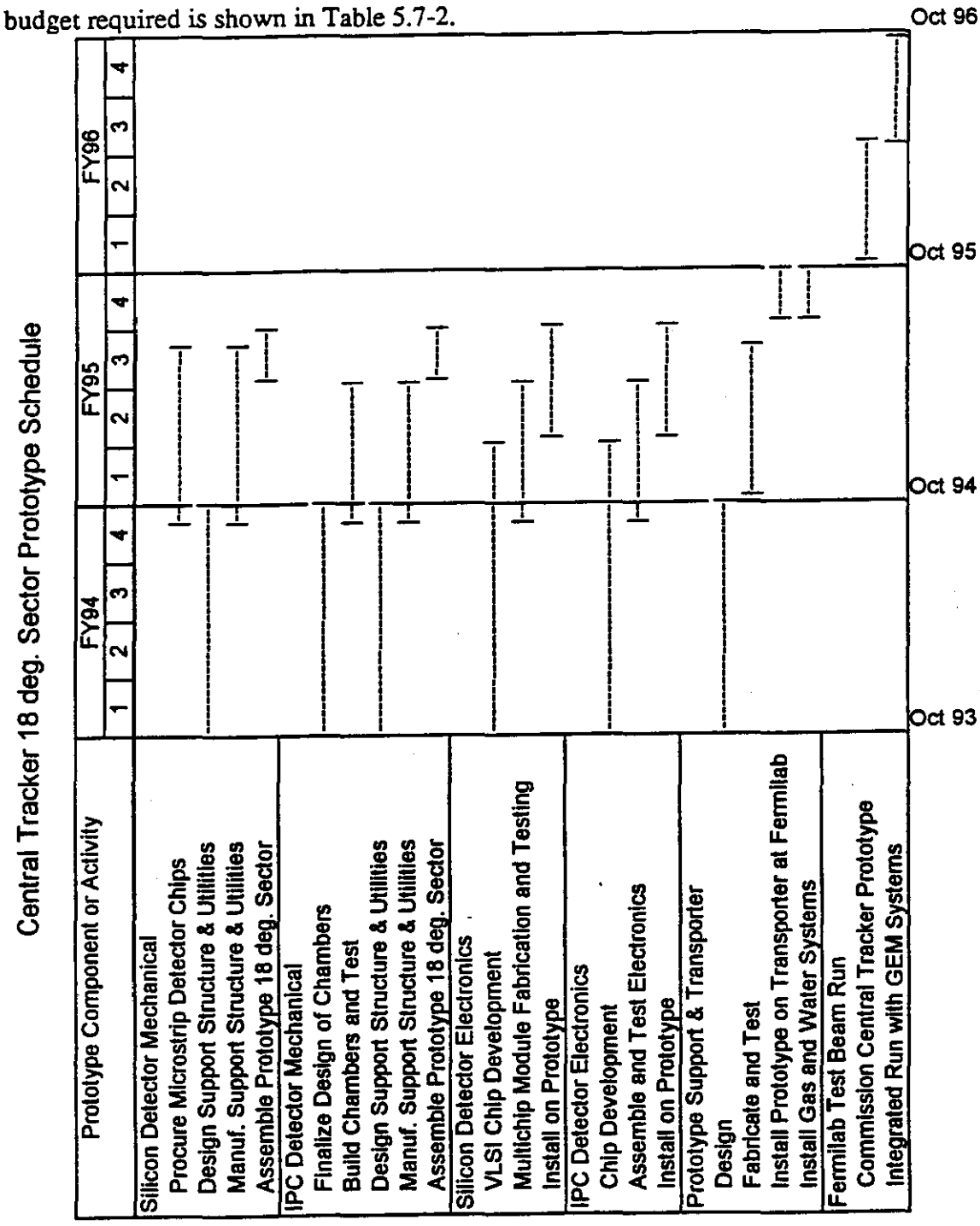

Table 5.7-1: Schedule

CENTRAL TRACKER
Research and Development Budgets
Including 18° Prototype

All values expressed in K$	1994		1995		1996		TOTALS		R&D by
	Engineering†	Procurement††	Engineering†	Procurement††	Engineering†	Procurement††	Engineering†	Procurement††	Subsystem
1. MECHANICAL									
a.) SILICON TRACKER									
LANL	615	470	615	975	615	100	1,845	1,545	3,645
Oregon	85		85		85		255		
Moscow / Vanderbilt	0		0		0		0		
Pittsburgh	0		0		0		0		
b.) IPC TRACKER									
Yale	252	350	252	803	252	50	756	1,203	3,165
LANL	312		312		312		936		
SSCL	90		90		90		270		
Rutgers	0		0		0		0		
c.) TEST BEAMS, INTEGRATION, PLATFORMS	0	100	0	450	0	50	0	600	600
Mechanical Engin / Proc	1,354	920	1,354	2,228	1,354	200	4,062	3,348	7,410
TOTAL MECHANICAL		2,274		3,582		1,554			
2.) ELECTRONICS									
a.) SILICON TRACKER									
LANL	560	355	560	580	560	50	1,680	985	2,815
Oregon	50		50		50		150		
b.) IPC TRACKER									
Indiana	85	350	85	989	85	150	255	1,489	2,716
BNL	120		120		120		360		
Oak Ridge	120		120		120		360		
Michigan	84		84		84		252		
Electronics Engin / Proc	1,019	705	1,019	1,569	1,019	200	3,057	2,474	5,531
TOTAL ELECTRONICS		1,724		2,568		1,219			
ENGIN / PROC by FY	2,373	1,625	2,373	3,797	2,373	400	7,119	5,822	12,941
TOTAL R&D by FY		3,998		6,170		2,773			

† defined as Engineering and Design and M&S in support of Engineering and Design

†† defined as Inspection, Procurement/Fabrication, and Assembly

Table 5.7-2: Budget

Chapter 6

Data Acquisition and Test Beam Trigger

A detailed description of the GEM Data Acquisition (DAQ) subsystems can be found in the GEM TDR [1]. The primary goal of the test beam DAQ is to provide a reliable system by which the detector subsystems can accumulate data, while taking the opportunity to model the concepts that will be used in the production DAQ system. The specific concepts that will be modeled are the switched event builder and the trigger supervisor which accepts Level 1 triggers and communicates with the Level 2/3 processor(s). The switched event-builder will allow easy integration of separate data flows into one, while also enabling the subsystems to take individual runs.

The test beam DAQ effort is being coordinated principally by members of GEM computing subsystem in cooperation with the detector and electronics subsystem groups, the SSC Physics Research Computing Department (PRCD) and the SSC PR Electronics/DAQ department.

This chapter first gives an overview of the event data flow in the electronics, DAQ and online systems. It then describes the overall layout of the proposed DAQ system and includes a short description of the test beam trigger system.

6.1 Event Data Flow Overview

A global overview of the event data flow is given in figure 6.1. Upstream of the GEM subdetectors under test are detectors which will be used for triggering the process of acquiring data. The event fragments will be assembled by the data acquisition system (DAQ) and move through the online processors to a data cache at Fermilab, then to permanent storage at the SSCL.

The remainder of this section will summarize the functions of the elements in figure 6.1. This chapter then presents more details about the DAQ and trigger systems. The electronics for the subsystems is discussed in chapter 7, while the online processors and data storage aspects are discussed in chapter 8.

1. Trigger

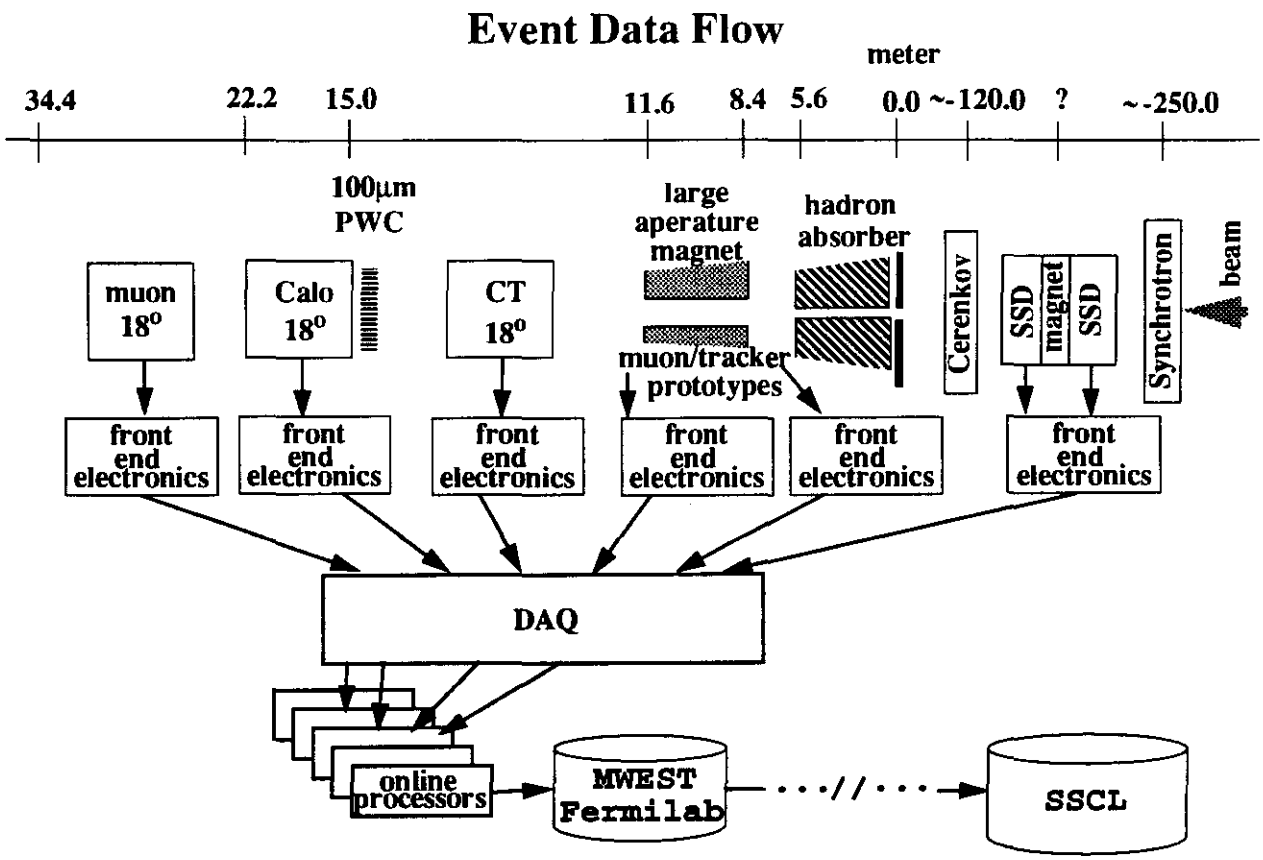

Figure 6.1: Overview of the data flow in the test beam setup. Particles in the beam trigger the experimental setup and create data. The data then flows through the various elements of the Electronics, DAQ and online systems to a permanent storage device.

The trigger that will be used for the test beam will be a typical one for such setups. By contrast, it will have little in common with the production GEM trigger system.

The trigger consists of a number of scintillators, Čerenkov and Synchrotron Radiation detectors. These detectors not only trigger the experiment, they also provide information about the incoming particles. The trigger is capable of providing single particle triggers for various particle types like e^-, μ^- and π^-. Additional information about the incoming particles is provided by a small chamber in front of the calorimeter.

The trigger system is discussed briefly in section 6.2.1.

2. Subsystem Electronics

The test beam provides a platform to test prototypes of the electronics that will be used in GEM. All three detector subsystems—tracker (silicon and IPC), calorimeter and muon (CSC)—will use prototypes of the final GEM electronics. The test beam plans for these components are discussed in sections 7.2 through 7.5.

The calorimeter group will test the calorimeter Level 1 trigger electronics and algorithms using a prototype of the production version. Calorimeter data will be processed

by this prototype and the results will be included in the data stream. Note, however, that this trigger will not be used to reject events. The test calorimeter Level 1 beam plans are discussed in section 7.6.

The tracker and muon groups have decided to use optical fibers to read out their electronics, just as is called for in the production system. The optical fibers will transport the data from the detector to the DAQ using prototype electronics

The (existing) test beam trigger detectors will continue to use standard CAMAC modules.

3. Subsystem Read-out Requirements

The DAQ must be prepared to connect to the detector subsystems with a variety of interfaces to their electronics. Here we present an overview of the modules to be read out.

- **Calorimeter.** The calorimeter will be comprised of an 18° sector, including the cryogenic electromagnetic calorimeter, the hadronic calorimeter, and the scintillating fiber calorimeter mounted outside of the cryogenic dewar. The readout electronics interface will evolve during the run and may include CAMAC, Fastbus, and VME. The long-term direction will be towards VME.
- **Muon.** The muon subsystem will read out an 18° sector and will test a smaller set of muon chambers inside a large aperature magnet. The system will have a production-style readout and will send data directly into an Event Data Collector (EDC) board that will designed for the test beam as a simple version of the production EDC.
- **Central Tracking.** The tracker group will also test of an 18° sector of their detector, both silicon and IPC's, and will additionally test just the IPC's in a large aperature magnet. As in the muon subsystem, data will be sent directly into simplified EDC's.

In addition to the detector subsystems, several other small detectors will be used for triggering and beam-tracking purposes. These include:

- **Čerenkov Detector.** This device carries the phototube signals over air core cables down the beamline to the front end of the the MWEST hall (upstream latch house) and are marked on a clocked shift register. This register is then readout through CAMAC when it receives a delayed trigger.
- **Synchroton Radiation Detector.** The signals from this device will probably be passed down to shift registers similar to that used by the Čerenkov and read out through CAMAC.
- **Beam Momentum SSD's.** These detectors write into a buffer memory the address and time stamp of all hits. To decrease the data rates, only those hits that are coincident in time with three planes are sent to the buffer. This buffer is then read out and decoded in a later stage to calculate the beam momentum.

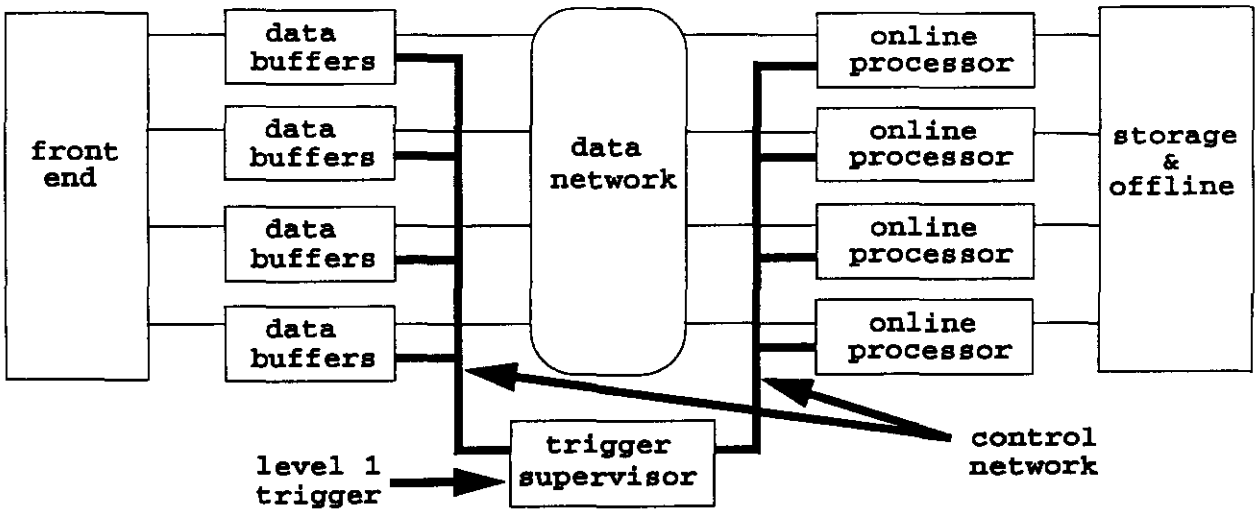

Figure 6.2: Overview of the implementation of the electronics and DAQ systems.

- **Calorimeter Pre-chambers.** In front of the calorimeter there is to be a small tracking chamber with approximately a 100 micron resolution and possible some scintillator for additional timing information. The read out system will probably be CAMAC or VME.

4. Data Acquisition

   The test beam data acquisition system will conceptually be a simplified version of the production system. A conceptual diagram of the test beam data acquisition system is shown in figure 6.2. This is a simplified scheme from the production DAQ scheme, as presented in figure 7–21 in the GEM TDR [1]. More details on the production DAQ system can be found in reference [28]. The spirit of the test beam DAQ will be to implement as many of the production *concepts* as is practical. The hardware and software implementations, however, may be radically different.

   As indicated in figure 6.2, the data of each subsystem will be collected in a single VME-crate, known as the "front end crate." This crate contains a processor, interfaces to other crates with subsystem electronics and receivers for the optical links.

   The front end crates are connected to the DAQ system. The DAQ system collects the data from all front end crates for an event and combines the data into local data buffers. A data-switch will be used to build events from the data fragments, similar to what is planned for the GEM production DAQ system. The data is then sent to the online system. The architecture of the DAQ system is discussed in section 6.2.2.

5. Online

   The on-line system will consist of a set of processors which will accept the data from the DAQ and send it to the data storage system. These processors may also be used to compress the data or to test Level 2 and Level 3 algorithms.

   The design of the online system is discussed in section 8.1.2.

6. Data storage

   The complete events are written to disks at FNAL. These disks provide space to store a few days worth of data. Long term storage will be at the SSCL. The data from the FNAL disk is copied over a T3-link to disks at the SSCL and then to tape-robot(s).

   The design of the storage system is discussed in section 8.1.3.

7. Control

   The test beam setup will be controlled by a Global Control System (GCS). The GCS distributes commands like "start" and "stop" to the elements of the system and monitors the status of the system. A graphical user interface (GUI) will most likely be provided. The GCS will also provide "slow control" functionality and interfaces to the accelerator.

   The GCS is discussed in section 8.1.1.

6.2 Fermilab Test Beam Plan

6.2.1 Trigger Architecture

The trigger for the test beam will be a standard beam trigger, reusing much of the existing hardware at MWEST. The beam trigger, acting as a Level 1 trigger, is built from beam scintillator counters in coincidence and veto and signals from the Čerenkov and the synchrotron radiation detector (SRD). The Čerenkov, SRD, and/or the use of a beam dump provide means of identification of e^-, π^- and μ beam trigger. A beam trigger rate of 100 Hz is achieved with a beam rate of $10^{3,4}$ beam particles per second.

The calorimeter subsystem is requesting a beam trigger within a ± 1 μsec time window, 100 ps time resolution (jitter) and a beam size spot of 2×2 or 2×1 inches in front of the calorimeter.

The muon subsystem is requesting a scintillator wall for muons from the beam halo in front of the 18° muon sector.

Random triggers and special calibration procedures outside the active beam spill will be provided; a detector subsystem person is expected to design and implement such special triggers.

Special studies to determine instantaneous rate limitation and measurement of pile up will be done under request of the detector subsystems.

ECL programmable logic units will be used to built the trigger logic.

Studies of calorimeter and muon trigger patterns from the prototype GEM trigger electronic cards are described in the electronics chapter.

6.2.2 DAQ Architecture

The GEM DAQ system has three goals: acquire data from the detector subsystem data reliably and send it to the online system, use architectural concepts from the production DAQ system, and promote standardization of front-end electronic protocols.

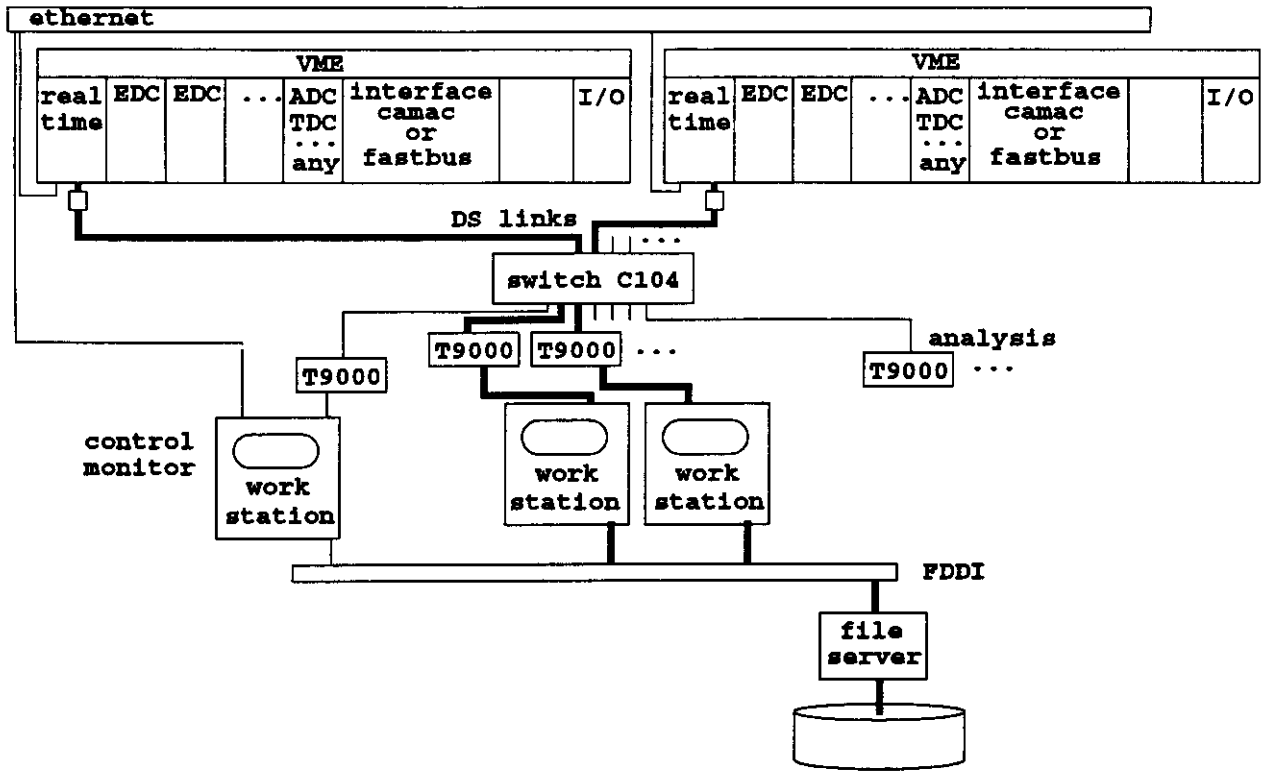

Figure 6.3: The baseline DAQ system.

While the baseline DAQ system will test concepts of the production DAQ system, it will be implemented with technology that is available today. A fallback system is also proposed. The decision of whether to use the baseline or fallback system will be made by the Fall of 1994. The basis for the two systems was worked out during several meetings, notes from which can be found in references [29] and [30].

Although the two systems are discussed independently, it should be noted that most of the hardware needed for the fallback solution is available regardless of which system will actually be used. Not only will this provide the option to switch back to the fallback solution at any given time, this hardware can also be used for local tests *before* a baseline DAQ system is delivered. Regardless of which solution is selected, there should always be a possibility to take data from a single subsystem before the DAQ-system is installed at Fermilab.

6.2.2.1 Baseline system

In the production DAQ system, a switch is employed to build a complete event from several hundred fragments from several hundred electronic modules, "Event Data Collectors" (EDC's), which themselves collect data from the front-end electronics. By comparison, the test beam DAQ system will be a small prototype of the production system with much smaller bandwidth requirements.

A switch-based DAQ system can be built today by creating a network based on the INMOS transputer [26]. A block diagram of the design is shown in figure 6.3. The test beam

DAQ can be divided into two parts: the data collection from the front end crates of the detector subsystems and the process of building a complete event.

6.2.2.2 Front End Crates

The data of each subsystem will be collected in a few (≤ 3) crates, known as the "front end crates." It has been agreed [30] that the front-end crates will be VME crates containing an MVME-162 processor [27] running VxWorks, an I/O module that communicates with the trigger and gating logic, and an arbitrary number of data sources. Figure 6.3 shows a few examples of front end crates.

The crate is controlled by the MVME-162 processor. This processor receives triggers through the I/O module, collects the data from the other boards in the crate and stores it in a to-be-determined standard format in VME accessible memory. All front end crates will use a common DAQ software package. The candidates for this package, which are already developed, include prDAQ [21] and DART [31]. The final choice will be made by fall of 1994.

The DAQ group will provide the framework software for the read-out of the front end crates. It is expected that the detector subsystems will provide the necessary code for the read-out of their modules, with assistance of the test beam DAQ group members. The software needed for the read-out of the crates is independent of the design of the event building step. Thus, crate-level read-out software can be used for stand-alone tests and data-taking with either the baseline or fallback solutions, assuming that the same event-formats and communication protocols will be used in all three cases.

The data-sources in the front end crates include, but are not limited to:

- CAMAC interfaces,
- Fastbus interfaces,
- VME DAQ boards like ADC's, TDC's or other miscellaneous read-out cards, and
- (prototype) simplified Event Data Collector (EDC) boards.

While the first 3 items on this list are standard, the last item requires some discussion.

In the production DAQ system, all front-end cards on the detector will be connected to the DAQ system through optical fibers. The card that receives the signals from the optical fibers is the "Event Data Collector" (EDC). The first function of this card is to store the data from the fibers into memory. For the testbeam, it is expected that the muon and tracker subsystems will have front-end cards with optical fibers. To accommodate these subsystems, an EDC with at least this functionality and the possibility to read the data in memory from VME will be made available. The block diagram of such an EDC is shown in figure 6.4. This mode of operation of an EDC is called the "passive" mode.

The second function of the EDC's in the production GEM DAQ system is to receive Level 1 triggers and transfer the appropriate data to the Level 2 and 3 processors. This requires a processor on each EDC board. Although it is not the baseline, as an R&D project we might want to test this in the testbeam (see section 6.3). For this reason, a T9000

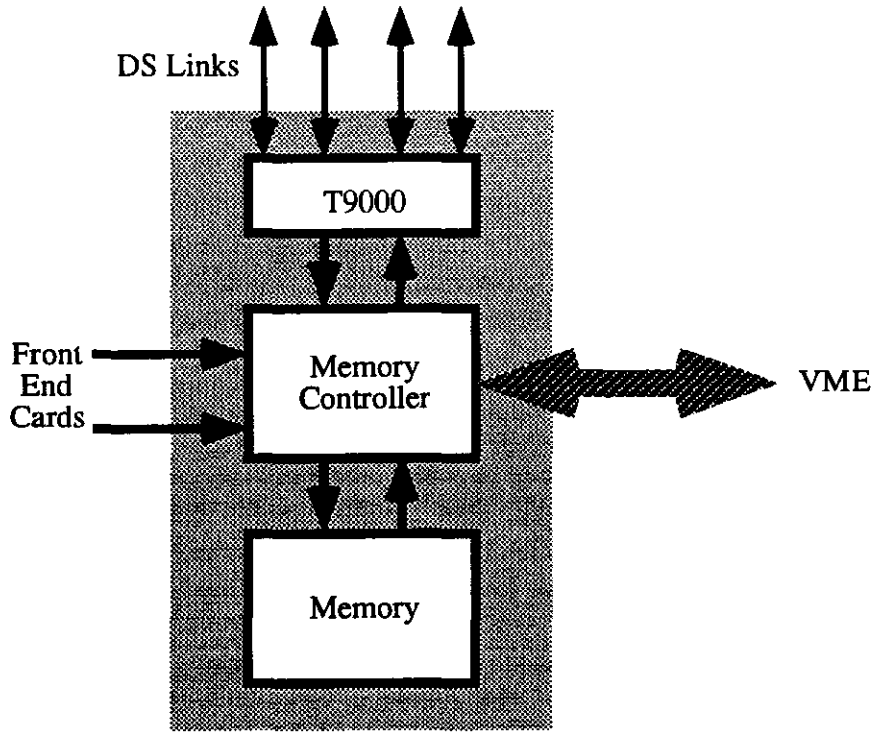

Figure 6.4: Block diagram of the prototype EDC. This board can operate in two modes: "passive" and "active." In the passive mode, data from the front end cards is put in memory. The data is then read-out by a VME-master. The T9000 is not used. In the "active" mode, the T9000 reads the data from memory as well as from VME and sends it out over the DS-links.

transputer may be put on the prototype EDC boards. This T9000 will control the EDC. This mode of operation of the EDC is called the "active" mode.

The simplified-EDC boards will be designed by groups from the SSCL and the UCSD. The protocols on the links will be determined by the design group of the production EDC's and the detector subsystems. As with all data-sources, it is expected that these groups will provide the necessary software to read-out the EDC's in the "passive" mode.

6.2.2.3 Event Building

After each front end crate has been read out, the data of all subsystems has to be combined into a single event, processed and sent to the online system. This is done by the transputer network shown in figure 6.3.

The event building starts with packetizing the data. The real time CPU reads the data from the data sources and combines the data into larger packets. While the data is being packetized, headers and word-counts will be attached to the packets.

Then the data is sent through a DS-link to a switch. The DS-links are bi-directional and can transfer up to 100 Mbit/s in each direction. At first, the transfer of the data will be controlled by the MVME-162 processor and the system will operate in a data-driven mode.

At a later stage, this task may be taken over by the processor on the EDC (see figure 6.4 and section 6.3).

The interface that will be required to connect a DS-link to an MVME-162 processor will be available as a single chip from INMOS [26]. A similar chip has been used in the ZEUS experiment and has proven to provide a reliable interface between transputers and VME-based processors [34].

The other end of the DS-links are connected to a C104 switch. This self-routing switch sends all data packets belonging to a certain event to a single T9000 transputer. This transputer puts the packets from all subsystems together, thus building the event. One or more T9000 transputers will be used as event-builders. The exact number will be determined later. Since the switch is self-routing, connecting more front end crates or transputers to the switch can be done with only minor changes in the software. The complete events are then sent to the online system.

Independent data paths for one or more subsystems can be realized by adding a second C104 switch. This switch will be connected to the front end crates of a particular subsystem and one or two of the T9000 transputers. This is, in fact nothing more than building another copy of the network shown in figure 6.3. Obviously, the software written for the first network can be used for this network as well.

The C104 switch can connect up to 32 subsystem VME-crates and T9000 transputers. The maximum bandwidth over the switch is of the order of 125 MByte/sec, which is much more than what is needed.

Events can be analyzed by the T9000 transputers that do the event-building. If the processing power of these chips (> 70 MIPS and > 15 MFLOPS each) is not sufficient, more T9000 transputers can be connected to the switch. These transputers can build events, analyze them and then send the complete events and the results of the analysis over the switch to the online system

It is expected that most of the communication software on the transputers will be written in OCCAM, the native language of the transputer. However since C++ compilers are available for transputers, it is expected that the same event analysis routines that are used in off-line analysis could be used in on-line analysis.

The network is controlled by a T9000 connected to a workstation. This "master" transputer takes care of booting the other transputers, downloads the network configuration to the switch, distributes commands like "start" and "stop" from the global control system to the other transputers and monitors the performance of the system.

6.2.2.4 Simulation of the system

Several groups are currently working on simulations of the GEM production DAQ system. These simulations can be extended to include the testbeam DAQ system for the purpose of optimizing the testbeam DAQ design. After the system has been built, the performance of the actual system can be compared with the simulations. This provides a method to check the simulations and will lead to a better understanding of the simulations of the production DAQ system.

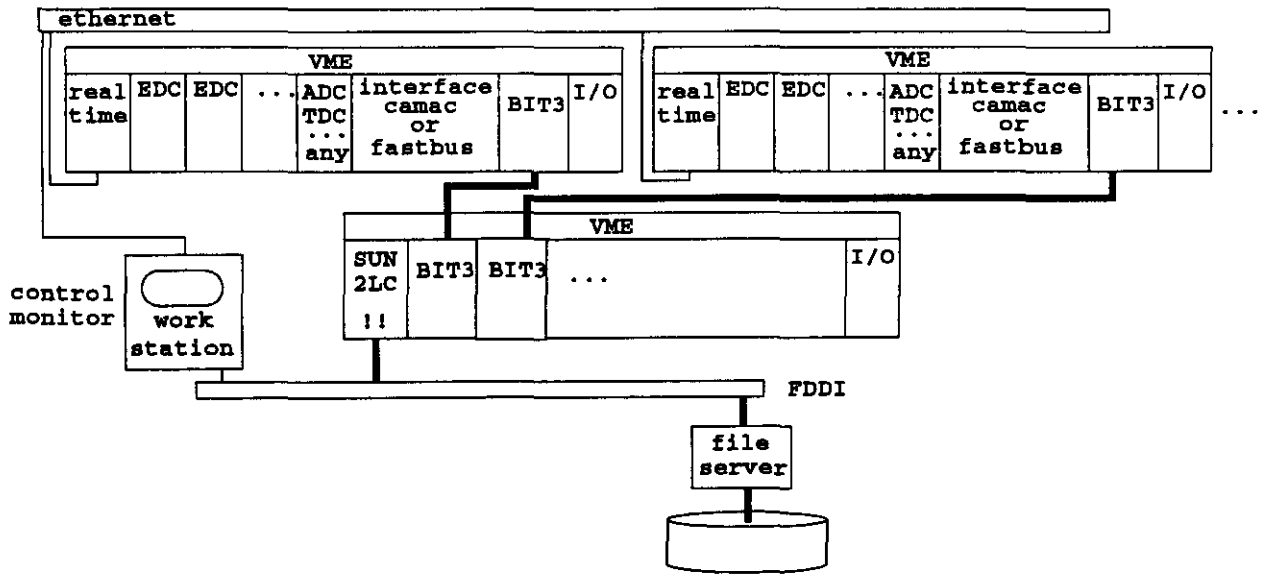

Figure 6.5: The fallback DAQ system.

6.2.2.5 The Fallback solution

The fallback solution is shown in figure 6.5. The same VME front end crates used for the baseline system could used to collect the data from all three detector subsystems. Most of the software necessary for the read-out of the crates will be identical to the software used for the baseline option.

The crates could then be connected by BIT3 links to another VME crate, into which the data from the front end crates could be memory-mapped. A single board computer, for example a SUN2LC SPARC card, could then build the event and transfer the data to the online system.

In the central VME crate, an existing, off-the-shelf, DAQ package could then be customized for use by the GEM test beam. Candidates for this package include prDAQ [21], UNIDAQ [33] and DART [31].

6.2.2.6 Stand alone data taking

Stand alone data taking is possible by inserting a single board computer, for example a SUN2LC SPARC card, into the front end VME crates. This is shown in figure 6.6. Together with an X-terminal, a minimal online system and a data storage device, this configuration provides a simple method to take data from a single subsystem. The prDAQ [21] package provides the necessary software to control this system.

This configuration will typically be used in the period before the test beam baseline DAQ is available, for tests of detector components before they are shipped to Fermilab and for small, stand-alone tests. It is expected that the detector subsystem groups will write all code necessary to customize the prDAQ package to their specific stand-alone needs.

It should be noted that configurations similar to the one shown in figure 6.6 have been used by the muon group for the TTR and by the tracker group for their test beam runs at

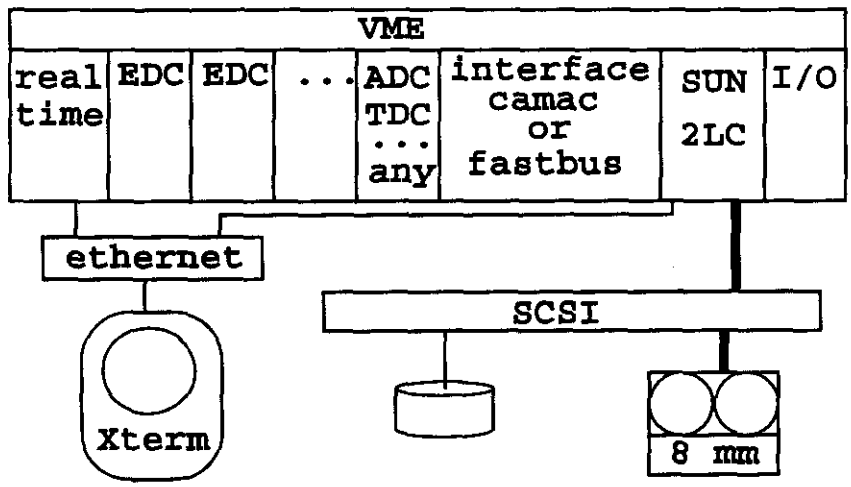

Figure 6.6: The system for stand-alone data taking.

BNL in July 1993. However, proper testing of the calorimeter will be limited unless it has at least some integration with the beam line particle tagging systems.

6.2.2.7 Interfaces and Controls

The DAQ system is controlled by a program on a workstation. This program communicates with and receives commands from the global control system, distributes them to the processors in the DAQ system and returns monitor- and error-messages to the global control system. The protocols for all messages will be defined at a later stage. Commercially available hardware interfaces will be used as much as deemed feasible.

6.3 Data Acquisition R&D Plans.

6.3.1 Initial DAQ R&D Goals.

Unlike the final GEM DAQ system, the initial version of the test beam DAQ system is data-driven. However, a successful implementation of this system would already accomplish the following:

- Test the feasibility of the system architecture of the GEM production DAQ. In the GEM design, a switch is employed to build a complete event from several hundred event fragments. In the testbeam DAQ system, switch protocols can be exercised and changed if necessary.
- Gain experience in areas of monitoring and debugging a GEM-like DAQ.
- Assist system simulations of the production DAQ by comparing results from the simulations with the testbeam DAQ.

- Learn about commercially available technology in this area. It is expected that the transputer technology evolves in the coming years, making it a possible candidate for an industrial solution to the event-building problem. If, however, another technology is chosen for the final GEM DAQ system, the experience gained with a transputer network is still useful.

- Test event-building algorithms. The events will arrive as fragments on the event-building transputers and have to be concatenated into a single event. The testbeam DAQ will provide a platform to test possible algorithms.

- Test event-filtering algorithms. At low trigger rates, we we do not plan to reject events but the transputers can still be used to study possible trigger algorithms, their performance and CPU usage. At higher trigger rates, not all events can be stored and the transputers have to filter or compress the data.

6.3.2 Phase II of the Baseline DAQ system.

The baseline system will evolve during the data-taking period. One interesting modification is the following:

- Connect the trigger to the controlling transputer.

- Switch to the "active" EDC mode.

With these minor hardware modifications, and some new software, one can simulate the production DAQ system even closer: For each trigger, the controlling transputer assigns the event to an event-building transputer. This transputer then request data from the EDC's, build the event and analyses it.

Undoubtably, there will be other ideas for the evolution of the system. For the moment it is important to realize that this system provides the ideal platform for GEM DAQ R&D during and after data-taking at Fermilab.

6.4 Schedules

6.4.1 DAQ R&D Schedule

The development of the baseline DAQ system starts as soon as this RDT is approved and the necessary funds are available. It is expected that the development of the system will take about 2 years. During the first year, we plan to:

- Acquire a small basic transputer setup consisting of 2 (or more) T9000 transputers, a C104 switch, cables, interfaces to a SPARC station and the necessary software. This setup will be used to get hands-on experience with transputers and for evaluation of the chips. If the T9000 chips are not yet available, the T800 transputers will be used in this setup.

- Develop a simulation of the system.
- Finalize the requirements for the system, specify the architecture for the system and finalize the design.
- Acquire the necessary hardware and/or software.
- Start the development of the EDC modules.
- If necessary, start with the development and design of other custom hardware.
- Start with the development of the software for the system.

During the second year, we plan to:

- Continue with development of hardware and software.
- Test the system at the SSCL.
- Install the complete system at Fermilab, a few months before data-taking starts, test and debug it.
- Compare the test-results with the design parameters and simulations of the system.

At this point, a working system will be available for data-taking. The system can also be used for DAQ R&D during or after the data-taking period, see section 6.3.

After the first year, a first prototype of the system should be available. This prototype has to be critically reviewed. If it turns out that the milestones cannot be met, then work on the fallback solution has to start. Since this technology exists in many proven varieties (see section 6.2.2.5), we feel that the customization of such an event-builder can be done easily in a few months. Thus, embarking for the next year on the baseline DAQ system does not present a risk for the overall GEM testbeam program.

6.4.2 Implementation of the DAQ at MWEST

Implementation and testing of the DAQ system will take advantage of those in residence at Fermilab. It is important to begin early to build a base of experts that can be called upon on short notice to solve problems of hardware and software glitches during the run. With the improvements in networks, a great deal of diagnostics can be done from remote sites, particularly in the case of software; however, the necessity of hands on repairs and diagnostics still exists. Resident experts can provide the needed continuity as non-residents rotate in and out of Fermilab. In order to assemble and test the DAQ system, it is important early on to be building and testing standard systems for the test beams at MWEST, which can be best provided by Fermilab residents.

The collaborators at MWEST will begin with a small test system similar to the stand alone system described in section 6.2.2.6, which has been purchased by Rochester and already exists at MWEST. From this, we intend to connect via AFS to SSC disks, so that DA software can be shared easily between MWEST and the SSCL as well as other institutions. GEM

software standards, will be followed. We initially plan to implement a high voltage control system, using the recommended computer language, C++. This will be useful later for tuning trigger scintillators etc. We can also adapt this to work with the beamline Čerenkov counter.

At an early date the options for the fallback DAQ system (see section 6.2.2.5) will be investigated so that it can be built quickly, if necessary. When pieces of the baseline event builder are ready, we will want to bring these to MWEST to build experience and assist in its integration.

The milestones in the DAQ implementation schedule at MWEST are:

- Assemble and bring up GEM standard test DA system – October 1993.
- Build high voltage diagnostic system in C++ – by January 1994.
- Investigate options for the fallback DAQ system – by March 1994.
- Acquire EDC's for readout tests – June 1994.
- Bring up hardware and software for the readout of the Čerenkov – January 1995.
- Assist in the check out of sub-systems and subsystem DA interface – throughout 1995.
- Working baseline event builder in place at MWEST – mid 1995.
- Exercise integrated system – mid 1995 until beam.
- Take data when beam arrives – fall 1995

6.4.3 Trigger implementation schedule

The trigger hardware will be assembled a few months prior to the time that data is to be taken.

The frame software for the programmable logic units needs to be ready prior to the run time.

The actual precision timing implementation and commissioning will require a few hours at the beginning of the run time. From there on, the timing is expected to be stable.

The tuning of the SRD, the Čerenkov, and beam momentum (beam line magnets) require the implementation of the slow controls prior to the run time, see the section on slow controls.

6.4.4 Phase II of the baseline DAQ system

All these plans (see section 6.3.2) plans will be scheduled during the quiet periods of the Fermilab testbeam, in such a way that they do not interfere with normal data-taking.

6.5 Budgets

This section lists the costs and schedules for the DAQ and trigger for the FNAL test beam. (Include overall operations costs, contingency, EDIA.)

Table 6.1: Costs of the first transputer development system

Item	*Cost [k$]*
2 T9000 transputers with an s-bus interface.	9.0
C104 Switch	1.0
Cables	1.0
Basic software	3.5
Sun SPARC station (provided by the electronics group or GEM-SSC).	0.0
Total	14.0

6.5.1 DAQ R&D Budget

The costs of the first test-setup is about 12 k$, more details are shown in table 6.1. Most of the equipment purchased for R&D purposes will be used to build the final system.

6.5.2 DAQ Implementation Budget

Table 6.2 contains a first estimate of the costs of the baseline DAQ system.

6.5.3 Trigger Implementation Budget

Table 6.3 lists the estimated equipment that will be used for the beam trigger. It is the present understanding that the listed equipment may be provided by PREP[1] subject to the MOU[2] between Fermilab and GEM.

6.6 Manpower, Responsibilities

Groups from the University of Rochester, SSCL and BNL will build the the trigger and DAQ systems. As we get closer to beam time, others are expected to join the testbeam DAQ and trigger groups. In addition, we fully expect a great deal of support from the various subsystems during assembly and running of the GEM test beam for both debugging and shift work.

6.6.1 DAQ R&D, implementation of the baseline system

The following people are expected to spend a fraction of their time on the DAQ R&D and the implementation of the baseline DAQ system:

- M. Botlo (SSCL, DAQ)

[1]PREP is the Pool and Repair Electronics facility at Fermilab.

[2]The MOU (Memorandum of Understanding) between Fermilab and GEM includes an agreement on the use and payment of the PREP services.

Table 6.2: Budget for the implementation of the baseline DAQ system. The items marked "subsystems" should be provided by the subsystems.

	Item	*# units*	*k$/unit*	*Total [k$]*
1.	**Front End crates**			
1.1	MVME 162's	Subsystems	–.–	–.–
1.2	EDC's	Subsystems	–.–	–.–
1.3	I/F 162–DS link	3...10	0.5	5.0
2.	**Transputer network**			
2.1	T9000 with S-bus I/F (Control, subsystems)	4	4.5	18.0
2.2	T9000 without S-bus I/F (Analysis)	0...4	4.0	16.0
2.3	C104	1...3	1.0	3.0
2.4	Cables	1	5.0	5.0
2.5	VME Crates for TP hardware	1...4	3.0	12.0
2.6	Basic Software	1	3.5	3.5
2.7	Other Software	1	7.0	7.0
3.	**Workstation**			
3.1	SUN ws, disk, monitor	1	12.0	12.0
3.2	FDDI, Ethernet cables and I/F		?.?	?.?
3.3	Maintenance contract	3 years	?.?	?.?
3.4	Online Workstations	Subsystems	–.–	–.–
4.	**Manpower**			
4.1	$\mathcal{O}(3)$ FTE's/year	3 years	?.?	?.?
4.2	Travel	1	?.?	?.?
5.	**Other**	1	?.?	?.?
	Total			$\geq$ **81.5**

- M. Bowden (SSCL, Electronics)
- J. Carrel (SSCL, Electronics)
- P. Dingus (SSCL, GEM)
- J. Dorenbosch (SSCL, DAQ)
- J. Dunlea (U.Roch, GEM)
- V. Kapoor (SSCL, Electronics)
- A. Morelos (SSCL, GEM)
- D. Ruggiero (U.Roch, GEM)
- H. Uijterwaal (SSCL, GEM)

Table 6.3: Estimated Trigger Equipment and Cost

	item	*# units*	*k$/unit*	*Total [k$]*
1	NIM discriminators	3	1.2	3.6
2	ECL discriminators	3	2.2	6.6
3	AND/OR NIM units	5	1.1	5.5
4	NIM fan in/out's	5	0.9	4.5
5	ECL programmable logic units	2	2.6	5.2
6	gate generators	5	1.5	7.5
7	ECL programmable delay	3	3.6	10.8
8	NIM-ECL-TTL level translators	5	1.6	8.0
9	pulse generators	2	5.0	10.0
10	NIM crates	3	1.6	4.8
11	CAMAC crates	3	2.7	8.1
12	serial CAMAC crate controllers	3	2.3	6.9
13	200 m cable for serial CAMAC	3	2.3	6.9
14	2 m cable for serial CAMAC	2	0.3	0.6
15	NIM visual scalers	2	1.1	2.2
16	CAMAC scalers	3	2.5	7.5
17	CAMAC to VME interface	1	5.0	5.0
	Total			103.7

- C. Zhao (U.Roch, GEM)

We expect that the total manpower available from these collaborators is sufficient to built the system according to schedule. The group will work together with the subsystem data-acquisition and computing groups led by S. McCorkle and G. Word respectively.

The implementation of the DAQ at MWEST will be coordinated by Jim Dunlea (U.Roch). The contacts responsible for the various interfaces to the DAQ are:

- test beam subsystem integration: Sean McCorkle (Brookhaven)
- Global Control System: Vladmir Glebov (SSCL)
- online, storage: Gary Word (SSCL)
- event builder: Henk Uijterwaal (SSCL)

6.6.2 Implementation of the trigger

Groups from the University of Rochester, BNL and SSCL are expected to build and organize the beam trigger.

Subsystem manpower, beyond the previous named institutions, is expected to work in different aspects of the trigger for their own special trigger needs, like calibration.

6.6.3 Phase II of the Baseline DAQ system

It is expected that most of the people working on the initial implementation of the system (see section 6.6.1), will also be involved in the DAQ R&D projects.

Chapter 7

Electronics

7.1 Electronics Summary

The GEM performance goals and the high SSC collision rate place severe demands on the readout electronics due to the high event rate coupled with the large channel count and data flow. Additionally each detector subsystem imposes unique requirements on its associated electronics readout system. In order to reduce the cable requirements and to minimize signal degradation, much of the electronics must be integrated on the detectors, particularly the inner silicon and IPC trackers. The primary GEM design goals of precision calorimetry and muon measurement place exacting demands on their electronic precision and calibration. Commercial components meeting the technical requirements are currently not available, necessitating the development of application-specific integrated circuits for each of the major subsystems.

In order to provide meaningful data to validate the critical electronics design areas it is the goal of the electronics subsystem to support the testbeam with designs that would be essentially identical to the final production system. Schedule constraints dictate that it is not possible to fully implement the production system, however the designs will incorporate many of the critical elements such as the custom designed integrated circuits. Each of the prototypes will be complete enough to demonstrate the viability of the electronics in a high rate beam environment, and will provide a testbed for possible design improvements.

The following sections provide detailed prototype functional descriptions and test approaches for each of the testbeam subsystems.

7.2 Silicon Tracker

7.2.1 Summary

This proposed silicon tracker electronics R&D effort is to design, fabricate and test a prototype system, to be used to verify the functional requirements and operations of the electronic designs for a future silicon tracker. The prototype is complete enough to demonstrate the operation of the electronics in a high rate beam environment, and will provide a testbed to

learn of possible design improvements. The prototype design follows the GEM TDR design as closely as possible.

7.2.2 Prototype Functional Description

The prototype design requirements are necessarily different from those of the future collider's, and there will be sensible engineering decisions to balance the cost and schedule of the R&D effort against a design and setup that are representative of future collider operations. The design specifications of the prototype should reflect most of the crucial operational parameters as anticipated from the future colliders, and still be flexible enough to realize the design within budget and schedule. Some of the most critical parameters include the per-channel power consumption, beam crossing time, data compression and readout data bit-rate, radiation hardness, and the signal to noise ratio of the front-end circuits. The key issues will be related to the efficiency of the electronics system for sensing tracks which pass through a silicon plane and the resulting tracking efficiency.

The specific packaging technology of the electronics, command and control, power distribution and cabling are to be optimized for the prototype so that the setup yields useful database for further improvements without undue cost and schedule constraints.

The external DAQ will be performed through the fiber optic links, through a prototype version of the GEM DAQ fiber optic receiver boards. The precise definition of this link will be one of the R&D tasks prior to the test beam operation. In addition, a PC based slow control system will be needed for initialization and monitoring of the electronics.

7.2.3 Prototype Test Approach

Prior to installation into the test beam, component checkout will be necessary. A test bench version of the data acquisition system will be needed for this purpose. For a complete checkout of the full silicon tracker test beam system, the test beam DAQ system should allow simultaneous data acquisition in the test beam DAQ so that equipment checkout can be performed parasitically with test beam operation. An alternative would be to have the DAQ module moved to a separate, stand-alone DAQ system. Either scenario would be acceptable.

7.2.4 Prototype Test Issues

The major risks are mainly due to the tight schedule that the effort lives with. The IC developments are on the critical path and should be given the highest priority. In addition, the MCM module design has not yet been verified and the NRE cost to do so is high.

There are several major R&D issues to be resolved in the electronics. The issue of noise and time-walk of the analog chip operating with the long ($16 - 18$ cm) strip detectors. While the design will be optimized for the two requirements given the power, the prototype design will favor a slightly higher power consumption rate than normal since the cooling requirements may not be as stringent as expected in future colliders. The problem due to interference from the logic pulses generated in the level discriminator and the digital

VLSI chips to the preamplifier front-end will also have to be worked out without incurring additional cost in developments.

The second involves the VHDL-based design of the digital chips which will have to be optimized for the most efficient use of the chip areas. The VHDL-based design makes it possible for the development of the chips more adaptable in mapping the design into different target foundries, but may also introduce inefficiency in die area usage. The use of MOSIS service and possibly others to produce the chips will require extra effort to optimize the layout. The storage and compression architectures are also areas for further research to arrive at the best possible solutions.

Multi-chip module production is the third major issue. HDI process mentioned earlier is the best option in dealing with the tremendous circuit layout density and heat dissipation requirements, but the NRE cost is quite high (in the neighborhood of 0.5 M$) for prototype production. It will be a difficult choice between conventional fabrication alternatives, which might not meet the ultimate design requirements, and the costly but ideally suited HDI technology. Further commercialization of the HDI may bring the NRE cost in the future and the slight lag of the MCM design phase from the VLSI chip development will allow us from making a hard choice right away.

The radiation hardness is one of the most demanding requirements imposed on the silicon tracker systems for future colliders. The designs of the integrated circuits are centered around that issue and its verification will be a goal of this effort.

7.3 IPC Tracker Electronics R&D

7.3.1 Summary

The IPC electronics system R&D program includes work needed verify that the rather novel approach taken to the readout of the IPC system, dictated by the SSC tracker environment, is viable, to develop the custom rad-hard integrated circuits used in the IPC readout system, as well as the very high density packaging of the front end components needed in this application, and finally, to develop fully all critical aspects of the overall system design, such as power and signal distribution, calibration, and the connections to the chamber and cooling systems.

7.3.2 Functional Description

The approach followed in the IPC readout system is somewhat unusual, in that neither a peak sensing circuit nor gated integrator is used to obtain the induced charge on the cathode pads. Instead, after the induced signals are amplified and shaped, the shaped signals are sampled at 16 ns intervals. These samples are stored in analog form in a switched capacitor array until the receipt of a trigger. At that time, the samples of interest are digitized, zero suppressed, and transmitted off the detector through a fiber optic link. For each pad with valid data, 3 to 4 samples are transmitted on each event. These correspond to a presample, which allows the baseline to be subtracted from subsequent samples, and the samples which span the shaped pulse. Because the time development of the signals on pads with induced

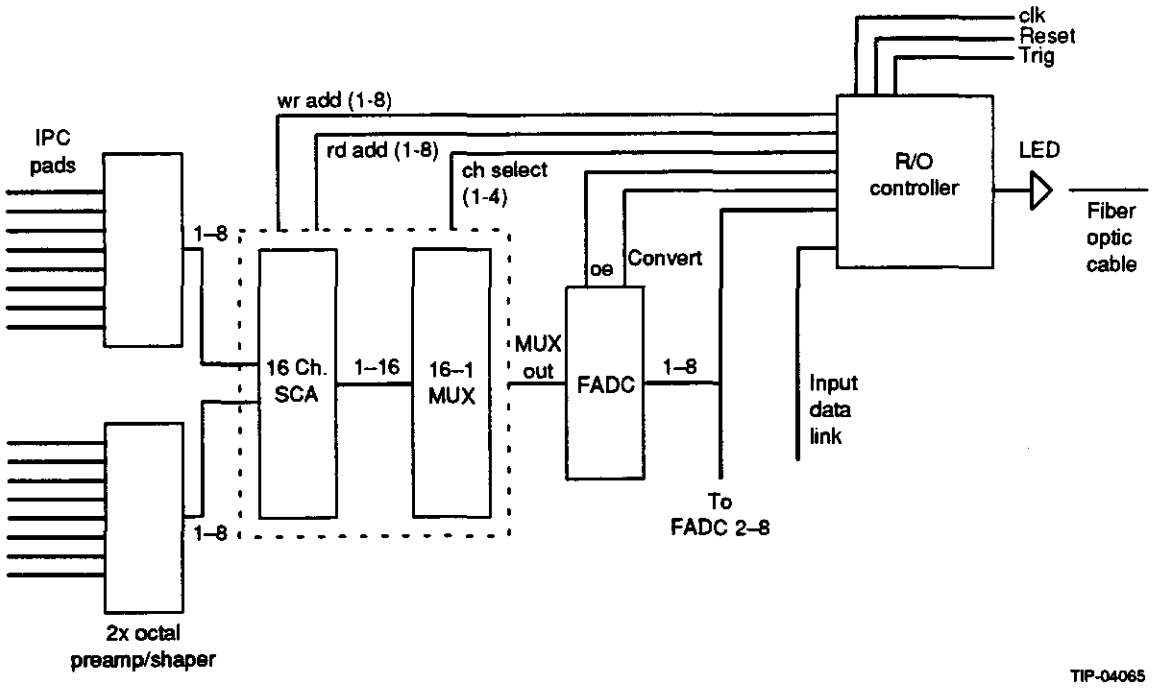

Figure 7.1: IPC readout architecture.

signals from the same avalanche are identical (in the absence of shaping time variations in the electronics), each of the samples from a set of adjacent pads can be used to obtain an independent position measurement. The basic components of the IPC readout architecture are illustrated in figure 7.1. Each of these components are described below.

7.3.3 Preamp-Shaper

The signals from the IPC cathode pads are input to octal preamp/shaping amplifier circuits, eight of which are contained on a single die. The gain of the preamp/shaper is 10 V/pC, and the nominal peaking time of the shaped output is 25 ns. The position resolution of the IPC system will be determined to a large extend by the signal to noise ratio of the readout chain, which is dominated by the noise contribution from the front end preamplifier transistor. As designed, the signal to noise performance of the amplifier is 2000 electrons for an input capacitance equal to the maximum expected in the IPC system. This noise figure has been verified on small scale prototypes, and will allow the 50 micron position resolution design goal of the IPC system to be met.

7.3.3.1 Analog Memory

The amplified signals from the shaper are input to an analog memory element, consisting of a switched capacitor array capable of simultaneous read and write operations. The inputs are sampled at the 60 Mhz SSC bunch crossing rate. The analog memory is packaged 16 channels to a chip, and includes a 16 to 1 analog multiplexer at the output. The readout of

the analog memory takes place through a amplifier on each channel having a settling time of 500 ns, which provides the input the multiplexer. We are now in the process of evaluating the first rad-hard analog memory prototypes, developed to meet the 2 Mrad ionizing radiation dose requirement for the IPC front end electronics.

7.3.3.2 FADC

The digitization of the sampled waveforms is accomplished using an 8 bit FADC. A rad hard FADC developed by Harris in the same CMOS process employed by us in the development of the amplifier and analog memory devices is commercially available, and meets our needs.

7.3.3.3 Readout Controller

Control of the analog memory write address generation and readout sequencing is handled by the readout controller. The analog memory itself is used to buffer data prior to readout, and the controller contains a status array containing the locations of memory locations awaiting readout. These locations are protected from being overwritten by the controller, allowing essentially deadtimeless operation. The readout controller also contains an internal buffer, used for building the output data packets. Finally, it is provides the interface to the clock, trigger, slow control, and calibration inputs. Each readout controller services 128 pad channels, and had a dedicated output data link.

7.3.3.4 Data Link

The data packets built by the readout controller are serialized, and output on a 60 Mhz bandwidth LED/fiber optic link. The approach used by the IPC system for the data link will be identical to that used by the Si Tracker, and it is expected that most of the development work for this component will be performed by that group.

7.3.4 Prototype Test Approach and Issues

The purpose of the FNAL beam test is to simulate as closely as possible the conditions which will be encountered at the SSC, and to evaluate the performance of the system in that environment. During the beam test, the IPC readout system will be tested primarily through measurements of the performance of the integrated IPC system. That is, measurements of the chamber position resolution as a function of position in the chamber, incident angle, rate, etc, will be used to evaluate the performance of the system, and in turn, the performance of the readout electronics. In addition, during the second phase of the beam test, in which the detector subsystems are operated as an integrated detector, the interactions between the IPC readout system and other elements of the GEM detector will be studied. In particular, the extent to which other subsystems introduce noise on the power and ground lines, or through RF pickup, will be investigated. Finally, the FNAL beam test will provide a means of testing the interface of this and other subsystems with the DAQ in a realistic environment. The IPC readout prototype which will be used for the FNAL test beam run will be functionally identical to the production hardware. However, some differences between the

FNAL prototype and the production hardware are likely to exist, and include the use of a FPGA based readout controller, rather than the final gate array, and the use of hybrids for packaging the front end electronics, rather than multichip modules, the development of which will not be complete prior to 1995.

The IPC subsystem for the FNAL beam test will consist of two complete barrel sectors of eight chambers apiece, and one forward sector with eight chambers. Each chamber requires roughly 1300 readout channels, resulting in a total channel count, with spares, of 34,000 channels. There will be approximately 250 fiber optic data links from these front ends to the DAQ. Roughly 3 kW of low voltage power will be required. Active cooling, of the same type envisioned for the production chambers, will be used on the FNAL prototypes.

7.4 Calorimeter Readout Electronics

7.4.1 Test Beam Prototype Functional Description (Overview and Requirements of the Readout)

The full GEM calorimeter contains approximately 125k channels. The readout must provide:

- 18 bits of dynamic range,
- a contribution to the constant term in the energy resolution of $< 0.2\%$,
- time resolution sufficient to uniquely identify the bunch crossing,
- storage for the calorimeter signals during the Level 1 latency of 2 μs,
- deadtimeless operation at a maximum Level 1 rate of 100 kHz,
- the transfer of fully digitized data to Level 2, with up to 5 samples per channel per Level 1 trigger.

A schematic of the readout chain is shown in figure 7.2. Preamplified signals will be transferred on short (several m) cables to "junction boxes" located on the outside of the cryostat. Cable drivers mounted there will drive the signals approximately 40 m to crates of electronics mounted on the wall of the experimental hall. There the signals will be received and split into two paths; one to the data acquisition (DAQ) hardware and the other to the Level 1 trigger summing electronics.

The DAQ signals will be split into two gain scales and shaped before being sampled at 60 MHz. The samples will be stored, most likely in analog form using switched-capacitor technology, awaiting a Level 1 trigger decision. A digital pipeline approach is also being investigated. Upon receipt of a Level 1 trigger, up to 5 samples per signal will be buffered awaiting digitization. Multiplexed and digitized samples will be processed locally and then sent over optic fibers to the Level 2 processing system.

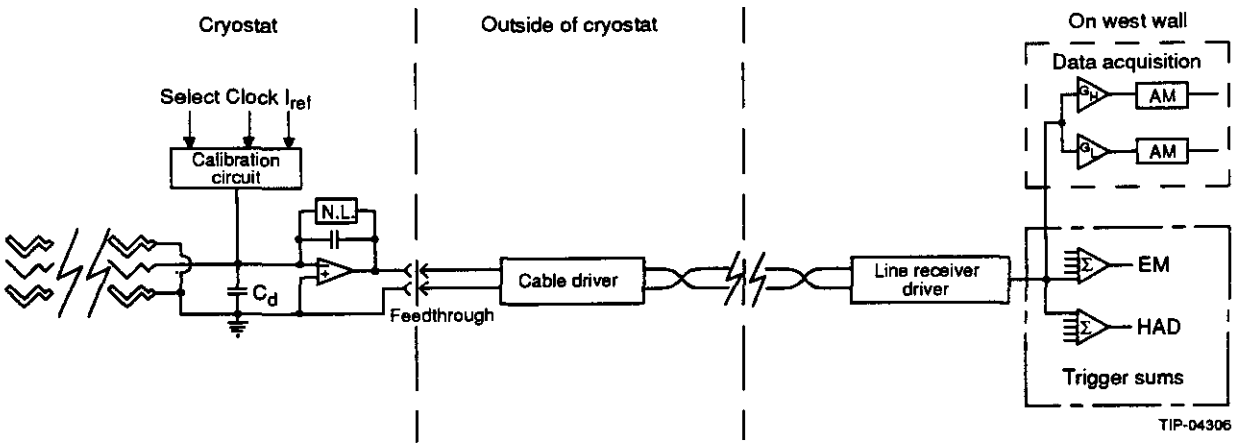

Figure 7.2: Schematic depicting the calorimeter readout chain.

7.4.2 Prototype Electronics for FNAL Test

For the FNAL test, approximately 4000 channels on "in-detector" electronics are required. These electronics include all components (preamplifiers, calibration circuits, cable drivers, signal cables, etc.) which are mounted either in or immediately on the cryostat, and are therefore not readily accessible. Those electronics which follow the 40m signal cables can be located in the counting house. In the interest of reducing the cost of the test program, only approximately 1000 channels of these components will be provided, since they can be "re-used" for different regions of the calorimeter by moving cables. The channel count must be large enough to cover a sufficient region of the calorimeter for complete containment of high energy hadron showers.

Goals of the FNAL test include testing and understanding the behavior and response of the calorimeter itself and, from an electronics viewpoint, determining as much as possible the performance of the readout electronics scheme.

Given these goals, the limited time available for custom prototype development before the FNAL test, and the 2002 turn-on of the SSC, we have developed the following prototype plans for the various components of the calorimeter readout chain:

- Preamplifier, Calibration Circuit - Hybrid versions with all the active circuitry incorporated in monolithic form, and only external resistors and capacitors used, will be available. These will be very similar to the final GEM design, and will include, in particular, the non-linear feedback of the preamplifier which is required to achieve the full dynamic range.

  It is possible that some of the 4000 channels will employ the fully hybrid versions of these circuits which were used successfully during the 1992 beam test at BNL. This approach will allow a comparison with previous results and also provide some margin in the prototype electronics production schedule.

- Cable Driver - Given their current state of development, it is difficult to guarantee design and production of sufficient quantities of prototypes of these devices in time for

the FNAL test turn-on. Some prototypes will be tested at FNAL, as available. As a backup, intermediate amplifiers with transformer coupling, as used in the 1992 BNL run, will be available.

- Shaper - Hybrid versions of the shaper will be housed, as they were at BNL, on separate boards. The existing "VGA" modules, with computer controlled gain, will be available.

- Sampling + Digitizing Electronics - Readout boards utilizing prototypes of GEM SCA's followed by commercial ADC's will be designed and produced. These boards will be designed to be read out by the DAQ via VME.

  Given the schedule, a relatively simple backup solution, similar to that used successfully at BNL, of S/H electronics followed by commercial ADC modules (FastBus or some other standard) will be provided. This approach will guarantee the existence of a well-understood electronic readout for the calorimeter before the turn-on of the FNAL test, as well as allow some flexibility in the development schedule of the SCA readout boards, thereby permitting development of a more sophisticated board which more closely resembles that envisioned for GEM.

7.5 Cathode Strip Chamber Readout

7.5.1 Summary

A complete description of the baseline Cathode Strip Chamber (CSC) readout can be found in Chapter 7 of the GEM TDR [1]. In this document, we present only a brief overview of that design and discuss the ways in which the Fermilab beam test system is likely to differ from the TDR system.

A system block diagram of the CSC readout electronics appears in figure 7.3. The system consists of three major board-level designs: the cathode front-end printed circuit boards (FEPCB), the anode FEPCB's, and the readout printed circuit board (ROPCB). The FEPCB's amplify, shape, and digitize the low-level signals from the chambers. The ROPCB provides the first levels of DAQ and the Level 1 trigger logic and transmits the data to the off-detector DAQ crates, *i.e.,* to the Event Data Collector (EDC) modules.

Figure 7.4 shows the physical layout of the 96-channel cathode FEPCB. The flow of signals is from top to bottom. There are two major layers of signal processing, the preamplifier-shaper (PASA) IC's, and a second set of IC's (ASIC#2) that are used to generate inputs to the Level 1 trigger logic. The logic implemented in the ASIC#2 chips identifies charged-track segments and is therefore useful in steering the readout—*i.e.,* only hits associated with local charged tracks need be read out.

The architecture of the anode chain is similar to that of the cathodes. However, owing to the relatively sparse nature of the anode signal readouts the anode chain consists of four 24-channel preamplifier boards followed by a 96-channel FEPCB. Also, the obvious differences in the input signals dictate that a significantly different preamp design be implemented.

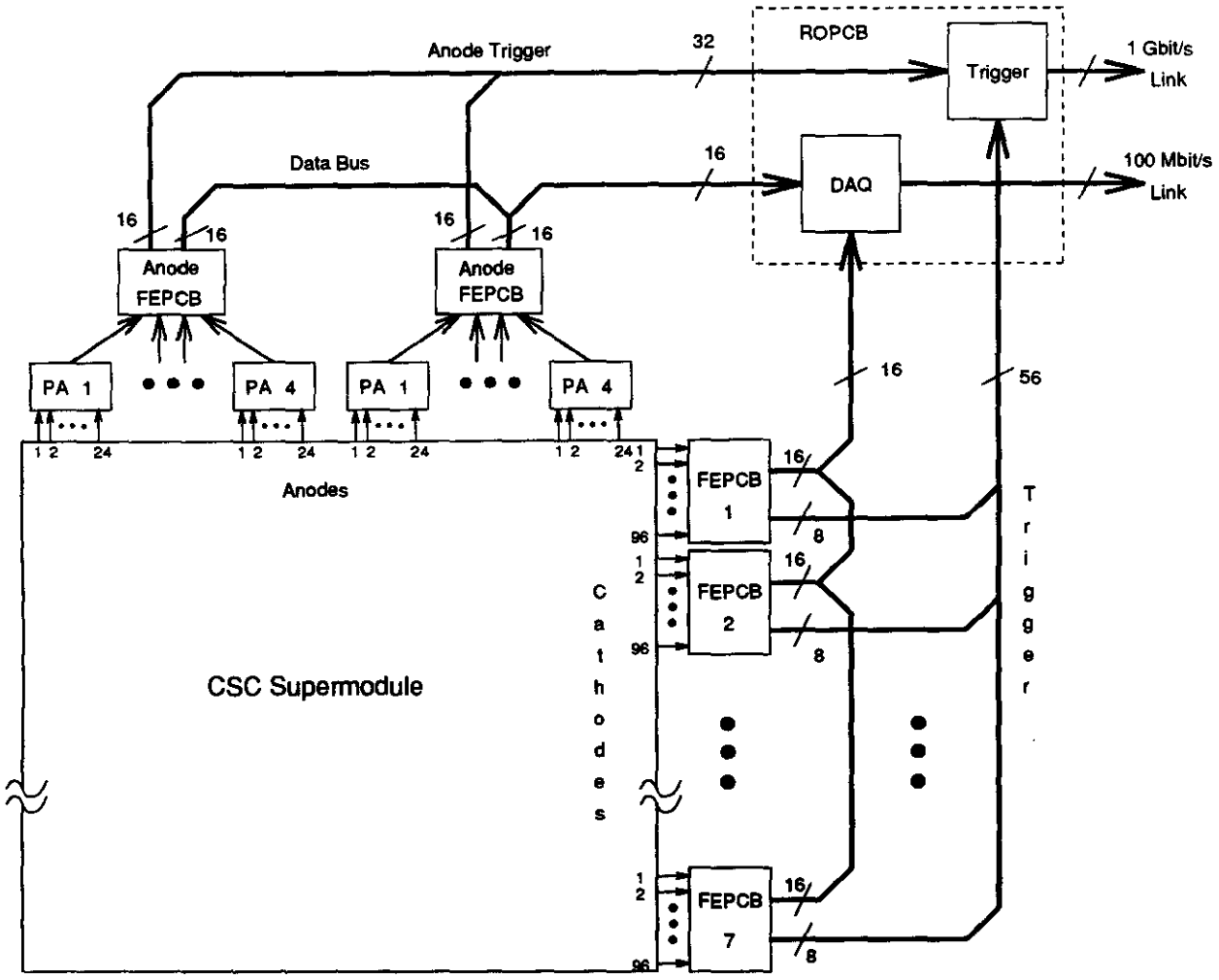

Figure 7.3: System block diagram for the readout, trigger, and DAQ system for the CSC's.

7.5.2 Prototype Functional Description

Table 7.1 summarizes the number of boards required for the tests. Sufficient boards will be produced to fully instrument the seven-module CSC sector in the Fermilab test beam with an allowance for spares and for other tests on and off site.

Ideally the prototype system would be essentially identical to the production system. However, schedule constraints dictate that it will not be possible to fully implement the production system in time for the Fermilab tests. Nonetheless the designs for the tests will incorporate as many of the key features of the production system as possible. One of the first orders of business will be identify areas where it is prudent to back off somewhat from the production design. This process will culminate in a Preliminary Design Requirements Review (PDRR) where a test-beam configuration will be formally adopted.

A preliminary analysis indicates that the following differences between the FNAL system and the baseline system are likely or possible:

- A less ambitious packaging strategy for the FEPCB's may be adopted. In particular,

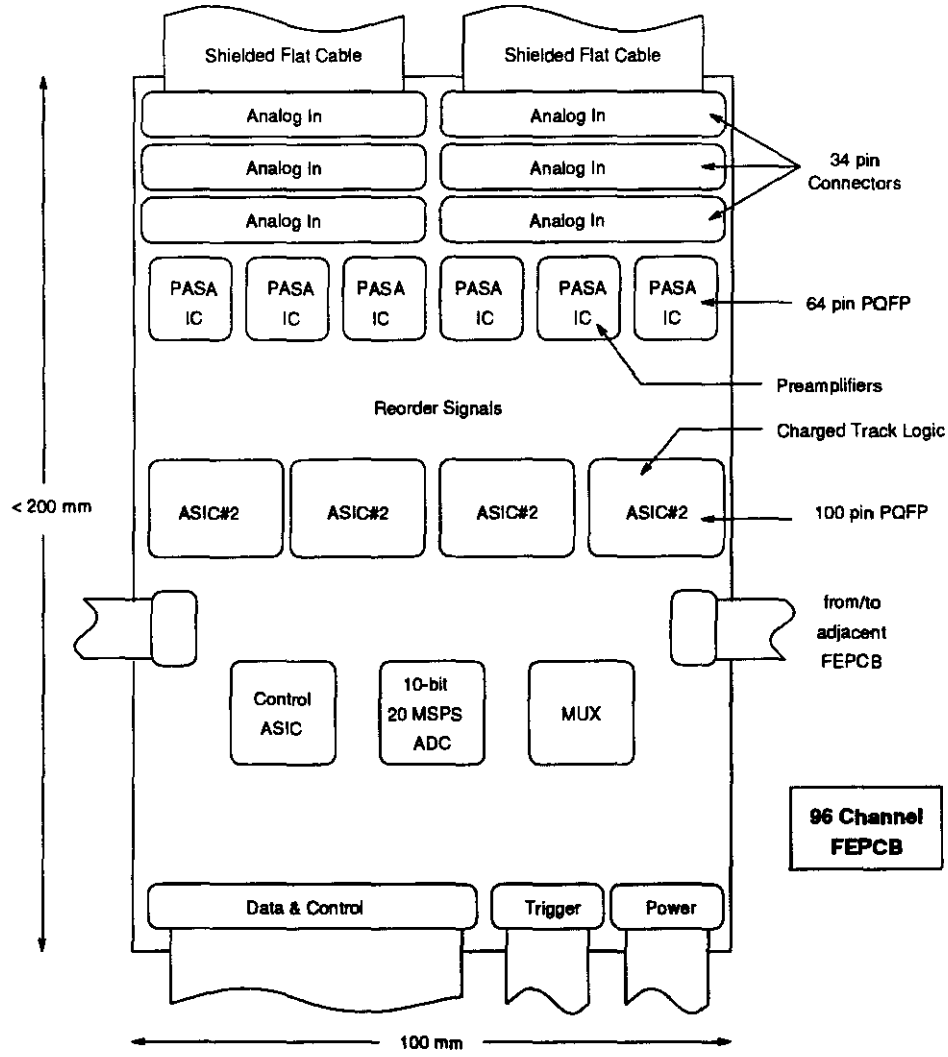

Figure 7.4: Physical layout of the 96-channel cathode FEPCB.

the $\leq$ 100 mm-width design goal for the cathode FEPCB's may be somewhat relaxed for the prototype FEPCB's. The 100 mm value is highly desirable in the production system since it simplifies the physical layout of the chambers. It is less critical in the prototype system.

- The control logic for the readout will be implemented using FPGA's instead of a full custom design or a gate array. The higher per-unit production costs associated with the FPGA are not significant for the small-scale system. Moreover, the added flexibility of an FPGA may prove useful in a prototype system where there are likely to be unexpected circumstances. Similar considerations will also apply to the ROPCB.

- The anode system readout may not be fully implemented. The baseline design calls for an anode readout that closely mirrors the cathode readout. Thus the "backend" IC's—*e.g.*, ASIC#2 and the ALP/control IC— will be the same or very similar to

Table 7.1: Summary of board counts for the test-beam CSC system.

Board Type	Channels/ Board	Boards for FNAL Test	Boards for Other Needs	Total Boards
Cathode FEPCB	96	56	24	80
Anode FEPCB1	24	56	24	80
Anode FEPCB2	96	14	6	20
ROPCB (Motherboard)	—	7	3	10

their cathode counterparts. Small differences in the arrangement of cathodes and anodes, however, will likely result in small differences in the designs for these circuits. Although the added engineering and non-recurring costs associated with the slightly modified designs are not significant in the context of a complete system, they may prove to be so for the FNAL system, where the schedule is very tight. Since most features of the design will be tested in the cathode system, a partial implementation of the anode electronics that is focussed on testing aspects of the readout peculiar to that subsystem represents the best approach. In view of their importance to the overall system performance, particular attention will be paid to the preamplifiers and the beam-crossing tagging circuitry.

- Certain slow control and monitoring functions, which in the production system will be incorporated into the ROPCB, will be separately implemented in the Fermilab system.

7.5.3 Prototype Test Approach

A set of test fixtures will be developed to test individual elements of the system—*i.e.*, FEPCB's, ROPCB's, and the various ASIC's. In view of the limited number of channels, these fixtures need not be as fully automated as those used for the production system. It is expected, however, that the experience gained in developing these fixtures will be useful in the specification and design of the production test fixtures.

7.5.4 Prototype Test Issues

The purpose of the test is to confirm that compact, low-cost, electronics that is suitable for chamber mounting can be produced and successfully operated under realistic conditions. In particular, we seek to verify that coherent noise from crosstalk and pickup in an accelerator environment can be reduced to below the level of the thermal noise. Also, although the number of channels is less than 1% of the total eventually required, it is large enough to test many facets of the process of mass production.

7.6 Calorimeter Trigger

7.6.1 Summary

There are a number of aspects of the calorimeter level 1 trigger logic which can be meaningfully tested with a section of the GEM calorimeter operating in a high energy test beam. These include studies of the timing properties of the trigger, both at the level of individual discriminators and at the level of jet sums, where the timing is given by digital filtering; studies of the efficiency and rejection power of the isolation logic used to identify isolated EM showers; studies of the operation of a real-time high speed transversal filter which will execute an optimal filtering algorithm for the jet sums and will provide inputs for the global sums in GEM; and tests of FPGA-based count logic, which will be used to identify the numbers of calorimeter clusters of various types.

In order to economize on manpower and to be able to meet the time schedule of the FNAL test, a prototype of only one of the 5 types of trigger modules (L1SUM) will be built for the FY95 FNAL beam test. The concepts for the other modules can be tested in three types of CAMAC modules, one of which already exists. A transversal filter test module, the design of which is well under way, can be used to understand the important features of the Global Sum module. The main functions of the Jetsum/Filter module are to sum and digitize the jetsum signal and to provide a trigger for the transversal filter. We plan to build a special digitizer module for the FNAL test, which will feed the transversal filter modules; the trigger logic will be done in a Xilinx FPGA chip which is housed in an existing CAMAC module (PCX).

We give below a brief summary of the measurements and tests to be carried out in order to understand the most critical issues regarding the GEM calorimeter trigger. We then describe the units to be constructed and describe the tasks needed to carry out the work. Finally we discuss the manpower requirements for the effort at Pitt.

7.6.2 Test Approach

The principal studies to be carried out for the calorimeter trigger in the beam test are:

- Amplitude and timing resolution measurements for the trigger jet sums through the use of a transversal filter. As has been discussed in the TDR, the ability to associate deposited energy of 20-30 GeV in a jet sum with an individual bunch crossing, in the presence of thermal and pileup noise, can only be carried out if a real-time optimal filter [22] is used. Although the pileup noise will not be present in the beam test, the performance of this filter for thermal noise alone is calculable, and measurements of its performance can be compared with these calculations. Such an analysis for an offline optimal filter for the BNL test data is currently under way [23], with encouraging results.

- Performance of the multilevel timing discriminator, particularly for low amplitude signals near the threshold for isolation vetos. Timing tests for a single-level discriminator were carried out in the BNL tests [3], where an on-line resolution of 1.1 ns was achieved

for signals in the range of 5-20 GeV. This resolution was dominated by the effects of different delays in the signals making up the trigger sum, and after correction for such effects, a resolution of 4.1 Gev-ns/E was seen, which was very close to the value predicted from thermal noise. The resolution studies need to be continued to understand the timing performance at the extremes of (a) very low energy deposits ($\sim$1 GeV for the EM section, $\sim$5 GeV for the hadronic section) near the isolation veto thresholds and (b) very high energy deposits (simulated in special-purpose preamps), where the common-mode rejection for the comparator becomes critical and the shaped waveform changes shape due to the nonlinearity of the preamplifier; above this region, the discriminator will switch to leading-edge timing [24].

- Tests of the efficiency and rejection power of the isolation logic used to define isolated electromagnetic showers at the trigger level. In the TDR we describe EM isolation logic based on the vetoing of large EM deposits by fixed thresholds in the hadronic sections behind the tower and in the neighboring EM sections. The efficiency for the $H \rightarrow 2\gamma$ trigger is directly related to the efficiency of this logic [25], and it is therefore important that its actual performance be compared against the Monte Carlo calculations and that its efficiency be optimized.

- Timing performance of the trigger system for events where there is enough energy deposit in a single cell to cause the preamplifier to enter its nonlinear region. In order to study this problem thoroughly with the available beams, some of the preamplifiers will be made with break points in a convenient energy region. As mentioned above, one of the tests of the performance of the timing discriminator is for large amplitude signals, where leading edge timing will be used. In addition, the transversal filter will utilize a second set of coefficients, which are chosen not to minimize the noise, which is unimportant at this energy, but to minimize dependence on pulse shape, which can become important [24]. The goal of this test is to ensure that the precautions taken to identify the proper bunch crossing for signals of all amplitudes are adequate.

- Measurement of the efficiency of algorithms used to define calorimeter clusters, which are needed for the trigger count logic. Among the general "primitives" to be delivered to the global level 1 trigger unit by the calorimeter logic are the numbers of EM showers, single hadrons, and jets. The counting of calorimeter clusters, especially for close-lying particles or jets, is reasonably crude at the trigger level and can introduce important inefficiencies for certain types of triggers. This problem can be studied in a Monte Carlo, but because of the importance of fluctuations in the recognition of merged showers, it is important to also study it with real particles in a calorimeter whose geometry is close to that of the final setup. This can be an especially tricky problem in the region where two calorimeters of different geometry are joined, as in the barrel-endcap joint in GEM.

We believe that the instrumentation we are planning to build will permit detailed studies of all of the above points, which are important for the continued development of the calorimeter trigger.

7.6.3 Prototype Functional Description

The L1SUM module is the lowest level module in the calorimeter level 1 trigger system. In the final GEM system, it will contain the following elements:

1. summing amplifiers to make the complete trigger sums from the (partial) current sums formed in the calorimeter readout modules
2. variable gain shaping amplifiers
3. multilevel discriminators
4. an FPGA (which can be downloaded remotely) for performing isolation logic
5. FADC digitization for monitoring of analog waveforms
6. control circuitry with analog switching for monitoring and test functions
7. module intercommunication for transfer of isolation logic data
8. high speed optical link for transmission of trigger data (or monitoring data when in diagnostic mode) to CR

We plan to build a prototype version of this board as a part of the beam test program. However, some of its functions will be implemented in other modules, so the unit we plan to build will be only a partial prototype. The functions of items 1 and 2 will be carried out by the Variable Gain Amplifier (VGA) modules and external shaping amplifiers to be produced by BNL Instrumentation Division as a part of the front end electronics. This is very similar to the system used in the BNL test [5]. With the exception of the optical link, the remainder of the circuits will be designed at Pitt, as will the layout of the PC board. We will use a commercial firm to produce the boards, which will be then stuffed and tested at Pitt. The basic circuit for item 3 has been built and tested in the BNL test [3]. This was a single level timing discriminator, whereas the GEM unit will need 7 levels, and we therefore plan to implement a set of seven-level timing discriminators on the prototype board. The FPGA-based isolation logic will also be fully implemented. The monitoring functions, which include switching of input waveforms to the input of the digitizer and the transmission of the digitized data to a remote location for display, will also be included in this module and could be a useful diagnostic tool in the beam tests. The isolation logic, including the sending and retrieval of data to/from neighboring modules will be fully implemented on the prototype board.

We plan to build a transversal filter module of the type required for the JETSUM/Filter board in the calorimeter level 1 trigger. This circuit, whose conceptual design is completed, will have a variety of test features to help us understand the operation of a real-time fast transversal filter. These features include:

- The ability to write into on-board memory a stream of numbers which simulate the output of a flash ADC looking at one of the trigger sums, and to trigger the processor to analyze these data at the required rate. The result of the filtering operation is stored in another on-board memory for examination in the computer.

- The ability to accept and process data in real time through a front panel input, with the output data available also through the front panel connection. The unit can be externally triggered, and a select line can be used to switch between two different sets of coefficients, as will be required for signals of large amplitude.

- The ability to regenerate either the input or output data in analog form, with a built in discriminator to permit the testing of trigger functions on either real or artificial data.

The transversal filter circuit is housed in a pair (1 CAMAC, 1 NIM) of modules for the purpose of separating the digital and analog functions. We plan to build 3 units, two of which will be used in the test (one for amplitude information and the other for timing). The third unit will serve as a spare but will normally be used at Pitt for bench tests with artificial data.

For the FNAL test, it will be necessary for the transversal filter modules to be driven by a fast digitizer of the type to be built on the JETSUM/Filter board. This will be a CAMAC module and will serve as a test for the ADC to be used on the final JETSUM/Filter board. In addition, the JETSUM/Filter board will contain logic to initiate the transversal filter on 4 successive bunch crossings, using data derived from the SP discriminators. This logic will be carried out in an FPGA on the JETSUM/Filter board, and this function can be emulated in the test through the use of our CAMAC PCX board.

In order to test the use of FPGA-based logic in a real beam environment, we have built a CAMAC module containing 32 inputs and 16 outputs, where the processing of the signals is done in a Xilinx model 3090 FPGA which can be downloaded from the CAMAC backplane. The module is currently being utilized in a trigger test in BNL experiment E877. Because it is a general purpose module, it can also be used in the beam test. For the FNAL test, we can implement in this module the algorithms used to count EM clusters, and since the final Count Logic board will contain similar FPGA chips, we will be able to test the design concepts for this board. In addition, as mentioned above, the PCX can be used to develop the start logic we need for the transversal filter. We thus propose to build 6 PCX modules for the FNAL test: 4 for the prototype count logic, permitting us to handle all 36 EM and 9 SP trigger towers contained in a 3×3 matrix of L1SUM boards, 1 for the transversal filter trigger logic, and 1 spare.

7.7 Electronics Tasks Summary

Tables 7.2 and 7.3 detail the tasks with the responsible organization required for the Fermilab Test Beam effort.

7.8 Electronics Cost.

Table 7.4 contains a first approximation of the electronics costs.

Table 7.2: Electronics Tasks

Element	*Task*	*Organization*
• Silicon Microstrip Readout	Design of bipolar front end VLSI chip	LANL
	Design of CMOS-I	LANL
	Design of CMOS-2D	LANL
	Design of CMOS-2A	LANL
	MCM packaging thermal/electrical properties. Test stations concept. Cabling.	LANL
	Preliminary clock distribution design	LANL
	Preliminary slow control design	LANL
	Design review	UO
• Interpolating pad chamber readout	Prototype readout controller IC	IU
	Readout controller PWB design	IU
	IPC control/data sets design	IU
	IPC MCM design	IU
	Update SCA design and fabricate	ORNL
	Design of bipolar front end preamp/shaper IC	ORNL
• Calorimeter	Design preamplifier	BNL
	Design monolithic P-channel circuit for calibration	BNL
	Design module	BNL
	Develop cable driver ASIC	SSCL
	Design shaper amplifier	NL
	Design SCA	NL
	Design R/O board for Fermilab test	NL
• Calorimeter Trigger	Design of transversal filter	PbU
	Design L1 sum board	PbU
• Muon Electronics	Circuit design and test 0f CMOS pre-amp/shaper IC	BNL
	Design integrated SCA (ASIC#2) chip and support circuitry	PU
	Design ALP IC	PU
	Design & fabricate cathode readout PCB	CU
	Design anode interface (PCB1)	BU
	Adopt cathode readout PWB for testbeam	BU
	Design CSC readout motherboard	HU
• Data Acquisition System	Document overall system design	SSCL
	Design fiber optic interface for testbeam	SSCL
	Design switch for testbeam event builder	SSCL
	Design event data collection module	UCSD
• System integration	Investigate transformer operation in magnetic field	SSCL
	Investigate commercial fiber optical link	SSCL
	Facility interface	SSCL
	Project management	SSCL

Table 7.3: Abbreviations used in the list of electronics tasks.

Abbr.	*Organization*
BNL	Brookhaven National Lab
BU	Boston University
CU	Colorado University
IU	Indiana University
HU	Houston University
LANL	Los Alamos National Lab
NL	Nevis Laboratory
ORNL	Oak Ridge National Lab
PbU	PittsBurgh University
PU	Princeton University
UO	University of Oregon
UCSD	University of California, San Diego

Table 7.4: Electronics Budget

Item	*FY'94* [*k*$]	*FY'95* [*k*$]	*FY'96* [*k*$]	*Total* [*k*$]
Silicon Tracker	965	1190	660	2815
IPC Tracker	759	1398	559	2716
Calorimeter	1120	1120	420	2660
Muon	825	725	600	2150
CAL Trigger	200	300	200	700
Muon Trigger	0	0	0	0
DAQ	560	560	500	1620
Integration/Management	300	300	300	900
Total	4729	5593	3239	13561

Chapter 8

Computing and Controls

A detailed description of the computing subsystems can be found in the GEM TDR [1]. The goal of the computing subsystem for the FNAL test beam program is to provide an integrated framework, both hardware and software, that is on an evolutionary path to the final GEM system. This is being carried out in cooperation with the test beam group, the subsystem groups, the SSC PR Computing department and the SSC PR Electronics/DAQ department.

The specific items to be worked on are:

- The Global Control System for the test beam: control and monitoring for the detector subsystems, control of transporters and manipulators, DAQ and online computing control, monitoring, alarm reporting and logging of equipment status.
- Online processes, to include the "Level 2/3" trigger. In the test beam case, the Level 2/3 trigger will likely be limited to event formatting and directing events to the correct output stream.
- Event storage for all events, in a storage system accessible to all GEM institutions.
- Databases for the test beam activity (configuration, calibration, production, etc.).
- Analysis tools for both the on-line and off-line software environment so that the data from the various subsystems can be reconstructed, the results plotted and manipulated interactively, and events displayed.
- Detailed simulations to determine if the detectors are performing correctly. The test beam must serve to validate these simulations, as they will provide the link between the test beam configuration and that of the complete GEM detector.
- Software and computer hardware standards.

All members of the GEM Computing group are committed to participate in this R&D program. The GEM Computing group at the present time consists of 13 institutions and 30 scientists, as listed in table 8.1. It is expected that others from the collaboration will join this effort, both those who will support their detector subsystems as well as others

Table 8.1: Computing Subsystem Membership

1. University of Arizona: M. Shupe
2. Brookhaven National Laboratory: S. McCorkle, H. Takai
3. California Institute of Technology: H. Newman, R. Mount
4. University of California, San Diego: J. Branson
5. University of Science and Technology of China (USTC), Hefei, China: Y.Z. Zhou
6. Lawrence Livermore National Laboratory: T. Wenaus
7. Louisiana State University: R. McNeil
8. University of Michigan: S. McKee
9. University of Rochester: J. Dunlea, C. Lirakis
10. Southern Methodist University: T. Skwarnicki
11. Stanford Linear Accelerator Center: T. Johnson
12. Superconducting Super Collider Laboratory: M. Bowden, L. Cormell, P. Dingus, Y. Fisyak, V. Glebov, J. Hilgart, K.W. McFarlane, A. Morelos, P. Padley, L.A. Roberts, I. Sheer, J. Thomas, H. Uijterwaal, J. Womersley, G. Word
13. University of Washington: T. Burnett

to assist with general computing and analysis tasks. Note that it is expected that some members of the computing subsystem may also be full-fledged members of another subsystem. The management of the Computing Subsystem and the technical design is performed by the Computing Subsystem Steering Committee which consists of K. McFarlane (chairman), J. Branson, T. Burnett, L. Cormell, J. Dunlea, J. Hilgart (secretary and PRCD liaison), T. Johnson, R. Mount, H. Newman, L. Roberts, I. Sheer, T. Wenaus, J. Womersley, G. Word, and S. Youssef (external advisor). The subsystem representatives in this program are summarized in table 8.2.

8.1 Fermilab Test Beam Plan

8.1.1 Global Control System

The Global Control System (GCS) for the GEM FNAL Test Beam effort provides "slow control" and monitoring for the detector subsystems, including data acquisition and online computing subsystems, a common human interface, and interfaces to external systems

Table 8.2: Subsystem Representatives

Subsystem / Task	Tracker	Calorimeter	Muon	Elec/DAQ	Computing
Coordinator	S.McKee	J.Womersley	R.McNeil	J.Dorenbosch	G.Word*
Controls	??	??	V.Glebov	J.Dorenbosch	H.Uijterwaal
Online	??	??	V.Glebov	P.Dingus	P.Padley
Databases	??	??	S.Kartik	??	J.Hilgart
Analysis	J.Thomas	??	T.Wenaus	J.Branson	G.Word
Simulation	S.McKee	J.Womersley	R.McNeil	M.Bowden	Y.Fisyak

* Overall Coordinator

(beamline, accelerator, etc.). The GCS Test Beam effort, besides its necessity for carrying out the Test Beam program, also is part of the R&D for the final GEM GCS. This R&D includes the gaining of experience in the required control and monitoring functions, and human interfaces, and the implementation of prototypes.

The scope of the GCS includes all hardware and software from user interfaces up to and including hardware modules for control and monitoring residing in the VME and industrial I/O crates that interface to actual sensors, motors and actuators. The actual sensors and actuators, including cabling to the modules in crates, are considered the responsibility of the specific subsystems.

GCS FNAL Test Beam activities are part of the R&D program for the GEM Global Control System. This effort provides an environment for testing and prototyping components of the planned GEM system. Specific goals include gaining experience in implementing and integrating a moderately large experimental control system, gaining experience and testing concepts in controling and monitoring of software systems (online run control and monitoring), and prototyping and testing ideas for a common user interface.

In addition to R&D goals, a "slow controls" and monitoring capability is required for Test Beam activities.

The major tasks that will be carried out by the GCS for each subsystem are:

1. **Central tracker.** Controls and position monitoring are required for the central tracker transporter. Controls and monitoring are required for the cooling, high voltage, alignment, and readout electronics for the silicon tracker. Controls and monitoring are required for the cooling, gas, high voltage, alignment, and readout electronics for the IPC tracker.

2. **Calorimeters.** There are two major calorimeter subsystems: the noble liquid electromagnetic and hadronic calorimeters, and the scintillator calorimeter. Both will reside on the same large transporter. Controls and position monitoring are required for the transporter. Controls and monitoring are required for high voltage and readout electronics for the scintillator calorimeter. Controls and monitoring are required for

temperature, pressure, liquid level, heaters, and readout electronics for the noble liquid calorimeters. A cryogenic controls system will also be required.

3. **Muon chambers.** There will be two muon systems: a small scale prototype that will be operated in a magnet, and a large scale system (full size chambers) with a prototype final alignment system. In each case controls and position monitoring are required for the transporters, and controls and monitoring for the cooling, gas system, high voltage, alignment system, and readout electronics. The chamber alignment system will require a significant development effort.

4. **Electronics crates.** Monitoring will be required for voltages, temperatures, humidity, water and airflow in the electronics crates and racks for detector associated electronics.

5. **DAQ and online computing.** Control and monitoring of DAQ and online computing. Some level of controls and monitoring are required for data acquisition hardware and software, including software downloading, system configuration, and status reporting. In addition to the online processing, this subsystem includes the archival file system and links to remote sites. Control and monitoring requirements for online computing hardware and software, including software initialization, system configuration, run control, and status reporting.

6. **MWEST Beamline and other relevant electronics.** In addition to controlling and monitoring beamline magnets, control and monitoring will be required for various beamline diagnostic and other instrumentation, including a beam-tagging Čerenkov counter, and a beam-tagging synchroton radiation detector, and beam position monitors. Most existing beamline control and monitoring functions are implemented with the FNAL EPICURE system. It will be desirable to implement a minimal interface between EPICURE and GCS to support at least the archival of some monitoring data via GCS.

7. **Safety and environmental systems.** It is assumed that there is a pre-existing environmental monitoring and safety system in MWEST at FNAL. It is desirable to implement a minimal interface to GCS to support archiving enviornmental and safety system data via GCS, and GCS alarm reporting. In addition there will be some interfaces required from GEM Test Beam subsystems to MWEST safety systems, and vice-versa. More detailed specifications must be developed.

8. **Configuration management** The complex and flexible running environment required for GEM FNAL Test Beam activities requires global configuration management capabilities that can easily and safely deal with various levels of subdetector integration, from completely independent subdetector operation to a fully integrated GEM "sector." These capabilities include configuring and synchronizing detector subsystem readout, online data processing and archiving, integration of detector subsystem control and monitoring (alarms for example) including safety systems, and archiving changes in the configuration. The Test Beam effort will provide a realistic environment for gaining experience in and testing prototype solutions for detector configuration and integration.

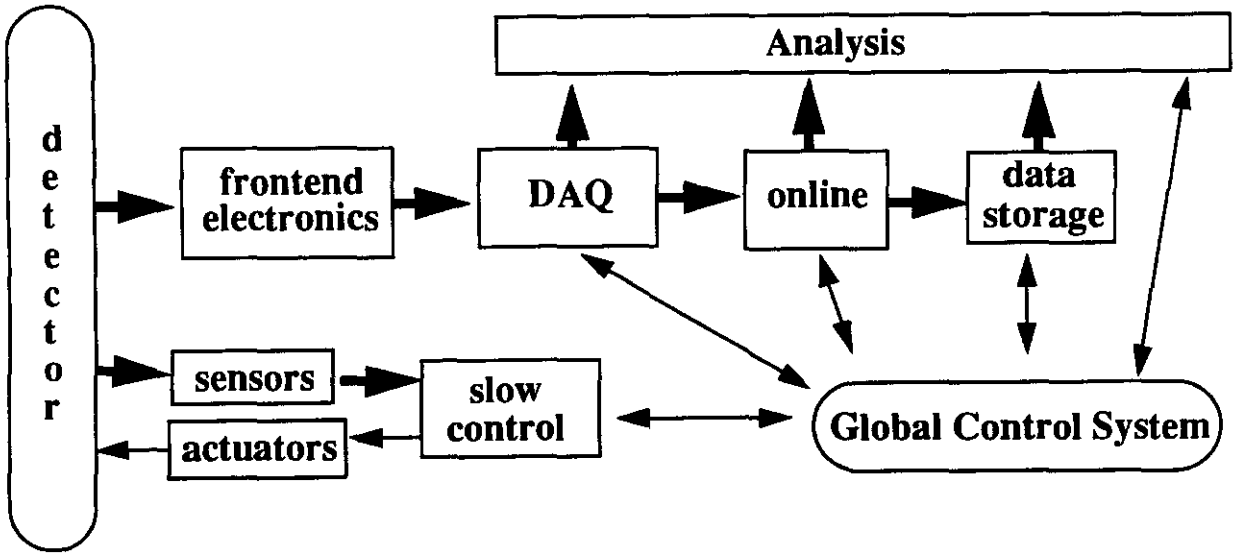

Figure 8.1: Layout of the Global Control System.

9. **Common user interface** It is a goal for the GEM detector and for the Test Beam activities to provide a common and uniform user interface for all human interactions. While resources and schedules may not permit achieving this goal completely for the Test Beam activities, the Test Beam environment will be useful for prototyping and gaining experiences with user interfaces and interface building tools. One goal of the Test Beam work should be a prototype common user interface.

Functionally the GCS for the FNAL Test Beam matches the functionality of the GEM GCS (see chapter 8 of the GEM TDR), with the exception of the GEM Magnet Subsystem, and different interfaces to external systems. Figure 8.1 gives a overview of the GCS connections with other subsystems. The GCS will control and monitor detector subsystems, DAQ and on-line computing, data storage and on-line analysis.

The Global Control System architecture is shown in Figure 8.2. It is supposed that each detector subsystem (Central Tracker, Calorimeter and Muon) will have its own sensors and actuators but all subsystems will be furnished with VME crate (EPICS crate) and GCS work station. Each detector subsystem will have its own (but presumably standard) hardware like electronics crates, High Voltage and Low Voltage power supply but each control subsystem will be supported by the same GCS software. The possibility of using commercial industrial control system is considered now for the calorimeter cryogenics subsystem. Such system can have its own work station or can be integrated into calorimeter GCS work station.

In the initial phase of the FNAL Beam Test program the detector subsystems will work in independent mode and will be controlled from a dedicated GCS work stations. In the final phase of the FNAL Beam Test program the detector subsystems will work in integrated mode and will be controlled from one GCS work station.

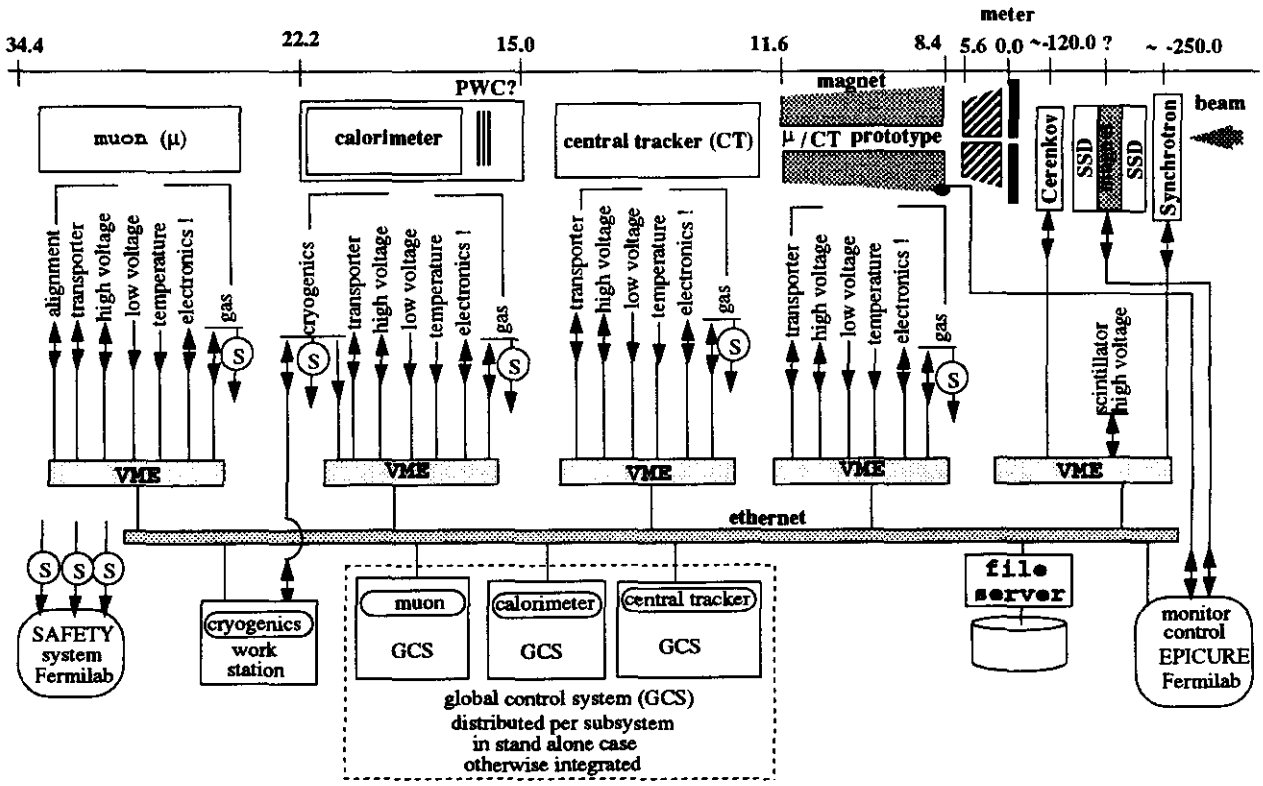

Figure 8.2: Architecture of the Global Control System.

8.1.2 Online

The data volume is dominated by the 18° sector readout channel count. The trigger rate for the 18° integrated mode is limited by the DAQ system to $\approx$ 1000 Hz. A safe 100 Hz trigger rate with no data filtering is chosen to estimate data sizes and rates.

The integrated baseline design of the data acquisition with front end crates for each subsystem transporting the data through DS links at 100 Mb/sec ($\approx$ 10 MB/sec) sets a limit on the trigger beam rate to $\approx$ 1000 Hz. The calorimeter data size centralized in a single VME crate put the strongest restriction on the trigger beam rate. Currently we are working on a safe trigger beam rate of 100 Hz without data filtering. The expected beam intensity is on the order of $10^{3,4}$ particles per second. Special studies to read the entire GEM sector at very high beam rate may be performed with distributed links between EDC's, the switch, and data filtering.

The data rates into the event builder are shown in tables 8.3, 8.4, and 8.5.

Table 8.3 shows the 18° sector rates which dominate all data sample. The number of channels read out is 5 % of the total instrumented CT and 10 % of the instrumented muon. The electromagnetic calorimeter will have the electronics for 432 channels. It is expected to disconnect and connect cables to survey the whole calorimeter sector, including the hadronic barrel.

Table 8.4 shows the rates from the quartz fiber forward calorimeter, small muon chambers,

Table 8.3: 18° Sector: channels and rates.

setup	optical fiber	channels	bits per channel	channels or samples readout	bytes readout	bandwidth to event builder @ 100 Hz (MB/sec)
μ	7	7500	16	750	1500	0.15
CT-si	60	76800	16	3840	7680	0.77
CT-ipc	250	34000	16	1700	3400	0.34
barrel em		3024	16	4320	8640	0.86
barrel h		134	16	134	268	0.03
barrel s		100	16	100	200	0.02
total	317	121424		10710	21420	2.17

Table 8.4: Prototypes: channels and rates.

setup	optical fiber	channels	bits per channel	bytes readout	bandwidth to event builder @ 100 Hz (KB/sec)
Quartz f c	*	100	16	200	20
μ	1	360	16	720	72
CT-IPC	1	144	16	288	29

* Only counting optical fibers which connect to EDC's.

and CT prototypes. The muon and CT prototypes will be in a magnetic field. All the instrumented channels will be read out.

Table 8.5 shows the expected rates from the beam track and beam ID devices.

The electromagnetic calorimeter will stage the electronics front end readout. There will be three stages, track and hold, sample 5 times with ZEUS pipeline and finally electronics that samples the signal 10 times. The final electronics resemble the GEM design. Table 8.6 shows the rates in each case. The highest rate is the DAQ design goal.

Table 8.7 shows the expected data sizes and rates for the GEM test beam at Fermilab. It is assumed that the entire 18° sector is taking data at once. The sector dominates the data volume.

In summary, the expected event size will be on the order of 21 kilobytes, with an anticipated event rate on the order of 100 events/second during a 20 second spill of particles from the FNAL particle beam. Thus the data rate over a spill is 21 kB/event * 100 event/second = 2.1 MB/s (20 second spill average). Additional information from slow control records will

Table 8.5: Beam Track/ID Devices: channels and rates.

setup	channels	bits per channel	bytes readout	bandwidth to event builder @ 100 Hz (KB/sec)
Čerenkov	24	16	24	4.8
Synchrotron	2	16	2	0.2
SSD beam				$\geq$ 10.0
PWC calo				$\leq$ 10.0

Table 8.6: Barrel Electromagnetic Calorimeter Stages: channels and rates.

stage	channels	bits per channel	channels or samples readout (432) instrumented	bytes readout	bandwidth to event builder @ 100 Hz (KB/sec)
a.track/hold	3024	16	432	864	86
b.zeus	3024	16	2160	4320	432
c.GEM	3024	16	4320	8640	864

be recorded along with the data, but this occupies a negligible amount of space.

Each 20 second spill is separated by 40 seconds of time during which a new spill is being prepared and no events are taken. (While some calibration data may be taken during these 40 seconds, the calibration data is assumed to be small compared to the beam-generated data.) Averaged over a minute, the data rate is 2.1 MB/s * 20s/60s = 0.7 MB/s.

During the course of roughly 24 hours of data taking, the detector will be moved to various locations, Allowing for 20% of the time over the course of an hour to be devoted to moving the detectors, the average data rate per hour is expected to be 0.7 MB/s * (1 - 20%) = 0.6 MB/s (hourly average).

The data transfer rates from the DAQ to permanent storage should be sufficient to keep from losing beam data. This implies a data transfer rate somewhat greater than the hourly-averaged rate of 0.6 MB/s. As a rough estimate, add 30% to the average rate, yielding an hourly-average data transfer rate of roughly 0.7 MB/s.

In view of the proposed architectural solution for data storage, it is planned to likewise off-load the computationally intensive tasks to the SSCL. Using an FNAL estimate of 1000 instructions/byte of I/O for event reconstruction, and the requirement to keep up with the hourly-averaged data rate of 0.6 MB/sec, we have the need for 600 MIPS of computing

Table 8.7: Sizes and Rates.

1	min	spill cycle
20	sec	active beam during spill
100	Hz	beam trigger rate inside the 20 sec active spill
80	%	run stop/start and calibration efficiency averaged over 8 hour period
30	%	nominal accelerator efficiency averaged over a week
2000		events collected during the 1 min cycle
2.52	10^8	events collected in one year, 30 and 80 % efficiency
100	Hz	output level 1 trigger rate (can go as high as 100 kHz)
100	Hz	output level 2 trigger (not defined, yet)
100	Hz	output level 3 trigger (Level 3 sets the data volume and rates for mass-storage)
21.4	kB	daq event size
2.14	MB/sec	data rate during active spill to master crate
0.71	MB/sec	data rate diluted during the 1 min cycle
33	Hz	event rate diluted during the 1 min cycle
1		event filter factor (> 1 if more than 100Hz)
1000	SSCUP	reconstruction (RECO) computational load
2	kB/spill	additional spill data, from slow control and monitor
0.71	MB/sec	daq+slow data rate during the 1 min cycle
16.45	GB	data from daq+slow in 8 hour period, with 80 % efficiency
0.002	GB	data from 2 all channel calibration runs performed in 8 hour period
3.29	GB	data enrichment from RECO and analysis, averaged in 8 hour period (estimated at 20 % of daq+RECO+slow)
0.69	MB/sec	storage data rate during an 8 hour period
0.21	MB/sec	storage data rate during a week period, 30 % efficiency
6.49	TB	annual data storage
5000	SSCUP	simulation computational load
0.2	TB	annual simulation storage
6.69	TB	annual total storage

power. It is reasonable to demand 50% above this amount for analysis and other offline purposes, for a total of about 1000 MIPS. This compute power needs to be available as a dedicated resource at the SSCL.

The remaining computing needs at FNAL, which will include file-serving, monitoring, and calibration, will be satisfied by one high-end file-server, able to sustain at least 3 MB/sec of file I/O, and roughly four workstations of the 50 MIPS variety. The file server should also

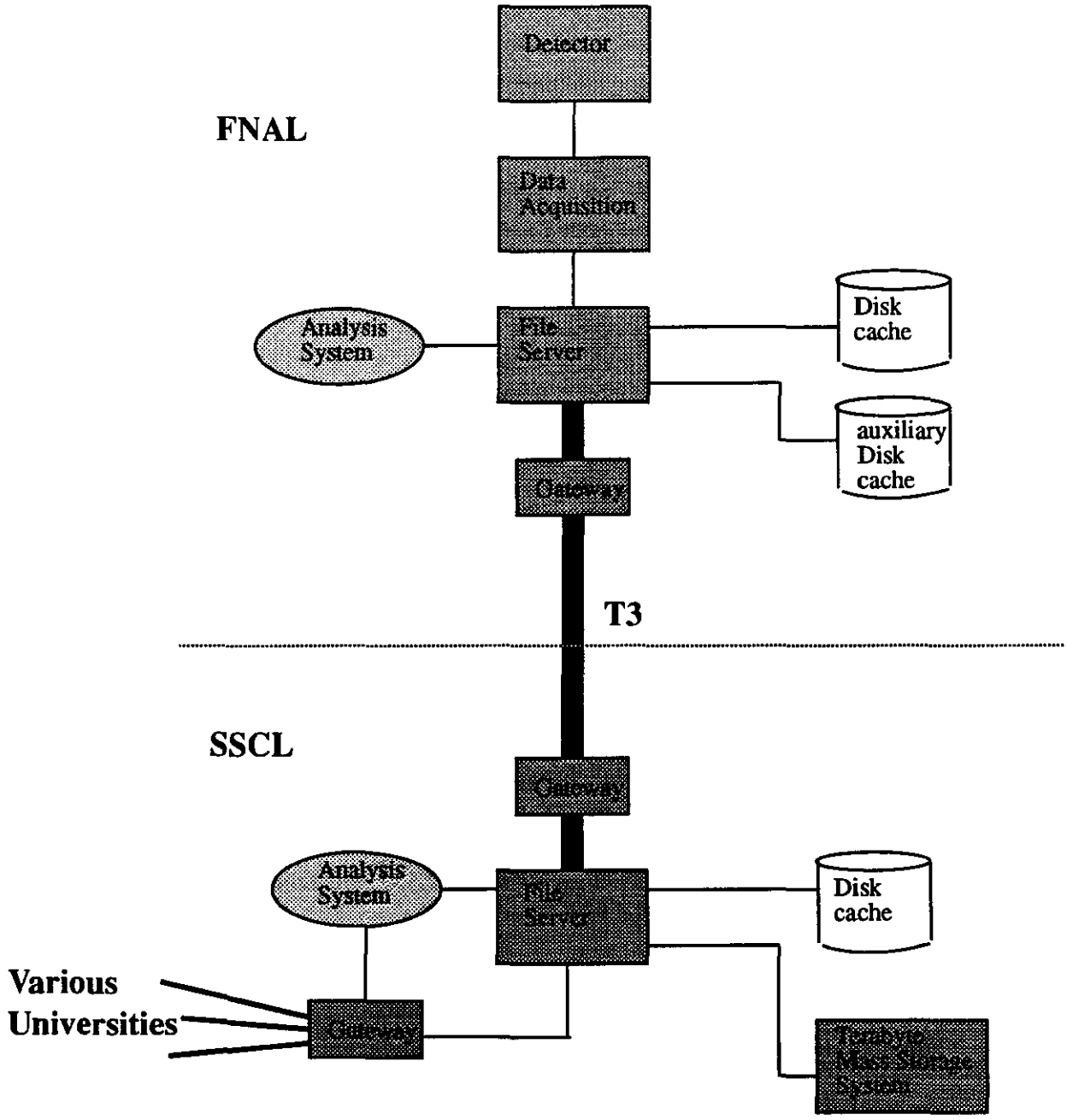

Figure 8.3: Online and data storage system for the GEM testbeam.

support about three workstations for offline analysis (described later).

A system architecture of the proposed online and data storage solution for the test beam is shown in Figure 8.3. The salient feature is the use of a high-bandwidth network (T3 has bi-directional 45 Mbits/sec bandwidth) to off-load the data from FNAL to a permanent store at the SSCL. Functionally, then, the online tasks will extend into the SSCL.

8.1.3 Data Storage

Presented here are the requirements which are used to determine the computing architecture that will be used for data storage. The information for reconstructed and simulated data size is currently a rough estimate.

1. Total Long Term Capacity

   According to the previous section, the expected yearly collection of data is on the order of 7 TB in size. An acceptable scenario might be to have on the order of 2 TB of storage available and tested by turn-on with about 0.5 TB of capacity added on average each month.

2. Accessibility of Long Term Data at SSCL

   It is desirable that all data be accessible at all times without human intervention. It is expected that large quantities of data will be available at the SSCL in a fast-cache with disk-like access times. A detailed study of the requirements of analysis and reconstruction will be performed to determine the amount of data which needs to be available on the fast-cache. One day's worth of data (48 GB) should be considered an absolute minimum, with on the order of 4 days (0.2 TB) being desirable.

3. Raw-Data Disk Cache at FNAL

   The size of the disk cache at FNAL that is required for data taking should be large enough to handle any reasonably expected non-scheduled outages of the remote mass storage system or links to it. An estimate of the raw-data disk cache may be made by requesting about a days worth of data, (48 GB).

4. Accessibility of Long Term Data at FNAL

   It is expected that all data that is taken at FNAL will always be visible at FNAL, even after the data has migrated to SSCL. Visibility at FNAL means that the data file will appear to still be on disk by the use of simple commands such as "`ls`," and that file sizes and time stamps will be available, so that the information that is returned by, *e.g.*, the "`ls -l`" command will always be available. Some distributed file system, such as AFS, might satisfy this requirement if the speed of cacheng can be demonstrated to be sufficient.

5. Auxiliary Disk Cache at FNAL

   To reduce the amount of data that must be transferred from Fermilab to SSCL, the processes, such as reconstruction and analysis, which tend to increase the amount of data, should be run on computers at the SSCL. Therefore, only a small additional disk cache is required at Fermilab for purposes such as calibration, small data subsets, etc. This should be about an additional 10 GB. These disks will serve as additional online data cache backup, should the need arise.

6. Additional Copies of Data

It is expected that the SSCL will be the sole central repository of the raw data. Data samples which are to be transferred outside of SSCL are expected to be created by those who want the data.

Note that it is anticipated, however, that one complete copy of the data will be made and stored in a different building, such as SSCL Central Facilities, for backup and disaster-recovery purposes.

7. Longevity of the Data

   GEM expects to refer to its test beam data for the life of the experiment, which means on the order of 15 years after it is first recorded.

In view of the quantity of data involved, and its expected longevity, it is foreseen to have the data repository's mass storage system at the SSCL rather than at FNAL. This will provide considerable labor savings by enlisting the technical help already employed at the SSCL. Moreover, the expected operation of a T3 link to FNAL will provide more than adequate bandwidth to the SSCL.

In view of the large amount of data and limited manpower available, a mass storage system with robotics for tape retrieval will be selected. Data caching will be implemented by a hierarchical storage system which will transparently migrate large, unused files to a slow-cache (tape), and keep heavily used files available via the fast-cache (disk). The SSCL's PRCD (Physics Research computing Department) will provide and implement the following components of this system: the mass store system, disk cache at SSCL, T3 link and gateways, and the hierarchical storage system. Vendors are currently being contacted.

In summary, the first year of GEM Test Beam at FNAL data will be collected at a rate of about 0.7 MB/s onto about 48 GB of disk cache (a day's worth), transparently transferred over a network with at least 0.7 MB/s dedicated throughput capacity to about 0.2 TB of disk cache at SSCL where it will be transferred again into tertiary storage with an initial capacity of about 2 TB, growing at the rate of about 0.5 TB each month, for a end-run capacity of 7 TB. The data will mainly be analyzed on CPUs at the SSCL. An additional 10 GB of disk space is required at FNAL for miscellaneous functions and as auxiliary caching space.

8.1.4 Reconstruction, Analysis and Simulation

The offline software environment for the test beam activity must enable rapid and convenient reconstruction, analysis and comparison with simulations for the data from the various detector systems. Fast feedback must be obtained to guide the run plan and to verify the functioning of the detector elements.

Reconstruction code will be used to digest the raw data from the particle's traversal of (or interaction within) the detector, and to create data entities to record the results. Analysis code allows manipulation, histogramming and refinement of these reconstructed entities.

The reconstruction and analysis operations are relatively simple by modern high energy physics standards. The number of channels is limited, generally only one particle interacts in

the apparatus, and the quantities to be derived are well defined and often known in advance (for example, particle energy is roughly known from the beam setting).

One of the important analysis tools, particularly in the early stages of data taking, will be an event display program. This will permit a rapid check of the quality of data and aid debugging of the reconstruction algorithms by pictorial representation of the raw data and the corresponding reconstructed entities.

At least one workstation per subsystem should be available at MWEST for the reconstruction and analysis of recently taken data. Network and CPU throughput should be sufficient to allow fast analysis of data files from the Fermilab disk cache. A reasonable goal is that it should not take much longer to process a datafile than it did to record it. At the hourly average rate of 0.6 MB/s assumed above, this would means individual data runs of 10^5 events ought to be processable in under an hour. This is adequate to permit the user to experiment with cuts and techniques with reasonable, though not outstanding, feedback. Once data has migrated to the longer term storage at SSCL, it is presumably of less immediate interest, and the turnaround time could be relaxed by a factor of two or so. An analysis of a series of such runs (for global fitting of parameters, for example) should still be able to be run in 24 hours.

The reconstruction and analysis computing system architecture that should be able to fulfill these requirements is one comprised of computing hardware both at Fermilab and at SSCL. The computing system at Fermilab will consist of three unix workstations of approximately 50 MIPS CPU each. The workstations will be connected to the fileserver machine in the same way as the global control system workstations and online processors. It is desirable, however, to locate them in a different room from the data-taking activity, if feasible.

The bulk of the reconstruction, analysis and simulation will be carried out using existing resources at SSCL (the PDSF system, GEM workgroup cluster) and at other collaborating institutions within GEM. The test beam-related processing will be a major consumer of GEM CPU time on PDSF. Roughly 5000 MIPS are expected to be available for GEM use on PDSF.

8.1.5 Computing Standards

Standards are being set for both the software and computing hardware components that will be used in the test beam run. Many of the standards have already been chosen. Some will require more evaluation to determine the most feasible option for the test beam run.

The hardware standards are driven by the need to limit the kinds of hardware that will be in use at MWest for which support will be required. The hardware standards for equipment at MWest will include standards for computing architectures; networking hardware; and tape drives and media.

1. Operating Systems

   The operating system for the GEM computers used in the test beam analysis farm will be a variant of UNIX, in compliance with TDR sections 8.6.3 and 8.7.1.

2. Graphical User Interface (GUI) Tools and Builders

   The Graphical User Interface will be based on X-windows. (For reference, see TDR section 8.7.1 item 2.)

3. File Systems

   All of the GEM Test Beam computers at FNAL will support NFS. In addition, most, if not all, will support a distributed file system, such as AFS, either directly or through an NFS translator. It is expected that the primary means by which the GEM computers at FNAL will implement the SSCL computing environment is by use of this distributed file system. In particular, the SSCL application server is expected to be visible to all GEM workstations at FNAL by means of the distributed file system. (For reference, see TDR section 8.7.1 item 3.)

4. Software Languages and Compilers

   The traditional software languages are restricted to be C, C++, and Fortran77 with the extensions for structures as realized by the native compilers on the PDSF computers. The dominant languages that will be used for the DAQ system are expected to be ANSI C or C++. The online system is expected to be written in ANSI C and/or C++. The analysis system will probably be written in some mixture of the three. (For reference, see TDR section 8.7.1 item 4.)

   The C and C++ compilers that will be used are gcc and g++, from GNU, as found in the "`/gem`" tree. The Fortran77 compilers that will be used are the native compilers as found on the SSCL application server.

5. Network Protocols

   The network protocol TCP/IP will be supported. (For reference, see TDR section 8.7.1 item 5.)

6. Code Management Tools

   The code management system will be CVS and will follow a practice of explicit releases. (For reference, see TDR section 8.7.1 item 6.)

7. Data Model and Data Definition Language (DDL)

   A standard data model will be defined for use by all of the GEM Test Beam computing tasks. One of the Data Definition Language that is under consideration is the chgen language, which is a part of the cheetah data management system.[32] (For reference, see TDR section 8.7.1 item 7.)

8. Programming Style Guide

   A programming style guide will be written and followed for all critical GEM Test Beam code. An object-oriented style will be adopted for all three languages. (For reference, see TDR section 8.7.1 item 8.)

9. InterProcess Communications (IPC) Tools

   Interprocess communication may be performed by several mechanisms. The preferred mechanism is the use of RPC messages. (For reference, see TDR section 8.8.3.)

10. Remote Procedure Calls (RPC) Tools

    The standard method of making Remote Procedure Calls (RPC's) will be by use of Sun's RPC library. Heavy use of Sun's rpcgen utility will be made. (For reference, see TDR section 8.8.3.)

11. Interface Definition Languages (IDL)

    The Interface Definition Languages (IDL), as it were, will be realized not so much by a formal IDL, as is used in commercial products, but through c-header files (Fortran-include files) which will give the prototypes (declare the Fortran functions) for the functions that are associated with a particular data structure. For those packages which provide RPC services, the package should also have an rpcgen-style file to define the remote services that are provided. (For reference, see TDR section 8.8.3.)

12. Data Management Tools

    There should be one main data management tool, which will be used for the i/o of all event data in all stages beyond the online system stage. One of the possible options for this tool is the cheetah system.[32] Where feasible, the same data management tool should be used in the DAQ system as well. If non-event data is kept in non-standard databases, then the appropriate interfaces will be written between such databases and the standard tool to permit ease of access to non-event data. Indirect access to the data will be possible from all supported languages. If feasible, direct access to the data may be possible from Fortran77 using the structures extensions realized in the supported Fortran compilers. (For reference, see TDR section 8.8.3.)

8.2 R&D Plan

This section describes the R&D plan for the GEM Computing subsystem for FY1994-FY1996, including the test beam work. It covers controls, on-line computing, off-line computing, and storage. The main goal is to make steady progress towards a production system through an incremental process of prototyping, and using, elements expected to be part of the final system. The test beam effort is an integral part of this process. Controls and online computing are part of the GEM detector WBS, while the off-line computing budget is the responsibility of the PRCD. Some of the off-line work will be done in cooperation with with SDC and PRCD, and we can benefit from exploiting commonalities between off-line and on-line software. In the GEM model, all storage is regarded as an off-line responsibility. For physics-related tasks, much will depend on the support of collaboration members.

8.2.1 Global Control System

The Global Control System that will be used at the Fermilab test beam is expected to be a prototype of the production system. The main compenents that are expected to be reused are the interface protocols between the GCS and the assorted other systems it controls.

8.2.2 On-line

The main project here is to develop a system for the FNAL test beam that is a small-scale model of the production system. This will require the development of hardware and software interfaces, to the DAQ on one side and to off-line or storage on the other. Methods of monitoring the activity of the system will be developed, as well as ways of giving real-time feedback of on-line analysis of data. The on-line analysis system is expected to share features and code with the software framework developed by PRCD (see below). Test systems consisting of one or more workstations will be built, transferring data from VME to disk arrays, and managing the relevant databases. Tools to monitor the activity of the on-line will be developed, as will methods of accessing the data flow to provide real-time feedback.

8.2.3 Data Storage

Appropriate databases are now crucial to HEP and our system model defines configuration, calibration, monitor and production databases as well as the electronic log book. Support from PRCD is requested for:

- evaluation and prototyping of database approaches for these databases,
- support for a geometry database (an example of a configuration database) in the short term for simulation support,
- databases for test beam support,
- R&D on approaches for the event data, both file-based and database, and
- R&D on multimedia approaches such as WWW (World Wide Web), including an electronic logbook.

Computing R&D will also be carried out within the GEM project to develop the databases needed for controls and on-line work: configuration, calibration, monitor, log book, and production. The storage system will be worked on jointly with PRCD.

8.2.4 Reconstruction, Analysis and Simulation

By the end of 1994, a first pass reconstruction code must be available. Each of the subsystems will provide the code to interpret the detector digitizations and perform pattern recognition and fits. The detector subsystems together with the Global Physics Group will develop the code which integrates the subsystems and derives physics hypotheses. The reconstruction

for the test beam will make use of the same code as in the full GEM reconstruction, plus additional code required by the test beam setup (such as beam momentum counters and synchrotron radiation detector).

The reconstruction code will run as an optional on-line process. It will accept raw data from the data acquisition system and processes it to produce abstract entities such as tracks and clusters.

Subdetector reconstruction code must perform the following tasks:

- pattern recognition and track finding (position and momentum fit) in central tracker,
- pattern recognition and track finding (position and momentum fit) in muon system,
- cluster finding, and energy, position and angle determination in the calorimeter.
- local and global alignment of the detector based on the reconstruction of the charged tracks, and
- beam particle tagging and momentum reconstruction using the Čerenkov, synchrotron radiation and silicon strip detectors.

Cross-detector reconstruction algorithms must then be developed to relate these entities for the integrated sector test, and reconstruct "physics" objects such as:

- muon identification on basis of central tracker track, calorimeter energy deposition and muon track, and
- electron identification on basis of central tracker track and isolated EM calorimeter shower.

The main simulation R&D task is to have simulated data available for all major running modes of all the subdetectors before the start of data taking. This is essential because the Monte Carlo forms a link between the test beam configuration and that of the final detector. The test beam, while intended to broadly reflect the arrangement of an 18° sector of GEM, differs in many details. As an example, the calorimeter in the test beam will be filled either all with argon or all with krypton; that in GEM will use krypton in the barrel and argon in the endcap. Consequently Monte Carlo simulations must be benchmarked and verified by their ability to reproduce the test beam data and then will be used to extrapolate to the expected performance of the full detector. Deviations between the test beam and Monte Carlo, whether because of detector or simulation problems, must be addressed as soon as possible and resolved within the running period because the Fermilab beam schedule will prevent us from running again for several years. In this respect we are attempting to learn from experience with the D0 test beam where such discrepancies between data and simulation were found only after data-taking had ended.

Because of this crucial role played by the Monte Carlo, it is important to understand the 'state of the art' in hadronic shower simulations and to know how much reliance can be placed upon them. Effort must therefore go into understanding the verification steps

undertaken by other experiments and by code developers, and the strengths and weaknesses of the various packages.

To generate several thousand simulated events for each class of running (electrons, pions and muons at various incident angles in tracker, calorimeter and muon detector) will realistically take several months, including some debugging time. A working simulation program should therefore be ready six months before the start of test beam data taking. Smaller numbers of simulated events should be available earlier than this to allow the development of reconstruction algorithms.

Studies will need to be performed using Monte Carlo events to explore how the data collected at the test beam will actually be used for calibration purposes. This will determine the run plan: how many events will be needed for each of the various studies, and at which energies, angles and with which particles these data should be taken.

Prototypes of the simulation and reconstruction code exist, in the form of a number of generally stand-alone programs which simulate the subdetectors of the full GEM detector. These prototypes take the form of programs developed to study detector design and physics performance issues (in most cases for the GEM TDR). However, they do not form a single system able to exchange data, nor do they share descriptions of the detector, nor do they describe the test beam setup. The simulation packages developed so far include a full GEANT description of GEM, SIGEM [35], and various detailed subdetector GEANT simulations of the EM calorimeters and the central tracker. Reconstruction and track-fitting code has been developed to process the output of these simulations and perform track finding and fitting, vertex reconstruction, calorimeter position, energy and angle reconstruction, and particle identification. The results of these reconstruction packages are described in the GEM TDR.

We have embarked on a program to unify and develop the disparate simulation codes into a flexible yet unified GEM simulation program. The basis of this program is the creation of the unified description of geometry and detector constants — a data base (GEOMDB). This will support both the test beam geometry and the full GEM geometry and will generate events with a standard output data format so that unified reconstruction code may be developed, applicable to both the test beam and the full detector. The following projects make up this R&D effort:

1. Geometry Builder Tool

   Work has begun, in collaboration with members of SDC, to design a flexible and interactive tool for the creation of detector geometry descriptions for simulation packages such as GEANT. Obviously this tool has application beyond GEM and indeed beyond the SSC. The tool will address the many requests from GEANT users for a GUI-based, interactive, graphical editing capability. The user will be able to read in an existing GEANT geometry structure, edit and display it, and then write it out again. It will also generate the appropriate calls to other GEANT-like packages, such as the SLAC GISMO package, and the MCNP neutron-transport code, thus enabling a common geometrical description to be used for all these simulations. It will support a text-file language that can be used to describe a detector and a tool to parse this language.

   An additional goal of this project is to develop an interface between CAD/CAM systems and the geometry data base. CAD systems have a rather sophisticated description

of geometries in comparison with the existing simulation programs. For this reason it is necessary to develop the simulation program's geometry description in the direction of a 'boundary representation' approach, Boolean algebra, etc. Some steps in this direction have been done in the new GEANT version 3.20.

The schedule calls for the availability of a first version of this tool, without necessarily all the graphical and interactive features or the CAD/CAM exchange capability, but supporting a text-file I/O language, by the end of 1993.

2. Describe test beam geometry using the Geometry Builder

   During the period 1/94 – 6/94 the test beam geometry description should be created using the Geometry Builder tool.

3. Describe GEM geometry using the Geometry Builder

   As a related task, but of lower priority, the full GEM detector geometry description should be created using the Geometry Builder tool (6/94 onwards).

4. Monte Carlo Generators and interfaces, including event pileup

   Event generation is a relatively simple proposition for the test beam as single particles are generally all that is required. However, some consideration will have to be given to pileup particles at high beam rates, and to the generation of secondaries from a target for the simulated "jet" studies. The event generation will be based on the existing **gemgen** package.

5. Particle Transport

   We plan to use primarily the GEANT package for particle transport and simulation of the physics of showering. This decision is based on the high degree of trust that can be placed in its results after a decade of confrontation with data for both electromagnetic and hadronic showers. We shall also evaluate the use of other options in parallel—one of the aims of the Geometry Builder project is to be able to easily run the same detector description within other transport packages such as GISMO, CALOR and MCNP.

6. Digitization

   Each detector subsystem will provide routines to simulate the digitized responses of their subsystem to hits generated by the particle transporter. This requires that a definition of data formats be agreed upon, and is scheduled to be completed by the end of 1994. Prototype efforts in this direction already exist for most subdetectors.

7. 3D Event Display

   By mid-1995 we aim to have developed a 3D visualization tool that permits real-time rotation of the detector shell, visualization of detector digitizations and particle traversal through the detector. This will use the same geometry description of the detector as the simulation. It will be based on the GEM GUI technology to have been selected by this time. Since this is potentially a complex task, we have a fall-back solution of using simpler two-dimensional displays, which may be adequate. The decision will depend on the resources available.

8.2.5 Software Framework

The GEM Computing Subsystem Framework group will develop a framework, as described in section 8.7.2 of the TDR, and for which the bulk of the effort will be provided by PRCD. A formal joint project has been established between PRCD, GEM and SDC to develop a software framework. We expect that prototype frameworks will be developed and used to support test beam work, especially for analysis. Specific elements of the framework which will be addressed are:

- data modeling/management/structures,
- interprocess communication and control (IPC),
- remote procedure calling (RPC),
- parallel processing support, and
- mixed language programming.

We will also establish a C++ pilot project in cooperation with PRCD, where the particular issues are the development of appropriate class libraries, developing methods of supporting object persistence and methods for object transport between processes.

8.2.6 Computing Infrastructure

Areas of computing systems infrastructure that are particularly important to GEM and for which some support is needed from PRCD are listed below. Of particular importance is development of hardware and software for support of test beam work at FNAL and elsewhere with a fully integrated system that demonstrates the overall features of a production system. Some of these projects might be suitable for a joint SSCL-vendor collaboration or for external funding, as being explored by PRCD.

- High-capacity networking,
- high speed I/O for standard workstations, and
- test generator for validation of hardware systems.

8.3 Computing Cost and Schedule Summaries

Table 8.8 lists the costs for Computing R&D for the years 1994–1996 and for the Test Beam.

The institution responsible for implementation of the Fermilab Test Beam GCS will be the SSCL. The following people have been identified as contacts and human resources for the GCS:

Coordinators:

1. V. Glebov (SSCL), overall controls coordinator

WBS	Description	Level 4 Total, k$	Level 3 Total, k$	Level 2 Total, k$
60.1	R&D			909
60.1.1	GCS		479	
60.1.1.1	Project Plan	67		
60.1.1.2	Test System	150		
60.1.1.3	Design	58		
60.1.1.4	Prototype Systems	134		
60.1.1.5	Test Beam Support	70		
60.1.2	Online		332	
60.1.2.1	Project Plan	10		
60.1.2.2	Test System	84		
60.1.2.3	Design	32		
60.1.2.4	Prototype Systems	133		
60.1.2.5	Test Beam Support	73		
60.1.3	Network and Comm.		98	
60.1.3.1	Digital Communications	39		
60.1.3.2	Human Communications	47		
60.1.3.3	Test Beam Support	12		
60.2	GCS			152
60.2.7	Test Beam Support		152	
60.3	Online			260
60.3.7	Test Beam Support		260	
60.4	Network and Communications			48
60.4.3	Test Beam Support		48	
60.5	Project Management			78
60.	Total			1,447

Table 8.8: Computing and Controls Cost Summary

2. J. Voyles (SSCL), transporter and cryogenics controls coordinator

Contacts:

1. TBD. silicon tracker
2. J. Musser (Indiana), IPC
3. Spisiak (Rochester), calorimeter transporter
4. W. Wisniewski (SSCL), noble liquid calorimeter
5. TBD, scintillator calorimeter
6. V. Glebov (SSCL), muon system

7. G. Word (SSCL), online computing
8. J. Voyles (SSCL), cryogenics
9. K. Freeman (SSCL), electronics crates monitoring, HV, LVPS
10. C. Lirakis (Rochester), EPICURE control system
11. G. Ginther (Rochester), safety systems

The cost of the off-line analysis and storage systems will be primarily carried by PRCD, with the help of the following people, who are expected to spend a significant fraction of their time working on offline software development for the test beam.

- Simulation Framework and Geometry: John Womersley (SSCL), Tomasz Skwarnicki (SMU), Toby Burnett (Washington), Brent Moore (Mississippi), Gary Word (SSCL)
- Central Tracker Simulation and Reconstruction: Melynda Brooks (LANL), Geoff Mills (LANL), Shawn McKee (Michigan)
- Calorimeter Simulation and Reconstruction: Michael Shupe (Arizona), Hong Ma (BNL), Michael Seman (Columbia), Christopher Lirakis (Rochester), Brent Moore (Mississippi)
- Muon System Simulation and Reconstruction: Yuri Fisyak (SSCL), Peter Dingus (SSCL), Torre Wenaus (LLNL)

The off-line software schedule and milestones can be summarized as:

- Develop Geometry Builder tool: now—12/93
- Use Geometry Builder to describe test beam setup: 1/94—6/94
- Define framework technologies (data formats etc.): now—3/94
- Define addressing and channel nomenclature: now—3/94
- Develop digitization code: 3/94—12/94
- Develop reconstruction algorithms: now—6/94
- Implement reconstruction code: 6/94—12/94
- Develop event display: 6/94—6/95
- Generate Monte Carlo events: for debugging and code development, 6/94—12/94; for production, 1/95 onward

Chapter 9

Safety, Quality, Reliability and Maintainability Engineering Requirements

9.1 Environment, Safety, and Health Requirements:

The design and operation of the GEM R&D&T systems will be required to eliminate or reduce to an acceptable level of risk the associated environmental and personnel hazards. The designers shall attempt to eliminate hazards from the design. If hazards are fundamental to the design, the design will mitigate the hazard to an acceptable level of risk. The hazard analysis will identify potential hazards and document the elimination of the hazard or, the mitigating action of the hazard which resulted in an acceptable level of risk. Hazard analysis will be provided for all systems, and reviewed and coordinated by the GEM ES&H Group. Mitigation is approved by the GEM Project Manager. Environment, Safety and Health (ES&H) issues will be addressed in accordance with policies and procedures described in the Fermilab and SSCL ES&H Manuals, GEM R&D&T Specifications, and in the GEM Project Management Plan.

All GEM ES&H-furnished safety systems will be functionally and communication compatible with the central monitoring station used at FNAL. Where possible, FNAL recommended hardware will be purchased to provide maximum compatibility. The experiment's slow control system integrates the safety control station (monitors, annunciates, and directs remedial action for the experiment) and will be designed to effectively communicate with the FNAL central monitoring station.

9.1.1 Magnet

The resistive 8000 G dipole and analysis magnets have return flux paths that present no significant hazard to personnel or equipment, operating nearby them. Field mapping will be performed as part of the physics performance qualification and the safety zones (protecting personnel with medical implants) at $\geq$ 10 G will be identified and protected. It is expected that the small fringe field will not pose any operational interference hazard to the vacuum

pumps or other nearby ferromagnetic equipment or structures. Medical screening procedures will identify those personnel who may be affected, and appropriate mitigating precautions will be implemented.

The high power and controls for these magnets will be reviewed and safety protection will be applied to prevent personnel shock or electrical shorts from occurring. The controls to the power source shall be capable of being locked out, when work is being performed on any energized power source. Fire hazards associated with electrical faults shall be protected by overcurrent shunt trip circuit breakers and ground fault circuit interrupters, as well as general smoke/fire detection devices that remove primary power.

The support structure for the large aperture (50×36 in^2) analysis and dipole magnets will be designed with a safety factor of ≥ 1.5 for it's yield strength. Footing attachments to the floor will be designed to prevent mechanical vibration and seismic shifting.

9.1.2 Test Gases

Cryogenic, gas and butane leak detection will be provided at specified locations throughout the distribution system, where leaks might be anticipated, cause personnel injury or ODH or where they could cause equipment damage. In case of leaks, a signal will be relayed to the safety control station.

The LAr and LKr used in the hadronic and endcap Calorimeter bath boxes, along with the N_2 used for cooling of the cryostat volume, will require that the existing ODH detection system at the MWEST facility be modified to detect localized small leaks as well as potentially catastrophic gross liquid spills draining to the pit area. additional sensors will be needed to protect these new inert gas sources. Sensing will be immediately external to the cryostat and any other experiment modules that contain inert test gases, as well as having the existing sensors at the bottom of the room walls. When the detector alarms at $\leq 19.5\%$ O_2, the room ventilation will be increased to allow for safe evacuation of personnel and removal of the leaking gases from the room or pit. The pit will be supplied with an effective gas evacuation exhaust system.

The butane and N_2 used in the tracker IPC and muon CSC chambers will be provided with flammable gas leak detection using the University of Houston SCARF Flammable Gas Detector or equivalent. (These have proven effective in the TTR application.) The $12-13$ sensor head capacity should be sufficient to monitor the butane system with ~ 2 ppb detection sensitivity. The N_2 inertion supplied within both ends of the tracker volume provides protection from the potential electrical ignition sources, and prevents oxygen from combining with any leaking butane. The butane leak sensors will be located immediately external to the tracker housing (at penetrations or connections) and at each gas delivery lines joints and at the vent stack (to monitor emission concentration).

The butane component of the muon chambers test gas mixture will be limited to $\leq 10\%$ concentration with the balance being non-combustible/flammable. These gases shall pose no hazard other than ODH, with no significant corrosive threat to hardware of facility. The exact concentration ratio of this mixture will be refined in the MWEST test; however in event will the concentration of the butane be increased to pose a combustible/flammable hazard without prior approval by the GEM Project and FERMI ES&H.

GEM ES&H will review and determine the safety requirements associated with any alternative test gases that are evaluated or used in any of the experimental modules.

9.1.3 Fire Protection

The largest combustible fuel source associated with the experiment may potentially be from the cryostat's optional use of a plastic foam insulation layer ($\sim$ 18" thick) applied to the exterior of the cold vessel. FNAL requires that this insulation either be of fire retardant composition or that the insulation be well protected from external ignition sources (fire, electrical arcing, or continuous contact heating); and the material liberates no highly toxic decomposition byproducts. GEM ES&H recommends that both polyurethane and poly vinylchloride type insulation be avoided, as they produce highly toxic decomposition byproducts (cyanide and chlorine/phosgene gases). Polystyrene will burn at an extremely rapid rate, but polyethylene presents the least toxicity hazards. With the safety requirements in place, the protection from the room sprinkler system appears adequate. In the event, internal liquid oxygen buildup from condensation within the insulation matrix or layers requires N_2 purging, sensors will be used to detect abnormal conditions of N_2 leakage.

The existing sprinkler suppression system at the MWEST facility must be reviewed to assure that it provides effective coverage of the facility and experiment in case of fire. No additional sprinkler or local suppression systems are anticipated. Smoke/fire detection systems (VESDA and IR type detectors) will be required within the electronic counting rooms, and possibly within the racks depending upon the amount of combustible load. Smoke/fire detection system will be controlled from the safety control station which will be integrated into the computing group's Slow Control System. Automatic room, rack, and experiment power shutdown will be required when a verified alarm condition occurs. GEM ES&H recommends that where a critical loss of data or equipment can occur from smoke or fire, that an automatic CO_2 local inertion system be applied (may be needed for the racks and counting room).

9.1.4 Electrical/Electronics

The primary hazards are presented from the type of cable insulation used and any exposed electrical connections. Cable insulation will comply to the NEC requirements as well as being low smoke density and fire retardant in accordance with the SSCL interim standard. It is recommended that the insulation be low or no halogen content, and that it be compatible with the radiation environment. Compliance with IEEE 1202, UL 1685 and ICEA S-66-524 is recommended, however, in lieu of compliance, mitigation through effective heat/smoke/fire detection and suppression is acceptable. Tray-rated cabling will be required, but no local detection or suppression is required except when low smoke/fire cabling is not used. Fiber optic cables are exempt from these requirements. Coaxial cables are recommended to have the same insulation properties as power. Refer to the LINAC-SSCL Specifications (AEJ-2110101-4) for guidance with safety of cable insulation. Proper separation of power and signal cabling is required; safety systems cabling will be separated from power cables. Cabling used in safety systems will be routed separately from all other cables.

The power supplies for facilities and experiment shall be enclosed, with access panel interlocks, and capability of lock-out power isolation. Verification of NEC compliance will be performed on the facilities and applicable parts of the experiment. Grounding shall utilize one common earth ground and GFIs, where appropriate.

Standard lightening protection will be provided for the MWEST facility, the experiment and it's electronics, coupled with the use of a grid earth-grounding system. Grounding will be in accordance with that described in the GEM TDR, graded to this experiment's scope. Transformers for primary power to the experiment and facility will be protected against strikes.

9.1.5 Radiation

Radiation safety will comply with the FNAL Radiation safety Program, as described in the FNAL Radiological Control Manual. A combination of hardware and procedural safety protection will be applied to preventing inadvertent access to the exposed test beam area. Protection method will be through the use of mechanical interlocked barriers, PASS-type system and administrative entry controls to protect personnel. Calibration radioactive sources will be controlled, through proper inventory, containment, and handling procedures. A permanent radiation monitoring system, supported by strict administrative controls, will be implemented at the MWEST facility. Personal dosimetry and periodic surveys will be used to monitor personnel exposure levels. A PASS-type system will incorporate radiation protection to prevent unauthorized entry into areas of the MWEST facility where radiation levels are in excess of the safe (20 mRem) limit. Interlocked gates, which can only be overridden by at least two intentional actions, will prevent access to the beam/radiation areas. It is anticipated that a PASS-type portal for personnel inventory and admittance-control, will be located at the primary means of access to the facility (counting room or exterior door).

9.1.6 ODH/Confined Space

The experiment will utilize the upgraded/expanded grid ODH monitoring system that currently exists at the MWEST facility. Additional sensors will be located near potential, critical leak points as determined by hazard and ODH analysis. An ODH analysis will be performed on the MWEST facility including the final design of the experiment to determine the risk classification; this will determine additional mitigating actions required to minimize the classification below levels requiring special procedures. The cryostat, calorimeter, pit, and gas mixing distribution facility will require local monitoring. Positive mechanical means will be provided to ensure that the portal access to within the cryostat remains open during occupancy. The pit will be monitored and is anticipated to be defined as a permit-required confined space, and will comply with FNAL ES&H Manual 5063. Exhaust and sump/pump will be provided for liquid/gas evacuation, whose operation is triggered by detection. Activation of the ODH alarm will initiate personnel evacuation from the MWEST facility.

9.1.7 Cryogenics

The dewars used are ASME code-stamped and will be reviewed for compatibility and operational acceptability in accordance with applicable FERMI procedure in their use of Argon, Krypton, and Nitrogen. The dewars, distribution lines and cryostat comply with all applicable FNAL ES&H 5031-34 requirements. The cold vessel will be code-stamped and ASME-compliant pressure relieving devices will be utilized. All delivery lines will be vacuum-jacketed and protected from mechanical damage. The vent lines within the cryogenic and vacuum systems will release either into the mechanical ventilation return duct or to outside atmosphere. Redundant overpressure protection is provided on the cryostat and supply dewars, with reliable, single protection provided at the experiment modules and gas mixing station. The spill path (cold vessel drain) and flow of cryogenic liquid to the pit will be directed away from the access ladder that must be provided in the pit. Redundant protection will be provided to prevent inadvertent mixing of the LAr and LKr in the recovery and supply portions of the distribution system. Cryogen compatible materials of construction will be used in the experiments design.

9.1.8 Transporter

GEM ES&H will review the transporter/manipulator and assure compliance of the design to FNAL ES&H requirements. Emergency stop buttons will be provided for use during maintenance and accident scenarios. Pinch/nip points will identified and guarded. The design yield strength safety factor for the system will be verified. University of Rochester will perform a hazard analysis in accordance with SSCL Procedure D10-000003, and provide for review their safety design with GEM ES&H and FNAL ES&H prior to installing equipment in MWEST.

9.1.9 HVAC

The minimum flow rate of supplied mechanical ventilation to the MWEST facility is recommended to be 2 air changes/hour, with boost capability to 4 air changes/hour minimum in case of ODH, gas release, or for smoke removal. Review will be performed on the acceptable discharge limits for ionized air from the facility to the outside environment. Containment and recirculating measures will be employed to meet the EIS-ALARA (As Low As Reasonably Achievable) emission guidelines. Vacuum pump output will discharge into the nearest ventilation return or to outside the facility. If the contaminants are vented into the room air return duct then non-hydrocarbon based pump oil should be used or sprinkler lines installed in the duct, to prevent ignition of oil condensate. Loss of room ventilation supply will sound an alarm at the safety control station, and may curtail ventilation-dependent operations. Heating will be remotely supplied; use of local space heaters is discouraged due to the use of butane within the tracker and muon chamber.

9.1.10 Environmental

The GEM R&D&T experiment will comply with the applicable parts of the FNAL ES&H Manual 8000 section. Radiation and heavy metals testing will be performed upon the experiments cooling water, prior to disposal. Generation of mixed hazardous waste stream is prohibited and not anticipated to occur. The effluent discharge from the experiment will be governed by FNAL ES&H requirements, which FNAL personnel will coordinate.

Interior lighting will be a minimum of 50 footcandles at the room floor, and will be on emergency power backup, providing a minimum of 1 footcandle at the floor.

Noise level contribution from the GEM R&D&T equipment will be designed or damped to a time-weighted average sound pressure level of $\leq$ 85 dBA. In no instance shall the equipment or area level exceed 115 dBA.

9.1.11 General

The GEM R&D&T shall present no safety hazards during delivery, assembly, installation, test, and operation by complying with applicable DOE Orders such as 5480.4, 5480.25 and 5481.1B and OSHA standards plus applicable state, local, and SSCL safety requirements. The Hazard Analyses will be performed on the experiment hardware, installation and integration, and shall identify the hazards and mitigating actions associated with the design, assembly, test, and operation of the Cryostat, Calorimeter, Muon, Tracker, and Magnet. The integration analysis will cover up to the defined interface points with the MWEST facilities. This analysis report shall also include a hazard list for the GEM R&D&T. Safety system parameters will be determined for the GEM R&D&T, where monitoring, detection, alarm annunciation, and suppression will be specified for smoke, fire, ODH, gas leak, and radiation hazards. Refer to the GEM R&D&T Safety Systems Specification GDT-0000XX for details.

MIL-STD-1472 shall be used as a guide to insure that the GEM R&D&T design is consistent and compatible with the human capabilities required to build, test, install, and repair the GEM R&D&T in a repeatable, consistent, effective, and safe manner. This includes tasks, tools, equipment, environment, personnel-equipment interfaces and other items required of the GEM R&D&T in meeting the requirements of this specification.

The GEM R&D&T piping shall comply with ANSI/ASME B 31.3 (Chemical Plant and Refinery Piping) Code. All other pressure vessel components shall comply with the ASME Boiler and Pressure Vessel Code, Section VIII. In cases of combined loads or geometries not explicitly covered by these codes, adequate supporting calculations shall be performed to insure that allowable Code stresses are not exceeded. Stresses in non-pressure boundary components, such as auxiliary equipment support structure and brackets, shall conform to the AISC Specification for the Design, Fabrication, and Erection of Structure Steel for Buildings.

Instrumentation and piping feedthroughs shall be reasonably accessible for repair or replacement without requiring major breaches of the cryostats. Feedthrough designs shall be optimized for reliability, assembly, safety, and maintenance. Designs shall be assessed for their life cycle survivability over the lifetime of the system. Piping feedthroughs shall also incorporate design features to minimize heat leakage into the cryostats and limit stress on lines during thermal cycling. Thermal cycling testing shall be performed, prior to acceptance

to determine typical failure rates. Wherever possible feedthrough bellows will be placed such that a positive external pressure is present to minimize squirm. Radiation levels present in the experimental area, when the beam is operational, will restrict access to the immediate area, except for intermittent occupation of the electronic counting rooms. Concrete shielding is present which will provide some exposure protection.

The cryostat cold vessel wall thickness will be of a sufficient thickness to provide protection against pressure differential buckling of the vessel, which potentially could occur due to separate vacuum systems for both vessels.

Load conditions on GEM R&D&T subsystem components shall include, but not necessarily be limited to gravity, static preload, seismic, steady-state and transient magnetic, steady-state and transient thermal, steady-state and transient pressure (cryogenic fluid or vacuum induced), transportation and handling, and environmental loading. Rings, shackles, and lugs shall be designed for a minimum yield factor of safety of 3.0 based on dead load (weights).

9.2 Codes, Standards, and Regulation Requirements:

The following documents form a part of this document to the extent specified herein. In the event of conflict between the documents referenced herein and the contents of this specification, the contents of this specification shall be considered a superseding requirement. However, if the design specified herein superceding a requirement does not comply with the intent of the superceding specification, that design shall comply with the requirement of the ES&H manual, D10–000001; Ch.1.3. In those instances where a document is referenced for use as a guide, the design agency must provide its own interpretation and verify proper applicability prior to its use. The systems and designs must meet the following codes and standards.

9.2.1 Government and Industry Regulations.

- CGA standards, P-1, etc.
- NEC, NFPA 70, ANSI C1 National Electric Code
- NEC, ANSI C2 National Electrical Safety Code
- NFPA 58 Standard for the Production, Storage, and Handling of Liquefied Petroleum Gas
- NFPA 59 Standard for the Production, Storage, and Handling of Liquefied Natural Gas
- Occupational Safety and Health Act (OSHA) 29 CFR 1910
- DOE Order 6430.1A General Design Criteria
- DOE Order 5480.25 Safety of Accelerator Facilities

- DOE Order 5481.1B Safety Analysis & Review System
- FNAL ES&H Manual
- ANSI B16.5 Pipe Flanges and Flanged Fittings
- ANSI B16.9 Factory-Made Wrought Steel Butt-welding Fittings
- ANSI B30 Hoisting & Rigging of Critical Components
- ANSI B31.1 Code for Power Piping
- ANSI B31.3 Chemical Plant and Petroleum Refinery Piping
- ANSI B31.5 Refrigeration Piping
- ANSI B31.6 Stainless Steel Pipe
- ASME Boiler and Pressure Vessel Code Section VIII
- AISC Structural Design Code
- AWS D1.1-90 Standard for Structural Welding Code Steel Notice 1, 12 Sep. 90
- AWS D1.2-90 Standard for Structural Welding Code Aluminum Notice 1, 12 Sep. 90
- MIL-STD-454 Standard General Requirements for Electronic Equipment
- MIL-STD-1472D Human Engineering Design Criteria for Military Systems, Equipment, and Facilities
- DOE Order 4700.1 Project Management System,
- DOE Order 5700.6C Quality Assurance
- DOE Order 5480.19 Conduct of Operations Requirements for DOE Facilities
- DOE-Engineering-Standard Implementation Guide for Quality Assurance Program for Basic and Applied Research, DOE-ER-STD-6001-92.

9.2.2 Fermilab and SSCL Documents

- P40-000013: SSCL Guideline 4.4, Engineering Drawings
- P40-000061: SSCL Reliability Guideline for Engineering, 3.20.1.
- P40-000061: SSCL Maintainability Guideline for Engineering, 3.20.2.
- P40-000070: Draft SSCL Guideline 3.2.1.1, Mechanical Engineering
- P40-000188: Minimum Recommended SSCL Seismic Design Requirements SSCL ES&H Manual

- SSC Laboratory Environment, Safety & Health Manual, D10-000001
- SSC Laboratory Quality Assurance Plan , D70-000001
- SSCL Engineering Management Plan, SSC Laboratory, E10-000029.
- GEM Project Management Plan, Gamma, Electron, Muon Detector Collaboration, GGT-000006.
- GEM Technical Design Report, April 1993, [1]
- FERMI RDT Safety Analysis Report, GGT-0000XX.
- GEM Configuration Management Policy , GGT-000009
- PRD Configuration Management Policy, R00-000003
- PRD QA 1.2, PRD Quality Implementation Plan, R00-000005
- D10-000003, SSCL Procedure, Hazard Analysis

9.3 Quality Assurance Requirements:

From the preliminary design to the final system installation, particular consideration must be given to quality assurance. All designs and processes will be required to be fully verified for compliance with established criteria for acceptance. Quality assurance will be executed in accordance with the DOE orders 4700.1 and 5700.6C, and the SSC Laboratory Quality Assurance Program , D70-000001 as described in the PRD Quality Implementation Plan and related procedures. Document control and configuration management will be carried out using procedures in Section 7.0 of the GEM Project Management Plan and in the PRD Configuration Management Policy, R00-000003. Quality assurance plans and procedures for designs or manufacturing processes taking place at institutions or in foreign countries must be approved by GEM Project Management.

9.4 Testing Requirements

Controls, materials, components, and subsystems will be tested prior to installation. Upon completion of installation and prior to start-up of the GEM electronic systems, the RDT systems must be fully commissioned through a series of tests. The tests will include performance tests for the heat rejection, pressure and leakage, flow and cryogenics, gas and butane quality requirements. In addition, systems will be tested to insure that fail-safe requirements are met. Operating Procedures, training, and operation and maintenance manuals will be provided as part of the design process. A detailed testing program will be described in a future Acceptance Test Plan Report (ATPR).

9.5 Reliability and Maintenance:

A GEM RDT Reliability Program shall be established and managed in conformance with P40-000061, the SSCL Reliability Engineering Guideline 3.20.1.

A maintainability program shall be established in accordance with the SSCL maintainability guidelines for engineering. The maintainability of the RDT systems must be readily achieved to minimize RDT downtime. Maintainability considerations shall include man-lift limits, accessibility, ease of maintenance, controls placements, placards for cautions/warnings and safety of maintenance. Hand tool selection shall be carefully considered due to the presence of a magnetic field, high voltage and radiation.

9.6 Design Reviews & Fabrication

Safety Design Review Committees will be established at FNAL to ensure that the RDT complies with all the applicable FNAL ES&H Requirements. Safety reviews by FNAL will be coordinated through GEM ES&H. Subcontractor QA programs will be reviewed prior to acceptance. This will include the vendors QA plans and procedures for fabrication. Design drawings, specifications, and user requirements for software will be reviewed.

Chapter 10

Budgets and Funding Requests

Cost estimates and schedules are included for each subsystem discussed in this document. Guidance provided to the subsystem leaders and authors was based upon budget assumptions which were assumed during the summer of 1993. GEM planned a full budget program for FY94 of $32 million. A middle budget plan assumed $25 million. A low budget scenario which did not permit much of the activity described in this document was also planned at $18 million. GEM management requested that the planning for this document should assume the middle budget scenario.

It was our plan to adjust the scope of the program proposed by GEM to match the final funding guidelines developed after the Congress and DOE provided the SSC funds ceiling for FY94. As the SSC project has been terminated we do not present a final budget and schedule for the proposed R&D activities beyond the individual estimates presented in the subsystem chapters. We do believe that the information included is the basis for planning a follow-on program to the SSC project.

Bibliography

[1] GEM collaboration, Technical Design Report, GEM TN–93–262(1993).

[2] W. Braunschweig et al., Nucl. Instr. and Methods, A275, 246-257(1989).

[3] O. Benary et al., Nucl. Instr. and Methods, A332, 78(1993).

[4] B. Aubert et al., Nucl. Instr. and Methods, A309, 438(1991),
B. Aubert et al., Nucl. Instr. and Methods, A321, 467(1992),
B. Aubert et al., Nucl. Instr. and Methods, A325, 116(1993).

[5] O. Benary et al., "Performance of an Accordion Electromagnetic Calorimeter with Liquid Krypton and Argon", Nucl. Instr. and Methods (submitted, 1993).

[6] O. Benary et al., "Performance of an Accordion Electromagnetic Calorimeter with Multiple Time Samples", Nucl. Instr. and Methods (submitted, 1993).

[7] C.W. Fabjan, CERN-EP/85-54(1985).

[8] D. Lazic, "Etude et mise au point d'un nouveau principe de calorimetre employant des fibres optiques en quartz", PHD thesis of Strasbourg University, France, May 1993.

[9] A. Savin in "Workshop on Forward Calorimetery", ITEP, Moscow, GEM TN–93–424.

[10] M. Diwan, Y. Fisyak et al., "Radiation Environment and Shielding for the GEM Experiment at the SSC", SSCL-SR-1223 and references therein.

[11] A. Beretvas, A. Byon-Wagner et al., Nucl. Instr. and Methods, A329, 50-61(1993)

[12] Judy K. Partin, "Fiber optics in high dose radiation fields", SPIE Vol.541 Radiation Effects in Optical Materials (1985),
J.B. Chesser, IEEE NS, vol.40, No.3,June 1993, pp.307-309 (and referencies therein).

[13] F. Lobkowitz, "GEM Barrel Calorimeter Hadronic Modules", GEM TN–93–311(1993)

[14] Yu. Efremenko et al., "Scintillating Barrel Calorimeter: Optimization of performance", GEM TN–93–349(1993).

[15] J. Rutherfoord, "GEM Forward Calorimetery: A General Description of the Liquid Argon Option", GEM TN–92–188(1992).

[16] J. Rutherfoord, "Testing for Effects of Ion Loading in Liquid Ionization Calorimeters", GEM TN–93–410(1993).

[17] "Monolithic Integrated Concepts for Muon Subsystem Structures"; Simpson Gumpertz & Heger Inc. Arlington, MA

[18] "GEM Muon Group Meeting - SSCL, July 12-13, 1993"; GEM TN-93-440

[19] "GEM Muon Group Meeting - SSCL, August 3-4, 1993"; GEM TN-93-451

[20] A.Chvyrov et al. "Spatial Resolution of 3.0 m × 0.3 m Dubna Prototype CSC" GEM TN-93-466

[21] prDAQ; "Data Acquisition for Detector Prototypes at the SSCL"; SSCL preprint 478; June 1993.

[22] W. E. Cleland and E. G. Stern, "Signal Processing Considerations for Liquid Ionization Calorimeters in a High Rate Environment", submitted to Nucl. Instr. and Methods, 1993.

[23] O. Benary, et al., "Liquid Ionization Calorimetry with Time-Sampled Signals", in preparation for submission to Nucl. Inst. and Methods, 1993.

[24] W. E. Cleland, "Timing Performance of the GEM Calorimeter Trigger for Large Signals", GEM TN–93–449(1993).

[25] M. Clemen and W.E. Cleland, "Detailed Studies of the Level 1 Calorimeter Trigger for Higgs $\rightarrow 2\gamma$", GEM TN–93–439(1993).

[26] INMOS ltd.; "The T9000 Transputer Products Overview Manual"; 1991.

[27] MVME–162, Product of Motorola, Inc.

[28] M. Bowden, J. Carrel, J. Dorenbosch, V.S. Kapoor, A. Romero, "GEM Data Acquisition System Preliminary Design Document," GEM–TN–471 (1993).

[29] "GEM Test Beam Meeting at FNAL: MWEST Conference Room," June 16–17, 1993, GEM–TN–418.

[30] "GEM Test Beam Meeting – SSCL," August 19, 1993, GEM-TN-93-456.

[31] DART, (Data Acquisition–Real Time), a product of Fermilab.

[32] Paul F. Kunz and Gary B. Word, "The Cheetah Data Management System," contributed paper to the Conference on Computing in High Energy Physics, Annecy, France, Sept. 21–25, 1992. Also available as SLAC-PUB-5930.

[33] C.Alan Fry, "UNIDAQ", SDC TN–93–478(1993).

[34] H. Uijterwaal; Ph.D. Thesis, University of Amsterdam, The Netherlands; 1992.

[35] Yu. Fisyak et al., GEM TN–93–438(1993).